Optimizing human Treg stability and target specificity for therapeutic applications

vorgelegt von

M.Sc.

Anna Nowak

geb. in Berlin

von der Fakultät III – Prozesswissenschaften
der Technischen Universität Berlin

zur Erlangung des akademischen Grades
Doctor rerum naturalium (Dr. rer. nat.)

genehmigte Dissertation

Promotionsausschuss:

Vorsitzender:	Prof. Dr. Lorenz Adrian
Gutachter:	Prof. Dr. Roland Lauster
Gutachter:	Prof. Dr. Jens Kurreck
Gutachter:	Prof. Dr. Alexander Scheffold

Tag der wissenschaftlichen Aussprache: 12.02.2018

Berlin 2018

Table of Contents

1 Introduction

1.1 The immune system

In order to protect themselves from pathogenic microorganisms, animals and plants have developed effective mechanisms to recognize and eliminate pathogenic invaders. The first line of defense is the innate immune system which comprises the unspecific recognition of pathogens and provides immediate defense. While mechanisms of innate immunity are present in most organisms, vertebrates have additionally developed an adaptive immune system that consists of highly specialized cells. Innate and adaptive immunity are mediated by humoral and cell-mediated components which comprise different mechanisms to target pathogenic invaders. While the former is mostly based on macromolecules that are found in extracellular fluids (e.g. antibodies, antimicrobial peptides), the latter consists of cells that directly respond to pathogens (e.g. phagocytes, T cells). Together, cell-mediated and humoral components of the innate and adaptive immune system provide complex and effective mechanisms that enable the recognition, elimination and long-lasting protection from intracellular and extracellular pathogens [1, 2].

1.1.1 Innate and adaptive immunity

The innate immune system is the first line of defense against pathogenic invaders which other than the adaptive immune system comprises generic mechanisms that enable immediate protection but do not provide long-lasting immunity. Among these mechanisms are physical barriers (e.g. mucosal surfaces) that prevent the invasion of microorganisms as well as proteins that induce inflammation (complement system) and cellular components that recognize and destroy pathogens (e.g. phagocytes, dendritic cells, natural killer cells). The recognition of pathogens by innate immune cells is mediated by pattern recognition receptors (e.g. toll-like receptors, TLRs) that bind conserved proteins that are present in various microorganisms. If the innate immune system fails to recognize and clear a pathogen, components of the adaptive immune system are activated to mount a more specific and efficient immune response [1]. The adaptive immune system enables the highly specific recognition and elimination of pathogens and can provide long-lasting protection. It comprises specialized lymphocytes, namely B cells and T cells that originate from a common lymphoid progenitor in the bone marrow. During their development in the thymus (T cells) or bone marrow (B cells), somatic recombination generates diverse repertoires of B cell and T cell receptors that bind particular antigens and form the basis for a highly specific recognition within the adaptive immune system [3, 4].

B cells are an important part of humoral immune responses as they can produce large amounts of antibodies that bind native proteins in their tertiary structure enabling efficient immune responses against extracellular microorganisms or toxins. B cell specificity is determined by a highly specific B cell receptor which can remain bound to the cellular surface or be secreted as antibody into the blood plasma. Upon antigen-specific activation via the B cell receptor, B cells proliferate and differentiate into plasma cells or memory B cells which can secrete large amounts of antibodies and are able to provide long-lasting immunity [2]. While antibodies target antigens that are outside of the cell, T cells are able to mediate an immune response against intracellular pathogens. T cells are an important part of cell-mediated immunity and recognize antigens that are processed and presented on the cell surface by major histocompatibility complexes (MHCs). T cell specificity is mediated by T cell receptors (TCRs) that are expressed on the surface of T cells which recognize antigens in their primary structure. Upon antigen-specific binding of MHC-peptide complexes, T cells proliferate and differentiate to mount an efficient immune response against pathogenic invaders (see 1.1.2). Once an infection is cleared by the adaptive immune system, most antigen-specific B and T cells are eliminated, but some become long-lasting memory cells. Upon binding of their previously encountered antigen they are able to mount a faster and stronger immune response providing the basis for long-term immunological memory [2].

1.1.2 T cells

T cells mature in the thymus and are an important part of cell-mediated immunity during adaptive immune responses. The T cell compartment consists of cytotoxic and helper T cells that differ in their phenotype and function but are similarly characterized by expression of a highly specific TCR which binds cognate antigens in an MHC-dependent manner. The TCR is a heterodimer and in most T cells is composed of an α and β chain whereas a minor subset (γδ T cells) consists of γ and δ chains (Figure 4A). Pairing of the two chains provides the structural composition for the highly specific interaction with MHC-peptide complexes [5]. To enable recognition of a large number of peptides, highly diverse TCR repertoires are generated by somatic recombination of variable (V) and joining (J) gene segments (α chain) or VJ and diversity (D) gene segments (β chain) resulting in over 10^{20} possible combinations [6]. Although a large number of TCRs are generated in the thymus, only about 5% are believed to enter the periphery as most T cells are eliminated during thymic selection [7]. This process is

essential to ensure functionality of T cell clones in the periphery but also to prevent reactivity against endogenous structures (see 1.1.3.1) [8].

The T cell compartment consists of cytotoxic T cells and helper T cells that have different functions during an adaptive immune response. Cytotoxic T cells are characterized by expression of CD8 which is a co-receptor for MHC class I molecules that are expressed on the surface of almost all cells. Upon recognition of foreign peptides, cytotoxic T cells mediate programmed cell death e.g. by secretion of cytotoxins or by expression of surface molecules that enable direct interaction with the target cell. This provides the immune system with the ability to directly eliminate cells that process and present foreign peptides on their surface upon infection with an intracellular pathogen [9]. In contrast, helper T cells (Th cells) express CD4 which is a co-receptor for MHC class II molecules that are expressed only on professional antigen presenting cells (APCs) such as dendritic cells, macrophages or B cells. Upon activation, CD4 T cells secrete cytokines and upregulate molecules that enable interaction with various cells of the immune system which allows modulation, such as amplification or suppression, of an immune response against intracellular or extracellular pathogens. Depending on the activating pathogen, CD4 T cells can differentiate into specialized Th subsets (e.g. Th1, Th2, Th17) that differ in their cytokine profile that corresponds to the respective immune reaction. Consequently, CD4 T cells are essential mediators of an adaptive immune response and comprise versatile mechanisms to modulate protective immune reactions [10].

1.1.3 Immune regulation

Based on the highly specific mechanisms of the adaptive immune system, pathogenic invaders can effectively be eliminated. However, the great potential of the immune system to cause inflammation and tissue damage requires tight controls that prevent its false activation which can otherwise result in chronic inflammation, autoimmunity or allergy. Immunological tolerance against self and harmless foreign antigens is induced in the thymus (central tolerance, see 1.1.3.1) or at peripheral sites (peripheral tolerance, see 1.1.3.2) and is essential for the maintenance of immune homeostasis [11].

1.1.3.1 Central tolerance

Central tolerance is a mechanism that affects T cell and B cell maturation and selection in the thymus or bone marrow before they enter the circulation. Selection of T cells is based on the specificity and affinity of the TCR and is an important mechanism to avoid self-reactivity in the periphery. Developing T cells are first selected based on their ability to bind self MHC-peptide complexes and clones that fail to bind die by neglect. Upon recognition of self MHC-peptide complexes, low and intermediate affinity interactions are positively selected to enter the periphery whereas high affinity clones that have the potential to recognize endogenous structures and cause autoimmunity are eliminated (Figure 1) [11]. Furthermore, it has been shown that intermediate affinity to self can promote commitment to a separate lineage of $CD4^+$ T cells that exhibits potent regulatory and suppressive functions (see 1.2) [12]. Although the precise mechanisms that induce commitment to the regulatory T cell (Treg) lineage are not fully understood, affinity to self has been proposed to be an important driver of Treg development in the thymus providing the basis for suppression of self-reactivity in the periphery (Figure 1).

The selection of clones based on their affinity to self requires the expression of autoantigens in the thymus. It has been shown that the transcription factor *Aire* (autoimmune regulator) upregulates expression of tissue-specific self-antigens in medullary thymic epithelial cells (mTECs). Consequently, *Aire* dysfunction results in a loss of central tolerance [13-16] which is characterized by a variety of autoimmune manifestations in patients suffering from Autoimmune Polyendocrinopathy Syndrome type 1 (APS-1) [17, 18]. Taken together, central tolerance is based on the careful selection of clones that enter the periphery and it is currently believed that T cells with high affinity interactions to self-antigens are eliminated during thymic selection whereas intermediate affinity promotes commitment to the Treg lineage (Figure 1).

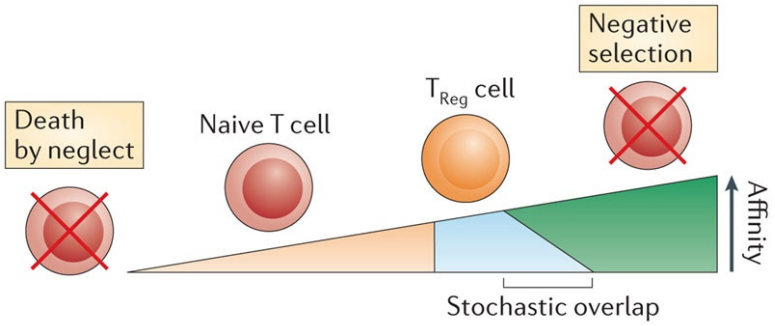

Figure 1: The affinity model of thymocyte selection. T cell selection in the thymus depends on the affinity of the T cell receptor to self-antigens. Clones that do not recognize self MHC-peptide complexes die by neglect while low and intermediate affinity clones are positively selected. Negative selection eliminates clones with high affinity interactions to prevent self-reactivity. Clones with intermediate affinity to self differentiate into Tregs, although a small range of stochastic overlap can generate either $CD4^+$ T cells or Tregs (figure derived from [19]).

1.1.3.2 Peripheral tolerance

Thymic selection of T cells represents an important mechanism to prevent self-reactivity in the periphery. Nevertheless, some self-reactive clones can escape thymic selection and also tolerance against harmless foreign antigens needs to be maintained in the periphery. Therefore, in addition to central tolerance, peripheral tolerance is essential to prevent immune reactions against endogenous structures but also against innocuous non-self antigens such as food or microbiota which can cause autoimmunity, chronic inflammation or allergy [20]. Mechanisms of peripheral tolerance include the elimination of self-reactive T cells that have left the thymus via e.g. anergy or deletion but also entail specialized cell subsets that are able to exert regulatory functions to control inflammatory immune reactions [11]. For example, tolerogenic APCs can suppress inflammation by insufficient co-stimulation resulting in impaired T cell activation and expansion. In addition, a tolerogenic environment can promote the acquisition of regulatory functions by CD4 T cells, e.g. by expression of the immunomodulatory cytokine IL-10 by type 1 regulatory T cells (Tr1 cells). Indeed, Tr1 cells have been shown to ameliorate inflammation in animal models of colitis [21], graft-versus-host-disease (GvHD) [22] and type 1 diabetes (T1D) [23]. Furthermore, regulatory T cells that are selected in the thymus based on their affinity to self-antigens are important mediators of tolerance in the periphery (see 1.2). Collectively, the T cell repertoire is shaped by careful selection processes in the thymus and periphery which provide T cells with specificities to efficiently eliminate pathogenic invaders while maintaining tolerance against self and harmless foreign antigens.

1.2 Regulatory T cells

Regulatory T cells (Tregs) are a small but highly specialized subset that is an important regulator of the immune system. Tregs develop as a separate lineage in the thymus and are believed to be selected based on their intermediate affinity to self-antigens (Figure 1). Because of their potent immunosuppressive functions they are important mediators of tolerance in spite of their low frequencies making up only ~2-3% of the human CD4 T cell compartment [24]. Tregs are mostly characterized by expression of high levels of the IL-2 receptor α-chain (CD25) and lack of expression of the IL7 receptor (CD127), although this signature is not exclusive to the Treg lineage. More importantly, the X chromosome encoded transcription factor Forkhead-Box-Protein 3 (FoxP3) has been identified as the lineage specification factor that is essential for Treg development and function [12, 25]. Consequently, its deficiency in mice (scurfy phenotype) and humans (IPEX syndrome) leads to severe systemic autoimmunity, allergy and inflammatory bowel disease underlining the importance of Tregs for the maintenance of tolerance [26, 27]. Although FoxP3 has been described as the key transcription factor that is critical for Treg development and function, its expression is not limited to Tregs and can be transiently upregulated by non-Tregs upon activation [28-30]. However, stable FoxP3 expression in thymic-derived Tregs is epigenetically imprinted within a highly conserved region in the FoxP3 locus (Treg-specific demethylated region, TSDR) that is demethylated in Tregs, but not in conventional T cells (Tcons) [31-34]. Furthermore, Treg-specific hypomethylation patterns that are essential for thymic Treg development and their stability in the periphery have been identified (e.g. *foxp3* intron 1, *ctla4* exon 2 and *ikfz4* intron 1) which together with concomitant expression of FoxP3 establish lineage stability in the periphery [35].

1.2.1 The peripheral Treg compartment

The immune system is frequently encountered with foreign antigens which can be harmful to the host and require protective immune reactions. In contrast, foreign antigens also include harmless structures such as microbiota, innocuous environmental antigens or food which have the potential to cause severe chronic inflammation or allergy. Therefore, immune reactions against such antigens need to be tightly controlled by mechanisms of peripheral tolerance which includes the circulation of regulatory cells in the periphery (see also 1.1.3.2) [20].

In spite of its well-established importance for the maintenance of tolerance, the composition of the peripheral Treg compartment remains poorly understood. In addition to FoxP3$^+$ Tregs that develop as a separate lineage from Tcons in the thymus, it has been shown that FoxP3$^+$ cells in the periphery can also derive from Tcons that have transiently acquired a regulatory phenotype (Figure 2; see 1.2.1.2). Furthermore, stability of thymic-derived Tregs in the periphery remains elusive as plasticity of the Treg phenotype has been observed which can potentially contribute to inflammatory immune pathologies (Figure 2; see 1.2.1.1). Collectively, heterogeneity and stability of the peripheral Treg compartment remain unknown and also their contribution to tolerance and inflammatory immune pathologies has not clearly been defined [36, 37]. For clear separation of Tregs that have developed in the thymus and Tregs that were induced in the periphery, a nomenclature that was proposed by Abbas et al. (2013) will be used throughout this work. In that way, thymic-derived Tregs (tTregs) can be distinguished from Tcons that have acquired FoxP3 expression *in vitro* (*in vitro*-induced Treg, iTreg) and Tregs that were induced extrathymically from Tcons *in vivo* (peripherally-derived, pTreg) [38].

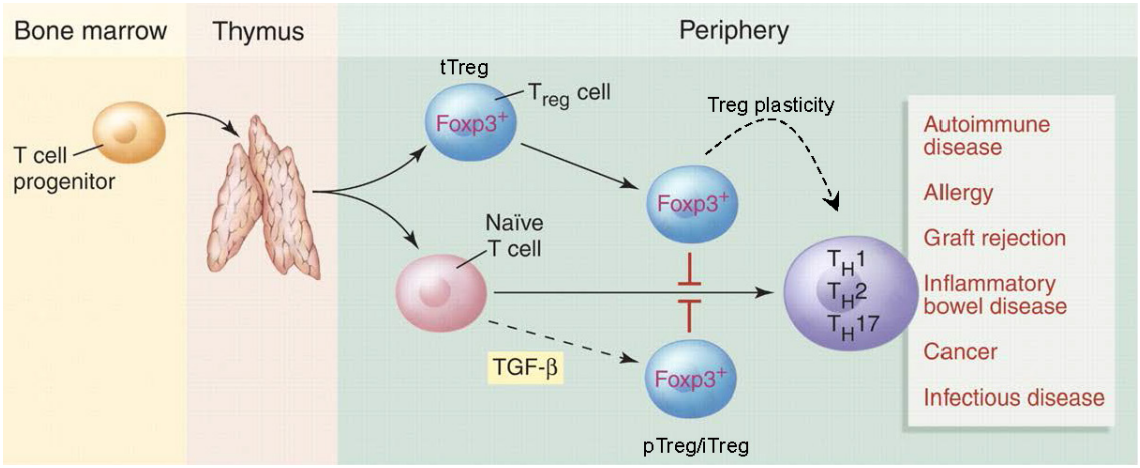

Figure 2. The peripheral Treg compartment. Naive T cells and tTregs develop separately in the thymus from a common T cell progenitor. In the periphery, naive T cells differentiate into effector cells (e.g. Th1, Th2, Th17) that mediate different immune responses which can be suppressed by Tregs. FoxP3$^+$ Tregs can either derive from the thymus (tTregs) or from Tcons that were extrathymically induced *in vitro* (iTregs) or *in vivo* (pTregs) which is dependent on TGF-β. In addition, it has been suggested that loss of a regulatory phenotype and plasticity of tTregs can contribute to inflammation (figure adapted from [39]).

1.2.1.1 Treg plasticity

Lineage stable tTregs develop in the thymus and exhibit potent immunosuppressive functions in the periphery. However, plasticity of inherently stable tTregs remains controversial. For example, downregulation of FoxP3, loss of suppressive capacity and expression of effector cytokines have been observed within the peripheral Treg compartment and have been proposed to contribute to heightened immune responses [36, 37, 40-43]. Such pathogenic conversion of Tregs has been shown to contribute to autoimmunity [44-46], allergy [47] and chronic inflammation [48] in mice but can also mediate protective immune responses against helminth infections [49]. However, it is not known whether these exTregs within the peripheral Treg compartment actually originate from *bona fide* tTregs or represent instability of pTregs. On the one hand, reprogramming of the Treg lineage under inflammatory conditions has been shown in mice indicating inherent instability of the Treg lineage [44, 45, 47-51]. In contrast, others have attributed plasticity to a minor Treg subset suggesting heterogeneity while showing overall stability of Tregs in the periphery [52-54]. Collectively, instability of the Treg lineage and its potential contribution to immune pathologies remain unknown.

Most studies that have analysed *in vivo* Treg stability have used lineage tracing of $FoxP3^+$ cells in mice. But also in humans Treg instability has been observed *in vitro* [55-59] which has been proposed to be restricted to the antigen-experienced memory Treg compartment as naive Tregs have been shown to be particularly stable [60-65]. Furthermore, expression of effector cytokines has been observed in Tregs derived from patients suffering from MS [66], T1D [67], arthritis [45, 68, 69], psoriasis [70] and inflammatory bowel disease [71-73], but also in healthy individuals [65]. These data question stability of the Treg lineage *in vivo* and even suggest a contribution of Treg plasticity to inflammatory immune pathologies. However, studies that have reported Treg instability in humans have analysed the polyclonal $CD25^+CD127^-$ Treg compartment *ex vivo* or after prior *in vitro* expansion which can contain variable degrees of effector cells. Furthermore, lack of Treg-specific activation markers has currently prevented analysis of antigen-specific Tregs and therefore lineage stability of Tregs during particular immune responses remains unknown [74, 75]. Collectively, due to a lack of markers it is currently impossible to unambiguously identify lineage stable tTregs *ex vivo* or within *in vitro* expanded cultures and therefore inherent Treg plasticity cannot be clearly distinguished from instability of pTregs. Consequently, plasticity can similarly derive from Treg reprogramming or cellular heterogeneity which currently

cannot be clearly separated. Taken together, the occurrence of Treg plasticity and its contribution to immune reactions in humans remain poorly understood.

1.2.1.2 Extrathymic Treg induction

In spite of their importance for the maintenance of tolerance, little is known about the antigen-specificity of the peripheral Treg compartment in humans. It is currently believed that Tregs develop based on their intermediate affinity to self to prevent auto-reactivity in the periphery while Tcon specificity is directed toward non-self to enable protective immune reactions (Figure 1) [76-83]. Nevertheless, tolerance needs to be maintained against harmless foreign antigens from e.g. the environment, commensals or food (see 1.1.3.2). Indeed, it has been shown that Tregs can control immune responses against non-self antigens in mice [84-91] and humans [92-97]. However, it is currently assumed that immune responses against foreign antigens are mediated by pTregs which are induced extrathymically from Tcons in the periphery. However, lack of markers to unambiguously distinguish tTregs from pTregs is currently limiting delineation of the peripheral Treg compartment in humans. Although Helios [98, 99] and Neuropilin 1 [100, 101] have been proposed to identify tTregs, their application for the separation of human tTregs and pTregs remains controversial [102-105]. More recently, CD137 has been shown to be upregulated on antigen-activated Tregs *ex vivo* which exhibited a stable Treg signature separating them from CD154-expressing Tcons suggesting a role for tTregs in the maintenance of tolerance against foreign antigens in humans [92, 96, 97, 106, 107]. Collectively, the specificity of pTregs as well as their contribution to regulatory immune responses in humans remain unknown.

Evidence for extrathymic Treg induction comes mostly from *in vitro* studies which have shown that particular conditions (IL-2, TGFβ) can induce FoxP3 expression and regulatory functions in naive Tcons (iTregs) [108-110]. Furthermore, pTreg induction has been observed *in vivo* in mice during chronic inflammation [111-113], autoimmunity [100, 101, 114, 115], within tumors [100], during helminth infection [116] and even under homeostatic conditions [117-122]. Similar to *in vitro* studies, *in vivo* Treg induction has been shown to require antigen-activation and TGF-β [101, 111, 112, 115, 119, 121, 123]. However, even in mice the origin of pTregs remains unclear as induction is mostly defined by acquisition of FoxP3 expression resulting in variable outcomes depending on the experimental system. Therefore, the extent and contribution of pTregs to the physiological Treg repertoire and to tolerance especially in humans remain elusive.

The inability to identify rare antigen-specific Tregs and Tcons has limited the characterization of immune responses against defined antigens [74, 75]. Therefore, the contribution of particular antigens to Treg-Tcon conversion, including extrathymic Treg induction and differentiation of tTregs into effector cells, has not been demonstrated in humans [74, 75]. More recently, sequencing of T cell receptors has emerged as novel technology to provide insight into the clonality of T cell populations and to track individual clones and their progeny. Using this method, studies have aimed to evaluate heterogeneity and plasticity of the peripheral Treg compartment in mice and humans by determining the clonal overlap between Tregs and Tcons. However in mice, studies have reported highly variable overlap ranging from less than 5% [124-126] to 20% [76, 77, 114, 127-129] up to 40% [130] depending on the approach. Similarly, results from humans have suggested variable degrees of Treg-Tcon conversion with notable TCR repertoire overlap within the polyclonal Treg compartment [131] as well as in response to tumor antigens [132] and CMV [133] while more recent studies have reported only limited overlap of the polyclonal Treg and Tcon compartments [134, 135].

Consequently, heterogeneity within the peripheral Treg compartment has been shown, yet whether it originates from the inability to unambiguously identify tTregs or represents physiological extrathymic Treg induction or potentially pathogenic Treg conversion cannot be clearly distinguished. Therefore, heterogeneity and stability of the peripheral Treg compartment remain unknown.

1.3 Regulatory T cell therapy

Regulatory T cells are important mediators of tolerance and are able to suppress inflammatory immune reactions in the periphery (see 1.2). Chronic inflammation or autoimmune diseases are caused by a temporary or long-lasting loss of tolerance against endogenous or harmless exogenous antigens that cause harmful immune reactions. Current therapeutic strategies focus on systemic immunosuppression which inhibits the immune system's capacity to react against infectious agents leaving patients severely immunocompromised. Since mechanisms that contribute to loss of tolerance are diverse and remain mostly unknown, the development of specific therapies is currently limited. Observations of impaired Treg frequency or function in autoimmune diseases such as multiple sclerosis (MS) [136-140], rheumatoid arthritis (RA) [141, 142] or systemic lupus erythematosus (SLE) [143-147] suggest a contribution of the Treg compartment to the development of inflammatory immune

pathologies. Furthermore, amelioration of inflammation by *in vivo* Treg expansion [148-152] or adoptive transfer [153] show the potency of Tregs for the treatment of inflammatory diseases. Therefore, Tregs emerge as promising therapeutic target to restore tolerance in patients that suffer from inflammatory immune pathologies.

1.3.1 Clinical Treg isolation

Therapeutic Tregs can contribute to the specific treatment of various immune pathologies. In addition to targeting Tregs *in vivo* [148-152], adoptive transfer of *in vitro* generated Tregs aims to increase Treg frequencies to restore tolerance. To this end, autologous Tregs are isolated from peripheral blood *ex vivo* followed by *in vitro* expansion to generate sufficient numbers before they are re-infused into the patient (Figure 3). Feasibility of using endogenous Treg populations to suppress immune reactions has been shown in different animal models for e.g. GvHD [154-158], MS [159], colitis [160], T1D [161] or arthritis [162, 163]. Furthermore, human Tregs have been shown to suppress transplant arteriosclerosis [164] as well as human skin [165-167] and islet [168] allograft rejection in humanized mouse models. However, unambiguous identification of Tregs remains a major challenge and also Treg plasticity has been observed questioning long-term stability of the Treg lineage (see 1.2.1.1). For clinical applications, stability of *in vitro* expanded Tregs needs to be ensured, but also long-term stability *in vivo* is required to prevent their differentiation into potentially pathogenic effector cells. However, to date little is known about Treg lineage stability which is mostly limited by the inability to unambiguously identify tTregs [36, 37]. Taken together, impurities of *in vitro* generated Tregs but also potential instability of Tregs *in vivo* raise significant safety concerns and represent a major obstacle for clinical use of Tregs [169, 170].

Clinical transfer of polyclonal Tregs, either *ex vivo* [171, 172] or following *in vitro* expansion [173-182], has been shown to be safe and effective in patients as treatment for GvHD and T1D. Furthermore, cord blood-derived $CD25^+$ Tregs, consisting mainly of naive Tregs, were successfully expanded *in vitro* and have proven safety and efficacy in allogeneic umbilical cord blood transplantation [174, 178, 179]. Alternatively, expanded $CD25^+CD127^-$ Tregs that were purified by fluorescence-activated cell sorting (FACS) have been used in autologous settings for the treatment of autoimmunity [173, 176, 177]. However, FACS sorting is still not routinely applicable under GMP-compatible conditions and even expansion of FACS sorted $CD25^+CD127^-$ Tregs fails to eliminate non-Treg contaminations [183, 184]. Currently, clinical Treg isolation

protocols are largely based on the magnetic separation of CD25-expressing T cells [171-174, 178, 179, 182, 185-188]. Although this enriches FoxP3$^+$ Tregs *ex vivo*, purity is highly variable and depends on the composition of the starting material, e.g. cord blood, adult peripheral blood or leukapheresis. Furthermore, also non-Tregs can acquire a CD25$^+$CD127$^-$ phenotype *in vivo* or upon *in vitro* culture including upregulation of FoxP3 without acquisition of regulatory functions (see 1.2.1.2). Collectively, the inability to clearly identify lineage stable Tregs compromises purity of *in vitro* generated Tregs and generates significant safety concerns for adoptive Treg transfer. More recently, converse expression of activation-induced CD137 and CD154 expression was shown to distinguish between CD137$^+$ Tregs and CD154$^+$ Tcons *ex vivo* enabling enrichment of antigen-specific Tregs that exhibited a stable Treg signature including TSDR demethylation and a Treg-specific expression profile [92, 96, 97, 106, 107]. Furthermore, following polyclonal stimulation of Tregs it was shown that exclusion of cells co-expressing CD137 and CD154 enabled enrichment of stable CD137$^+$ Tregs *ex vivo* [107]. However, applicability of this marker combination for optimization of stability of therapeutic Tregs remains elusive but could strongly improve current protocols. Collectively, the great potential of Tregs to mediate immunosuppression in various inflammatory immune pathologies has been shown, yet successful Treg therapy requires the optimization of Treg isolation and expansion protocols to improve purity and stability of therapeutic Tregs [170].

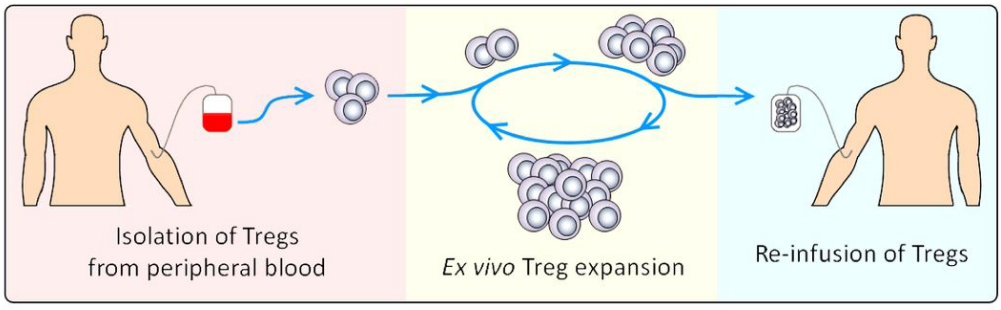

Figure 3: Schematic diagram of adoptive Treg transfer. For adoptive transfer, Tregs are isolated from the peripheral blood of patients, expanded *in vitro* and re-infused back into the patient (figure modified from [189]).

1.3.2 Generation of antigen-specific Tregs

For therapeutic Treg transfer, large numbers are currently required in spite of their high suppressive potential. Since only low numbers can be isolated from the peripheral blood, extensive *in vitro* expansion is needed which compromises Treg purity (see

1.3.1). Therefore, increasing the potency of clinical Tregs can significantly reduce required numbers and consequently augment efficacy and safety of Treg therapy. It has been shown that endogenous antigen-specific Tregs reactive against disease-relevant antigens are of higher potency than polyclonal populations in murine models for e.g. T1D [161] or GvHD [154-158, 166, 167] and therefore much lower cell numbers were required to mediate potent immunosuppression. Furthermore, protocols for *in vitro* generation of human alloantigen-specific Tregs have been developed [167, 190-192]. Yet, application of antigen-specific Tregs for adoptive transfer is currently limited by lack of knowledge about disease-relevant Treg targets and technological difficulties that are currently limiting the large-scale isolation and expansion of antigen-specific Tregs. Therefore, novel approaches, including genetic engineering of Tregs to introduce defined specificities are currently evaluated to improve efficacy of adoptive Treg transfer.

1.3.2.1 TCR gene transfer

T cell specificity is mediated by expression of a defined TCR that consists of an α and β chain (Figure 4A, see also 1.1.2). However, cells that express a particular TCR are extremely rare and therefore TCR gene transfer aims to introduce defined specificities into a large number of T cells by genetic engineering. For therapeutic applications, TCRs that recognize disease-relevant antigens can be isolated to generate an expression construct which can be integrated into donor T cells [193]. This approach enables the introduction of a defined specificity into a large number of T cells which has successfully been implemented into the clinic for the treatment of cancer [194-199]. Furthermore, in animal models for e.g. experimental autoimmune encephalomyelitis (EAE) [79, 200], GvHD [201, 202], T1D [203-205] and arthritis [206, 207], Tregs with transgenic TCRs have been shown to ameliorate inflammation and also human antigen-specific Tregs have been generated by TCR gene transfer *in vitro* [208-210]. These findings highlight the potential of genetically modified T cells to mediate antigen-specific immune responses which can be used for the redirection of Treg specificity toward defined antigens for targeted immunosuppression.

In spite of their therapeutic potential, the identification and isolation of endogenous antigen-specific T cells remains a major challenge and especially the identification of disease-relevant Treg-derived TCRs is currently limited. Furthermore, mispairing of endogenous αβ chains with transgenic αβ chains can generate novel, potentially harmful specificities that can result in harmful off-target activation of transgenic T cells.

In addition, TCRs bind antigens in an MHC-dependent manner which requires the generation of different TCRs for individual patients or at least patient groups. Consequently, clinical application of TCR therapy is currently limited by multiple challenges and therefore novel strategies are needed to improve the safety and efficacy of genetically modified T cells with a redirected specificity.

1.3.2.2 Chimeric antigen receptors

Chimeric antigen receptors (CARs) emerge as promising alternative for the generation of antigen-specific T cells. Other than TCRs, CARs are artificial receptors that contain an antibody-type specificity that can bind surface antigens independent of MHC (Figure 4B). The specific recognition of particular antigens by CAR-T cells is mediated by antibody-derived single chain variable fragments (scFv) with an extracellular spacer domain that are coupled via a transmembrane region to an intracellular TCR-derived signaling domain [211, 212]. This enables MHC-independent binding of surface antigens resulting in T cell activation by TCR-derived intracellular signaling domains. The potential of chimeric receptors to mediate antitumor activity in mice has already been described many years ago [213-217]. Yet, promising clinical results were only obtained recently in the treatment of hematological malignancies targeting $CD19^+$ B cells [218-220]. In spite of their efficacy in the treatment of hematological malignancies, many challenges remain (e.g. targeting solid tumors, toxic side effects, on-target-off-tumor activity), but novel strategies are aiming to increase safety and efficacy of CAR-T cells not only for cancer [221], but also to treat chronic immune pathologies such as HIV [222-224] or fungal infections [225].

In addition, CARs emerge as novel strategy for the *in vitro* generation of antigen-specific Tregs that have the potential to mediate tolerance in inflammatory immune pathologies. Since disease-relevant TCRs for Treg activation are mostly unknown, CARs emerge as promising technology to redirect Treg specificity toward a large variety of surface antigens. In murine models, redirected CAR-Tregs reactive against myelin basic protein were able to ameliorate EAE [226] and also CAR-Tregs specific for 2,4,6-trinitrophenol (TNP) or carcinoembryonic antigen (CEA) were successfully redirected to the colon where they were highly potent in suppressing colitis and development of its associated colorectal cancer [227-229]. More recently, human CAR-Tregs were redirected toward HLA-A2 as commonly mismatched antigen in transplantation and have been shown to suppress xenogeneic GvHD [230-232]. Furthermore, it has been demonstrated that CAR-Tregs have the potential to

ameliorate allergic airway inflammation [233] and to prevent neutralizing immune responses against Factor VIII in mice [234]. Together these findings highlight the wide-ranging potential of CAR-Tregs to mediate antigen-specific tolerance in different immune pathologies. However, the identification of disease-relevant target antigens as prerequisite for the *in vitro* generation of antigen-specific Tregs remains a major challenge and is currently limiting CAR-Treg application for different immune pathologies. Nevertheless, Tregs emerge as a promising target to harness the immune system's potential to regulate immune reactions which can contribute to the specific treatment of chronic inflammation and autoimmune disease.

In conclusion, the potential of Tregs to mediate tolerance is well-established and currently emerging as promising therapeutic approach for the treatment of chronic inflammation and autoimmune disease. Nevertheless, little is known about the heterogeneity, stability and specificity of the peripheral Treg compartment in humans which not only generates significant safety concerns for adoptive transfer, but also questions inherent stability of the Treg lineage and its contribution to regulatory immune responses.

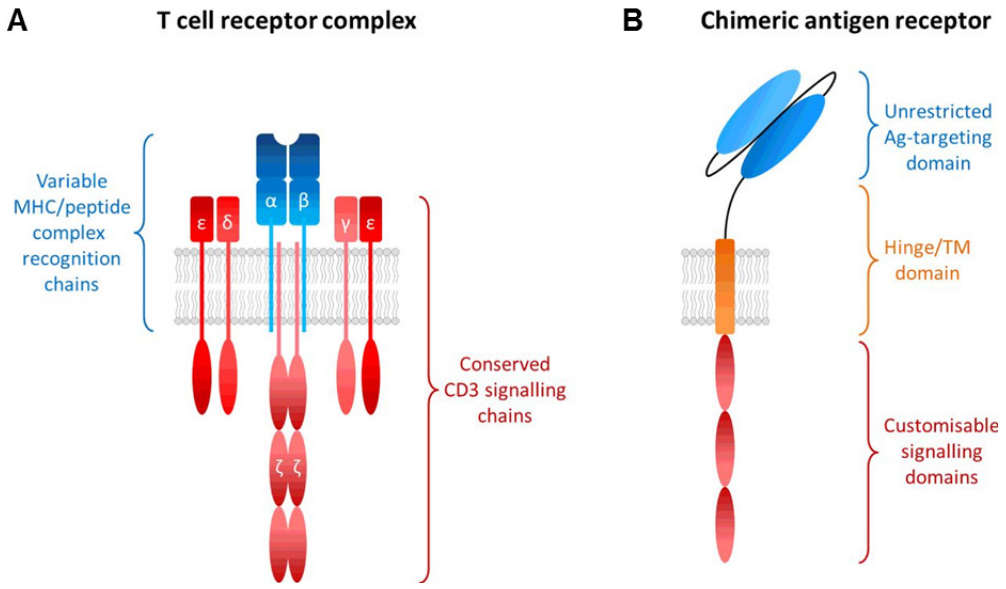

Figure 4: Schematic diagram of receptors for the redirection of T cell specificity. (A) T cell receptor complexes consist of an αβ heterodimer that binds peptides presented on MHC complexes; T cell activation is mediated by the ζ chain and TCR-associated proteins (CD3ε,δ,γ). **(B)** Chimeric antigen receptors consist of an antibody-derived antigen-binding moiety that is coupled to intracellular signaling domains via a flexible hinge and transmembrane domain (figure modified from [189]).

2 Aim

The immunosuppressive potential of regulatory T cells (Treg) is currently evaluated for the treatment of chronic inflammation and autoimmune disease. Yet, to date their clinical application is still limited as little is known about the stability and specificity of the human Treg compartment. Therefore, this study aimed to optimize efficacy and safety of *in vitro* generated Tregs as well as to provide insight into the heterogeneity and stability of the physiological Treg compartment in humans.

In this study, novel markers for the identification and isolation of stable Tregs were to be identified as *in vitro* modification and expansion severely compromise Treg purity and there are currently no markers for the unambiguous identification of Tregs and conventional T cells (Tcons) *ex vivo* or after prior expansion. CD137 and CD154 expression have recently been shown to distinguish between antigen-activated Tregs and Tcons *ex vivo*. Whether this Treg signature is also maintained after *in vitro* activation and expansion and still allows discrimination of stable from instable Tregs or effector T cells is not known but would strongly improve current possibilities for the generation of therapeutic Treg. Furthermore, the unambiguous identification of stable antigen-activated Tregs was to enable comprehensive analysis of the stability of the physiological Treg compartment in humans *in vitro* and *in vivo* as well as in response to specific antigens. Collectively, these findings can provide insight into the currently unknown contribution of heterogeneity and plasticity to the human Treg compartment.

Secondly, this study aimed to improve efficacy of *in vitro* generated Tregs by optimizing their antigen-specificity. In spite of the heightened suppressive potential of antigen-specific Tregs, lack of knowledge about disease-relevant target antigens has prevented the identification and isolation of highly potent antigen-specific Tregs for the treatment of inflammatory immune pathologies. Therefore, chimeric antigen receptors (CARs) are currently investigated to redirect Treg specificity toward defined antigens. In this study, Treg specificity was to be redirected toward an exogenous antigen to provide a system for targeted Treg activation that is dependent on antigen application. Furthermore, the identification of Treg-specific activation markers was to provide insight into specific requirements of *in vitro* Treg activation for augmented CAR-Treg functionality.

Taken together, these data can provide novel tools for the optimization of Treg efficacy and safety in a clinical environment as well as improve understanding of the composition of the physiological Treg compartment that is essential for the maintenance of tolerance.

3 Material and Methods

3.1 Material

3.1.1 Reagents and kits

Table 1: Reagents

Reagent	Source
1,4-Dithiothreitol (DTT)	Sigma-Aldrich, Schnelldorf
2-Propanol (ROTISOLV® ≥ 99,95%)	Carl Roth, Karlsruhe
2X Reaction Mix (CellsDirect™)	Thermo Fisher Scientific, Schwerte
3,5-bistrifluoromethyl pyrazole (BTP1)	In house [235]
4',6-diamidino-2-phenylindol (DAPI)	Sigma-Aldrich, Schnelldorf
Acetic acid (96%)	Carl Roth, Karlsruhe
Adenosine triphosphate (ATP)	New England Biolabs, Frankfurt a.M.
Agencourt Ampure XP beads	Beckman Coulter, Krefeld
AluI (10U/µl)	New England Biolabs, Frankfurt a.M.
Anti-Biotin MacsiBeads	Miltenyi Biotec, Bergisch Gladbach
Anti-CD62L microbeads, mouse	Miltenyi Biotec, Bergisch Gladbach
Anti-CD90.2 microbeads, mouse	Miltenyi Biotec, Bergisch Gladbach
Brefeldin A	Sigma-Aldrich, Schnelldorf
Candida albicans (lysate)	Greer Laboratories, Lenoir, NC, USA
Collagenase NB 8 Broad Range from C*lostridium histolyticum*	Serva Electrophoresis GmbH, Heidelberg
Cytomegalovirus (lysate)	Siemens Healthcare Diagnostics, Erlangen, Germany
D+ Glucose	Merck, Darmstadt
D+ Maltose Monohydrate	Sigma-Aldrich, Schnelldorf
Deoxyribunucleotides (dATP, dCTP, dGTP, dTTP)	Solis BioDyne, Tartu, Estonia
Dextran 500 (MW: 500,000)	Carl Roth, Karlsruhe
Dextrin	Sigma-Aldrich, Schnelldorf
Dimethylsulfoxid (DMSO)	Sigma-Aldrich, Schnelldorf
DNase I from bovine pancreas	Sigma-Aldrich, Schnelldorf
Escherichia coli (lysate)	ATCC, LGC Standards GmbH, Wesel, Germany
Ethanol (≥99,5%, 96%)	Carl Roth, Karlsruhe
FastStart Universal Probe Master (ROX)	Roche Diagnostics, Mannheim
Fc receptor (FcR) Blocking Reagent, human	Miltenyi Biotec, Bergisch Gladbach
Ficoll-Paque™ PLUS (1,078g/ml)	GE Healthcare Life Sciences, Freiburg

Table 1 (continued): Reagents

Reagent	Source
FITC-Dextran 2000 (MW: 2,000,000)	Sigma-Aldrich, Schnelldorf
Formaldehyde	Carl Roth, Karlsruhe
Hot FirePol® DNA Polymerase (5U/µl)	Solis BioDyne, Tartu, Estonia
HotStar PCR Buffer (10x)	Qiagen, Hilden
HotStar Taq™ DNA Polymerase (5U/µl)	Qiagen, Hilden
Ionomycin	Sigma-Aldrich, Schnelldorf
Klenow Fragment (5U/µl)	New England Biolabs, Frankfurt a.M.
Lamda DNA	NEB, Frankfurt a.M.
PCR Buffer BD (10x)	Solis BioDyne, Tartu, Estonia
Pefabloc	Sigma-Aldrich, Schnelldorf
Percoll	GE Healthcare Life Sciences, Freiburg
Phorbol-12-myristat-13-acetat (PMA)	Sigma-Aldrich, Schnelldorf
Propidium iodide	Sigma-Aldrich, Schnelldorf
Protaminsulfate (from salmon)	Sigma-Aldrich, Schnelldorf
Proteinase K (20mg/ml)	Sigma-Aldrich, Schnelldorf
Retronectin	Takara Bio via Clontech Laboratories, Saint-Germain-en-Laye, France
SUPERnase In™ RNase Inhibitor	Thermo Fisher Scientific, Schwerte
SuperScript® III RT/Platinum® Taq Mix	Thermo Fisher Scientific, Schwerte
SYBR® Green PCR Master Mix	Thermo Fisher Scientific, Schwerte
T4 DNA Ligase	New England Biolabs, Frankfurt a.M.
TaqMan™ Universla PCR Master Mix	Thermo Fisher Scientific, Schwerte
Tris	Carl Roth, Karlsruhe
Triton X-100	Sigma-Aldrich, Schnelldorf
Trypan blue	Biochrom, Berlin
twin.tec® 96 well plates	Eppendorf, Hamburg

Table 2: Cell separation reagents and kits

Reagent	Source
AllPrep® DNA/RNA Micro Kit	Qiagen, Hilden
AllPrep® DNA/RNA Mini Kit	Qiagen, Hilden
Anti-Biotin microbeads	Miltenyi Biotec, Bergisch Gladbach
Anti-CD25 microbeads II, human	Miltenyi Biotec, Bergisch Gladbach
Anti-CD3 microbeads, human	Miltenyi Biotec, Bergisch Gladbach
Anti-CD4 microbeads, human	Miltenyi Biotec, Bergisch Gladbach
Anti-PE microbeads	Miltenyi Biotec, Bergisch Gladbach
C1™ Single-Cell Auto Prep Array IFC (5-10µm)	Fluidigm, South San Francisco, CA, USA
C1™ Single-Cell Auto Prep Reagent Kit	Fluidigm, South San Francisco, CA, USA
CellTrace™ Violet Cell Proliferation Kit	Thermo Fisher Scientific, Schwerte
EpiTect Bisulfite Kit	Qiagen, Hilden
EZ DNA Methylation Kit Gold	Zymo Research, Freiburg
FoxP3 staining buffer set	Miltenyi Biotec, Bergisch Gladbach
FoxP3 staining buffer set	ebioscience, Frankfurt a.M.
GE 48.48 Dynamic Array™ Sample and Assay Loading Reagent Kit IFC	Fluidigm, South San Francisco, CA, USA
Gel/PCR DNA Fragments Extraction Kit	Geneaid, New Taipei City, Taiwan
Inside Stain Kit	Miltenyi Biotec, Bergisch Gladbach
MiSeq Reagent Kit v3	Illumina, Inc., San Diego, USA
QIAamp® DNA Blood Mini Kit	Qiagen, Hilden
Qubit™ ds DNA HS Assay Kit	Thermo Fisher Scientific, Schwerte
Quick-DNA™ Miniprep Kit	Zymo Research, Freiburg
Rneasy Mini Kit	Qiagen, Hilden
Single Cell-to-CT™ Kit	Thermo Fisher Scientific, Schwerte
Treg expansion kit	Miltenyi Biotec, Bergisch Gladbach
Treg suppression inspector, human	Miltenyi Biotec, Bergisch Gladbach

3.1.2 Buffers and media

Table 3: Buffers for cell isolation, transfection and fluorescent labeling

2x HBS Buffer		
136,89mM	NaCl	Carl Roth, Karlsruhe
4,96mM	KCl	Carl Roth, Karlsruhe
1,76mM	Na_2HPO_4	Carl Roth, Karlsruhe
20,98mM	HEPES	Carl Roth, Karlsruhe
	in ddH_2O (pH = 6,75 – 6,76)	
Calcium Loading Buffer		
1mM	$CaCl_2$ x 2 H_2O	Carl Roth, Karlsruhe
1mM	$MgCl_2$	Carl Roth, Karlsruhe
20mM	HEPES	Carl Roth, Karlsruhe
	in PBS/BSA	
Colon Washing Buffer		
100U/ml	Gibco® penicillin/	Thermo Fisher Scientific, Schwerte
100µg/ml	streptomycin	Thermo Fisher Scientific, Schwerte
0.25µg/ml	Amphotericin B	Sigma-Aldrich, Schnelldorf
10µg/ml	Gentamicin	Sigma-Aldrich, Schnelldorf
	in Gibco® Hank's Balanced Salt Solution (HBSS)	Thermo Fisher Scientific, Schwerte
Phosphate-buffered saline (PBS)		
137mM	NaCl,	Carl Roth, Karlsruhe
2.7mM	KCl	Carl Roth, Karlsruhe
1.5mM	KH_2PO_4	Carl Roth, Karlsruhe
8.9 mM	Na_2HPO_4 x 2 H_2O	Carl Roth, Karlsruhe
	in ddH_2O (pH = 7,2)	
PBS/BSA		
0.5%	BSA	Sigma-Aldrich, Schnelldorf
	in PBS	
PBS/BSA/EDTA		
0.5%	BSA	Sigma-Aldrich, Schnelldorf
2mM	EDTA	Promega, Mannheim
	in PBS	

Table 4: Cell culture media

Treg expansion medium		
100U/ml	IL-2 (GMP-grade)	Miltenyi Biotec, Bergisch Gladbach
100U/ml	Gibco® penicillin/	Thermo Fisher Scientific, Schwerte
100µg/ml	streptomycin	Thermo Fisher Scientific, Schwerte
5% (v/v)	Human serum from male AB plasma	Sigma-Aldrich, Schnelldorf
100nmol	Rapamycin (GMP-grade)	Miltenyi Biotec, Bergisch Gladbach
	in TexMACS™	Miltenyi Biotec, Bergisch Gladbach
Tcon expansion medium		
200U/ml	IL-2 (Proleukin®)	Novartis, Nürnberg
100U/ml	Gibco® penicillin/	Thermo Fisher Scientific, Schwerte
100µg/ml	streptomycin	Thermo Fisher Scientific, Schwerte
5% (v/v)	Human serum from male AB plasma	Sigma-Aldrich, Schnelldorf
	in TexMACS™	Miltenyi Biotec, Bergisch Gladbach
T cell resting medium		
100U/ml	Gibco® penicillin/	Thermo Fisher Scientific, Schwerte
100µg/ml	streptomycin	Thermo Fisher Scientific, Schwerte
5% (v/v)	Human serum from male AB plasma	Sigma-Aldrich, Schnelldorf
	in Gibco® Roswell Park Memorial Institute Medium (RPMI) 1640	Thermo Fisher Scientific, Schwerte
Treg cloning medium		
100U/ml	IL-2 (GMP-grade)	Miltenyi Biotec, Bergisch Gladbach
100U/ml	Gibco® penicillin/	Thermo Fisher Scientific, Schwerte
100µg/ml	streptomycin	Thermo Fisher Scientific, Schwerte
10% (v/v)	Human serum from male AB plasma	Sigma-Aldrich, Schnelldorf
100nmol	Rapamycin (GMP-grade)	Miltenyi Biotec, Bergisch Gladbach
20µM	2-Mercaptoethanol	Thermo Fisher Scientific, Schwerte
1µg/ml	anti-CD28 antibodies	Miltenyi Biotec, Bergisch Gladbach
	in TexMACS™	Miltenyi Biotec, Bergisch Gladbach
Tcon cloning medium		
200U/ml	IL-2 (Proleukin®)	Novartis, Nürnberg
100U/ml	Gibco® penicillin/	Thermo Fisher Scientific, Schwerte
100µg/ml	streptomycin	Thermo Fisher Scientific, Schwerte
10% (v/v)	Human serum from male AB plasma	Sigma-Aldrich, Schnelldorf
20µM	2-Mercaptoethanol	Thermo Fisher Scientific, Schwerte
	in TexMACS™	Miltenyi Biotec, Bergisch Gladbach

Table 4 (continued): Cell culture media

Complete DMEM		
10%	Fetal Calf Serum (FCS)	Biowest, Nuaillé, France
100U/ml	Gibco® penicillin/	Thermo Fisher Scientific, Schwerte
100µg/ml	streptomycin	Thermo Fisher Scientific, Schwerte
50µM	2-Mercaptoethanol	Thermo Fisher Scientific, Schwerte
	in Gibco® Dulbecco's Modified Eagle Medium (DMEM)	Thermo Fisher Scientific, Schwerte

3.1.3 Equipment and software

Table 5: Equipment

Equipment	Source
ABI 7500 Cycler	Thermo Fisher Scientific, Schwerte
Amnis® ImageStream X Mark II	Merck, Darmstadt
Cell Sorter, FACSAria™	BD, Heidelberg
Cell Sorter, FACSAria™ II	BD, Heidelberg
Cell Sorter, Influx™	BD, Heidelberg
Flow Cytometer, FACSCanto™	BD, Heidelberg
Flow Cytometer, LSR II	BD, Heidelberg
Flow Cytometer, MACSQuant	Miltenyi Biotech, Bergisch Gladbach
Gammacell® 40 Exactor	Best Theratronics, Kanata, ON, Canada
MACS® manual separators	Miltenyi Biotech, Bergisch Gladbach
StepOnePlus™ Real-Time PCR System	Thermo Fischer Scientific, Schwerte

Table 6: Software

Software	Source
FlowJo X 10.0.7	TreeStar, Inc, Ashland, OR, USA
GraphPad Prism	GraphPad Software Inc., La Jolla, CA, USA
IDEAS® software v6.1	Merck, Darmstadt
INSPIRE® software	Merck, Darmstadt
MACSQuantify™	Miltenyi Biotech, Bergisch Gladbach
RStudio v0.98.501	RStudio Inc., Boston, MA, USA
SINGuLAR™ Analysis Toolset R package	Fluidigm, South San Francisco, CA, USA
StepOne Software v2.3	Thermo Fischer Scientific, Schwerte

3.1.4 Primers and gene expression assays

Bisulfite specific primers for epigenetic analysis (see 3.3.8.2) were designed by the group of Prof. Dr. J. Walter at the Saarland University and obtained from biomers.net; sequences are listed in Table 7. Primer pairs that are marked with an asterisk (*) were used for the generation of hairpin constructs for hairpin bisulfite PCR (see 3.3.8.2). Primers for the detection of CAR constructs (see 3.3.9.3) were designed by D. Lock at Miltenyi Biotech and were obtained from TIBMolbiol; sequences are shown in Table 8. Gene expression assays for high-throughput qPCR (see 3.3.9.1 and 3.3.9.2) are listed in Table 9 and were obtained from Thermo Fisher Scientific.

Table 7: Bisulfite-specific primers

Target	Amplicon location (Human GRCh37/hg19)	Primer sequence (5' → 3')	
		Forward	Reverse
ctla4	chr2:204700499-204700960(+)	GTAGTTGTATGTATTTATTTATTTAAATTTT	CCTTTAATACAAACCAATCTATC
foxp3 promoter	chrX:49121125-49121322(+)	TGGTGAAGTGGATTGATAGAAAAGG	TATAAAAACCCCCCCCCACC
		GGATTATTAGAAGAGAGAGGTTTG*	CTACTCTCCCCTACCAAATATAAA*
foxp3 enhancer	chrX:49116207-49116607(+)	ATATAGAAGGGGATGTTTAGATGT	AATACTCTCCCAAACCCTTATTC
		TATTATATAGAAGGGGATGTTTAGATGT*	CCCCATTATACAAAAAAAAATACT*
foxp3 TSDR	chrX:49117051-49117387(+)	TGTTTGGGGGTAGAGGATTT	TATCACCCCACCTAAACCAA
		TAAGTTTGTTGTAGGATAGGGTAGTTAG*	ATAAAATATCTACCCTCTTCTCTTCCTC*
ikzf2	chr2:213988928-213989329(+)	TATGGGTGTATGTTTTTGTGTGT	CATTACATAACATATCCACTTATAC
il2ra	chr10:6079456-6079933(+)	TATTTGTATTTAGTGAAGATTAGAATAA	CTTCTAATTTAAATTTCCCAAAAAAAC
lrrc32	chr11:76379042-76379386(+)	TTTTTAGTGAGTATAGTATTAAGTTTTT	CTATAATCAAAACCAAAATTAAAATAAC
cd40lg	chrX:135739037-135739484(+)	ATTTTGTAAAGATTAATAGGTTTTAAGA	CATAATAATAATAACTATCCATATATTAC
tnfrsf9	chr1:8000840-8001383(+)	TAGATTTTGAGATTTTAGGGTTG	TCATACCAAATTCTAAAATTCTTTC
A-tailing hairpin linker		GGGCCCATDDDDDDDDATGGGCCCT*	

Table 8: Primers for the detection of Dextran-CAR constructs

Construct	Primer location	Primer sequence (5' → 3')
CD137-CD3ζ	CD137 fwd CD137 rev	CTTCCCGGAGGAAGAAGAGG CAAGGTTCAGCTCGTTGTAG
w/o-CD3ζ	CD3ζ fwd CD3ζ rev	TGTACTGCCTGCAGCGAGTC TATCCAGCACGTCGTATTCC
ICOS-CD3ζ	ICOS fwd CD3ζ rev	CTGACCGATGTGACACTGAG TATCCAGCACGTCGTATTCC
CD28-CD3ζ	CD28 fwd CD28 rev	CTGTACTGCCTGCAGAGAAG GGTGCGTATGGCTGGTAATG
CD134-CD3ζ	OX40 fwd CD3ζ rev	CTGGCCAAGATCAGTACTCG TATCCAGCACGTCGTATTCC
Housekeeping	GAPDH fwd GAPDH rev	AGGGCTGCTTTTAACTCTGGT CTCCTCCCACACCAGCTTTG

Table 9: Gene expression assays

Target	Taqman® Gene Expression Assay ID
b2m	Hs00187842_m1
bach2	Hs00222364_m1
bcl2	Hs00608023_m1
bcl6	Hs00153368_m1
ccr8	Hs00174764_m1
cd40lg	Hs00163934_m1
csf2	Hs00929873_m1
ctla4	Hs03044418_m1
cxcr6	Hs00174843_m1
fas	Hs00907755_m1
fcrl3	Hs00901693_m1
foxp3	Hs00203958_m1/Hs01085834_m1
gapdh	Hs99999905_m1
gata3	Hs00231122_m1/Hs00922328_m1
gzmb	Hs04261345_m1
havcr2	Hs00958623_m1
icos	Hs04261471_m1
ifnγ	Hs00989291_m1
ikzf2	Hs00212361_m1
ikzf4	Hs00223842_m1/Hs01042455_m1
il10	Hs00961622_m1
il17a	Hs00174383_m1

Table 9 (continued): Gene expression assays

Target	Taqman® Gene Expression Assay ID
il1r2	Hs01030384_m1
il2	Hs00174114_m1
il21	Hs00222327_m1
il22	Hs01574154_m1
il2ra	Hs00907779_m1
il32	Hs00992441_m1
il7r	Hs00902334_m1/Hs00904815_m1
lrrc32	Hs00194136_m1
maf	Hs04185012_s1/Hs00193519_m1
nfatc2	Hs00905452_m1
pdcd1	Hs01550088_m1
prdm1	Hs01068503_m1
rorc	Hs01076122_m1
tgfβ1	Hs00998133_m1
tigit	Hs00545087_m1
tnf	Hs01113624_g1/Hs99999043_m1
tnfrsf18	Hs00188346_m1
tnfrsf4	Hs00533968_m1
tnfrsf9	Hs00155512_m1
ArrayControl™ RNA Spikes	-

3.2 Methods

3.2.1 T cell isolation and expansion

Leukapheresis products from healthy donors were obtained from the Charité University hospital in Berlin with informed consent according to ethical guidelines. Leukapheresis filters were reconstituted with PBS/EDTA, layered onto Ficoll-Paque and centrifuged for 35min at 445g at room temperature. The interphase was carefully removed and washed twice with PBS/EDTA (300g, 15min and 200g, 10min at 4°C). PBMCs were counted using trypan blue with 3% acetic acid to exclude dead cells and erythrocytes. T cells were isolated from PBMCs by magnetic activated cell sorting (MACS, Miltenyi Biotec, Bergisch Gladbach) using magnetic particles coupled to antibodies (microbeads). PBMCs were labeled with anti-CD25 or anti-CD4 microbeads for 15min at 4°C. Cells were washed and $CD25^+$ or $CD4^+$ cells were enriched using columns composed of ferromagnetic spheres within a magnetic field. For expansion, $CD25^+$ Tregs were cultured in Treg expansion medium (Table 4) in the presence of Treg expansion beads (4:1 bead-to-cell ratio) and fresh medium was added every 2-3 days. Before 6h restimulation, $CD25^+$ Tregs were rested for 1-4 days in T cell resting medium (Table 4) without magnetic particles before activation with Treg expansion beads (4:1 bead-to-cell ratio) or 10ng/ml PMA and 500ng/ml Ionomycin. To block potential downregulation of CD154 upon ligation, 1µg/ml anti-CD40 antibodies were added during 6h activation when CD154 was stained on the surface.

3.2.2 Isolation of cells from human tissue

Human tissue was obtained from patients who underwent surgery and gave informed consent according to ethical guidelines (EA1/233/09, EA1/008/16, EA1/266/12, EA1/290/13, EA1/094/15). Cells from tissue were obtained by mechanical (tonsil, thymus, lung) and/or enzymatic (colon) disruption of the tissue. For stimulation, either total lymphocytes (tonsil, thymus) or CD4-enriched T cells (lung, colon) were rested overnight in T cell resting medium (Table 4) before 6h restimulation with 10ng/ml PMA and 500ng/ml Ionomycin in the presence of 1µg/ml anti-CD40 antibodies.

Tonsil samples were obtained from patients who underwent tonsillectomy and the tissue was cut into small pieces in PBS/EDTA. Homogenized tissue was passed through a 100µm cell strainer, layered onto Ficoll-Paque and centrifuged for 35min at 445g. The interphase was carefully removed and washed twice with PBS/EDTA (300g,

15min and 200g, 10min at 4°C). Cells were counted and cultured overnight before stimulation. Thymic tissue was obtained from patients who underwent cardiac surgery and samples were mechanically processed by the group of Prof. Dr. I.-K. Na who provided stroma cell-depleted cell lysates that were rested overnight before stimulation. Colon samples were kindly provided by Prof. Dr. D. Baumgart and D. Metzke from the Charité University hospital in Berlin. Mucosal tissue was washed for 5min on a shaker in Colon Washing Buffer (Table 3). For tissue lysis, samples were incubated for 15min at 37°C in HBSS + 5mM DTT while shaking at 150rpm. Lysed tissue was vortexed for 15s before washing 2 x 5min in HBSS and 1 x 5min in RPMI + 10% FCS + 100U/ml penicillin, 100µg/ml streptomycin. The tissue was cut into small pieces and digested for 60-90min at 37°C in RPMI + 10% FCS + 100U/ml penicillin, 100µg/ml streptomycin supplemented with 1,5mg/ml collagenase NB 8 and 20µg/ml DNAse I at 170rpm. Digested tissue was passed through a metal strainer and a 100µm cell strainer before counting. T cells were isolated using CD4 microbeads as described above (see 3.3.1) and rested overnight before restimulation. Lung tissue was obtained from lung explants or biopsies and cut into small pieces in RPMI1640 medium. Homogenized tissue was passed through a 100µm cell strainer and centrifuged for 10min at 1000rpm at 4°C. Lymphocytes were obtained by Percoll gradient centrifugation at 1000g for 30min at RT. Percoll was diluted 10:1 with 10x PBS and cells were resuspended in 40% Percoll (diluted in RPMI1640) and layered onto 80% Percoll (diluted in RPMI1640). The interphase was carefully removed, filtered (100µm) and washed for 15min at 400g at 4°C. T cells were isolated using CD4 microbeads as described above (see 3.3.1) and rested overnight before restimulation.

3.2.3 Generation of T cell clones

Single cell naive clones ($CD4^+CD25^+CD127^-CD45RO^-CCR7^+CD45RA^+$) or 10 cells/well memory clones ($CD4^+CD25^+CD127^-CD45RO^+CD45RA^-$) were sorted from CD25-enriched Tregs into 96 well plates (round bottom) with 5 x 10^4 irradiated (30 Gy) autologous or allogeneic (pooled from 3 donors) feeder cells in 100µl Treg cloning medium (Table 4). Single cell CD137/CD154 Treg clones ($CD4^+CD25^+CD127^-$) were sorted likewise after *ex vivo* 6h stimulation with Treg expansion beads (4:1 bead-to-cell ratio). On day 1, beads at a 2:1 ratio (bead-to-feeder cell) were added. $CD4^+$ memory Tcon clones were generated by single cell sorting of $CD4^+CD25^-CD127^+CD45RO^+$ T cells into 96wp with 5 x 10^4 irradiated (30 Gy) autologous or allogeneic (pooled from 3 donors) feeder cells in 100µl Tcon cloning medium (Table 4) with 30ng/ml anti-CD3 and 1µg/ml anti-CD28 antibodies. On d7, 5 x 10^4 irradiated (30 Gy) allogeneic feeder

cells (pooled from 3 donors) were added in 100µl Treg or Tcon expansion medium (Table 4), respectively. After 2-3 weeks, yellow wells were transferred to 96 well plates (flat bottom) and clones were expanded before analysis after 4-5 weeks. During expansion, fresh Treg expansion medium or Tcon expansion medium (Table 4) were added every 2-3 days. Before restimulation, cells were rested for 2 days in T cell resting medium (Table 4) before stimulation with 10ng/ml PMA and 500ng/ml Ionomycin for intracellular cytokine staining. FoxP3 staining was performed in unstimulated clones that were obtained directly from the culture. Cloning efficiencies were 22.14% (± 8.13% SD) for naive Tregs, 10.07 % (± 10.28% SD) for memory Tregs, 18.23% (± 8.10% SD) for $CD137^+CD154^-$ Tregs, 34.37% (± 8.90% SD) for $CD137^+CD154^+$ Tregs and 21.09 % (± 4.45% SD) for memory Tcons.

3.2.4 Antigen-reactive T cell enrichment (ARTE)

The identification of antigen-reactive T cells is based on the converse expression of CD137 and CD154 on Tregs and Tcons after 6h antigenic stimulation, respectively [106, 107]. CD137- and CD154-expressing cells were isolated by fluorescent labeling and subsequent magnetic enrichment as described in 3.2. To this end, 2-5 x 10^7 PBMC were cultured overnight in T cell resting medium before 6h stimulation with respective antigens (40µg/ml *E. coli*, 40µg/ml C. albicans, 10µg/ml CMV) in the presence of 1µg/ml anti-CD40 and 1µg/ml anti-CD28 pure antibodies. Cells were stained with CD154-Biotin and CD137-PE and magnetically enriched with anti-Biotin and anti-PE microbeads, surface staining of additional markers was performed on the column. CMV-reactive T cells were isolated from CMV seropositive donors.

3.2.5 *In vitro* Treg suppression assay

The *in vitro* suppressive capacity of Tregs was analysed by inhibition of proliferation of $CD4^+$ responder T cells (Tresps). Tregs and Tresps were distinguished by opposite HLA-A2 expression. Expanded Tregs were rested for 1-4 days in T cell resting medium (Table 4) without expansion beads before co-culture with Tresps. Tresps were isolated *ex vivo* and stained for 15min at 37°C in PBS with CellTrace™ Violet Cell Proliferation Kit at a final concentration of 2.5µM. Staining was blocked with FCS for 2min at RT and cells were washed twice with PBS. A total of 5 x 10^4 Tresps were co-cultured in different ratios with Tregs in 96 well flat bottom plates in T cell resting medium (Table 4) for 5-7 days. Proliferation of Tresps was assessed by dilution of CellTrace™ Violet

Cell Proliferation Dye. The percentage of inhibition was calculated as $\frac{(A-B)}{A} x\ 100$ where A: uninhibited Tresps and B: inhibited Tresps.

Treg suppression requires their activation and also Tresps need to be activated to proliferate. For polyclonal activation, Tregs and Tresps were activated by the same stimulus using anti-CD3/-CD28. To this end, Treg Suppression Inspector beads were added to the culture according to manufacturer's instructions. Analysis of the suppressive capacities of CAR-Tregs upon dextran-specific stimulation required independent activation of Tresps. Therefore, Tresps were activated by allogeneic stimulation using $CD4^+$ Tresps from 3 pooled donors. To this end, irradiated allogeneic APCs (CD3-depleted PBMCs, irradiated at 30Gy) were added to the co-culture at a 1:1 ratio. For activation of CAR-Tregs, bead-bound dextran (1:100) was added to the culture.

3.2.6 Genetic engineering of Tregs

Genetic engineering of Tregs was based on the stable integration of a transgene using lentiviral vectors. To this end, replication-deficient lentiviral particles containing the transgene were generated (see 3.3.6.1) and activated primary human T cells were infected (see 3.3.6.2) resulting in stable integration of the transgene into the host genome.

3.2.6.1 Production of lentiviral particles

Dextran-CAR constructs were generated and provided by Dr. A. Kaiser and D. Lock (Miltenyi Biotec, Bergisch Gladbach, Table 10). All CAR-constructs contained an AC146-derived scFv, a CD8 transmembrane domain and a P2A-linked ΔLNGFR for detection of transfected and transduced cells. Constructs that differed in their extracellular spacer contained a human IgG4 hinge (L, M, XS) or a human CD8 hinge (S) together with CD137-CD3ζ signaling (Table 10). Different signaling domains were coupled to ectodomains with an XS IgG4 hinge (Table 10).

Lentiviral supernatants were generated by co-transfection of HEK293T cells with the expression vector and packaging plasmids. The 2nd generation lentiviral packaging plasmids pCMVΔR8.74 and pMDG2.VSV-G were used for the packaging of lentiviral particles. One day prior to transfection, 3 x 10^6 HEK293T cells were seeded in a 10cm cell culture dish in complete DMEM (Table 4). Cells were transiently transfected with

0,84µg pMDG-2.VSV-G, 5,16µg pCMVΔR8.74 and 3,35µg Dextran-CAR plasmids diluted in ddH_2O supplemented with 2,5M $CaCl_2$. While aerating, 2ml of 2x HBS buffer (Table 3) were slowly added to the solution and 2ml of the transfection solution were added dropwise to the cells. The medium containing the transfection solution was removed after 4h and cells were washed twice with pre-warmed PBS before fresh complete DMEM was added. After 48 hours, lentiviral supernatants were harvested, filtered (0,45µm) and used directly or stored at -80°C for up to 6 months.

Table 10: Dextran-CAR constructs

Spacer domains				
Construct	Spacer	Co-stimulation	Signaling	Size (bp)
L	Hinge CH2-CH3 IgG4	CD137	CD3ζ	9339
M	Hinge CH3 IgG4	CD137	CD3ζ	9012
XS	Hinge IgG4	CD137	CD3ζ	8691
S	Hinge CD8	CD137	CD3ζ	8790
Signaling domains				
Construct	Spacer	Co-stimulation	Signaling	Size (bp)
w/o-CD3ζ	Hinge IgG4	-	CD3ζ	8568
ICOS-CD3ζ	Hinge IgG4	ICOS	CD3ζ	8688
CD28-CD3ζ	Hinge IgG4	CD28	CD3ζ	8697
CD137-CD3ζ	Hinge IgG4	CD137	CD3ζ	8691
CD134-CD3ζ	Hinge IgG4	CD134	CD3ζ	8700
PD1-CD3ζ	Hinge IgG4	PD-1	CD3ζ	8865
CD137-CD3ε	Hinge IgG4	CD137	CD3ε	8529
CD28-CD3ε	Hinge IgG4	CD28	CD3ε	8526

3.2.6.2 Lentiviral transduction of T cells

$CD25^+$ Tregs were activated in Treg expansion medium (Table 4) in the presence of Treg expansion beads at a bead-to-cell ratio of 4:1. $CD4^+$ Tcons were activated in Tcon expansion medium (Table 4) in the presence of 30ng/ml anti-CD3 and 1µg/ml anti-CD28. On d3, culture medium was replaced with the respective lentiviral supernatants supplemented with 4µg/ml protaminsulfate and cells were spinoculated on retronectin-coated 96 well plates for 90min at 800g and 32°C. After centrifugation, viral supernatant was removed and fresh culture medium was added to the cells. Transduction efficiency was assessed on d2 or d3 after transduction by staining of LNGFR on the cellular surface. For restimulation, magnetic particles were removed on

d7-d8 and expanded Tregs were rested for 1-4 days in T cell resting medium (Table 4). Tregs were activated with 10ng/ml PMA and 500ng/ml Ionomycin, Treg expansion beads (4:1 bead-to-cell ratio), bead-bound dextran (anti-mouse CD90.2/CD62L microbeads in PBS, 1:100), 2µg/ml soluble FITC-Dextran (MW 2 x 10^6), 1nMol D+ Glucose, 1nMol D+ Maltose, 2µg/ml Dextrin or 1nmol Dextran (MW 5 x 10^5) for 6h. For expansion, bead-bound dextran (1:100) or Treg expansion beads (4:1 bead-to-cell ratio) were added in Treg expansion medium (Table 4).

3.2.7 Flow-cytometry

For flow cytometric detection of extracellular and intracellular antigens, cells were stained with antibodies from Table 11 as described in 3.3.7.1 - 3.3.7.6. All data were acquired on a FACS Canto/LSRII or MACS Quant Analyzer, adsorption and emission of used fluorochromes are shown in Table 12. FlowJo vX.0.7 or MACSQuantify™ were used for data analysis.

Table 11: Antibodies

Antibodies for flow cytometric detection			
Specificity	Fluorochrome	Clone	Source
CD3, human	VioBlue®	BW264/56	Miltenyi Biotec, Bergisch Gladbach
CD4, human	PE-Vio770 APC-Vio770 VioGreen™ FITC VioBlue®	VIT4	Miltenyi Biotec, Bergisch Gladbach
CD8, human	APC-Vio770 PerCP VioGreen™	BW135/80	Miltenyi Biotec, Bergisch Gladbach
CD14, human	PerCP VioGreen™	TÜK4	Miltenyi Biotec, Bergisch Gladbach
CD20, human	VioGreen™ PerCP	LT20	Miltenyi Biotec, Bergisch Gladbach
CD25, human	BV421™	3G10	Biolegend, Koblenz
CD25, human	PE APC VioBright™ FITC	3G10	Miltenyi Biotec, Bergisch Gladbach

Table 11 (continued): Antibodies

Specificity	Fluorochrome	Clone	Source
CD69, human	FITC APC APC-Vio®770	FN50	Miltenyi Biotec, Bergisch Gladbach
CD127, human	FITC PE-Vio®770 PE	MB15-18C9	Miltenyi Biotec, Bergisch Gladbach
CD137, human	PE VioBright™FITC	4B4-1	Miltenyi Biotec, Bergisch Gladbach
CD154, human	APC VioBlue® Biotin	5C8	Miltenyi Biotec, Bergisch Gladbach
CD154, human	PECy7 APC	TRAP1	in house (DRFZ)
CD45RA, human	APC-Vio®770 APC VioGreen™	T6D11	Miltenyi Biotec, Bergisch Gladbach
CD45RO, human	PE-Vio®770 APC-Vio®770 PerCP	UCHL1	Miltenyi Biotec, Bergisch Gladbach
FoxP3, human/mouse	APC	3G3	Miltenyi Biotec, Bergisch Gladbach
FoxP3, human/mouse	PerCP	PCH101	ebioscience, Frankfurt a.M.
GARP, human	Alexa Fluor® 647	G14D9	Biolegend, Koblenz
Helios, human/mouse	PE FITC	22F6	Miltenyi Biotec, Bergisch Gladbach
HLA-A2, human	PE	REA517	Miltenyi Biotec, Bergisch Gladbach
IFN-γ, human	PerCP-Cy5.5	4S.B3	Biolegend, Koblenz
IFN-γ, human	FITC	45-15	Miltenyi Biotec, Bergisch Gladbach
IL-2, human	APC-Vio®770	N7.48A	Miltenyi Biotec, Bergisch Gladbach
IL-10, human	APC	JES3-9D7	Miltenyi Biotec, Bergisch Gladbach
IL-17, human	FITC APC-Vio®770	CZ8-23G1	Miltenyi Biotec, Bergisch Gladbach

Table 11 (continued): Antibodies

Specificity	Fluorochrome	Clone	Source
LAP, human	PE	CH6-17E5.1	Miltenyi Biotec, Bergisch Gladbach
LNGFR (CD271), human	PE PE-Vio®770	ME20.4-1H.4	Miltenyi Biotec, Bergisch Gladbach
NFAT-1, human	FITC	1	BD, Heidelberg
Phospho-ZAP-70/SYK (Y319/Y352), human/mouse	PE	n3kobu5	ebioscience, Frankfurt a.M.
TNF-α, human	PE-Vio®770	CA2	Miltenyi Biotec, Bergisch Gladbach
Activating and blocking antibodies			
Specificity	Fluorochrome	Clone	Source
CD28, human	Pure (functional grade)	15E8	Miltenyi Biotec, Bergisch Gladbach
CD3, human	Pure (functional grade)	OKT3	Miltenyi Biotec, Bergisch Gladbach
CD40, human	Pure (functional grade)	HB14	Miltenyi Biotec, Bergisch Gladbach

Table 12: Fluorochromes

Fluorochrome	$Excitation_{max}$ (nm)	$Emission_{max}$ (nm)
DAPI	359	461
Brilliant Violet 421™	407	421
CellTrace™ Violet	405	450
VioBlue®	400	452
Indo-1 AM	346	475
VioGreen™	388	520
Viobility™ 405/520 Fixable Dye	405	520
VioBright™ FITC	496	522
FITC	495	520
PE	565	578
Propidium Iodide	493	632
PerCP	482	675
PerCP-Cy5.5	482	690
PE-Vio®770	565	775

Table 12 (continued): Fluorochromes

Fluorochrome	$Excitation_{max}$ (nm)	$Emission_{max}$ (nm)
Alexa Fluor® 647	650	665
APC	652	660
APC-Vio®770	652	775

3.2.7.1 Fluorescent labeling of surface molecules

For fluorescent labeling of surface molecules, cells were washed for 5min at 500g at 4°C with PBS/BSA/EDTA (Table 3) and stained with different combinations of surface antibodies (Table 11). Staining was performed for 10min at 4°C in PBS/BSA/EDTA or if Viobility™ 405/520 Fixable Dye was used, cells were washed and stained for 20min at RT in PBS (Table 3). After surface staining, cells were washed and either resuspended in PBS/BSA/EDTA for analysis or cell sorting (see 3.3.7.3) or fixed and permeabilized for intracellular or intranuclear staining (see 3.3.7.2).

3.2.7.2 Fluorescent labeling of intracellular and intranuclear proteins

After staining of surface molecules as described in 3.3.7.1, cells were fixed and permeabilized for staining of intracellular or intranuclear proteins. For staining of FoxP3, cells were fixed and stained using the FoxP3 buffer kit. For fixation, cells were resuspended in Fixation/Permeabilization solution for 30min at 4°C, intranuclear staining was performed in permeabilization buffer for 30min at 4°C according to the manufacturer's manual. For intracellular cytokine staining, cells were restimulated with 10ng/ml PMA and 500ng/ml Ionomycin for 6h in the presence of 5µg/ml Brefeldin A for the last 4h. After surface staining, cells were fixed for 15min at RT and stained with respective antibodies (Table 11) upon permeabilization for 10min at RT using the Inside Stain Kit. When analysed together with cytokines, CD137 and CD154 were stained intracellularly.

3.2.7.3 Fluorescence activated cell sorting

Sorting of live cells is based on the separation of populations according to the expression of fluorescently labeled surface antigens. For the sorting of live cells, surface staining was performed as described in 3.3.7.1 with antibodies from Table 11. Cells were resuspended in PBS/BSA/EDTA (Table 3) at a concentration of 5 x 10^7

cells/ml and propidum iodide was added before sorting to exclude dead cells. Cells were sorted on a FACS Aria™/Aria™ II or Influx™ cell sorter either into 96-well-plates or protein-coated 5ml or 1.5ml tubes. Sorted cells were counted and their purity was determined before they were cultured or used for downstream analysis.

3.2.7.4 Flow-cytometric detection of ZAP70 phosphorylation

Phosphorylated ZAP70 (pZAP70) was stained intracellularly after activation. Before stimulation, Tregs were rested for 1-4 days without activation in T cell resting medium (Table 4) before incubation with 10µg/ml soluble FITC-Dextran at 37°C degrees. After 5 minutes, cells were fixed directly according to manufacturer's recommendations using the ebioscience FoxP3 Staining Buffer Set. After fixation, permeabilization and intracellular staining with CD4, LNGFR and pZAP70 antibodies were performed.

3.2.7.5 Nuclear localization of NFATc2

Localization of NFATc2 within single cells was analysed by combination of flow cytometry with microscopy on an AMNIS ImageStream X Mark II. $CD25^+$ Tregs were isolated *ex vivo* and stimulated in T cell resting medium (Table 4) with 10ng/ml PMA and 500ng/ml Ionomycin. After 6h, cells were harvested and fixed in 3% Formaldehyde for 20min at RT and then stained with CD4-PECy7, CD137-PE, CD154-Alexa647, and NFATc2-FITC in 0.1% (v/v) Triton-X for 30min at RT. Before analysis, 2µg/ml DAPI was added for nuclear staining. Nuclear localization of NFATc2 was analysed on AMNIS ImageStream X Mark II using ISPIRE® software, data was analysed with IDEAS® software. Analysis of nuclear localization of NFATc2 is based on the similarity of the images of the nucleus (DAPI) with NFATc2. To this end each cell is allocated a similarity score with higher scores indicating more similar images.

3.2.7.6 Calcium Flux Assay

$CD25^+$ Tregs were isolated *ex vivo* and stimulated with Treg expansion beads (4:1 bead-to-cell ratio) in T cell resting medium (Table 4). After 6h, cells were stained with 4µM Indo-1 AM Calcium Sensor Dye for 30min at 37°C in Calcium Loading Buffer (Table 3). Cells were washed with Calcium Loading Buffer and surface staining with antibodies against CD4, CD137 and CD154 was performed in PBS/BSA/EDTA. Cells were warmed up to 37°C before measurement on a LSRII Flow Cytometer. After approximately 30s of acquisition, the calcium ionophore Ionomcyin was added at 1µg/ml and the remaining sample was measured. Peak emission of Indo-1 AM Calcium

Sensor Dye shifts upon calcium binding from 475nm (unbound) to 410nm (bound) enabling the quantification of changes in intracellular calcium concentrations (Table 12).

3.2.8 Epigenetic analysis

Analysis of the epigenome is based on the conversion of unmodified cytosine to uracil upon treatment with bisulfite which enables evaluation of the methylation status of every cytosine either by gene-specific amplification (see 3.3.8.1) or sequencing (see 3.3.8.2).

3.2.8.1 Methylation-sensitive TSDR real-time PCR

Cells were frozen in 200µl PBS at -80°C before analysis which was done by K. Vogt in cooperation with Prof. Dr. B. Sawitzki (BCRT Berlin). Genomic DNA was isolated with the QIAamp® DNA Blood Mini Kit. Bisulfite conversion of 50-1200ng genomic DNA was performed with EpiTect Bisulfite Kit. Real-time PCR was done in a final reaction volume of 20µl with 10µl FastStart Universal Probe Master, 100ng Lamda DNA, 5pmol methylation or non-methylation specific probe, 30pmol methylation or non-methylation specific primers and at least 1ng bisulfite-treated DNA or plasmid standard. Samples were analyzed in triplicates on an ABI 7500 Cycler under the following conditions: 1 cycle of 10min 95°C and 45 cycles of 15s 95°C followed by 1min 61°C. The percentage of FoxP3 TSDR was then calculated by dividing the nonmethylated copy-number by the total genomic FoxP3 copy-number.

3.2.8.2 Deep bisulfite amplicon sequencing

$CD137^{+}CD154^{-}$ Tregs and $CD137^{+}CD154^{+}$ Tregs from male donors were sorted, pooled and frozen as dry pellets at -80°C. Deep bisulfite sequencing was done by P. Giehr and J. Gottfreund in cooperation with Prof. Dr. J. Walter (Saarland University). Cells were thawed and digested with lysis buffer (10mM Tris, 5mM EDTA, pH 8.0) with 1mg/ml Proteinase K at 55°C overnight. For deep sequencing of Treg signature regions (Table 7), cell lysates were used directly for bisulfite conversion. To analyse methylation of complementary strands within individual DNA molecules by hairpin bisulfite sequencing, DNA was enzymatically cut and strands were covalently linked by hairpin molecules. To this end, cell lysates were incubated with 1mM Pefabloc for 1h at RT after Proteinase K treatment. DNA was digested with 10U AluI at 37°C overnight.

Digestion was stopped at 80°C for 20min and blunt ends were tailed with 5µM dATP and 6U Klenow enzyme for 30min at 37°C. The reaction was stopped at 80°C for 30min. Strands were ligated with 5µM AluI/A-tailing hairpin linker (Table 7), 20µM ATP and 200U T4 DNA ligase at 16°C overnight. For bisulfite conversion, 100ng DNA were treated with EZ-DNA methylation Gold kit according to manufacturer's instructions. PCR was performed with either 2.5U HOT FIREPol® DNA Polymerase or 1.5U HotStar Taq™ DNA Polymerase with 20ng bisulfite-treated DNA, 0.2mM dNTPs and 0.17µM bisulfite-specific primers (Table 7) according to manufacturer's recommendations. PCR products were amplified under the following conditions: 1 cycle of 15min 95°C and 42 cycles of 1min 95°C, 2min annealing (90min for generation of hairpin constructs), 1min 72°C followed by 7min 72°C. Amplicons were purified with Agencourt Ampure XP beads according to manufacturer's instructions. Hairpin amplicons were gel purified using Gel/PCR DNA Fragments Extraction Kit according to manufacturer's instructions. Purified amplicons were sequenced on the Illumina MiSeq platform using MiSeq Reagent Kit v3 at the NGS sequencing unit of Prof. Dr. J. Walter at Saarland University. Data analysis was perfomed with BiQ Analyzer HT [236] by P. Giehr and J. Gottfreund (Saarland University). Sequencing results were processed and filtered according to sequence identity (>0.9), bisulfite conversion (>0.95) and fraction of unrecognized sites (<0.1). The mean methylation value and CpG methylation pattern maps were generated for each amplicon.

3.2.9 Quantification of gene expression

3.2.9.1 High throughput real-time PCR

High throughput real-time PCR was done by M. Stäber in cooperation with Dr. L. Lozza (MPI for infection biology, Berlin) using the Biomark™ HD system which is based on automated PCR reactions within integrated fluidic circuits (IFCs). $CD25^+$ Tregs were isolated *ex vivo* and stimulated for 6h with Treg expansion beads in the presence of 1µg/ml anti-CD40 pure antibodies. After 6h, $CD4^+CD25^+CD127^-CD45RO^+$ $CD137^+CD154^-$ and $CD137^+CD154^+$ Tregs were FACS purified for analysis of gene expression. A total of 300 cells (100 cells/donor) were sorted into twin.tec® 96 well plates with 5µl of 2X CellsDirect™ Reaction Mix and 0.1µl of 20U/µl SUPERnase In™ RNase Inhibitor and stored at -80°C. Reverse transcription was performed with TaqMan® Gene Expression Assays (Table 9) and SuperScript® III RT/Platinum® Taq Mix. Real-time PCR was performed using 48.48 Sample/Loading Kit and analysed on a

Biomark™ HD according to manufacturer's instructions. Gene expression was normalized to expression of GAPDH.

3.2.9.2 Single cell gene expression

For single cell gene expression analysis, $CD25^+$ Tregs or $CD25^-$ Tcons were stimulated for 6h with 10ng/ml PMA and 500ng/ml Ionomycin in T cell resting medium (Table 4) in the presence of 1µg/ml anti-CD40 pure antibodies. $CD137^+CD154^-$ Tregs and $CD137^+CD154^+$ Tregs as well as $CD137^-CD154^+$ Tcons (all $CD45RO^+$) were FACS purified and frozen in FCS + 10% DMSO at -80°C overnight or in the gas phase of liquid nitrogen at ≤ -150°C for 1-2 weeks before analysis. Single cell gene expression was done by K. Vogt in cooperation with Prof. Dr. B. Sawitzki (BCRT Berlin). Single cells were captured and lysed in individual reaction chambers of an IFC using the C1™ system before high throughput gene expression analysis was performed using the Biomark™ HD system. For capturing of single cells, cells were loaded onto C1™ Single-Cell Auto Prep Array IFC (5-10µm) using C1™ Single-Cell Auto Prep Reagent Kit. Cells were imaged and wells with single cells were documented. Cell lysis, reverse transcription and pre-amplification were performed with C1™ Single-Cell Auto Prep Reagent Kit and Single Cell-to-CT™ Kit on a C1™ System. Pre-amplified products were harvested and real-time PCR was performed with TaqMan™ Universal PCR Master Mix and TaqMan® Gene Expression Assays (Table 9) with 48.48 Sample and Assay Loading Reagent Kit IFC according to manufacturer's recommendations on a Biomark™ HD (also see 3.3.9.1). Single cells were filtered according their expression of B2M (Ct ≤16) and gene expression was analysed using the SINGuLAR™ Analysis Toolset R package for RStudio v0.98.501.

3.2.9.3 Detection of Dextran-CAR constructs by quantitative real-time PCR

The competitive expansion of Dex-CAR constructs with different signaling domains was analysed by qPCR using primers that bind within the signaling domain that are unique to the particular construct (Table 8). DNA was isolated by Qiagen DNA Mini Kit or Zymo Research *Quick*-DNA™ Miniprep Kit according to manufacturer's instructions and expression of the different constructs was analysed using 1x SYBR® Green PCR Master Mix and 500nMol forward and reverse primers (57°C annealing temperature), respectively. Expression was analysed on a StepOne™ Real-Time PCR System and normalized to expression of GAPDH. Relative expression of different time points was

normalized to the beginning of the culture to account for different efficiencies of the PCR depending on the primers.

3.2.10 Sequencing of TCRVβ chains

CD25-enriched Tregs were isolated from PBMCs *ex vivo* and stimulated for 6h with 10ng/ml PMA and 500ng/ml Ionomycin in the presence of 1µg/ml anti-CD40 antibodies. For the isolation of antigen-specific Tregs and Tcons, PBMCs were stimulated with different antigens and antigen-specific Tregs and Tcons were simultaneously enriched by ARTE as described in 3.3.4. $CD137^{+}CD154^{-}$ Tregs, $CD137^{+}CD154^{+}$ Tregs and $CD137^{-}CD154^{+}$ Tcons were FACS purified and genomic DNA was isolated with AllPrep® DNA/RNA Mini or Micro Kit. Sequencing of TCRVβ chains was done by Dr. U. Stervbo and Dr. M. Nienen in cooperation with Prof. Dr. N. Babel (BCRT Berlin/Ruhr University of Bochum). To this end, TCR-β loci were amplified as previously described [237] and library preparation and sequencing was performed using Illumina MiSeq at NGS core facility at the BCRT in Berlin. High quality reads (average quality score >30) were processed with IMSEQ [238] and each clonotype was assigned an ID (Vβ-/Jβ-gene identity, CDR3 amino acid sequence). Similarity was quantified by Yue-Clayton similarity index (YC_{Sim}) where 0 indicates dissimilarity and 1 identifies identical populations [239].

3.2.11 Statistical analysis

All data are summarizing different donors and experiments which were analysed with GraphPad Prism. Significances were calculated with Prism using paired t test, unpaired t test, Wilcoxon matched pairs test, Mann-Whitney U test (for the comparison of two groups) or repeated measures ANOVA, one way analysis of variance, Friedman test or Kruskal-Wallis test in combination with Dunns or Tukeys post hoc tests (for the comparison of more than two groups) depending on the parametric or non-parametric distribution and the paired or unpaired nature of the respective data set. The exact tests that were performed are specified in the respective figure legends. Significances are indicated with $p \leq 0.05$: *, $p \leq 0.01$: ** and $p \leq 0.001$: ***.

4 Results

4.1 Identification of stable Tregs by $CD137^+CD154^-$ expression

The immunosuppressive potential of Tregs emerges as important target for clinical applications. For adoptive transfer, Tregs are isolated from the peripheral blood of patients followed by *in vitro* expansion to generate sufficient numbers (see 1.3, Figure 3). However, *in vitro* expansion compromises purity and increases the risk of introducing contaminating effector cells. Current protocols for clinical isolation of human Tregs are based on the expression of CD25, yet in spite of optimized protocols insufficient purity remains a major concern for adoptive therapy [153]. Currently, there are no unambiguous surface markers to identify stable $FoxP3^+$ Tregs *ex vivo* or within *in vitro* expanded cultures limiting their therapeutic potential. Therefore, this study aimed to define markers for the identification and isolation of highly stable Tregs *ex vivo* and after prior *in vitro* expansion for optimized stability of therapeutic Tregs.

4.1.1 CD137 and CD154 expression within the human Treg compartment

It has been shown that CD154 is expressed selectively on Tcons after 6h stimulation *ex vivo* while antigen-activated Tregs are characterized by CD137 expression [92, 96, 97, 107]. To investigate the potential of converse CD137 and CD154 expression to distinguish between Tregs and contaminating Tcons within the human polyclonal $CD25^+CD127^-$ Treg compartment, expression of CD137 and CD154 were analysed upon activation of $CD25^+CD127^-$ Tregs *ex vivo*. Following stimulation with anti-CD3/-CD28, most Tregs upregulated CD137 of which a small subset co-expressed CD154 (Figure 5A,B). In addition, a very minor $CD154^+$ population lacked CD137 expression which most likely represents contaminating Tcons. To determine phenotypic differences between $CD137^+CD154^-$ Tregs and $CD137^+CD154^+$ Tregs, gene expression of selected Treg-associated markers and effector cytokines was analysed. Among CD137-expressing Tregs, $CD154^+$ and $CD154^-$ cells were defined by expression of Treg-associated markers such as *foxp3*, *ikzf2* (HELIOS), *tigit*, *il2ra* (CD25) and *tgfβ1* which were expressed at lower levels in $CD137^+CD154^+$ Tregs (Figure 5C). In contrast, effector cytokines (*il2, il17a, ifnγ, tnfα*) were exclusively expressed by $CD137^+CD154^+$ Tregs and completely absent in $CD137^+CD154^-$ Tregs. These data show striking differences regarding the phenotype of the two Treg populations within the $CD25^+CD127^-$ Treg compartment. Interestingly, high levels of the regulatory cytokine *il10* were detected exclusively in $CD137^+CD154^+$ Tregs indicating a regulatory potential in spite of their limited ability to express other Treg-associated markers (Figure 5C). Furthermore, these data suggest distinct regulatory mechanisms

of $CD137^+CD154^-$ Tregs that lack IL-10 expression. These data show the co-existence of $CD137^+CD154^-$ Tregs and $CD137^+CD154^+$ Tregs within the human $CD25^+CD127^-$ Treg compartment that differ in their expression of Treg-associated markers and effector molecules. While $CD137^+CD154^-$ Tregs exhibited a transcriptional Treg phenotype, $CD137^+CD154^+$ Tregs were characterized by a compromised transcriptional Treg signature.

$CD137^+CD154^-$ Tregs expressed high levels of Treg-associated markers. However, long-term stability of the Treg phenotype and stable expression of Treg-associated genes are regulated by epigenetic marks. Indeed, Treg stability has been closely linked to the demethylation of specific Treg signature genes that have been shown to be differentially methylated in Tregs and Tcons [240, 241]. To investigate differential stability of $CD137^+CD154^-$ Tregs and $CD137^+CD154^+$ Tregs on an epigenetic level, local-deep bisulfite sequencing of regions within *foxp3, ctla4, ikzf2*, *lrrc32*, *il2ra*, *tnfrsf9* and *cd40lg* that were shown to be differentially methylated in Tregs and Tcons was performed [241]. $CD137^+CD154^-$ Tregs exhibited a completely demethylated TSDR and were highly demethylated at all other analysed regions indicating remarkable epigenetic stability (Figure 5D). In contrast, $CD137^+CD154^+$ Tregs were partially methylated at all analysed Treg-associated regions revealing an instable Treg signature (Figure 5D). These findings show that $CD137^+CD154^-$ Tregs are characterized by a stable Treg signature providing evidence for their thymic origin and long-term stability in the periphery. In contrast, $CD137^+CD154^+$ Tregs exhibited an instable Treg signature with significant methylation of Treg-associated regions. However, compared to conventional central memory T cells (T_{CM}), $CD137^+CD154^+$ Tregs were hypomethylated at these regions clearly separating this regulatory subset from Tcons (Figure 5D). Therefore, $CD137^+CD154^+$ Tregs did not represent contaminating effector cells but rather exhibited an intermediate Treg-Tcon signature. It is important to note that also *tnfrsf9* (CD137) and *cd40lg* (CD154) were differentially methylated indicating that the ability to express either of these markers was at least partially imprinted on an epigenetic level. In summary, these data show that the human $CD25^+CD127^-$ Treg compartment contained stable $CD137^+CD154^-$ Tregs with a prototypic Treg signature and instable $CD137^+CD154^+$ Tregs with an intermediate Treg-Tcon signature revealing notable heterogeneity within the peripheral Treg compartment.

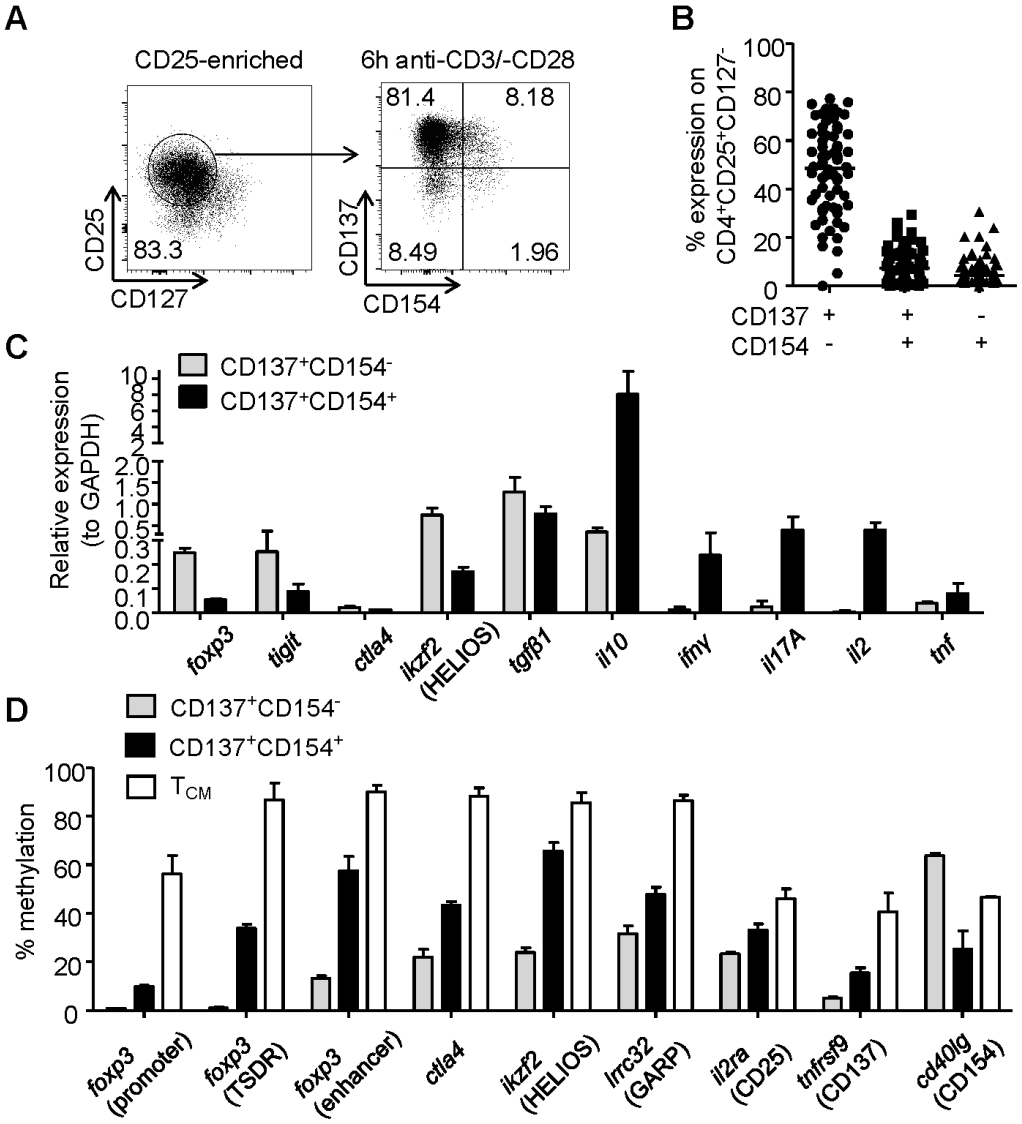

Figure 5: Phenotype of CD137$^+$CD154$^-$ Tregs and CD137$^+$CD154$^+$ Tregs *ex vivo*. (A-D) CD25-enriched Tregs were activated for 6h with anti-CD3/-CD28. **(A,B)** CD137 and CD154 expression were analysed on CD25$^+$CD127$^-$ Tregs; **(A)** representative dot plot of one donor and **(B)** statistical summary of several donors (n=68, 17 independent experiments were performed). CD137$^+$CD154$^-$ Tregs and CD137$^+$CD154$^+$ Tregs (CD25$^+$CD127$^-$CD45RO$^+$) were sorted for analysis of **(C)** gene expression (2 independent experiments were performed, 3 donors were pooled for each experiment) and **(D)** mean methylation of indicated regions (data from two independent experiments are shown, 5 and 6 male donors were pooled for each experiment); data from T_{CM} were obtained from Durek et al., 2016 [242]. **(B)** Each dot represents one donor, lines indicate median, **(C,D)** mean + SEM is shown.

4.1.1.1 Molecular regulation of CD154 expression on Tregs

CD154 expression on activated Tregs distinguished between stable $CD137^+CD154^-$ Tregs and effector-like $CD137^+CD154^+$ cells (Figure 5C,D). Differential methylation of *cd40lg* was observed (Figure 5D), but how CD154 expression on Tregs is regulated remains unclear. Expression of CD137 has been described to be NFκB-dependent whereas CD154 expression is mediated by NFAT (nuclear factor of activated T cells) [243]. The NFAT family consists of five transcription factors (NFAT1-5) of which NFAT1, 2, 4 and 5 are essential for T cell development and function. NFAT expression exhibits a certain level of redundancy and together with other transcription factors is crucial for the regulation of gene expression upon translocation into the nucleus [244]. To elucidate molecular differences that mediate activation-induced expression of CD154 and potentially also upregulation of other effector functions on Tregs, molecular mechanisms downstream of TCR activation were analysed.

Since NFAT is ubiquitously expressed in all T cells, mean fluorescent intensity (MFI) of NFATc2 was analysed to investigate differences in the expression level per cell. Interestingly, the MFI of NFATc2 was increased in $CD137^+CD154^+$ Tregs compared to $CD137^+CD154^-$ Tregs indicating higher levels of NFATc2 expression within CD154-expressing Tregs (Figure 6A). NFAT-dependent gene regulation requires its translocation into the nucleus. Therefore, nuclear NFAT translocation was blocked by BTP1 which is a highly selective inhibitor of NFAT activation [235]. Blocking of nuclear NFAT translocation by BTP1 reduced expression of IL-2 in activated Tregs showing the functionality of NFAT inhibition (Figure 6B). Furthermore, expression of CD154 was inhibited by BTP1 whereas an effect on CD137 expression was only observed at high concentrations (Figure 6C). Although BTP1 is highly specific for blocking nuclear translocation of NFAT [235], an effect on NFκB cannot be excluded which can result in inhibition of CD137 expression especially at high concentrations (Figure 6C). Taken together, these data suggest that expression of CD154, IL-2 and most likely also other effector molecules in Tregs were regulated by NFAT which was differentially expressed in $CD137^+CD154^-$ Tregs and $CD137^+CD154^+$ Tregs. Therefore, molecular adaptations within the peripheral Treg compartment represent a potential mechanism for the regulation of effector functions in Tregs.

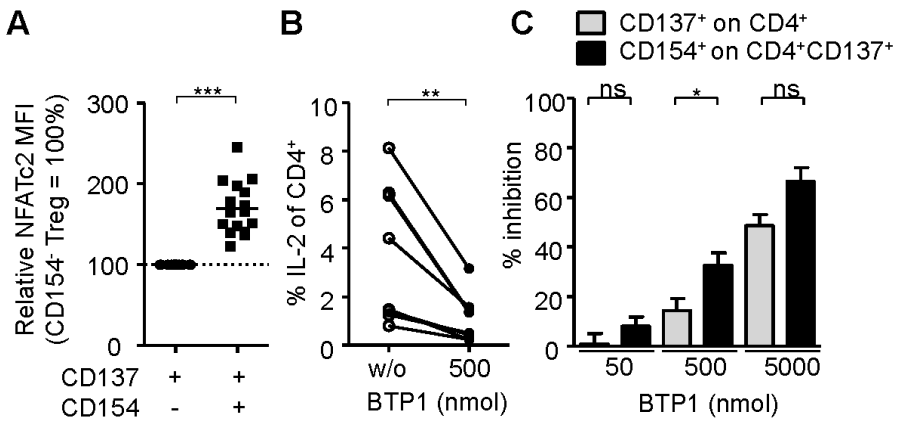

Figure 6: CD154 expression on Tregs is dependent on nuclear NFAT. (A-C) CD25$^+$ Tregs were isolated and restimulated for 6h *ex vivo*. **(A)** NFAT expression was analysed after 6h stimulation with PMA/Ionomycin, the MFI (geometric mean) of NFATc2 was normalized to CD137$^+$CD154$^-$ Tregs (n=17, 6 independent experiments were performed). **(B-C)** BTP1 was added 20min prior to 6h stimulation with anti-CD3/-CD28 before analysis of **(B)** IL-2 expression (n=8, 2 independent experiments were performed) and **(C)** CD137 and CD154 expression (n=8, 3 independent experiments were performed). **(C)** Inhibition of CD137 and CD154 was calculated based on expression without BTP1. Statistical significances were determined by **(A)** one sample t test, **(B)** paired t test or **(C)** Mann-Whitney test. **(A,B)** Each dot represents one donor with **(A)** mean, **(C)** mean + SEM is shown.

Differential expression of NFATc2 was observed in CD137$^+$CD154$^-$ Tregs and CD137$^+$CD154$^+$ Tregs and also dependence of CD154 expression on nuclear NFAT translocation was shown (Figure 6A-C). However, it remains unclear whether an inability to upregulate CD154 derives from the lower levels of NFAT per cell (Figure 6A) or insufficient translocation into the nucleus in CD137$^+$CD154$^-$ Tregs. To address this question, flow cytometric detection was combined with imaging to provide a detailed analysis of NFAT localization within individual cells. This method enabled the separation of cytoplasmic from nuclear NFATc2 in CD137$^+$CD154$^-$ Tregs and CD137$^+$CD154$^+$ Tregs (Figure 7A). Nuclear translocation was analysed on a single cell level by allocating a similarity score to each cell based on the similarity of the images of NFATc2 and the nucleus which was defined by DAPI staining. Within CD137$^+$CD154$^+$ Tregs almost all cells had translocated NFATc2 into the nucleus whereas significant amounts of cytoplasmic NFATc2 were detected within CD137$^+$CD154$^-$ Tregs (Figure 7B). Nevertheless, nuclear NFATc2 was also detected within CD137$^+$CD154$^-$ cells showing that translocation itself was not sufficient to induce CD154 expression within individual cells (Figure 7B).

Collectively, NFATc2 translocation was higher in CD137$^+$CD154$^+$ Tregs (Figure 7C) indicating that not only lower expression but also inefficient nuclear translocation contributed to lack of CD154 expression on CD137$^+$ Tregs. These data indicate differential signaling mechanisms upon stimulation which can have the potential to contribute to the regulation of the expression of effector molecules in Tregs.

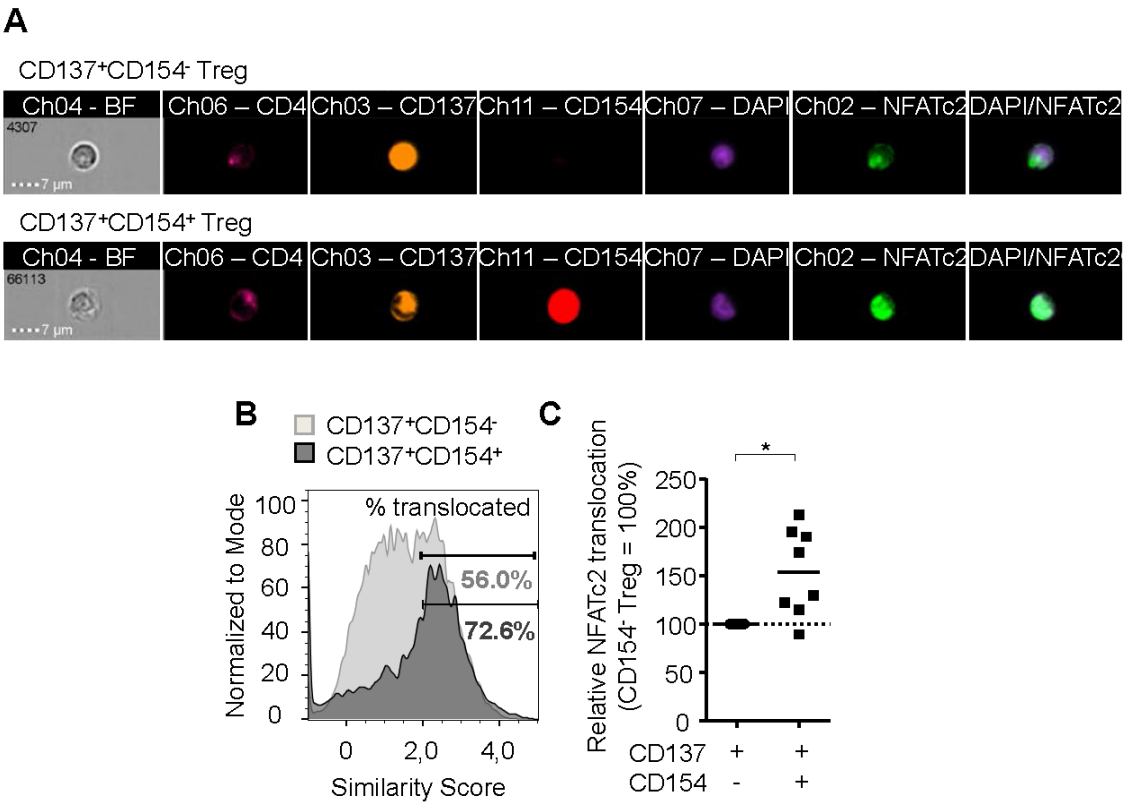

Figure 7: Nuclear translocation of NFATc2 in Tregs. (A-C) Nuclear translocation of NFATc2 was analysed after 6h stimulation with PMA/Ionomycin. **(A)** Representative image of one cell of CD137$^+$CD154$^-$ Tregs (top) and CD137$^+$CD154$^+$ Tregs (bottom). **(B-C)** A similarity score was allocated to each cell based on the similarity of the images of NFATc2 and the nucleus (DAPI); higher similarity scores indicate more similar images. **(B)** Representative histogram of one donor; **(C)** the percentage of cells that had translocated NFATc2 was determined based on **(B)** and normalized to CD137$^+$CD154$^-$ Tregs (n=8, 3 independent experiments were performed); **(C)** statistical significances were determined by one sample t test, each dot represents one donor, lines indicate mean.

Here it was shown that the transcription factor NFAT represents an important mechanism contributing to the regulation of CD154 expression on Tregs. Within CD137$^+$CD154$^-$ Tregs, nuclear NFATc2 was significantly reduced indicating inefficient translocation (Figure 7C). Nuclear import of NFAT requires calcium-dependent dephosphorylation which emerges as potential mechanism upstream of NFAT-dependent gene regulation in Tregs [245]. Therefore, intracellular calcium levels were

analysed within $CD137^+CD154^-$ Tregs and $CD137^+CD154^+$ Tregs to investigate molecular differences downstream of TCR activation. To analyse calcium influx, cells were stained with a calcium indicator dye which shifts emission upon calcium-binding. To this end, changes in the intracellular calcium concentration were measured in $CD137^+CD154^-$ Tregs and $CD137^+CD154^+$ Tregs upon stimulation with the calcium ionophore ionomycin. Changes in intracellular calcium were quantified by determining the ratio of bound to unbound calcium over the time of acquisition with addition of ionomycin after ~30 seconds (Figure 8A). There was a stronger calcium influx in $CD137^+CD154^+$ Tregs compared to $CD137^+CD154^-$ Tregs after addition of ionomycin (Figure 8A) resulting in overall higher levels of bound calcium as determined by the area under the curve (Figure 8B) and higher maximum values (Figure 8C). These data suggest reduced or delayed signal transduction in $CD137^+CD154^-$ Tregs following stimulation. Consequently, reduced calcium signaling in $CD137^+CD154^-$ Tregs can represent a potential mechanism to limit nuclear translocation of NFAT upon TCR activation and therefore expression of effector molecules.

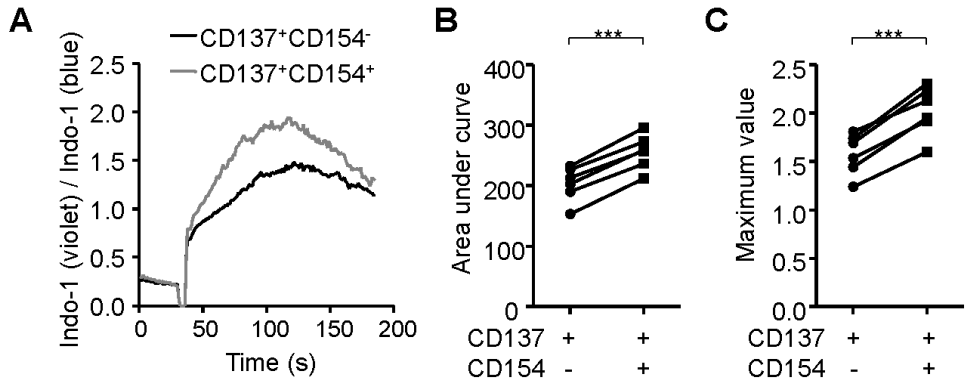

Figure 8: Calcium influx in $CD137^+CD154^-$ Tregs and $CD137^+CD154^+$ Tregs. (A-C) $CD25^+$ Tregs were isolated and stimulated *ex vivo* for 6h with anti-CD3/-CD28. **(A)** Mean value for each time point of the ratio of bound to unbound calcium after addition of 10µg/ml Ionomycin after 30-40s is shown. **(B-C)** Differences between $CD137^+CD154^-$ Tregs and $CD137^+CD154^+$ Tregs were quantified by analysis of **(B)** the area under the curve and **(C)** the maximum value of the curves that are shown in **(A)**. **(B-C)** Statistical significances were determined by paired t test (n=6, 2 different experiments were performed); **(B,C)** each dot represents one donor.

Taken together, these data show that CD154 expression on Tregs was associated with molecular adaptations downstream of TCR signaling. It can be speculated that reduced calcium influx mediated lower levels and inefficient nuclear translocation of NFATc2 in $CD137^+CD154^-$ Tregs. This can represent an important mechanism that contributes to phenotypic differences between $CD154^-$ Tregs and $CD154^+$ Tregs.

4.1.2 CD137 and CD154 expression within expanded Treg cultures

Here it was shown that activation-induced CD137 and CD154 expression distinguished between epigenetically stable $CD137^+CD154^-$ Tregs and effector-like $CD137^+CD154^+$ Tregs within the peripheral Treg compartment (Figure 5A-D). Therefore, $CD137^+CD154^-$ expression enabled the purification of Tregs *ex vivo*, yet it remains elusive whether stable Tregs can similarly be identified after prior *in vitro* expansion. This represents a particular challenge as the generation of sufficient numbers for Treg-based therapies or the modification of Treg functionality e.g. by genetic engineering requires prolonged *in vitro* expansion.

To date, clinical Treg isolation is based on CD25 expression which can routinely be applied under GMP-compatible conditions. Treg isolation by CD25 microbeads enabled the enrichment of $FoxP3^+$ cells from peripheral blood *ex vivo* (Figure 9A). However, notable frequencies of $FoxP3^-$ cells were detected within enriched populations which potentially represent transiently activated Tcons that have upregulated CD25 (Figure 9A). Since Treg frequencies were low *ex vivo*, Tregs were expanded for 2-3 weeks in the presence of IL-2, rapamycin and anti-CD3/-CD28 which have been shown to favor expansion of Tregs [246, 247]. Upon polyclonal expansion, frequencies of $FoxP3^+$ cells significantly decreased resulting in cultures with only 41.01% (mean ± 14.50% St.Dev.) FoxP3-expressing cells compared to 65.79% (mean ± 10.46% St.Dev.) at the beginning of expansion (Figure 9B). Furthermore, CD25 was expressed by almost all cells and CD127 was lost and could therefore no longer distinguish between Tregs and contaminating Tcons (Figure 9A). These data suggest either downregulation of FoxP3 by Tregs or an outgrowth of non-Tregs in spite of optimized culture conditions. In addition to a loss of FoxP3, significant amounts of pro-inflammatory cytokines (IFN-γ, IL-17, IL-2, TNF-α) were detected within expanded cultures indicating notable numbers of cells that exhibited an effector-like phenotype which can have a strong inflammatory potential (Figure 9C). Taken together, *in vitro* expansion of $CD25^+$ Tregs, which is required to generate sufficient numbers for therapeutic applications, resulted in compromised purity of expanded cultures. Impurities can either derive from inherent Treg instability or contaminations with effector cells *ex vivo.* Irrespective of their origin, inflammatory effector cells generate significant safety concerns for adoptive therapy and therefore novel strategies for the identification and isolation of stable Tregs *ex vivo* and after prior *in vitro* expansion are required.

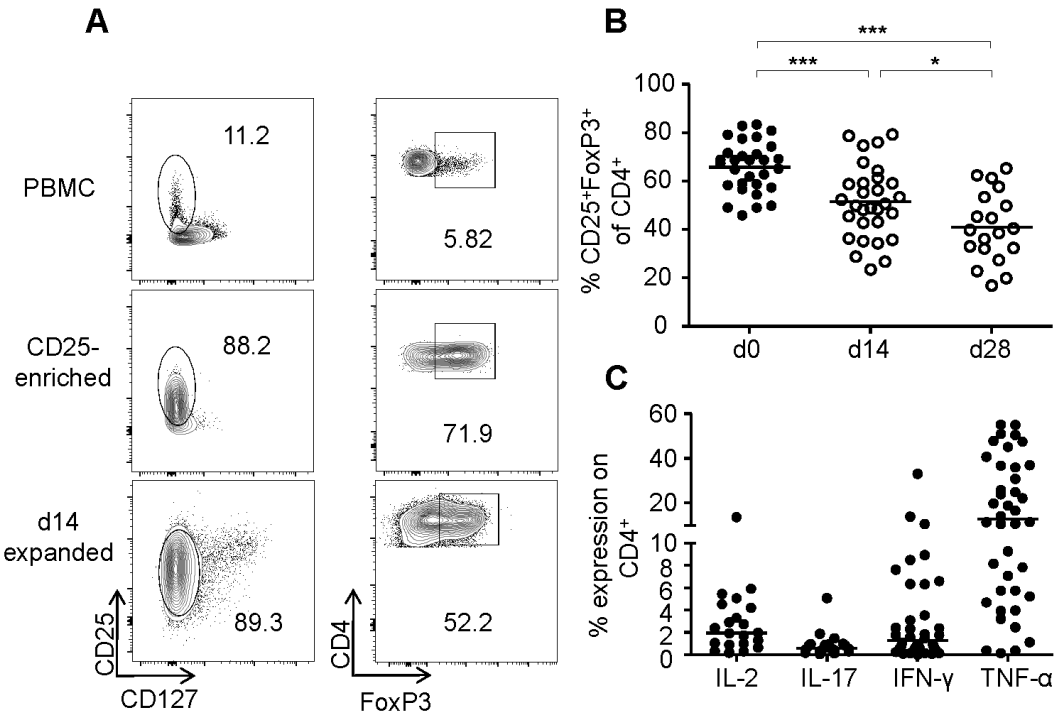

Figure 9: Treg expansion compromises purity. (A-C) CD25$^+$ Tregs were sorted and expanded before analysis of **(A,B)** FoxP3 and **(C)** cytokine expression; **(A)** representative dot plot of one donor and **(B)** statistical analysis of several donors (n=30 from 9 independent experiments for d0 and d14, n=19 from 7 different experiments for d28). **(C)** Cytokine expression was analysed on d28 after 6h restimulation with PMA/Ionomycin (n=38 from 12 different experiments for IFN-γ, n=40 from 13 different experiments for TNF-α, n=19 from 7 different experiments for IL-17 and n=17 from 6 different experiments for IL-2). **(B)** Statistical significances were determined by One Way analyis of variance; lines indicate **(B)** mean or **(C)** median.

In vitro expansion of CD25$^+$ Tregs resulted in compromised purity including loss of FoxP3 expression and upregulation of effector cytokines which can derive from contaminations at the beginning of the culture or Treg instability. CD137$^+$CD154$^-$ expression was shown to be upregulated on an epigenetically stable Treg subset *ex vivo* whereas co-expression of CD154 identified an effector-like Treg subset with an instable transcriptional and epigenetic Treg signature (Figure 5C,D). To investigate stability of Tregs after prior *in vitro* expansion, CD137 and CD154 expression were analysed on expanded Tregs after 6h stimulation. Similar to Tregs *ex vivo* (Figure 5B), the majority of cells exhibited a CD137$^+$CD154$^-$ phenotype after expansion with a small percentage of cells that expressed CD154 of which some co-expressed CD137 (Figure 10A,B). Frequencies of FoxP3$^+$ Tregs varied between subsets and were significantly increased within CD137$^+$CD154$^-$ Tregs compared to cells expressing CD154 (Figure

10C,D). Lowest levels of FoxP3 were detected within CD137$^-$CD154$^+$ cells which most likely represent contaminating effector cells. Therefore, phenotypic differences between CD154$^+$ and CD154$^-$ Tregs that were observed *ex vivo* were maintained upon expansion and CD137$^+$CD154$^-$ expression was similarly able to selectively identify FoxP3$^+$ Tregs.

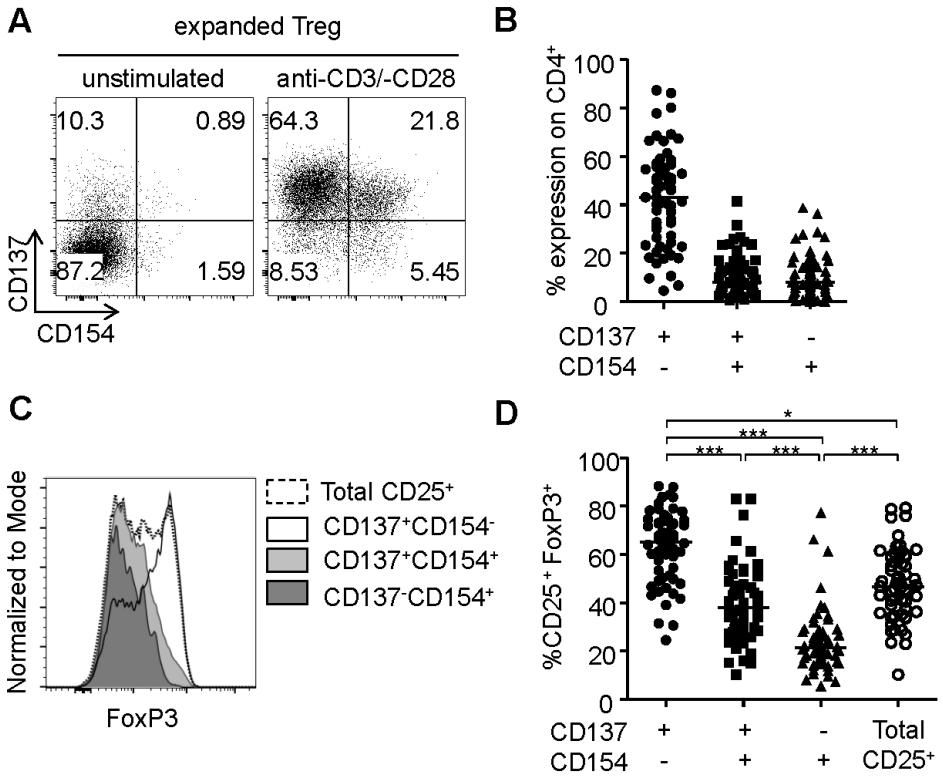

Figure 10: CD137 and CD154 expression within expanded Treg cultures. (A-D) CD25$^+$ Tregs were isolated and expanded *in vitro* before restimulation with anti-CD3/-CD28. **(A,B)** CD137 and CD154 expression were analysed. **(A)** Representative dot plot of one donor and **(B)** statistical summary of several donors (n=64, 21 independent experiments were performed). **(C,D)** FoxP3 expression was analysed on the different subsets after 6h stimulation, **(C)** representative histogram of one donor and **(D)** statistical summary of several donors (n=61, 20 independent experiments were performed). **(D)** Statistical significances were determined by Kruskal-Wallis test. **(B,D)** Each dot represents one donor, lines indicate median.

Differences in FoxP3 expression were observed between CD137$^+$CD154$^-$ Tregs and CD137$^+$CD154$^+$ Tregs within *in vitro* expanded cultures (Figure 10C,D). To determine their epigenetic stability, TSDR demethylation was analysed. In line with epigenetic stability of CD137$^+$CD154$^-$ Tregs *ex vivo* (Figure 5D), CD137$^+$CD154$^-$ Tregs exhibited an almost completely demethylated TSDR after expansion which was strongly methylated in CD137$^+$CD154$^+$ Tregs and completely methylated in CD137$^-$CD154$^+$ cells

(Figure 11A). These data show that $CD137^+CD154^-$ expression was able to identify epigenetically imprinted Tregs within *in vitro* expanded cultures. Furthermore, these data confirm the notion that $CD137^-CD154^+$ expression identified contaminating Tcons whereas $CD137^+CD154^+$ Tregs exhibited intermediate levels of TSDR demethylation (Figure 11A). Remarkably, a strong correlation was observed between $CD137^+CD154^-$ expression and TSDR demethylation within expanded Treg cultures (Figure 11C) which was even more significant than the association of FoxP3 expression with TSDR demethylation (Figure 11B). These data reveal the striking potential of $CD137^+CD154^-$ expression as surrogate surface marker for the identification of epigenetically stable FoxP3-expressing Tregs even after prior *in vitro* expansion.

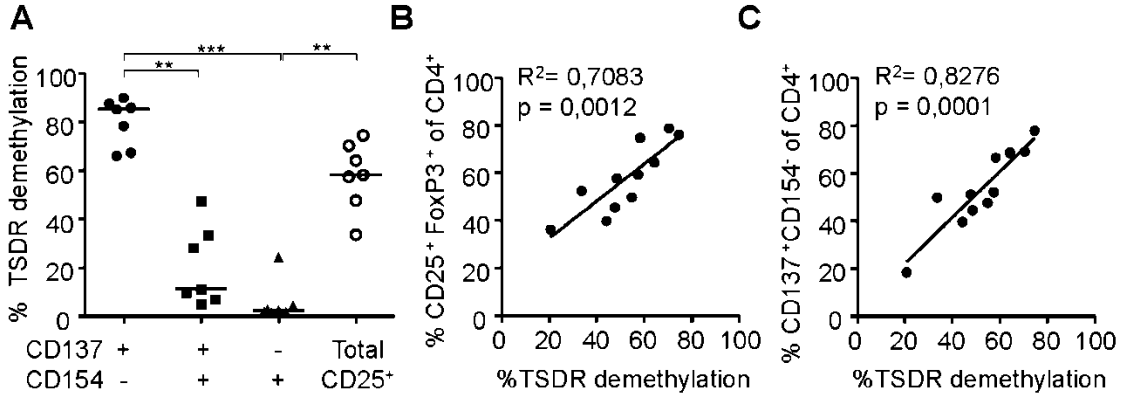

Figure 11: Epigenetic stability of $CD137^+CD154^-$ Tregs and $CD137^+CD154^+$ Tregs. (A) Tregs were sorted from expanded cultures according to CD137 and CD154 expression and TSDR demethylation was analysed (n=7, 2 independent experiments were performed). **(B-C)** CD25-enriched Tregs were expanded for 14 or 28 days before analysis of TSDR demethylation; correlation of TSDR demethylation with **(B)** FoxP3 and **(C)** $CD137^+CD154^-$ expression are shown (n=11, 3 independent experiments were performed). Statistical significances were determined by **(A)** Kruskal-Wallis test or **(B,C)** linear regression analysis. **(A)** Each dot represents one donor, lines indicate median.

Within expanded Treg cultures, $CD137^+CD154^-$ expression identified epigenetically stable $FoxP3^+$ Tregs while $CD137^+CD154^+$ Tregs were characterized by a hypermethylated TSDR (Figure 11A) and low levels of FoxP3 expression (Figure 10C,D). Next, a more detailed phenotypic analysis was to provide insight into potential functional differences between $CD137^+CD154^-$ Tregs and $CD137^+CD154^+$ Tregs. In line with their transcriptional signature *ex vivo* (Figure 5C), high protein levels of the Treg-associated markers LAP and GARP were detected within $CD137^+CD154^-$ Tregs while expression was significantly reduced within $CD137^+CD154^+$ Tregs (Figure 12A). LAP and GARP have been shown to contribute to contact-dependent TGF-β-mediated suppression representing an important regulatory mechanism [248]. In line with these

findings, CD137$^+$CD154$^-$ Tregs were more suppressive than CD137$^+$CD154$^+$ Tregs in an *in vitro* suppression assay showing different functionality and underlining the heightened regulatory potential of CD137$^+$CD154$^-$ Tregs (Figure 12B). In addition, expression of pro-inflammatory cytokines was limited to CD137$^+$CD154$^+$ Tregs and except for TNF-α almost completely absent in CD137$^+$CD154$^-$ Tregs (Figure 12C). Interestingly, as observed on a transcriptional level (Figure 5C), IL-10 was expressed almost exclusively by CD137$^+$CD154$^+$ Tregs (Figure 12C). IL-10 expression might represent an important regulatory mechanism for this particular subset suggesting functional differences between CD137$^+$CD154$^+$ Tregs and CD137$^+$CD154$^-$ Tregs. Nevertheless, IL-10 expression was low and *in vitro* suppression was compromised in CD137$^+$CD154$^+$ Tregs suggesting only a minor regulatory potential of this subset which was rather characterized by an effector-like phenotype.

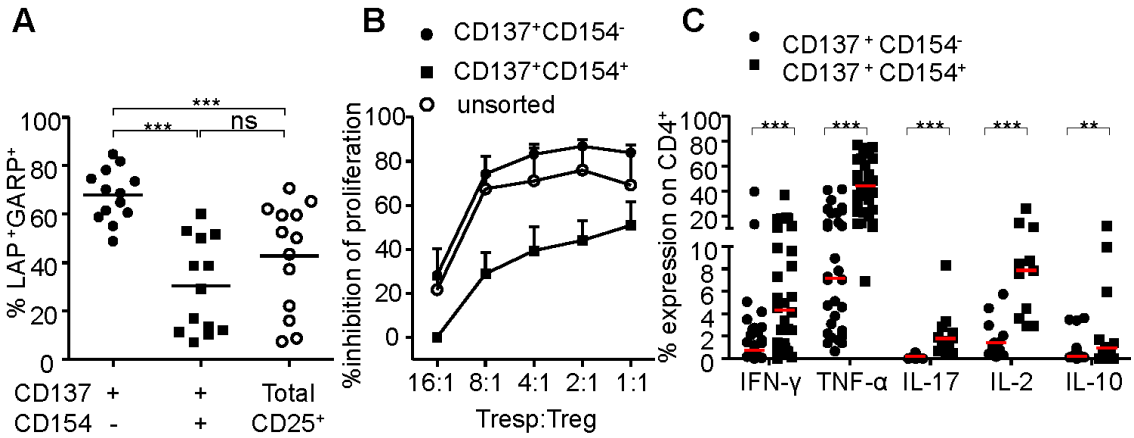

Figure 12: Phenotype of CD137$^+$CD154$^-$ Tregs and CD137$^+$CD154$^+$ Tregs within expanded cultures. (A,C) CD25$^+$ Tregs were isolated and expanded *in vitro* before restimulation with PMA/Ionomycin. **(A)** Expression of LAP and GARP were analysed after 24h (n=13, 4 independent experiments were performed). **(C)** Expression of INF-γ, TNF-α (n=30 from 9 different experiments), IL-17, IL-2 (n=11, 4 different experiments) and IL-10 (n=17, 6 independent experiments) were analysed after 6h stimulation. **(B)** Tregs were sorted from expanded CD25$^+$ cultures according to CD137 and CD154 expression, total CD25$^+$ Tregs represent unsorted samples; all populations were expanded for another 10 days before *in vitro* suppression of CD4$^+$CD25$^-$ Tresps was analysed (n=4-6, 2 independent experiments were performed); inhibition of proliferation relative to untreated Tresps is shown. Statistical significances were determined by **(A)** repeated measures ANOVA or **(C)** Wilcoxon signed-rank test. **(A,C)** Each dot represents one donor and lines indicate **(A)** mean or **(C)** median, **(B)** mean + SEM is shown.

Taken together, these data show that CD137 and CD154 expression distinguished between epigenetically stable CD137$^+$CD154$^-$ Tregs and effector-like CD137$^+$CD154$^+$ Tregs not only *ex vivo*, but also after prior *in vitro* expansion. While lack of CD154 expression identified a Treg subset that expressed high levels of FoxP3 and almost completely lacked cytokine expression, CD137$^+$CD154$^+$ Tregs exhibited a strongly

methylated TSDR and were characterized by reduced levels of FoxP3 and high levels of effector cytokines. Although the origin and function of $CD137^{+}CD154^{+}$ Tregs remain to be determined, the potency of $CD137^{+}CD154^{-}$ expression as Treg-specific activation signature becomes evident and can enable the identification and isolation of lineage stable Tregs for the purification of clinical products for adoptive Treg transfer.

4.2 *In vitro* generation of antigen-specific Tregs

Chronic inflammatory diseases are currently believed to be the consequence of effector cells that target harmless, mostly unknown autoantigens resulting in the destruction of healthy tissue such as the CNS during multiple sclerosis, pancreatic islets during T1D or cartilage tissue during rheumatoid arthritis [249]. To suppress inflammatory immune reactions and restore immune homeostasis, Tregs emerge as important target for clinical applications (see 1.3). Adoptive transfer of *in vitro* expanded Tregs has demonstrated their potential to treat inflammatory immune pathologies. Nevertheless, their therapeutic application is currently limited by insufficient technologies for the isolation and large-scale expansion of highly potent antigen-specific Tregs. Therefore, chimeric antigen receptors (CARs) are currently emerging to redirect Treg specificity for clinical applications (see 1.3.2.2). Current approaches using CAR technology to generate antigen-specific Tregs have focused on endogenous antigens such as HLA-A2 [230-232]. However, disease-relevant Treg targets are often unknown and expression is often not limited to inflamed tissues. Therefore, Treg specificity was redirected toward an exogenous antigen for targeted activation of CAR-Tregs.

4.2.1 Generation of dextran-specific CAR-Tregs

In this study, antigen-specific Tregs were generated by *in vitro* genetic engineering using a chimeric antigen receptor to redirect Treg specificity toward dextran to provide an inducible system by linking Treg activation to the application of an exogenous antigen. Dextran is a branched polysaccharide consisting of several glucose molecules that are linked by α-1,6 and α-1,3 glycosidic linkages resulting in lengths of 3-2000 kDa. Dextran-reactive Tregs were generated by genetic engineering of human $CD25^{+}$ Tregs using a lentiviral expression vector encoding a dextran-specific CAR. The construct contained a dextran-specific scFv which was connected to a short (12aa) IgG4-derived hinge to provide flexibility for efficient antigen-binding. The ectodomain was connected via a CD8-derived transmembrane domain to an intracellular signaling

moiety consisting of CD3ζ in combination with CD137 co-stimulation (Figure 13A). To detect transduced cells, truncated human low-affinity nerve growth factor receptor (LNGFR) was included in the expression vector which could be stained on the surface after successful lentiviral transduction (Figure 13B). LNGFR expression was detected after lentiviral transduction although levels were highly variable with an average of 20.75% (mean ± 9.84% St.Dev.; Figure 13C). Although LNGFR expression identified transduced cells, it does not provide insight into the efficiency of the transcription and translation of the receptor. Therefore, receptor expression was quantified by analyzing antigen-binding within transduced cells. To this end, Tregs were incubated with FITC-labeled dextran which enabled direct flow cytometric detection of dextran-binding cells. Dextran was bound selectively by $LNGFR^+$ and not $LNGFR^-$ cells within the same culture in a concentration-dependent manner with only minor unspecific binding by $LNGFR^-$ Tregs at high concentrations (Figure 13D,E). These data show functional expression of the CAR on transduced $LNGFR^+$ Tregs although not all $LNGFR^+$ cells were able to bind dextran suggesting inefficient transcription or translation of the transgene (Figure 13E). Since it was bound efficiently and enabled tracking of dextran-binding cells, FITC-Dextran with a molecular weight of 2,000,000 g/mol was used throughout this work to detect CAR-Tregs unless specified otherwise.

Dextran consists of several glucose molecules and can therefore structurally resemble other saccharides that are commonly encountered and could have the potency to induce off-target activation of CAR-Tregs. To this end, the degree of cross-reactive binding by CAR-Tregs was analysed by incubation with glucose (monosaccharide), maltose (disaccharide), dextrin (polysaccharide) or dextran (polysaccharide) before staining with FITC-Dextran. FITC-Dextran staining was only blocked by soluble or bead-bound dextran, but not by any other tested saccharides (Figure 13D,F). Consequently, CAR-Tregs selectively bound dextran showing no cross-reactive binding of CAR-Tregs with other saccharides highlighting their specificity. Furthermore, CAR-Tregs similarly bound soluble and bead-bound dextran and also different molecular weights (500,000g/mol and 2,000,000 g/mol) providing flexible opportunities regarding antigen application. Taken together, specificity for dextran was introduced into human Tregs by *in vitro* genetic engineering using a chimeric antigen receptor. CAR-Tregs were able to selectively bind dextran and therefore emerge as system for targeted activation of Tregs *in vitro* and *in vivo*.

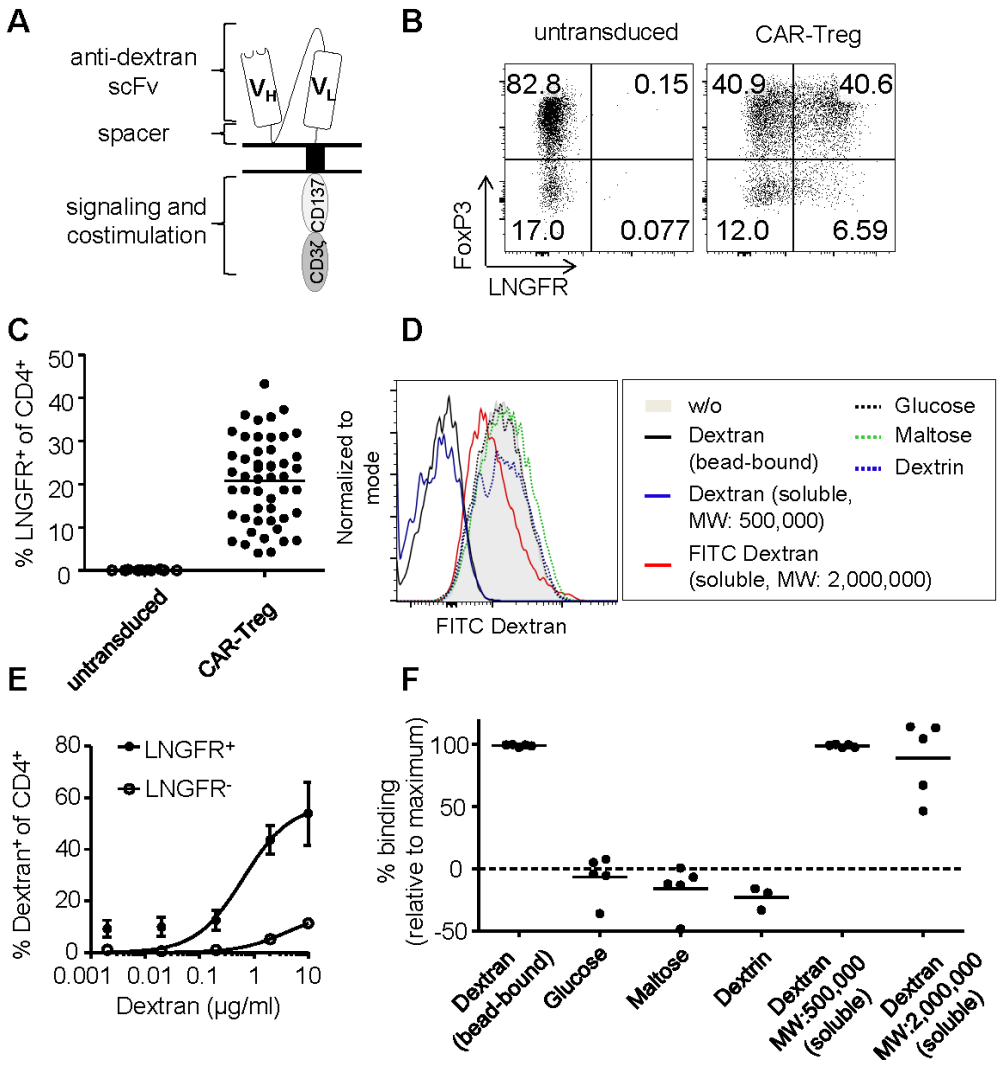

Figure 13: Generation of dextran-specific CAR-Tregs. (A) Schematic diagram of the dextran-specific CAR construct. **(B-F)** CAR-Tregs were generated by lentiviral transduction which was analysed by **(B-C)** LNGFR expression; **(B)** representative dot plot of one donor and **(C)** statistical analysis of several donors (n=50 from 16 independent experiments for CAR-Tregs and n=12 from 4 different experiments for untransduced Tregs). **(D-F)** CAR expression and specificity was analysed by incubation with different saccharides before staining with FITC dextran; **(D)** representative histogram of one donor and **(F)** statistical analysis of several donors (n=5-9, 2-3 independent experiments were performed); the percentage of bound antigen was calculated as relative frequency of FITC-Dextran$^+$ cells in the treated samples compared to the untreated control. **(E)** CAR surface expression was analysed by binding of FITC-Dextran (n=3-9 from 1-3 independent experiments). Each dot in **(C,F)** represents one donor and lines indicate mean; **(E)** mean ± SEM is shown.

CAR-Tregs were generated by lentiviral transduction which stably integrates the transgene into the host genome. To investigate a potential influence of viral transduction and CAR expression on Treg function, the phenotype of CAR-Tregs was analysed. FoxP3 as most important Treg marker was similarly expressed by LNGFR$^+$

and LNGFR$^-$ Tregs indicating no immediate effects on the phenotype of CAR-Tregs (Figure 14A). To provide a more comprehensive phenotypic analysis, gene expression of several Treg-associated markers (*foxp3, ctla4, ikzf4*, *tigit*, *ikzf2*, *tnfrsf9*, *tgfb1*) and pro-inflammatory cytokines (*il2, ifnγ, tnf, il5, csf2*) were analysed after polyclonal stimulation. LNGFR$^+$ Tregs expressed similarly high levels of Treg markers compared to LNGFR$^-$ Tregs and lacked expression of pro-inflammatory cytokines (Figure 14B). Although expression of *ctla4* and *ikzf4* was low, this was not dependent on CAR expression and was similarly observed in LNGFR$^-$ Tregs. Collectively, there was no apparent influence of CAR expression on the Treg phenotype which was maintained by CAR-Tregs.

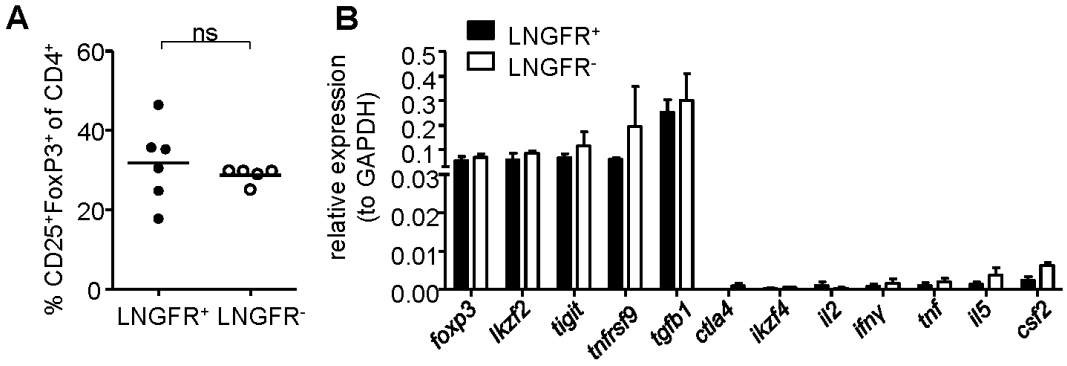

Figure 14: Phenotype of CAR-Tregs. (A) LNGFR$^+$ Tregs and LNGFR$^-$ Tregs were sorted and expanded for 10 days before staining of FoxP3 (n=5-6 from 2 independent experiments). **(B)** Transduced Tregs were activated for 6h with anti-CD3/-CD28 and LNGFR$^+$ Tregs and LNGFR$^-$ Tregs were sorted for gene expression analysis (n=3, 1 experiment was performed). **(A)** Statistical significance was analysed by Mann Whitney test. **(A)** Each dot represents one donor, line indicates mean; **(B)** mean + SEM is shown.

4.2.2 CD137 expression identifies antigen-activated CAR-Tregs

Here, Treg specificity was redirected toward an exogenous antigen by expression of a dextran-specific CAR. CAR-Tregs maintained their Treg phenotype (Figure 14A,B) and bound dextran (Figure 13D-F), but their functionality requires efficient signal transduction and Treg activation. To date, lack of Treg-specific activation markers has limited identification, isolation and characterization of antigen-reactive Tregs on a single cell level. CD137 has been described to be upregulated specifically on Tregs after short-term antigen-specific stimulation *ex vivo* and was furthermore shown here to identify activated Tregs after prior *in vitro* expansion [92, 96, 97, 107].

CD137 expression was analysed on transduced Tregs after 6h stimulation with dextran to determine antigen-specific activation of CAR-Tregs. Although the origin and function of $CD137^+CD154^+$ Tregs remain unclear, they only represented a small subset within the Treg compartment and clearly exhibited a partial Treg signature (see 4.1). Therefore, expression of CD137, regardless of CD154 expression, was analysed to determine activation of CAR-Tregs. CD137 was upregulated selectively on $LNGFR^+$ Tregs while $LNGFR^-$ Tregs within the same culture were not activated (Figure 15A,B). These data were in line with the selective binding of dextran by $LNGFR^+$ cells and show efficient activation of CAR-Tregs upon antigen-binding. As dextran was not bound by all $LNGFR^+$ cells (Figure 13E), CAR-Tregs were activated with FITC-Dextran to directly track activation of antigen-binding cells. Dextran-binding was stable over the time of stimulation showing stable receptor-ligand interaction enabling analysis of dextran-binding cells after 6h stimulation (Figure 15D). Following activation, CD137 was upregulated selectively on cells that had bound dextran showing specific activation of dextran-binding cells while indicating only minor unspecific activation (Figure 15C,E).

CD137 has been shown to be upregulated on Tregs upon TCR stimulation and was now applied to the identification of antigen-activated CAR-Tregs. The selective induction of CD137 on $LNGFR^+$ CAR-Tregs already indicated that expression was induced upon CAR-mediated stimulation. Nevertheless, to directly control that CD137 expression was induced by CAR and not TCR stimulation, down-regulation of CD3 as pivotal event in endogenous T cell activation was analysed after 6h stimulation [250]. CD3 was down-regulated on $CD137^+$ cells upon TCR but not CAR stimulation confirming that CD137 expression was induced by CAR-mediated stimulation independent of the endogenous TCR (Figure 15F). Since CD137 expression enabled rapid analysis of CAR-Treg activation *in vitro*, cross-reactivity with other polysaccharides was again evaluated by CD137 expression after 6h incubation with glucose, maltose and dextrin. In line with the selective binding of dextran (Figure 13F), CAR-Tregs were not activated with other saccharides whereas bead-bound and soluble (500,000g/mol and 2,000,000 g/mol) dextran induced CD137 upregulation (Figure 15G). These data underline the antigen-specificity of CAR-Tregs and demonstrate the potency of CD137 expression for the detection of antigen-activated CAR-Tregs. Taken together, these data show redirection of Treg specificity toward an exogenous antigen by expression of a dextran-specific CAR. CAR-Tregs selectively bound dextran and antigen-specific activation could readily be identified by CD137

expression which emerges as marker for the rapid analysis of CAR-mediated Treg activation *in vitro*.

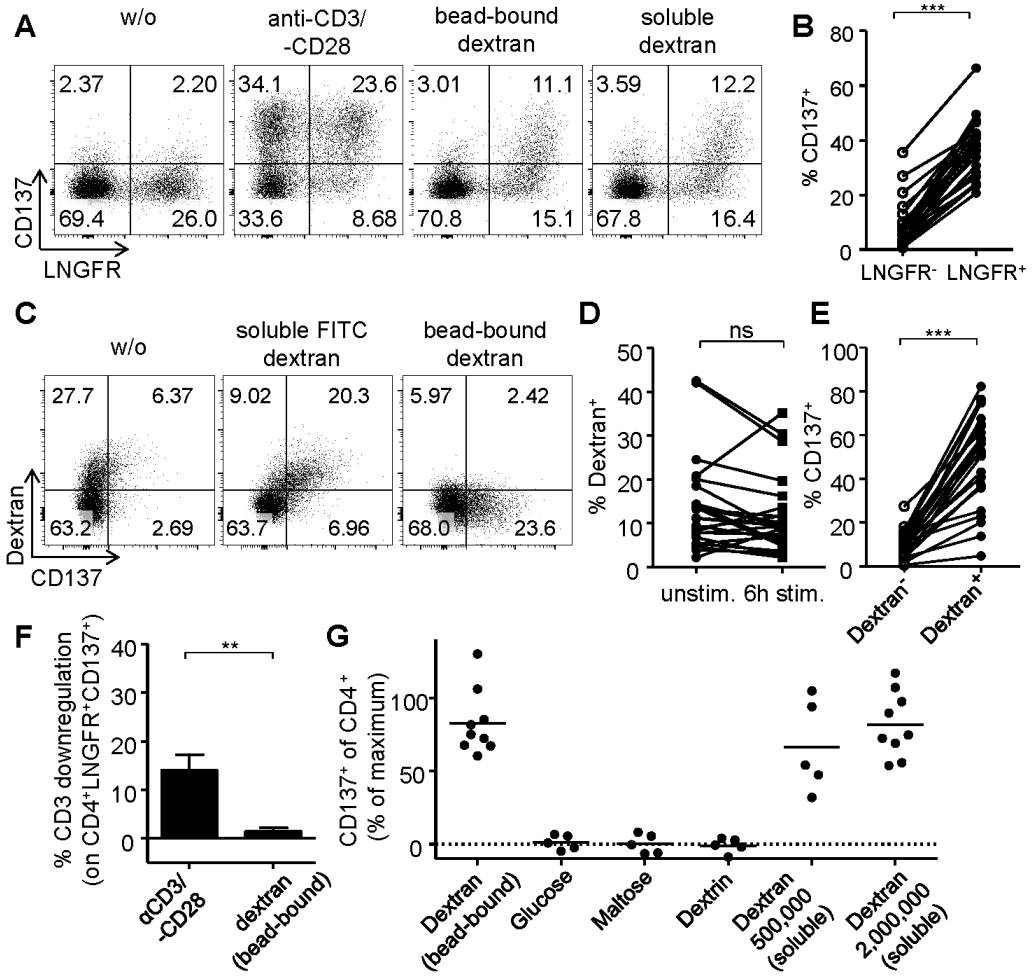

Figure 15: CD137 expression identifies antigen-activated CAR-Tregs. (A-G) CAR-Tregs were activated for 6h before analysis. **(A,B)** CD137 expression on LNGFR$^+$ Tregs and LNGFR$^-$ Tregs is shown; **(A)** representative dot plot of one donor and **(B)** statistical analysis of several donors (n=21, 7 experiments were performed). **(C-E)** Activation of dextran-binding cells was analysed; **(C)** representative dot plot of one donor and **(D-E)** statistical summary of several donors (n=25, 9 experiments were performed). **(D)** Dextran-binding was analysed after 6h stimulation with FITC-labeled dextran (6h stim.) compared to staining of unstimulated samples (unstim.); **(E)** CD137 expression was analysed on dextran$^+$ and dextran$^-$ cells. **(F)** CD3 surface expression was analysed after 6h stimulation with anti-CD3/-CD28 or bead-bound dextran (n=11, 4 experiments were performed); downregulation was calculated as ((A-B)/A)x100 with CD3 expression on A: unstimulated LNGFR$^+$ Tregs and B: CD137$^+$LNGFR$^+$ Tregs. **(G)** Specificity of CAR-Tregs was analysed by CD137 expression after incubation with different saccharides, unstimulated background was subtracted from each sample and CD137 expression was normalized to the maximum of dextran-binding cells in the unstimulated sample (n=5-9, 2-3 experiments were performed). **(B,D,E,F)** Statistical significances were calculated by paired t tests. **(B,D,E,G)** Each dot represents one donor, lines indicate mean; **(F)** mean + SEM is shown.

4.2.3 Optimizing CAR design for augmented Treg efficacy

CAR-Tregs were generated by lentiviral transduction and dextran-specific activation was shown *in vitro* (see 4.2.1 and 4.2.2). However, functionality of CAR-Tregs can strongly depend on the structure of the construct and therefore efficacy of CAR-Treg therapy requires optimization of CAR design for improved Treg function. To date, studies that have investigated the impact of CAR design on T cell function have focused on effector cells as analysis of Treg activation has been limited by lack of specific activation markers. In this study, CD137 was identified as marker that was specifically upregulated on antigen-activated CAR-Tregs separating them from CD154-expressing Tcons. Therefore, analysis of CD137 expression provides the opportunity to selectively evaluate the impact of CAR design on Treg function within *in vitro* cultures enabling the optimization of CAR-Treg efficacy.

4.2.3.1 The extracellular spacer domain affects CAR-Treg activation

CAR-Treg activation requires stable antigen-binding which can be influenced by the extracellular spacer domain. Indeed, it has been shown that the extracellular spacer significantly influences CAR-T cell activation depending on the size, structure and expression pattern of the target antigen [251-257]. Dextran is a very large polysaccharide and therefore antigen-binding can be particularly dependent on the size and flexibility of the extracellular spacer. To analyse the impact of the size of the spacer domain on antigen-binding and CAR-Treg activation, dextran-specific CAR-Tregs with long (L, 228aa), medium (M, 119aa), short (S, 45aa) and very short (XS, 12aa) extracellular spacer domains that contained IgG4-derived (L, M, XS) or CD8-derived (S) hinges were generated (Figure 16A) [253]. Efficiency of lentiviral transduction as determined by LNGFR expression was similar between constructs (Figure 16B), but major differences in antigen-binding were observed within transduced cells (Figure 16C). Most efficient binding was facilitated by S domains although binding was also observed by L and XS spacers albeit at lower frequencies (Figure 16C). In contrast, binding was almost completely abrogated by M spacer domains revealing significant differences in antigen-binding by variable spacer lengths (Figure 16C). To investigate the impact of the spacer domain on CAR-Treg activation, CD137 expression was analysed after dextran-specific stimulation. Since antigen-binding was highly variable between constructs, activation was analysed directly on cells that had bound dextran. Following 6h stimulation with soluble FITC-Dextran, CAR-Tregs with an XS spacer were activated most efficiently whereas other domains failed to initiate Treg

activation in spite of antigen-binding (Figure 16D). Interestingly, S spacer domains that exhibited the most efficient antigen-binding (Figure 16C), were not activated by dextran suggesting insufficient stability of the receptor-ligand interaction that failed to initiate intracellular signaling and Treg activation. These data show that antigen-binding *per se* was not sufficient to mediate CAR-Treg activation and highlight the potential of CD137 expression to rapidly analyse *in vitro* Treg activation for optimized CAR design.

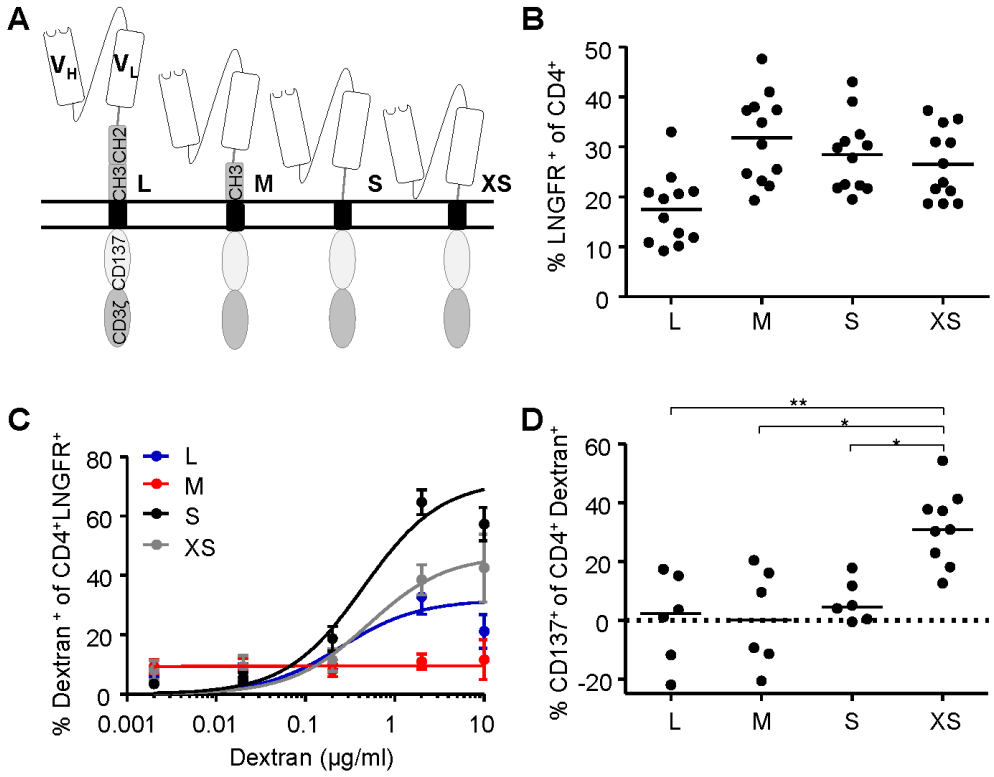

Figure 16: The impact of the extracellular spacer domain on CAR-Treg activation. (A) Schematic diagram of CAR constructs with different spacer lengths (L=large, M=medium, S=small, XS=very small). **(B)** LNGFR expression (n=12, 4 different experiments were performed) and **(C)** dextran-binding are shown (n=3-9, 1-3 different experiments were performed). **(D)** CD137 expression was analysed after restimulation with soluble FITC-Dextran, expression on unstimulated samples was subtracted (n=6-9, 2-3 independent experiments). **(D)** Statistical significances were calculated by Kruskal-Wallis test. **(B,D)** Each dot represents one donor, lines indicate **(B)** mean or **(D)** median; **(C)** mean ± SEM is shown.

4.2.3.2 The impact of co-stimulation on CAR-Treg function

Comparison of different spacer domains revealed a significant impact of CAR design on antigen-binding and CAR-Treg activation. Following antigen-binding, signal transduction is mediated by the intracellular signaling domain which is derived from the endogenous TCR complex. The addition of one (2^{nd} generation CAR) or two (3^{rd} generation CAR) co-stimulatory domains (e.g. CD28, CD137) to the CD3ζ signaling domain have been shown to increase persistence, proliferation and effector functions of $CD4^+$ and $CD8^+$ CAR-T cells *in vitro* and *in vivo* [258-265]. To evaluate the impact of co-stimulation on CAR-Treg function *in vitro*, dextran-specific CAR constructs consisting of an optimized XS spacer domain combined with different co-stimulatory domains (CD28, CD137, ICOS, CD134, PD-1) together with CD3ζ or CD3ε signaling were generated (Figure 17A).

LNGFR expression was similar between constructs (Figure 17B), but there was high variability in the efficiency of dextran-binding within transduced cells (Figure 17C). Particularly CAR-Tregs with ICOS co-stimulation and CDε signaling exhibited significantly reduced binding of dextran even within transduced $LNGFR^+$ cells showing inefficient CAR expression on the surface or an inability to bind dextran in spite of CAR expression (Figure 17C). It has been shown that steric effects can affect stability of CAR complexes which can provide an explanation for instability of these particular constructs [266-268]. Nevertheless, most commonly used domains including CD3ζ with CD28, CD137, CD134 or no co-stimulation were similarly expressed and could therefore be compared in regard to their ability to activate Tregs (Figure 17C). To investigate the effect of different co-stimulatory domains on Treg activation, expression of CD137 was analysed after 6h stimulation with bead-bound dextran. As expected, constructs that failed to bind dextran did not induce CD137 expression once more underlining the specificity of CD137 expression to identify antigen-activated CAR-Tregs (Figure 17C,D). Interestingly, among CAR-Tregs that exhibited functional antigen-binding, CAR-Tregs were only activated with CD137 or to a lesser extent CD134 co-stimulation, but not with other commonly used signaling moieties such as CD28-CD3ζ or CD3ζ alone (Figure 17D). These data reveal a striking impact of co-stimulation on CAR-Treg activation which can rapidly be analysed by CD137 expression. Interestingly, Tregs were shown to benefit from CD137, but not CD28 co-stimulation suggesting a significant impact of intracellular signaling on CAR-Treg functionality. Collectively, CD137 expression can contribute to the optimization of CAR-Treg efficacy by rapid *in vitro* screening of Treg activation.

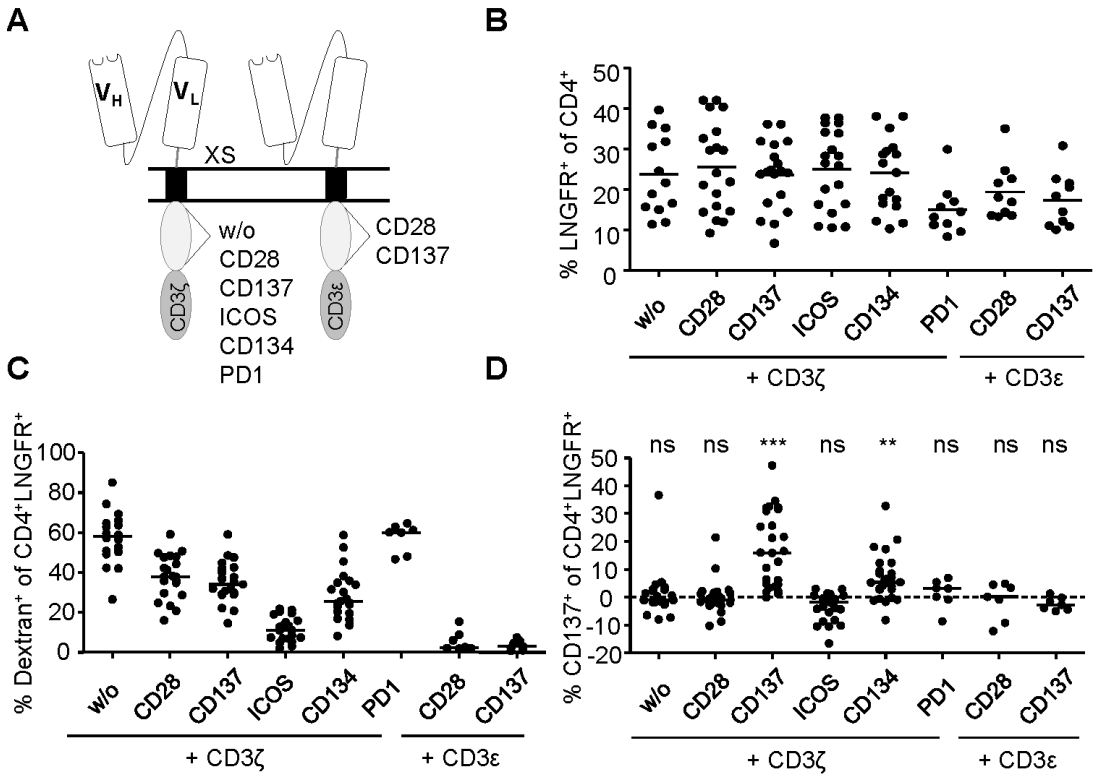

Figure 17: The impact of co-stimulation on CAR-Treg activation. (A) Schematic diagram of CAR constructs with different signaling domains. **(B)** LNGFR expression (n=10-19 from 3-6 different experiments) and **(C)** dextran-binding (n=7-21 from 2-7 independent experiments) are shown. **(D)** CD137 expression was analysed after restimulation with bead-bound dextran, CD137 expression of unstimulated samples was subtracted (n=7-26, 2-8 different experiments were performed). **(D)** Statistical significances were calculated by Wilcoxon signed rank test and indicate activation above background. **(B-D)** Each dot represents one donor and lines indicate the **(B)** mean or **(C,D)** median.

Analysis of CAR-Treg activation revealed that commonly used CD28 co-stimulation did not induce Treg activation in spite of efficient antigen-binding (Figure 17C,D). Thus, the CAR was expressed on the cellular surface but failed to provide intracellular signaling which can derive from insufficient co-stimulation or dysfunctional signaling domains. To investigate the functionality of the constructs and to elucidate the ability of the different signaling domains to initiate proximal signaling, phosphorylation of the protein tyrosine kinase ZAP70 was analysed. Upon TCR stimulation, ZAP70 is phosphorylated (pZAP70) after recruitment to ITAMs within CD3ζ initiating early signaling events [269]. Upon stimulation with soluble dextran, pZAP70 was only detected in $LNGFR^+$ Tregs but not in $LNGFR^-$ cells confirming its selective phosphorylation after CAR-mediated activation (Figure 18A,B). Phosphorylation in constructs containing CD3ε was completely absent and also CD3ζ-ICOS signaling did not initiate proximal signaling

events (Figure 18B). These data are in line with lack of antigen-binding and confirm the specificity of ZAP70 phosphorylation in dextran-reactive CAR-Tregs (Figure 17C). Interestingly, high frequencies of pZAP70 were detected in CAR-Tregs with CD28 or no co-stimulation although there was no CD137 upregulation (Figure 18B, Figure 17D). These data show that antigen-binding by these constructs induced proximal signaling events which yet did not result in Treg activation providing further evidence for the heightened potential of CD137 co-stimulation for CAR-Treg activation.

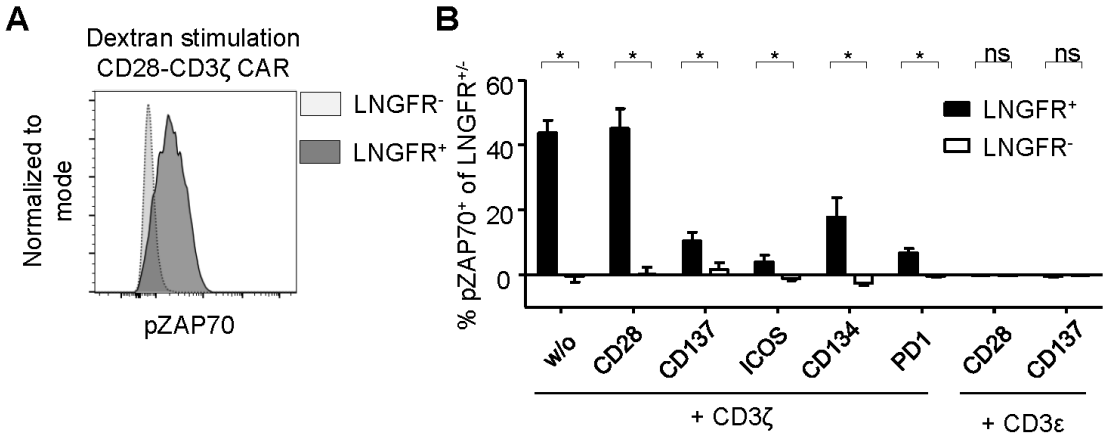

Figure 18: ZAP70 phosphorylation upon CAR-Treg activation. (A-B) Phosphorylation of ZAP70 in LNGFR$^+$ Tregs and LNGFR$^-$ Tregs was analysed after 5min incubation with soluble dextran; **(A)** representative histogram of one sample and **(B)** statistical summary of several donors and constructs (n=7, 2 independent experiments were performed). **(B)** Statistical significances were calculated by paired t test, mean + SEM is shown.

In contrast to other studies that have generated human CAR-Tregs with CD28 co-stimulation [230-232], dextran-specific CAR-Tregs were not activated by CD28-CD3ζ signaling although functionality of the CD28-CD3ζ CAR was confirmed by initiation of proximal signaling events (Figure 17D, Figure 18B). To further analyse the impact of co-stimulation on T cell activation and to investigate potential differences in the signaling requirements of Tregs and Tcons, activation of CAR-expressing CD4$^+$ Tcons was analysed. Tcons were transduced with different CD3ζ-CAR constructs containing CD28, ICOS, CD137, CD134 or no co-stimulation. Dextran was bound by LNGFR$^+$ Tcons, although levels were lower in CAR-Tcons with ICOS co-stimulation (Figure 19A). These findings provide further evidence for overall instability of some CARs. Next, activation of CAR-Tcons by bead-bound dextran was analysed by expression of the Tcon-specific activation marker CD154 [106, 107]. Interestingly, differences in Tcon activation were less pronounced compared to Tregs with notable CAR-Tcon activation

with CD28, CD137, CD134 or no co-stimulation (Figure 19B). Only low levels of activation were observed with ICOS co-stimulation which also exhibited reduced binding of dextran (Figure 19A). However, overall levels of CD154 induction were low and variable between donors (Figure 19B). To directly compare efficiency of the most commonly used signaling domains with CD137 and CD28 co-stimulation, activated $CD154^+$ CAR-Tcons were sorted after 6h stimulation with bead-bound dextran and expanded before restimulation. Isolation of antigen-specific CAR-Tcons enabled the direct comparison of dextran-reactive cells and therefore could reveal a potential impact of small differences that were observed within bulk cultures (Figure 19B). Following restimulation, CAR-Tcons with CD137 and CD28 co-stimulation were activated although CD28 co-stimulation was even slightly more efficient (Figure 19C). These findings are in line with the higher potency of CD28-CD3ζ signaling that was observed in bulk cultures (Figure 19B). These data further confirm overall functionality of CARs with CD28-CD3ζ signaling and show that different co-stimulatory domains can have a variable impact on Tcons and Tregs. Therefore, functionality of different constructs needs to be evaluated separately which can rapidly be determined by converse expression of CD137 and CD154 on Tregs and Tcons, respectively.

It was shown that CD28 co-stimulation had a significantly different impact on Tcons and Tregs. To investigate whether this differential activation derived from differences in proximal signaling events, ZAP70 phosphorylation was analysed after dextran-specific stimulation of CAR-Tcons. Interestingly, ZAP70 phosphorylation was similar to Tregs with higher levels of pZAP70 with CD28 co-stimulation compared to CD137 (Figure 19D). Therefore, it can be speculated that ZAP70 phosphorylation was more potent in inducing downstream signaling in Tcons with CD28 co-stimulation compared to Tregs. These data show that similar proximal signaling events can have a differential impact on the activation of Tregs and Tcons indicating differences in the signal transduction downstream of ZAP70 phosphorylation. Taken together, functionality of the CD28-CD3ζ CAR construct was confirmed by analysis of CAR-Tcon activation and was shown to exhibit augmented potency compared to CD137 co-stimulation in Tcons. Therefore, it can be speculated that activation of Tregs and Tcons was dependent on differential signaling requirements upon CAR-mediated stimulation. While CD28-CD3ζ was potent in activating CAR-Tcons, CAR-Tregs required CD137-CD3ζ signaling for efficient activation.

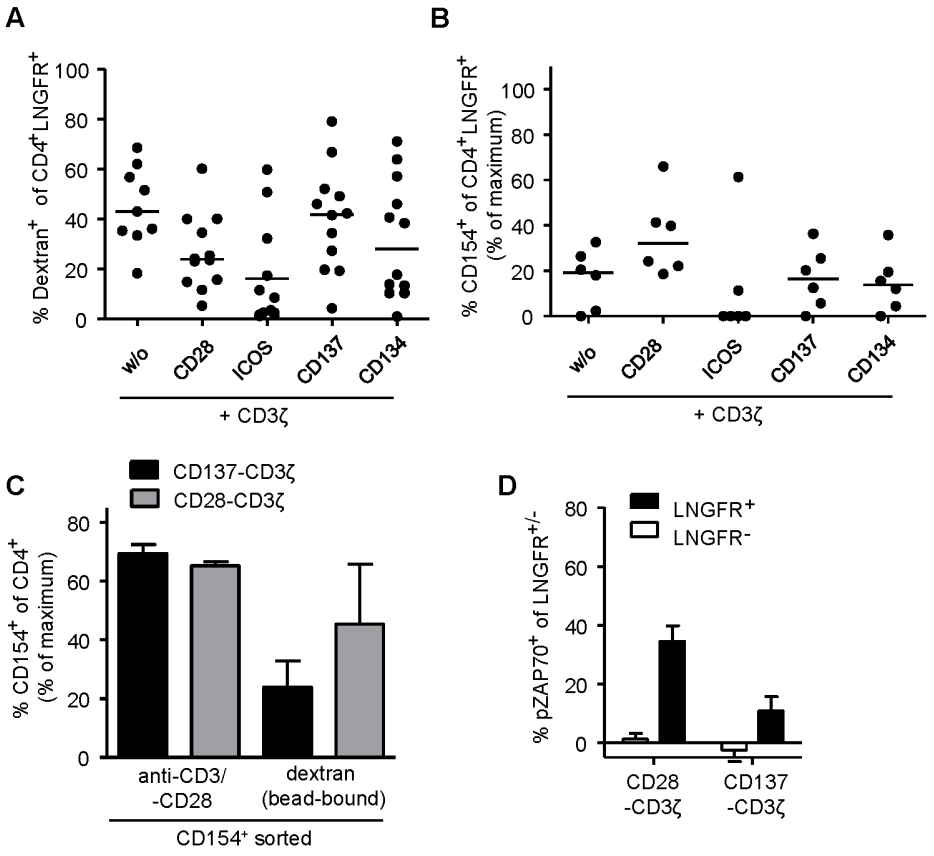

Figure 19: The impact of co-stimulation on conventional CAR-T cells. (A-B) $CD4^+$ Tcons were transduced and restimulated for 6h. **(A)** Dextran-binding of unstimulated samples (n=9-12, 3-4 independent experiments were performed) and **(B)** CD154 expression after stimulation with bead-bound dextran are shown (n=6, 2 independent experiments were performed), unstimulated background was subtracted from each sample and CD154 expression was normalized to the maximum of dextran-binding cells in the unstimulated sample. **(C)** $CD154^+$ Tcons were sorted after 6h stimulation with bead-bound dextran and expanded before restimulation with anti-CD3/-CD28 or bead-bound dextran (n=6 for CD137-CD3ζ and n=3 for CD28-CD3ζ from 1 experiment). **(D)** Phosphorylation of ZAP70 in $LNGFR^+$ and $LNGFR^-$ T cells was analysed after 5min incubation with soluble dextran (n=3-6 from 2 independent experiments). **(A,B)** Each dot represents one donor, lines indicate median; **(C,D)** mean + SEM is shown.

It was shown here that CD137, but not CD28 co-stimulation induced dextran-specific CD137 expression on CAR-Tregs (Figure 17D). However, co-stimulatory domains have not only been described to influence immediate T cell activation, but to contribute to persistence and proliferation of CAR-T cells *in vivo* [270]. To elucidate differences between CAR constructs upon dextran-specific expansion *in vitro*, CAR-Tregs with different signaling domains were expanded in the presence of anti-CD3/-CD28 or bead-bound dextran. LNGFR was stained on expanded cultures at the beginning of the culture and on d17 after antigen-specific expansion. Enrichment of $LNGFR^+$ cells was calculated based on the ratio of $LNGFR^+$ and $LNGFR^-$ cells at the beginning and end of

the culture. Enrichment of CAR-Tregs with CD137 and CD134 co-stimulation was more pronounced compared to other co-stimulatory domains after dextran-specific expansion whereas polyclonal activation did not specifically enrich CAR-Tregs (Figure 20A,B). These findings indicate stronger proliferation of CAR-Tregs with CD137 and CD134 co-stimulation providing them with a selective advantage compared to LNGFR$^-$ cells in the same culture. These findings are in line with superior activation of CAR-Tregs with CD137 and to a lesser extent CD134 co-stimulation (Figure 17D). However, differences between CARs were low with strong variations between donors and experiments. It is important to note that Tregs were activated with anti-CD3/-CD28 *ex vivo* to enable efficient lentiviral transduction. Polyclonal stimulation was removed before antigen-specific expansion of CAR-Tregs and therefore dextran was supposed to serve as specific stimulus for CAR-Tregs for the time of the culture. Nevertheless, unspecific proliferation as result of the original stimulation cannot be excluded and can contribute to the high variability.

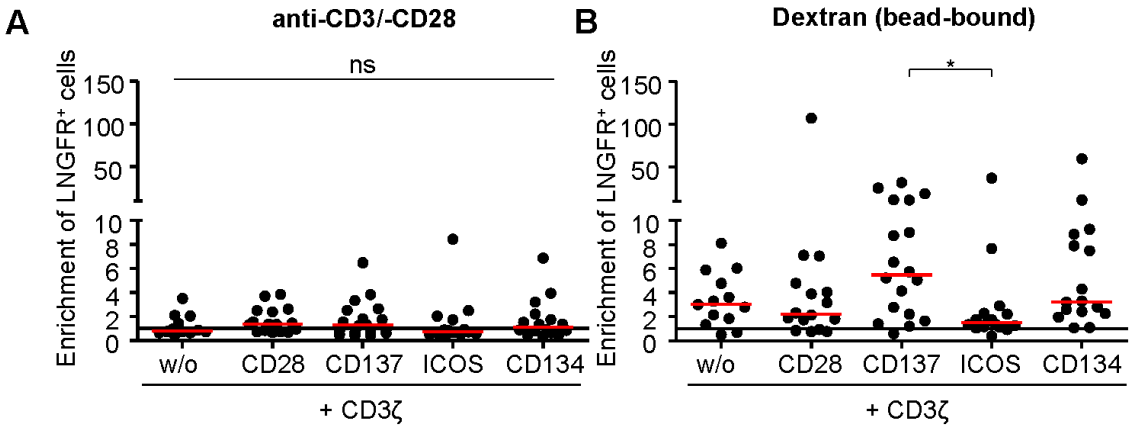

Figure 20: Expansion of CAR-Tregs with different signaling domains. (A-B) Tregs were expanded in the presence of **(A)** anti-CD3/-CD28 or **(B)** bead-bound dextran and enrichment of LNGFR$^+$ cells on d17 was calculated as the ratio of LNGFR$^-$/LNGFR$^+$ Tregs on d0 multiplied with the ratio of LNGFR$^+$/LNGFR$^-$ Tregs on d17 (n=13-18 from 4-6 independent experiments). Statistical significances were calculated by Kruskal-Wallis test; each dot represents one donor with lines representing the **(A)** median or **(B)** mean.

High variability was observed when CAR-Tregs with different signaling domains were expanded separately *in vitro*. Therefore, comparison of the different constructs within a competitive setting was to enable direct comparison within a single culture. To this end, CAR-Tregs with different signaling domains were pooled and expansion of the different constructs was determined by quantitative real-time PCR (qPCR). Separation of constructs was enabled by specific primers that were spanning construct-specific

regions within the intracellular signaling domains (Table 8). To account for different efficiencies of the PCR reactions depending on the primers, relative expression levels were determined at the beginning of the culture to which subsequent expression levels were normalized.

Upon dextran-specific expansion of pooled CAR-Tregs with different signaling domains, there was an enrichment of $LNGFR^+$ cells only in the presence of dextran compared to stimulation with anti-CD3/-CD28 showing selective enrichment of CAR-Tregs (Figure 21A). It is important to note that the beads that were used for polyclonal stimulation also contained dextran and could therefore also be bound by the CAR. However, their high affinity for CD3 and CD28 most likely favors interaction with the TCR and therefore selective expansion of $LNGFR^+$ cells was only observed at later time points of polyclonal expansion (Figure 21A). To ensure that enrichment of $LNGFR^+$ cells during dextran-specific expansion was not merely a result of apoptosis of $LNGFR^-$ cells, absolute expansion was determined. Similar levels of expansion were detected within cultures expanded with bead-bound dextran or anti-CD3/-CD28 showing that accumulation of $LNGFR^+$ cells was a result of antigen-specific expansion of CAR-Tregs (Figure 21B).

Antigen-specific expansion of pooled CAR-Tregs with different signaling domains resulted in expansion of $LNGFR^+$ cells. To investigate a potential outgrowth of a particular construct within this pooled culture, relative expression of the different signaling domains was determined by qPCR and normalized to the beginning of the culture. To exclude high variability based on differential transcription of the constructs, genomic DNA was used as template. Within this competitive co-culture, there was selective expansion of CAR-Tregs with CD137-CD3ζ signaling in the presence of dextran while polyclonal expansion did not favor any construct (Figure 21C,D). Therefore, CD137 provided the most potent co-stimulation for dextran-specific expansion of CAR-Tregs *in vitro*. Although CD28 co-stimulation did not induce CD137 expression in almost all donors (Figure 17D), there was significant ZAP70 phosphorylation and also expansion in some donors indicating a certain degree of functionality (Figure 21D). Conversely, CD134 co-stimulation induced CD137 expression in some cells (Figure 17D), yet it did not provide an advantage for proliferation suggesting suboptimal co-stimulation (Figure 21D). Therefore, functionality of e.g. CD28 or CD134 co-stimulation cannot be excluded although it appeared to be highly variable. In contrast, CD137-CD3ζ signaling was shown to consistently correlate

with increased functionality in almost all donors including potent *in vitro* activation and expansion indicating their overall heightened potential.

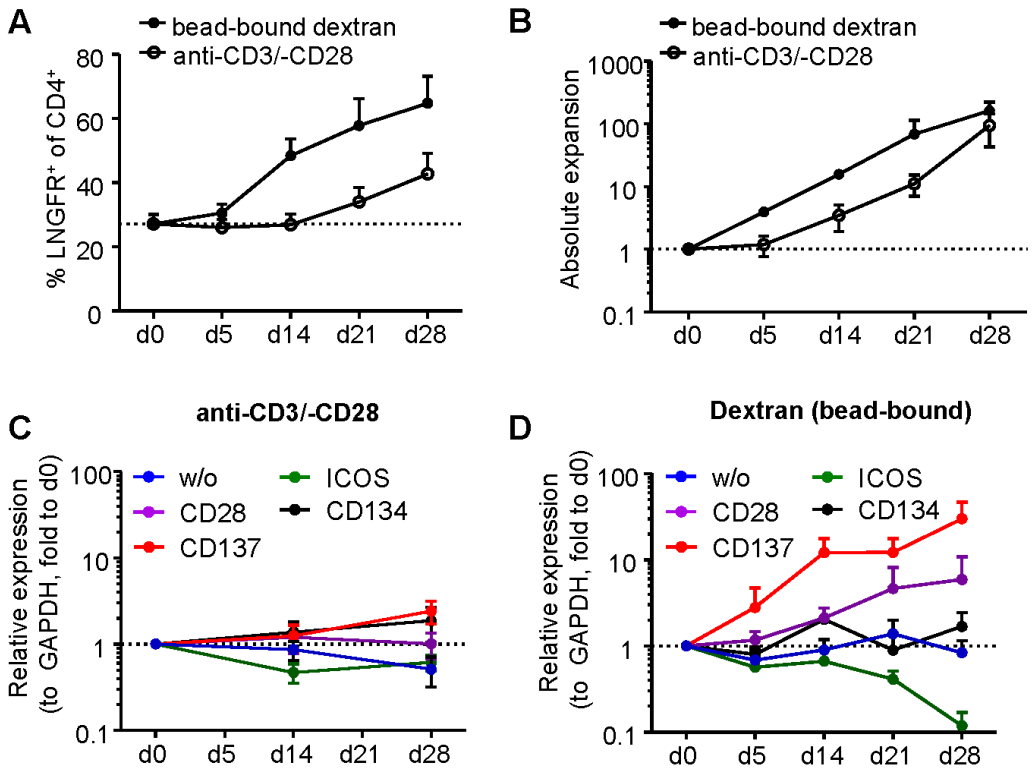

Figure 21: Expansion of CAR-Tregs with different signaling domains in a competitive co-culture. (A-D) CAR-Tregs with different signaling domains were pooled and expanded in the presence of anti-CD3/-CD28 or bead-bound dextran. **(A)** LNGFR expression and **(B)** absolute expansion were analysed (n=5-7, 2-3 different experiments were performed). **(C-D)** Relative expression of the different signaling domains after expansion with **(C)** anti-CD3/-CD28 or **(D)** bead-bound dextran was quantified by qPCR (n=7, 3 different experiments were performed). **(A-D)** Mean + SEM is shown.

Taken together, CD137 expression emerges as Treg-specific activation signature that can be applied to the rapid analysis of Treg activation *in vitro* which enabled the optimization of CAR-Treg efficacy. CAR-Treg activation was shown to require a very short spacer domain which in combination with CD137-CD3ζ signaling enabled potent activation and expansion of dextran-specific CAR-Tregs *in vitro*.

4.2.4 Isolation of dextran-reactive CAR-Tregs

Treg specificity was redirected toward dextran by CAR expression and receptor design was optimized for augmented Treg functionality. For clinical applications, CAR-Tregs need to be enriched prior to transfer which can be achieved either by antigen-specific expansion or by direct sorting of transduced cells. To evaluate the possibility to enrich CAR-Tregs by antigen-specific expansion, Tregs consisting of an optimized XS spacer and intracellular CD137-CD3ζ signaling were generated and expanded in the presence of bead-bound dextran. During *in vitro* culture in the presence of bead-bound dextran, CAR-Tregs selectively expanded resulting in an enrichment of CAR-Tregs after 2 weeks (Figure 22A). In contrast, expansion with anti-CD3/-CD28 did not favor $LNGFR^+$ Tregs but similarly expanded $LNGFR^-$ cells (Figure 22B). Similar to the high variability that was observed in previous experiments (Figure 20B), purities were variable between experiments and donors and therefore only partially enabled purification of CAR-Treg.

Alternatively, increasing CAR-Treg purity by FACS sorting of transduced cells followed by polyclonal expansion was evaluated. To this end, sorting of $LNGFR^+$ cells was investigated to enrich CAR-Tregs for expansion. In addition, sorting of $CD137^+$ Tregs after dextran-specific stimulation was analysed to increase potency of sorted CAR-Tregs as CD137 expression was shown to specifically identify antigen-activated CAR-Tregs (see 4.2.2). Both sorting strategies similarly enriched $LNGFR^+$ cells and also frequencies of dextran-binding cells were comparable after expansion (Figure 22C,D). However, upon antigen-specific restimulation, CD137 expression was increased when Tregs were sorted by CD137 expression compared to isolation by LNGFR expression (Figure 22E). Furthermore, dextran-reactive cells were almost completely absent within $CD137^-$ sorted cells showing that most antigen-specific CAR-Tregs had expressed CD137 upon the initial stimulation (Figure 22E). These data show that CD137 expression enabled the identification of highly reactive CAR-Treg clones which maintained transgene expression upon expansion. Therefore, CD137 expression emerges as Treg-specific activation marker to isolate potent antigen-reactive CAR-Tregs without prior enrichment of transduced cells.

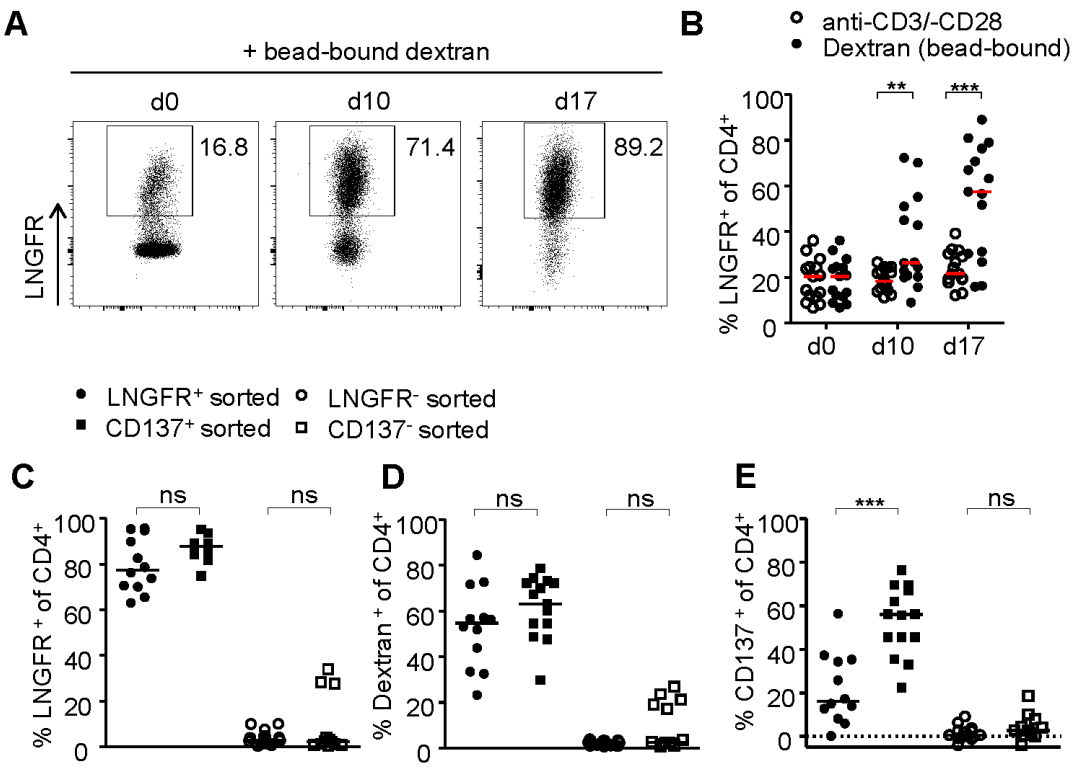

Figure 22: Isolation of CAR-Tregs. (A,B) Tregs were expanded in the presence of anti-CD3/-CD28 or bead-bound dextran and LNGFR expression was analysed on d0, d10 and d17; **(A)** representative dot plot of one donor and **(B)** statistical summary of several donors (n=25 from 5 different experiments). **(C-E)** Unstimulated LNGFR$^+$ Tregs or CD137$^+$LNGFR$^+$ Tregs after 6h stimulation with bead-bound dextran were sorted and expanded with anti-CD3/-28 (LNGFR$^+$ sorted) or without further stimulation (CD137$^+$ sorted) for 14 days before staining of **(C)** LNGFR, **(D)** dextran and **(E)** CD137 expression after restimulation with bead-bound dextran (n=12, 4 independent experiments for LNGFR sorted; n=15, 5 different experiments for CD137 sorted). Statistical significances were calculated by **(B)** paired t test or **(C-E)** Mann Whitney test; **(B-E)** each dot represents one donor, lines indicate median.

CAR-Tregs were specifically activated and expanded by dextran, yet their regulatory potential depends on their suppressive capacities upon antigen-specific activation. Therefore, the *in vitro* potential of dextran-activated CAR-Tregs to suppress Tcons that were activated by allogeneic stimulation was evaluated. CAR-Tregs were enriched by sorting of LNGFR$^+$ cells and by the isolation of dextran-specific CD137$^+$ cells which were shown to be highly reactive after expansion (Figure 22E). LNGFR$^+$ sorted CAR-Tregs were slightly more suppressive than LNGFR$^-$ Tregs at low Tresp-to-Treg ratios (Figure 23A). However, the effect was not dependent on antigen application as it was similarly observed without stimulation (Figure 23B). Likewise, CD137$^+$ sorted Tregs were suppressive, yet the addition of dextran did not have a significant effect and also CD137$^-$ sorted Tregs were similarly able to inhibit Tresp proliferation (Figure 23C,D). These findings either show lack of suppression upon CAR stimulation or are caused by

technical limitations of this *in vitro* assay. It is important to note that Tregs were activated *ex vivo* by anti-CD3/-CD28 for efficient lentiviral transduction and expansion of CAR^+ Tregs and CAR^- Tregs. It can be speculated that this prior expansion induced Treg activation which resulted in unspecific suppression even in the absence of stimulation masking a potential effect of CAR-mediated activation. Furthermore, remaining dextran can be present in unstimulated samples as magnetic particles used for the isolation and expansion consist of dextran and cannot be fully removed from expanded cultures. Therefore, more sensitive *in vitro* assays as well as analysis of *in vivo* suppression are required to elucidate the antigen-specific suppressive potential of dextran-specific CAR-Tregs.

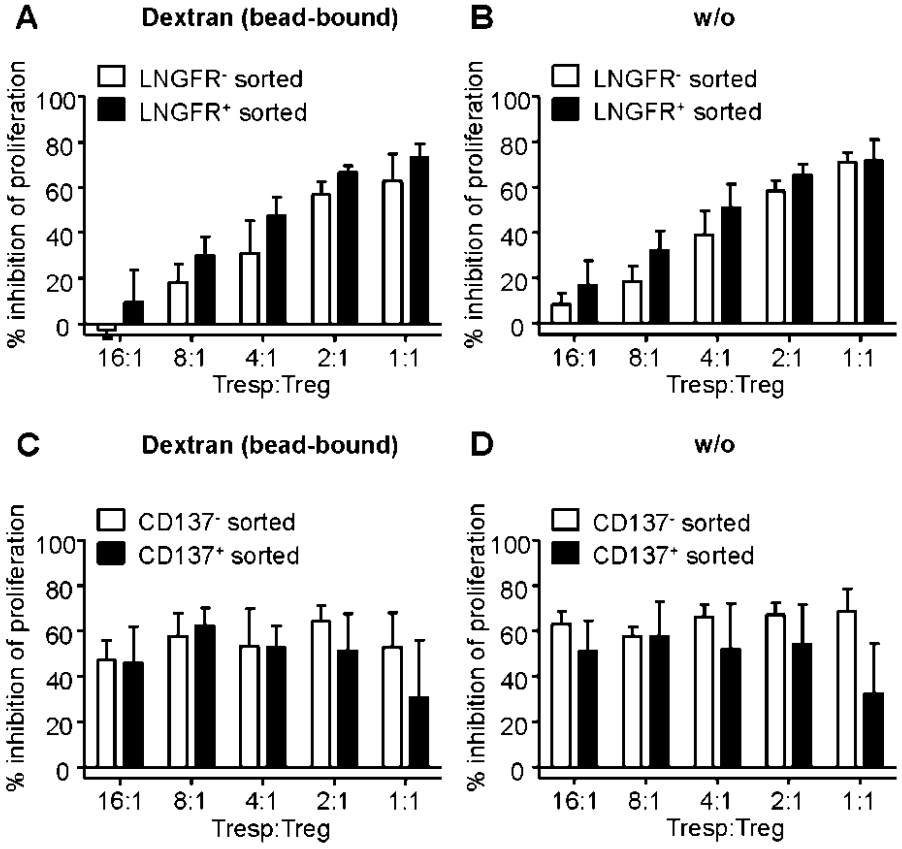

Figure 23: *In vitro* suppressive capacity of CAR-Tregs. (A-D) CAR^+ Tregs and CAR^- Tregs were sorted and expanded with anti-CD3/-CD28 before suppression of allogeneic $CD4^+$ Tresps was analysed in the presence of **(A,C)** bead-bound dextran or **(B,D)** without stimulation (w/o); inhibition of proliferation is shown. **(A,B)** Tregs were sorted based on LNGFR expression (n=5-6, 2 independent experiments were performed). **(C,D)** Tregs were sorted based on CD137 expression after 6h stimulation with bead-bound dextran (n=6, 2 independent experiments were performed). **(A-D)** Mean + SEM is shown.

4.2.5 Purification of stable antigen-reactive CAR-Tregs

In this study, Treg specificity was redirected toward dextran which enabled targeted activation of Tregs upon antigen application. *In vitro* generation of CAR-Tregs can significantly increase efficacy of Treg therapy, yet antigen-specific Tregs with disease-amplifying potential require heightened safety measures regarding Treg instabilities or non-Treg contaminations. CD137 was upregulated on highly reactive, dextran-specific CAR-Tregs upon stimulation and therefore enabled the identification and isolation of potent CAR-Tregs. However, it was shown here that a small subset of $CD137^+$ Tregs co-expressed CD154 after polyclonal stimulation which exhibited an instable Treg-Tcon phenotype including expression of effector cytokines. In contrast, $CD137^+CD154^-$ expression identified epigenetically stable Tregs after 6h polyclonal stimulation *ex vivo* and after prior *in vitro* expansion (see 4.1). Therefore, $CD137^+CD154^-$ expression was to be evaluated for the purification of stable *in vitro* generated antigen-specific CAR-Tregs.

To purify *in vitro* generated CAR-Tregs by co-staining of CD137 and CD154 and to evaluate the potential of this Treg-specific activation signature to identify stable antigen-specific CAR-Tregs, $LNGFR^+$ Tregs were sorted and expanded *in vitro*. Following 6h dextran-specific restimulation, CD137 was selectively upregulated although variable levels of $CD154^+$ cells were also observed (Figure 24A,C). These findings reveal notable frequencies of effector-like cells that were specific for dextran which can provide a significant safety risk regarding therapeutic applications. In line with previous observations after polyclonal stimulation, $CD137^+CD154^-$ expression identified activated CAR-Tregs that expressed high levels of FoxP3 (Figure 24B,D) and low levels of IL-2 and TNF-α (Figure 24E). In contrast, CD137 and CD154 co-expression identified antigen-reactive cells that exhibited an effector-like phenotype with low levels of FoxP3 (Figure 24B,D) and high levels of pro-inflammatory cytokines (Figure 24E). Therefore, dextran-reactive cells with an inflammatory potential can readily be eliminated from expanded cultures by CD154 expression whereas $CD137^+CD154^-$ expression identified antigen-reactive CAR-Tregs that expressed high levels of FoxP3 and lacked expression of effector cytokines.

In summary, human Tregs were engineered to express a dextran-reactive CAR which enabled their *in vitro* redirection toward an exogenous antigen. Stable antigen-specific Tregs were identified by $CD137^+CD154^-$ expression which emerges as Treg-specific

activation signature to optimize CAR design for augmented CAR-Treg efficacy as well as to improve stability and safety of therapeutic Tregs.

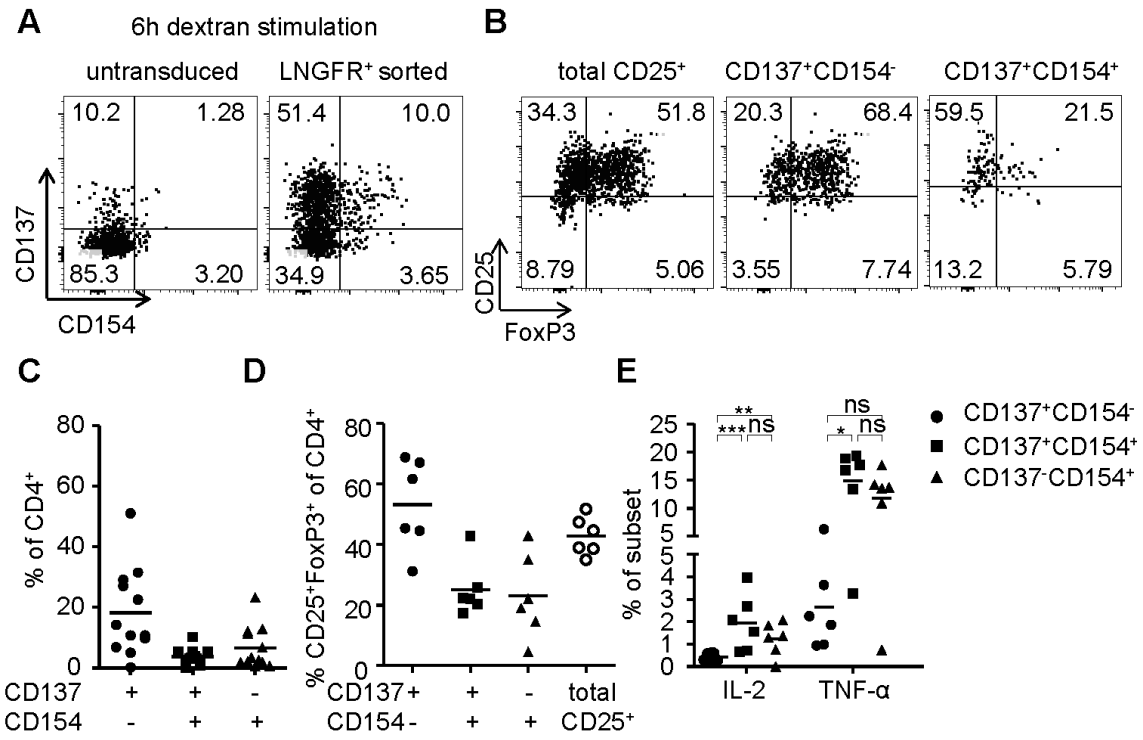

Figure 24: Identification of FoxP3$^+$ CAR-Tregs by CD137$^+$CD154$^-$ expression. (A-E) CAR-Tregs were sorted by LNGFR expression and expanded for 10 days before 6h restimulation with bead-bound dextran. **(A,C)** Expression of CD137 and CD154 (n=12, 4 independent experiments), **(B,D)** FoxP3 and **(E)** IL-2 and TNFα (n=6, 2 independent experiments) were analysed. **(A,B)** Representative dot plot of one donor and **(C,D)** statistical summary of several donors are shown. Statistical significances were determined by **(D)** repeated measures ANOVA or **(E)** Wilcoxon signed-rank test. **(C-E)** Each dot represents one donor, lines indicate mean.

4.3 Heterogeneity and stability of the peripheral Treg compartment

$CD137^+CD154^-$ expression was shown to identify antigen-activated Tregs that exhibited a stable epigenetic and transcriptional Treg signature *ex vivo* and after prolonged *in vitro* expansion. In contrast, a small subset that co-expressed CD137 and CD154 was identified within the peripheral Treg compartment which exhibited an intermediate Treg-Tcon phenotype and expressed significant amounts of effector cytokines (see 4.1 and 4.2.5). These findings clearly show a certain level of heterogeneity and potential instability within the peripheral $CD25^+CD127^-$ Treg compartment that correlates with the expression of CD137 and CD154. In addition to the purification of *in vitro* generated Tregs, long-term stability of Tregs *in vivo* is essential for adoptive Treg transfer, yet little is known about Treg stability in humans. Therefore, comprehensive analysis of $CD137^+CD154^-$ Tregs and $CD137^+CD154^+$ Tregs was to provide insight into the stability and heterogeneity of the physiological Treg compartment in humans.

4.3.1 Heterogeneity within $CD137^+CD154^+$ Tregs

Expression of effector molecules and compromised suppressive capacity within the $CD25^+CD127^-$ Treg compartment were limited to a small $CD137^+CD154^+$ Treg subset *ex vivo* and after prior *in vitro* expansion (see 4.1 and 4.2.5). However, it remains unclear whether this subset represented an inherently stable and functionally distinct population or was characterized by cellular heterogeneity or phenotypic plasticity. To investigate their stability *in vitro*, $CD137^+CD154^+$ Tregs were sorted and expanded before re-analysis of CD137 and CD154 expression. $CD137^+CD154^+$ Tregs gave rise to heterogeneous populations containing cells that had lost either CD137 or CD154 expression following restimulation while others maintained expression of both markers (Figure 25A). These data indicate that $CD137^+CD154^+$ expression was not stably maintained by this subset which rather represented a transient phenotype. Interestingly, cells that had lost CD154 expression were highly positive for FoxP3 expression and lacked expression of effector cytokines while $CD154^+$ cells maintained effector functions (Figure 25B-G). These data suggest that $CD137^+CD154^+$ Tregs were not an inherently stable Treg subset and underline the correlation of $CD137^+CD154^-$ expression with a Treg phenotype. However, it remains unknown whether heterogeneity within $CD137^+CD154^+$ Tregs derived from phenotypic plasticity of

inherently stable clones or identified a transitional state of conversion between the Treg and Tcon compartment.

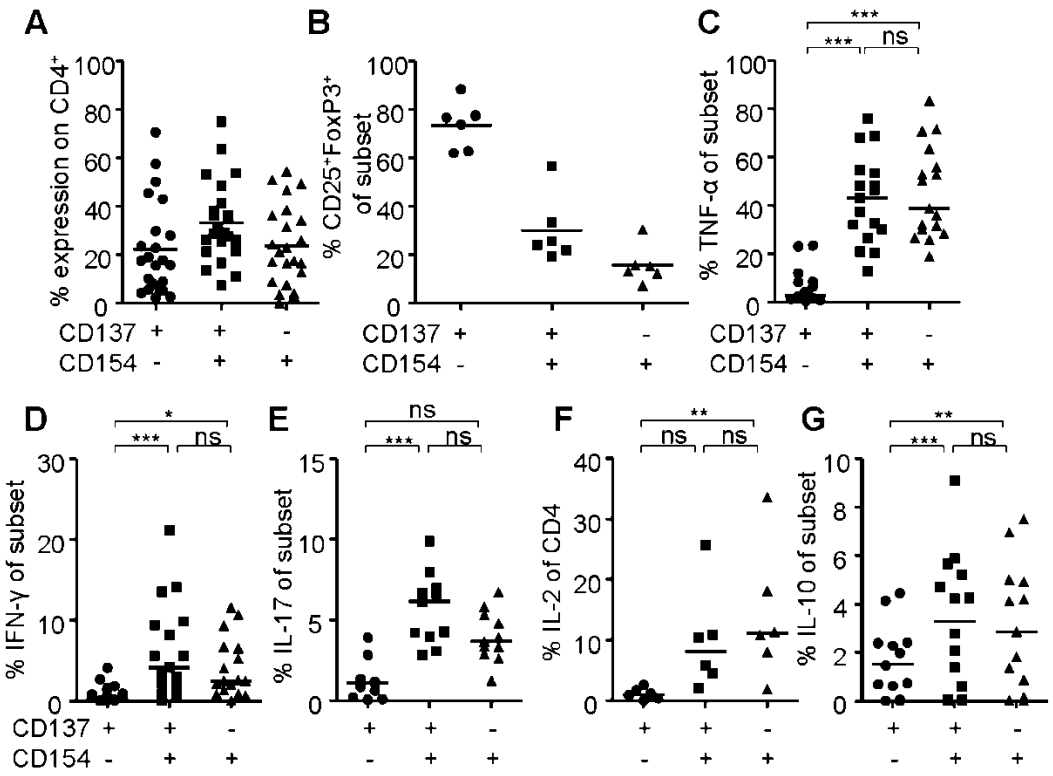

Figure 25: Stability of CD137$^+$CD154$^+$ Tregs. (A-G) CD137$^+$CD154$^+$ Tregs were sorted from expanded Treg cultures and expanded for 10-12 days before analysis of **(A)** CD137 and CD154 expression (n=23, 8 different experiments were performed). Expression of **(B)** FoxP3 (n= 6 from 2 different experiments), **(C)** TNF-α, **(D)** IFN-γ (n=17, 6 independent experiments), **(E)** IL-17 (n=11, 4 different experiments), **(F)** IL-2 (n=8, 2 different experiments) and **(G)** IL-10 (n=14, 5 different experiments) were analysed on CD137/CD154 expressing cells after 6h restimulation with PMA/Ionomycin. Statistical significances were determined by **(C,D,E,F)** Friedman test or **(G)** repeated measures ANOVA. **(A-G)** Each dot represents one donor, lines indicate **(B,C,D,E,F)** median or **(A,G)** mean.

4.3.1.1 Clonal heterogeneity within CD137$^+$CD154$^+$ Tregs

CD137$^+$CD154$^+$ Tregs exhibited and intermediate Treg-Tcon phenotype and also expansion of CD137$^+$CD154$^+$ Tregs revealed notable heterogeneity (see 4.1, Figure 25A-G). These observations can either derive from phenotypic plasticity of inherently stable clones or the occurrence of cellular intermediates of Treg-Tcon conversion. However, within bulk populations the impact of individual clones cannot be determined and therefore the source of heterogeneity cannot be clearly defined. To provide insight into the stability of CD137$^+$CD154$^+$ Tregs on a clonal level, single cell clones were

generated. Similar to bulk populations (Figure 25A), expression of CD137 and CD154 was highly variable between expanded clones but also within individual clonal populations. Some clonal populations completely lost CD154 expression while others maintained co-expression of both markers and only few lost CD137 (Figure 26A,B). These data show once more that $CD137^+CD154^+$ expression was not stably maintained by a distinct Treg subset, but rather reveal heterogeneous expression on a clonal level. Whereas $CD137^+CD154^+$ expression was partly maintained within bulk cultures (Figure 25A), the majority of clonal populations exhibited a $CD137^+CD154^-$ phenotype, although expression of CD154 was variable even within clonal populations (Figure 26B). Since only few populations maintained expression of CD137 and CD154, these data provide further evidence for heterogeneity within $CD137^+CD154^+$ Tregs which was now shown to derive from diversity on a clonal level.

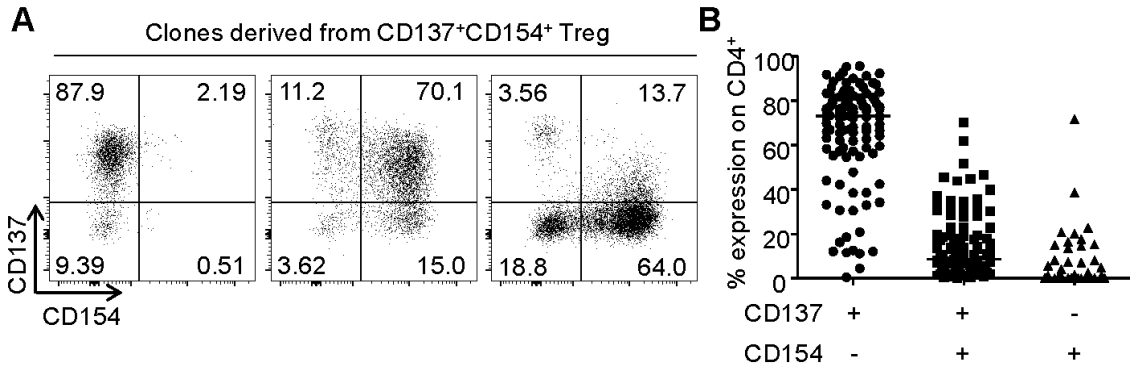

Figure 26: CD137 and CD154 expression on single cell clones within $CD137^+CD154^+$ Tregs. Single cell $CD4^+CD25^+CD127^-CD137^+CD154^+$ Treg clones (2 donors, 2 independent experiments were performed) were sorted and expanded before analysis. **(A-B)** CD137 and CD154 expression were analysed after 6h restimulation with PMA/Ionomycin; **(A)** representative dot plot of individual clonal populations and **(B)** statistical summary of several clones (107 clones). **(B)** Lines indicate median.

Most clones within $CD137^+CD154^+$ Tregs did not maintain co-expression of both markers upon expansion but exhibited variable expression levels of CD137 and CD154 (Figure 26A,B). These findings suggest heterogeneity in regard to CD137 and CD154 expression, yet underlying phenotypic plasticity of individual clones remains elusive. To enable phenotypic analysis of clonal heterogeneity, clonal populations shown in Figure 26 were arbitrarily classified according to their expression of $CD137^+CD154^-$ which was shown to correlate with Treg identity in previous experiments (see 4.1; Figure 11C). To this end, clonal populations that expressed ≥60% $CD137^+CD154^-$ were characterized as Treg-like clones whereas Tcon-like clones were classified as cultures that contained

<60% $CD137^+CD154^-$ cells after expansion (Figure 27A). Within clonal populations derived from $CD137^+CD154^+$ Tregs, cytokine-producing cells were enriched within Tcon-like clones that mostly maintained CD154 expression which was highly significant for TNF-α and IL-2 (Figure 27D). Similarly, IL-10 expression was increased in Tcon-like clones which was in line with its selective expression in CD154-expressing cells within polyclonal cultures (Figure 27C, Figure 5C, Figure 12C). In contrast, FoxP3 expression was similarly heterogeneous in Treg-like and Tcon-like clones (Figure 27B-D) and it has been shown to be less specific for a stable Treg phenotype within clonally expanded populations [271]. Collectively, significant phenotypic differences were observed within clonal populations derived from $CD137^+CD154^+$ Tregs which contained Treg-like clones that lacked expression of effector cytokines and Tcon-like clones that exhibited an effector-like phenotype. Therefore, heterogeneity that was observed regarding CD137 and CD154 expression was reflected on a phenotypic level. However, it remains unclear whether Tcon-like clones represented contaminating effector cells or Tregs that had acquired effector functions. To further investigate the phenotype of Tcon-like clones, their phenotype was compared to clonal populations derived from Tcons. Interestingly, in comparison to clones derived from Tcons, FoxP3 and IL-10 expression were increased in Tcon-like clones (Figure 27B,C) while high levels effector cytokines where mostly detected in clones derived from Tcons (Figure 27D).

Taken together, heterogeneity of $CD137^+CD154^+$ Tregs was shown to derive from diversity on a clonal level revealing Treg-like and Tcon-like clones that differed in the expression of effector cytokines. Although Tcon-like clones exhibited an effector-like phenotype, they did not resemble clones derived from Tcons but were rather characterized by an intermediate Treg-Tcon signature. These data show that diverse expression of CD137 and CD154 on expanded $CD137^+CD154^+$ Tregs correlated with phenotypic heterogeneity which further demonstrates cellular heterogeneity within this subset.

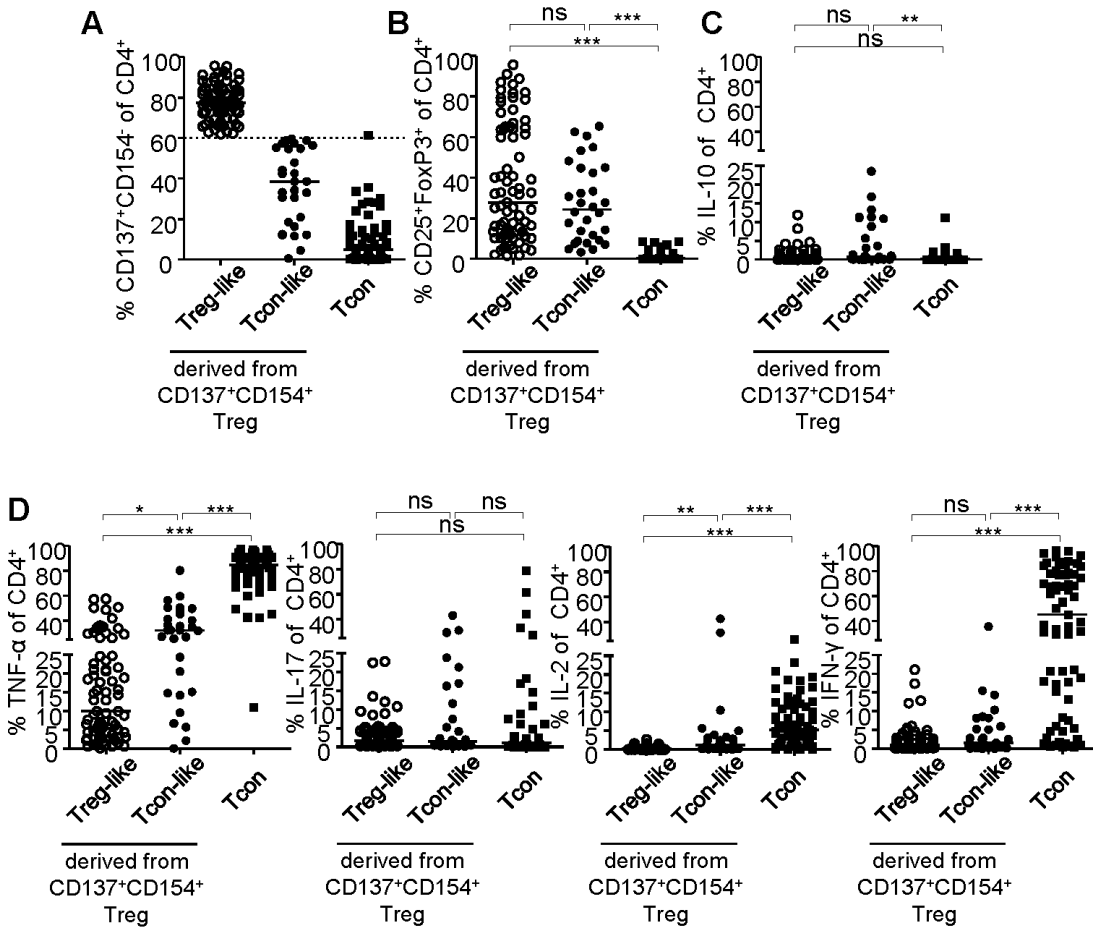

Figure 27: Clonal heterogeneity within CD137$^+$CD154$^+$ Tregs. (A-D) Single cell CD4$^+$CD25$^+$CD127$^-$CD137$^+$CD154$^+$ Treg clones (n=2, 2 independent experiments were performed) and CD4$^+$CD25$^-$CD127$^+$CD45RO$^+$ Tcon clones (n=4, 2 independent experiments were performed) were sorted and expanded before analysis. **(A)** CD137 and CD154 expression and **(C-D)** cytokine expression were analysed after 6h restimulation with PMA/Ionomycin, **(B)** FoxP3 expression was analysed in unstimulated samples. **(A-D)** Clones derived from CD137$^+$CD154$^+$ Tregs were grouped into Treg-like clones (>60% CD137$^+$CD154$^-$ expression) and Tcon-like clones (<60% CD137$^+$CD154$^-$ expression) as shown in **(A)**. A total of 77 Treg-like clones, 30 Tcon-like clones and 69 Tcon clones were analysed. Statistical significances were determined by **(B-D)** Kruskal-Wallis test, lines in **(A-D)** indicate median.

4.3.1.2 Single cell gene expression in CD137$^+$CD154$^+$ Tregs, CD137$^+$CD154$^-$ Tregs and CD137$^-$CD154$^+$ Tcons

Analysis of clonal populations derived from CD137$^+$CD154$^+$ Tregs revealed Treg-like and Tcon-like clones that exhibited differential expression of effector cytokines (Figure 27A-D). To provide insight into heterogeneity and cell-to-cell variation of CD137$^+$CD154$^+$ Tregs directly *ex vivo*, expression of 41 selected target genes (including 2 housekeeping genes) was analysed in 93 single cells derived from

CD137$^+$CD154$^-$ Tregs, 91 cells from CD137$^+$CD154$^+$ Tregs and 47 cells from CD137$^-$ CD154$^+$ Tcons. Based on 39 target genes including e.g. Treg-associated markers, effector cytokines and transcription factors (Figure 28B), principal component analysis (PCA) revealed a complete separation of CD137$^+$CD154$^-$ Tregs and CD137$^-$CD154$^+$ Tcons along PC1 which accounted for most of the variance (28.93%; Figure 28A). These data highlight their distinct transcriptional profiles based on the expression of the analysed target genes. Interestingly, the majority of CD137$^+$CD154$^+$ Tregs clustered closely with CD137$^+$CD154$^-$ Tregs although some were transcriptionally more similar to CD137$^-$CD154$^+$ Tcons (Figure 28A). These findings reflect the heterogeneity that was observed within clonally expanded populations providing further evidence for the co-existence of Treg-like and Tcon-like cells within CD137$^+$CD154$^+$ Tregs.

A

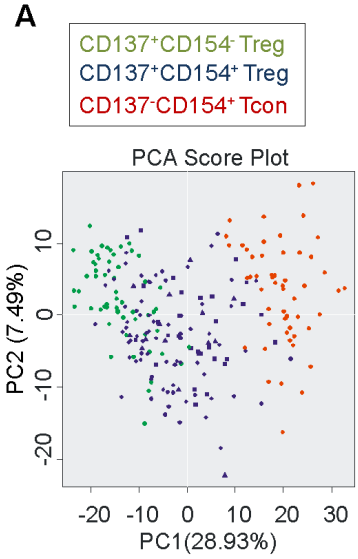

B

1	*bach2*	9	*fas*	17	*ikzf2*	25	*il2ra*	33	*rorc*
2	*bcl2*	10	*fcrl3*	18	*ikzf4*	26	*il32*	34	*tgfβ1*
3	*bcl6*	11	*foxp3*	19	*il10*	27	*il7r*	35	*tigit*
4	*ccr8*	12	*gata3*	20	*il17a*	28	*lrrc32*	36	*tnf*
5	*cd40lg*	13	*gzmb*	21	*il1r2*	29	*maf*	37	*tnfrsf18*
6	*csf2*	14	*havcr2*	22	*il2*	30	*nfatc2*	38	*tnfrsf4*
7	*ctla4*	15	*icos*	23	*il21*	31	*pdcd1*	39	*tnfrsf9*
8	*cxcr6*	16	*ifnγ*	24	*il22*	32	*prdm1*		

Figure 28: PCA analysis of single cell gene expression. (A) CD4$^+$CD25$^+$ Tregs and CD4$^+$CD25$^-$ Tcons were stimulated for 6h with PMA/Ionomycin and sorted according to CD137 and CD154 expression. **(A)** PCA analysis of single cell gene expression of 39 target genes that are shown in **(B)**; different symbols in **(A)** indicate individual donors (93 cells from 2 donors for CD137$^+$CD154$^-$ Tregs, 91 cells from 5 donors for CD137$^+$CD154$^+$ Tregs and 47 cells for CD137$^-$ CD154$^+$ Tcons from 1-2 individual experiments were analysed).

Principal component analysis provided an overview about the overall similarity of the different populations based on the transcriptional signature of the analysed target genes (Figure 28A,B). Next, a more detailed analysis was to provide insight into the expression of selected targets within single cells. Using hierarchical clustering analysis based on the expression of 39 target genes (Figure 28B), there was a very clear separation of all cells into three distinct clusters (Figure 29). Most strikingly, there was

a complete separation of $CD137^{-}CD154^{+}$ Tcons (cluster III) from $CD137^{+}CD154^{-}$ Tregs (cluster I) which was similarly observed by PCA analysis (Figure 28A). These findings underline the transcriptional signature of $CD137^{+}CD154^{-}$ Tregs that was completely distinct from $CD137^{-}CD154^{+}$ Tcons. In contrast, $CD137^{+}CD154^{+}$ Tregs contained cells that clustered closely with $CD137^{-}CD154^{+}$ Tcons (cluster II) as well as cells that transcriptionally resembled $CD137^{+}CD154^{-}$ Tregs (cluster I; Figure 29). Within the latter (cluster I), high levels of Treg-associated markers (e.g. *helios, garp, tigit*) were detected whereas effector cytokines (e.g. *ifn-γ, il-2*) were almost completely absent. On the other hand, a significant proportion of cells derived from $CD137^{+}CD154^{+}$ Tregs expressed reduced levels of Treg-associated markers and clustered closely with Tcons (cluster II). These findings confirm cellular heterogeneity and further demonstrate the co-existence of Treg-like and Tcon-like cells within $CD137^{+}CD154^{+}$ Tregs that was similarly observed on a clonal level. Interestingly, even within these Tcon-like cells (cluster II) there was no significant expression of effector cytokines which were almost exclusively detected within Tcons (cluster III). In contrast to data derived from clonal populations (Figure 27C), IL-10 expression was not restricted to $CD137^{+}CD154^{+}$ Tregs but similarly observed in cells derived from Tcons (Figure 29). In line with previous observations, cytokine expression was almost completely absent within $CD137^{+}CD154^{-}$ Tregs even on a single cell level.

Taken together, these data show that $CD137^{+}CD154^{+}$ Tregs consisted equally of Treg-like and Tcon-like cells that in spite of the co-expression of both markers represented a heterogeneous population. Single cell analysis showed that $CD137^{+}CD154^{+}$ expression did not continuously correlate with expression of effector cytokines suggesting that although cytokine expression appeared to be limited to CD154-expressing cells, CD154 expression was not sufficient to induce effector functions. Furthermore it is important to note that Treg identity of $CD137^{+}CD154^{-}$ cells was confirmed on a single cell level as high levels of Treg markers and low levels of effector cytokines were homogenously observed within individual cells of this subset.

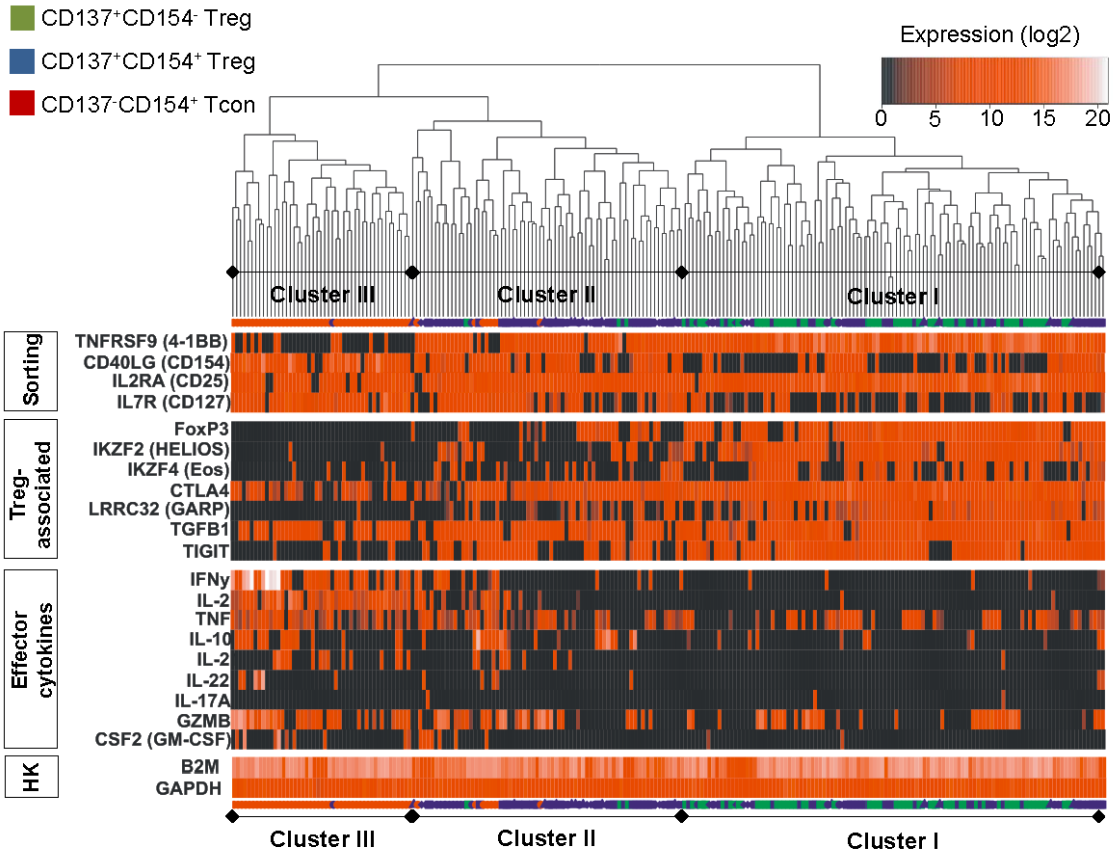

Figure 29: Hierarchical clustering of single cells. $CD4^+CD25^+$ Tregs and $CD4^+CD25^-$ Tcons were stimulated for 6h with PMA/Ionomycin and sorted according to CD137 and CD154 expression. Hierarchical clustering was performed based on expression of 39 target genes (Figure 28B) in single cells, housekeeping (HK) genes (*gapdh, b2m*) were not included for clustering; expression is shown as log2. A total of 93 cells from 2 donors for $CD137^+CD154^-$ Tregs, 91 cells from 5 donors for $CD137^+CD154^+$ Tregs and 47 cells for $CD137^-CD154^+$ Tcons from 1-2 individual experiments were analysed.

4.3.1.3 CD137 and CD154 co-expression identifies epigenetically imprinted Tregs and Tcons

Single cell analysis showed that heterogeneity within $CD137^+CD154^+$ Tregs derived from the co-existence of Treg-like and Tcon-like cells. However, it remains unclear whether this mixture represented convergence of inherently stable cells or identified cellular intermediates that were undergoing conversion between the Treg and Tcon compartment. Lineage identity of Tregs and Tcons can be determined by epigenetic analysis of the TSDR which is completely demethylated in Tregs, but not in Tcons [31-34]. Analysis of bulk cultures has revealed intermediate levels of TSDR methylation in $CD137^+CD154^+$ Tregs (Figure 5D, Figure 11A). However within bulk cultures, it cannot

be distinguished between homogenous de-/methylation of both strands or differential methylation of complementary strands within a single DNA molecule (hemimethylation). While the former would indicate a mixture of cells, the latter could provide strong evidence for ongoing de-/methylation processes and therefore potential conversion between the Treg and Tcon compartment.

Conventional epigenetic methods enable the distinction between methylated and unmethylated DNA but fail to capture dynamic processes within individual cells. To analyse whether CD137 and CD154 co-expression identified a transitional population between the Treg and Tcon compartment, methylation of complementary DNA molecules was analysed by hairpin bisulfite sequencing. This method is based on the covalent linking of complementary DNA strands by a hairpin linker after enzymatic cleavage of genomic DNA. Following bisulfite treatment, methylation of complementary strands within single DNA molecules can be analysed enabling the distinction between methylated, demethylated and hemimethylated DNA molecules. While $CD137^{+}CD154^{-}$ Tregs were completely demethylated at *foxp3* (promoter, TSDR, enhancer; Figure 30A), $CD137^{+}CD154^{+}$ Tregs contained cells that were completely methylated or unmethylated with only few cells that exhibited hemimethylated DNA (Figure 30B). These data confirm epigenetic stability of $CD137^{+}CD154^{-}$ Tregs on a single cell level and show that intermediate levels of TSDR methylation within $CD137^{+}CD154^{+}$ Tregs derived from a mixture of methylated and unmethylated cells while providing no evidence for transitional processes.

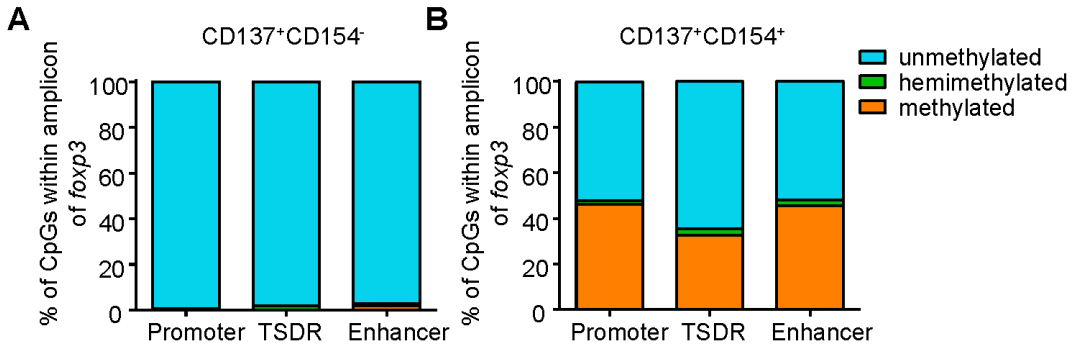

Figure 30: Hairpin bisulfite sequencing of $CD137^{+}CD154^{-}$ Tregs and $CD137^{+}CD154^{+}$ Tregs. **(A-B)** Methylation of single DNA molecules was analysed by hairpin bisulfite sequencing (pool of 5 male donors from one experiment). The percentage of unmethylated, hemimethylated and methylated CpGs within the indicated regions (promoter, TSDR and an enhancer) of *foxp3* of **(A)** $CD137^{+}CD154^{-}$ Tregs and **(B)** $CD137^{+}CD154^{+}$ Tregs are shown.

Analysis of complementary strands of single DNA molecules revealed a mixture of epigenetically stable Tregs and Tcons within the $CD137^+CD154^+$ Treg subset showing that CD137 and CD154 co-expression did not identify cellular transitions between the Treg and Tcon compartment (Figure 30B). However, hairpin bisulfite sequencing was done directly *ex vivo* and it cannot be excluded that epigenetic reprogramming is induced upon proliferation. To evaluate stability of this distinct epigenetic pattern upon *in vitro* expansion, methylation of expanded clonal populations that were generated from $CD137^+CD154^+$ Tregs was analysed. In line with the co-existence of unmethylated and methylated cells within $CD137^+CD154^+$ Tregs *ex vivo* (Figure 30B), clonal populations were either completely methylated or demethylated at the TSDR indicating the co-existence of epigenetically imprinted clones (Figure 31A). Furthermore, TSDR demethylation strongly correlated with $CD137^+CD154^-$ expression showing that the separation of Treg-like clones and Tcon-like clones based on $CD137^+CD154^-$ expression in Figure 27 represented the epigenetic state of the clones (Figure 31B). Furthermore, differential methylation was observed at the FoxP3 promoter although low methylation levels were also observed in Tcon-like clones (Figure 31A). These data confirm that $CD137^+CD154^+$ Tregs consisted of epigenetically imprinted Treg-like and Tcon-like clones which maintained their epigenetic stability upon prolonged expansion but differed in their ability to retain CD154 expression.

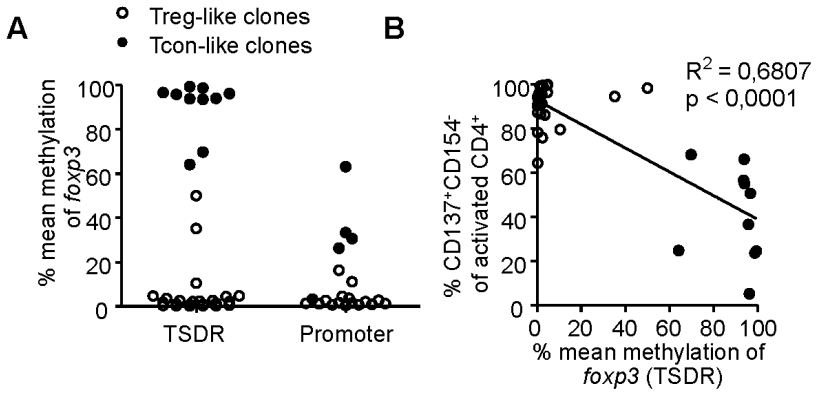

Figure 31: TSDR demethylation within clones derived from $CD137^+CD154^+$ Tregs. Single cell $CD4^+CD25^+CD127^-CD137^+CD154^+$ Treg clones were sorted and expanded before analysis (n=2, 2 independent experiments were performed). **(A)** Mean methylation of *foxp3* TSDR (33 clones) and *foxp3* promoter (21 clones) were analysed. **(B)** Correlation of $CD137^+CD154^-$ expression with mean methylation of *foxp3* TSDR; $CD137^+CD154^-$ expression was calculated relative to activated cells that upregulated CD137 and/or CD154. **(A-B)** Clones were grouped into Treg-like clones (open circles) and Tcon-like clones (closed circles) according to TSDR demethylation in **(A)**; Treg-like clones were defined as clones with ≤ 50% mean methylation. **(B)** Statistical significances were determined by linear regression analysis. Each dot represents one clone.

Epigenetic analysis of $CD137^+CD154^+$ Tregs has shown the presence of lineage stable Tregs within this subset. Therefore, it becomes clear that some Tregs can transiently upregulate CD154 in spite of TSDR demethylation. However, it remains unknown how differential expression of CD154 is regulated in Tregs. On the one hand, molecular differences in $CD154^+$ and $CD154^-$ cells have been observed (see 4.1.1.1) and also differential methylation of *cd40lg* (CD154) was shown in bulk populations *ex vivo* (Figure 5D). To investigate whether the ability to upregulate CD154 was epigenetically imprinted within expanded clones derived from $CD137^+CD154^+$ Tregs, methylation of *cd40lg* was analysed. Clones were classified into Treg-like clones and Tcon-like clones based on TSDR demethylation (Figure 31A). Methylation of *cd40lg* was heterogeneous indicating that CD154 expression was not stably imprinted within this subset in spite of CD154 expression by all cells at the time of sorting. Moreover, expression of CD154 did not correlate with methylation of *cd40lg* as some Treg-like clones exhibited partially demethylated *cd40lg* although the protein itself was not expressed. Conversely, some Tcon-like clones expressed CD154 in spite of *cd40lg* methylation (Figure 32A). The TSDR is a highly conserved, epigenetically imprinted region that enables the separation of Tregs and Tcons and therefore represents an exceptionally stable epigenetic mark. In contrast, expression of most genes is regulated by epigenetic modifications within promoter regions. Indeed, the FoxP3 promoter was demethylated in Treg-like clones but only partially methylated in Tcon-like clones indicating a permissive state that can enable transient expression of FoxP3 in Tcons independent of lineage stability (Figure 31A, Figure 32B). It can be assumed that the weak correlation of CD154 expression with *cd40lg* methylation derives from the analysed region (intron 4), which was not located within the promoter and therefore its demethylation might not be required for protein expression (Figure 32A). Consequently, it remains unclear to what degree CD154 expression is epigenetically imprinted on Tregs.

Taken together, comprehensive single cell analysis of $CD137^+CD154^+$ Tregs revealed phenotypic heterogeneity which derived from the co-existence of epigenetically imprinted Tregs and Tcons. These data show a certain degree of phenotypic plasticity of Tregs and Tcons that similarly co-express CD137 and CD154, yet they provide no evidence for transitional processes within this subset.

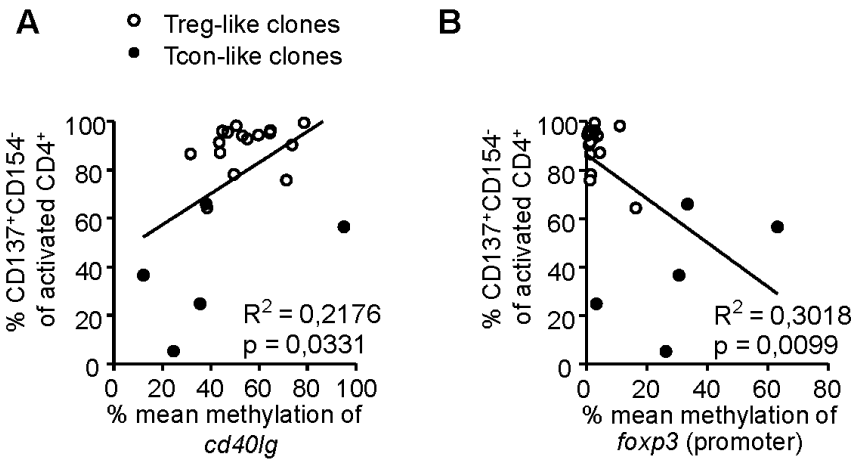

Figure 32: Generation of single cell clones from CD137$^+$CD154$^+$ Tregs. Single cell CD4$^+$CD25$^+$CD127$^-$CD137$^+$CD154$^+$ Treg clones were sorted and expanded before analysis (n=2, 2 independent experiments were performed). Correlation of CD137$^+$CD154$^-$ expression with mean methylation of **(A)** *cd40lg* and **(B)** *foxp3* promoter is shown, CD137$^+$CD154$^-$ expression was calculated relative to activated cells that upregulated CD137 and/or CD154. Clones were grouped into Treg-like clones (open circles) and Tcon-like (closed circles) according to TSDR demethylation (as shown in Figure 31A). **(A-B)** Statistical significances were determined by linear regression analysis; each dot represents one clone.

4.3.2 Plasticity of Tregs *in vitro*

In-depth analysis of CD137$^+$CD154$^+$ Tregs revealed the presence of epigenetically imprinted Tregs within this effector-like subset (Figure 30B, Figure 31A). These data indicate a certain degree of transient phenotypic plasticity within lineage stable Tregs which includes the upregulation of CD154 and potentially also expression of effector molecules. To analyse plasticity of epigenetically imprinted Tregs *in vitro*, CD137$^+$CD154$^-$ Tregs were sorted after 6h stimulation from expanded Treg cultures and expanded for another 10-12 days. In spite of high purities before expansion, CD137$^+$CD154$^-$ sorted Tregs exhibited some CD154 expression following restimulation after expansion showing acquisition of CD154 expression (Figure 33A,B). However, there was no loss of TSDR demethylation upon expansion of CD137$^+$CD154$^-$ Tregs indicating maintenance of epigenetic stability that was independent of CD154 acquisition (Figure 33C). Nevertheless, CD154 expression correlated with the upregulation of effector cytokines which were not expressed by Tregs that maintained a CD137$^+$CD154$^-$ phenotype (Figure 33D). Collectively, CD154 expression could be acquired by some stable Tregs upon expansion and therefore emerges as important marker for the identification of cells that have the potency to express effector molecules. Furthermore, CD137$^+$CD154$^-$ expression was once more shown to correlate

with a stable Treg phenotype and lack of effector cytokines expression. These data show that CD137$^+$CD154$^-$ Tregs exhibited a certain degree of phenotypic plasticity *in vitro* as they could partially acquire effector functions along with CD154 expression while maintaining epigenetic stability. Still, CD154 acquisition was rare and a CD137$^+$CD154$^-$ phenotype was maintained by most cells.

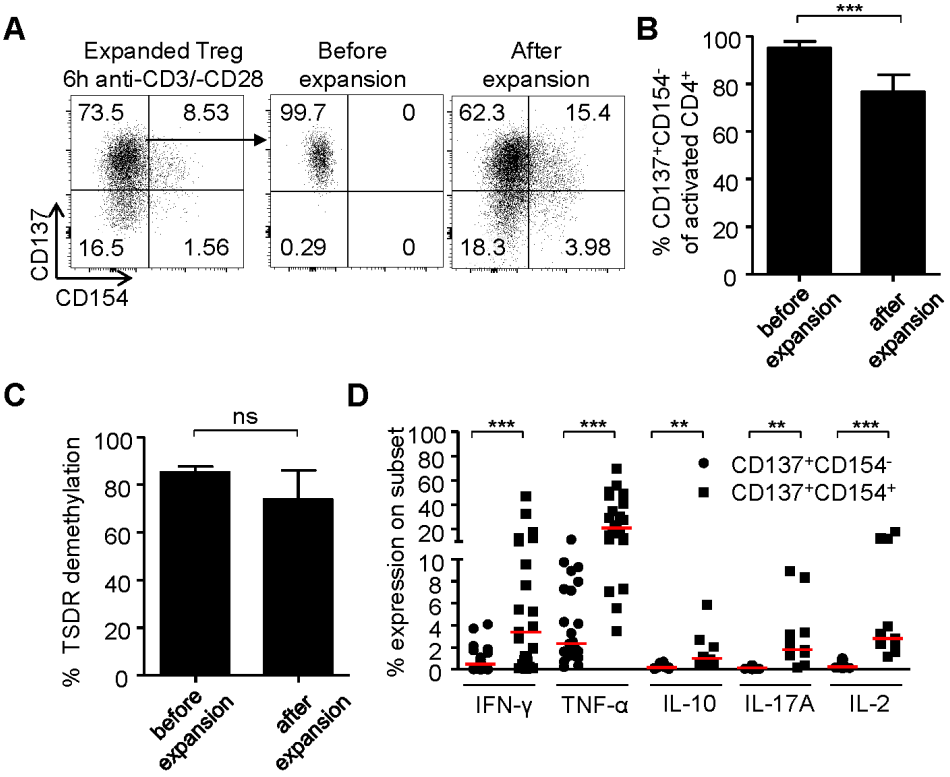

Figure 33: Stability of CD137$^+$CD154$^-$ Tregs *in vitro*. (A-D) CD137$^+$CD154$^-$ Tregs were sorted from expanded CD25$^+$ Treg cultures and further expanded for 10-12 days before analysis. **(A-B)** CD137 and CD154 expression were analysed before and after expansion; **(A)** representative dot plot of one donor and **(B)** statistical summary of several donors (n=8 from 3 experiments before expansion and n=28 from 9 experiments after expansion). **(C)** TSDR demethylation of CD137$^+$CD154$^-$ Tregs was analysed before and after expansion (n=4, 1 experiment was performed). **(D)** CD137$^+$CD154$^-$ Tregs were expanded and restimulated for 6h with PMA/Ionomycin before expression of IFN-γ, TNF-α (n=28 from 10 different experiments), IL-17 (n=16, 6 different experiments), IL-2 (n=11, 4 different experiments) and IL-10 (n=19, 7 independent experiments) were analysed on CD137$^+$CD154$^-$ and CD137$^+$CD154$^+$ cells. Statistical significances were determined by **(B,C)** Mann-Whitney test or **(D)** Wilcoxon signed-rank test. **(B,C)** Median + interquartile range are shown; **(D)** each dot represents one donor, lines indicate median.

In vitro expansion of CD137$^+$CD154$^-$ Tregs revealed a certain degree of phenotypic plasticity including expression of CD154 and upregulation of effector cytokines (Figure 33A,B,D). It has been proposed that instability is restricted to the memory Treg compartment as naive Tregs have been shown to represent a particularly stable subset *in vitro* [60-64]. To investigate stability of naive and memory Tregs in regard to CD137

and CD154 expression, naive and memory Tregs were sorted and expanded separately before analysis. Interestingly, similar frequencies of CD154-expressing cells were detected within both subsets indicating that plasticity was not limited to the memory Treg compartment (Figure 34A). To track stability of individual clones, single cell Treg clones were generated from naive, memory and $CD137^{+}CD154^{-}$ Tregs (Figure 34B-D). Most clonally expanded populations were of remarkable stability with only some that contained a small percentage of CD154-expressing cells (Figure 34B). Nevertheless, the majority of clones maintained epigenetic stability indicating that the naive as well as the memory Treg compartment were stable upon prolonged *in vitro* expansion (Figure 34C). These data suggest that minor phenotypic plasticity that was observed within bulk cultures of $CD137^{+}CD154^{-}$, naive and memory Tregs derived from individual clones, but not inherent instability. Intermediate levels of TSDR demethylation were observed in some clonal populations derived from memory Tregs (Figure 34C). It is important to note that the cloning efficiency of memory Tregs was significantly lower than that of the other Treg populations. Therefore, 10 cells/well were sorted to generate memory clones which can result in oligoclonal populations. Although it can be assumed that most clonal populations originated from a single clone, the contribution of clonal heterogeneity cannot be fully excluded for this subset.

Independent of the starting population, the acquisition of CD154 expression by individual clones was accompanied by an upregulation of effector cytokine expression (IFN-γ, TNF-α, IL-2, IL-17A) showing that although rare, some clones can exhibit phenotypic plasticity (Figure 34D). Nevertheless, plasticity was not accompanied by epigenetic instability as TDSR demethylation was maintained (Figure 34C). These findings are in line with the absence of hemimethylation within $CD137^{+}CD154^{-}$ Tregs *ex vivo* which collectively provide no evidence for epigenetic reprogramming of stable Tregs *in vivo* or *in vitro* (Figure 30A). It is important to note that although restricted to CD154-expressing cells, cytokine expression was rather low. Furthermore, within single cells derived from $CD137^{+}CD154^{+}$ Tregs only very few cytokine-producing cells were detected in spite of CD154 expression (Figure 29). These data show that although they were limited to the $CD154^{+}$ compartment, effector functions were extremely rare within the peripheral Treg compartment and not always induced along with CD154.

Taken together, these data show that plasticity within the peripheral Treg compartment, including CD154 expression and upregulation of effector cytokines, originated from individual clones that maintained epigenetic stability. Nevertheless, the majority of the naive and memory Treg compartment was remarkably stable *in vitro* indicating only a minor contribution of Treg plasticity to the peripheral Treg compartment in humans.

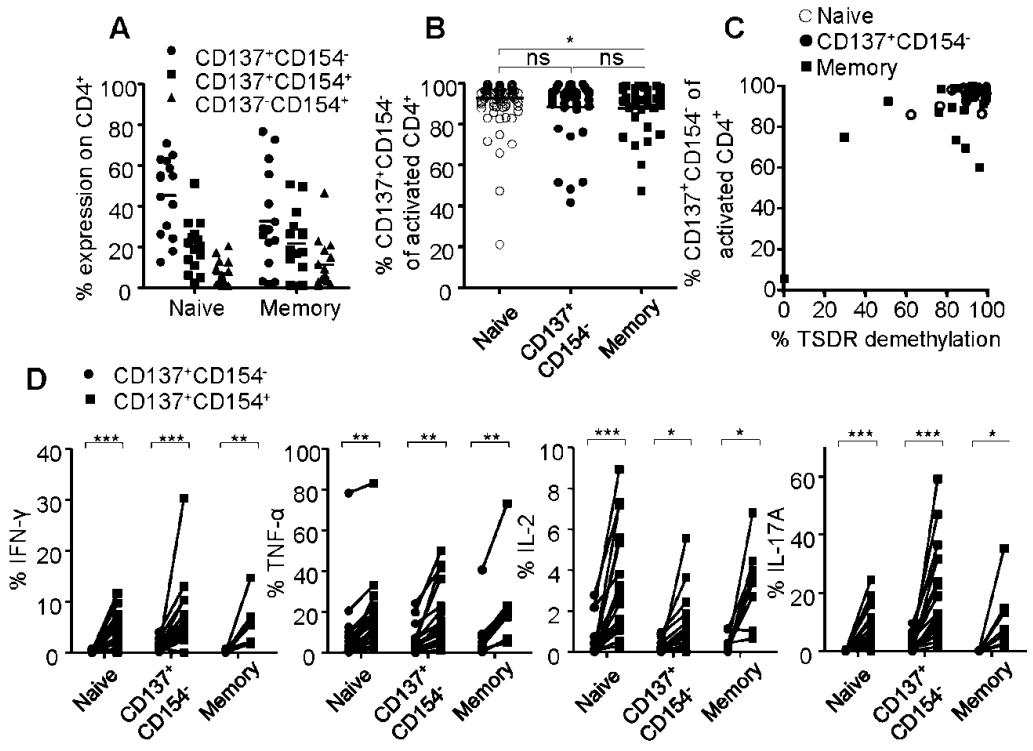

Figure 34: Stability of clones within the peripheral Treg compartment. (A) Naive ($CD45RO^-CCR7^+CD45RA^+$) and memory ($CD45RO^+CD45RA^-$) Tregs were sorted *ex vivo* and expanded for 14 days before CD137 and CD154 expression were analysed after 6h restimulation with PMA/Ionomycin (n=15, 5 independent experiments were performed). **(B-D)** Treg clones were generated from naive ($CD45RO^-CCR7^+CD45RA^+$), memory ($CD45RO^+CD45RA^-$) and $CD137^+CD154^-$ Tregs and expanded before analysis. **(B)** $CD137^+CD154^-$ expression was analysed on 96 naive (n=6, 4 different experiments), 37 $CD137^+CD154^-$ (n=2, 2 independent experiments) and 32 memory clones (n=3, 3 independent experiments). **(C)** Correlation of $CD137^+CD154^-$ expression (relative to activated cells that upregulated CD137 and/or CD154) with TSDR demethylation is shown of $CD137^+CD154^-$ clones (5 clones, n=1 from one experiment), naive clones (20 clones, n=2 from 2 different experiments) and memory sorted clones (19 clones, n=2 from 2 different experiments). **(D)** Cytokine expression was analysed after 6h restimulation with PMA/Ionomycin, expression on $CD137^+CD154^-$ and $CD137^+CD154^+$ cells was analysed (consideration of clones with >5% $CD137^+CD154^+$ expression). Statistical significances were determined by **(B)** Kruskal-Wallis test or **(D)** Wilcoxon signed-rank test. **(A-D)** Each dot represents one clone, lines indicate mean.

4.3.3 Plasticity of Tregs *ex vivo*

The presence of epigenetically imprinted Tregs within $CD137^+CD154^+$ cells indicated a certain degree of plasticity within the lineage stable Treg compartment. Furthermore, phenotypic plasticity of stable Tregs was observed upon *in vitro* expansion, but was shown to be limited to individual clones. Overall, these data show stability of the peripheral Treg compartment in humans with only minor phenotypic plasticity. However, it is important to note that analysis was limited to Tregs derived from peripheral blood of healthy individuals and it can be speculated that plasticity might be increased during inflammation or at local sites. To address the stability of Tregs that were exposed to different environments *in vivo*, CD137 and CD154 expression were analysed on $CD25^+CD127^-$ Tregs from human thymus, tonsil, lung and colon and compared to peripheral blood. It is important to note that thymic samples were obtained from young individuals and therefore can be expected to contain mostly naive cells whereas samples from tonsil, lung and colon were obtained from patients with acute or chronic inflammation. Furthermore, samples were obtained from different donors, including different ages, and therefore donor variability cannot be fully excluded for comparisons between different tissues. Nevertheless, these findings can provide insight into the stability of Tregs that were exposed to different conditions *in vivo*.

To identify Tregs in different tissues, cells were stained for expression of CD25, CD127 and FoxP3. The percentage of $CD25^+CD127^-$ Tregs was slightly increased in tonsil samples while frequencies within other tissues were similar to peripheral blood (Figure 35B). It is important to note that tonsils are highly immunocompetent organs and that tonsillectomies are often the result of continuous local inflammation. Consequently, high frequencies of $CD25^+CD127^-$ cells can derive from strong inflammatory immune reactions resulting in activation of Tcons. In line with this notion, FoxP3 expression within the $CD25^+CD127^-$ compartment was low in tonsils, but similarly in Tregs derived from other tissues compared to blood (Figure 35C). These findings either suggest inefficient FoxP3 staining or significant numbers of non-Tregs within the tissue-derived $CD25^+CD127^-$ Treg compartment.

To determine plasticity within the $CD25^+CD127^-$ Treg compartment, frequencies of $CD137^+CD154^-$ cells were determined after 6h stimulation. $CD137^+CD154^-$ expression was highly variable and rather low in the tissue (Figure 35A,D), but similar to frequencies of FoxP3-expressing cells (Figure 35C). These data suggest significant amounts of non-Tregs that exhibited a $CD25^+CD127^-$ phenotype in the different tissues.

To evaluate Treg plasticity and to account for different levels of activation, CD137 and CD154 expression were analysed relative to all activated cells that upregulated CD137 and/or CD154 (Figure 35E-G). High frequencies of $CD137^{-}CD154^{+}$ cells were detected in some samples and provide further evidence for the occurrence of Tcons within the tissue-derived $CD25^{+}CD127^{-}$ Treg compartment. However, there were only low levels of $CD137^{+}CD154^{+}$ expression indicating that Treg plasticity was rare even within mucosal tissues such as lung or colon where most cells exhibited a $CD137^{+}CD154^{-}$ phenotype (Figure 35E,F). Interestingly, $CD137^{+}CD154^{+}$ expression was almost completely absent on Tregs derived from thymus compared to other analysed organs (Figure 35F). As the thymus mostly contains naive cells, these data indicate that the human Treg compartment is shaped in the periphery upon antigen encounter which can contribute to Treg plasticity in local tissues. Nevertheless, overall levels of CD154 expression were low showing that similar to observations *in vitro*, the majority of the human Treg compartment in blood and tissue was remarkably stable *in vivo*.

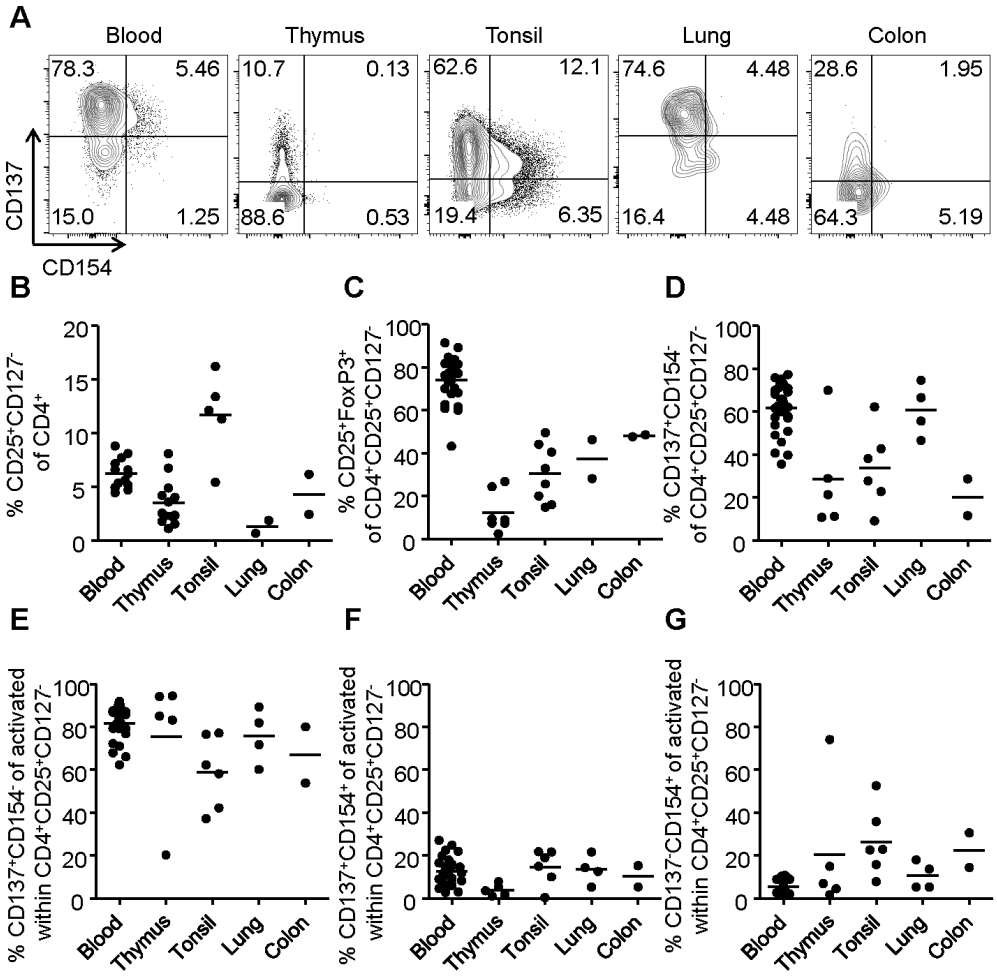

Figure 35: CD137 and CD154 expression within human tissue. (A-G) Tregs from different tissues were analysed *ex vivo*. Expression of **(B)** $CD25^+CD127^-$, **(C)** FoxP3 and **(A,D-G)** CD137 and CD154 were analysed on Tregs derived from peripheral blood (n=14-30, 2-5 independent experiments), thymus (n=5-13, 5-13 independent experiments), tonsil (n=5-8, 5-8 independent experiments), lung (n=2-4, 1-3 independent experiments) and colon (n=2, 2 independent experiments). **(A,D-G)** CD137 and CD154 expression were analysed after 6h restimulation with anti-CD3/-CD28 (blood) or PMA/Ionomycin (thymus, tonsil, lung, colon) on $CD4^+CD25^+CD127^-$ Tregs; **(A)** representative dot plot of one donor and **(D-G)** statistical summary of several donors. **(E-G)** Expression is shown relative to activated cells that upregulated CD137 and/or CD154. **(B-G)** Each dot represents one donor, lines indicate mean.

4.3.4 The T cell receptor repertoire of human Tregs

The peripheral Treg compartment is important for the maintenance of tolerance against self and non-self antigens. Here, the peripheral Treg compartment was shown to contain stable, possibly thymic-derived $CD137^+CD154^-$ Tregs and instable effector-like $CD137^+CD154^+$ Tregs. In-depth analysis revealed the co-existence of stable Tregs and Tcons within $CD137^+CD154^+$ Tregs while providing no evidence for transitional

processes within this subset. These data clearly show a minor contribution of non-Tregs to the peripheral Treg compartment but suggest a certain degree of transient phenotypic plasticity of Tregs and Tcons that co-express CD137 and CD154. To elucidate the clonal origin of $CD137^{+}CD154^{-}$ Tregs and $CD137^{+}CD154^{+}$ Tregs, sequencing of the TCR repertoire was to enable tracking of individual clones and their progeny within the peripheral Treg compartment and during antigen-specific immune responses. These findings were to provide insight into the clonal relationship of Tregs and Tcons and reveal clonal progenitors of $CD137^{+}CD154^{-}$ Tregs and $CD137^{+}CD154^{+}$ Tregs to ultimately elucidate conversion between the Treg and Tcon compartment.

4.3.4.1 The polyclonal TCR repertoire of the peripheral Treg compartment

$CD137^{+}CD154^{-}$ expression enabled the identification of lineage stable Tregs and their separation from contaminating Tcons and instable Tregs that were shown to co-exist within the $CD137^{+}CD154^{+}$ Treg subset. Therefore, analysis of the TCR repertoire of $CD137^{+}CD154^{-}$ Tregs, $CD137^{+}CD154^{+}$ Tregs and $CD137^{-}CD154^{+}$ Tcons was to provide insight into the clonal overlap of Tregs and Tcons in humans as well as to clarify the clonal origin of $CD137^{+}CD154^{+}$ Tregs. To this end, the TCR Vβ chains of $CD137^{+}CD154^{-}$ Tregs and $CD137^{+}CD154^{+}$ Tregs were sequenced and compared to $CD137^{-}CD154^{+}$ Tcons. Interestingly, the TCR repertoire of $CD137^{+}CD154^{-}$ Tregs was distinct from $CD137^{-}CD154^{+}$ Tcons with only 0.48% (mean ± 0.08% St.Dev.) shared sequences (Figure 36A,B). Similarly, distinct repertoires were confirmed when the clonality of both populations was taken into account using the Yue-Clayton similarity index underlining the lack of overlap between $CD137^{+}CD154^{-}$ Tregs and $CD137^{-}CD154^{+}$ Tcons (Figure 36B). These data suggest that $CD137^{+}CD154^{-}$ Tregs and $CD137^{-}CD154^{+}$ Tcons derive from different lineages and are defined by separate TCR repertoires providing further evidence for the thymic origin of $CD137^{+}CD154^{-}$ Tregs. To confirm that lack of overlap between Tregs and Tcons was not due to technical limitations, the repertoires of $CD137^{+}CD154^{-}$ Tregs and $CD137^{-}CD154^{-}$ Tregs were compared (Figure 36B). $CD137^{-}CD154^{-}$ Tregs (total Treg) most likely represent a heterogeneous population that is, for as yet unknown reasons, not properly activated upon stimulation. However, it can be assumed that this subset contains a significant proportion of clones that is shared with $CD137^{+}CD154^{-}$ Tregs and can therefore be used as internal control to detect overlapping sequences. Indeed, notable overlap was observed between both Treg populations (17.33% mean ± 5.0% St.Dev.) confirming

that shared sequences could readily be detected highlighting the distinct clonality of $CD137^{+}CD154^{-}$ Tregs and $CD137^{-}CD154^{+}$ Tcons in the periphery providing no evidence for conversion between the Treg and Tcon compartment (Figure 36A,B).

Tcon-derived sequences were absent in $CD137^{+}CD154^{-}$ Tregs but enriched within $CD137^{+}CD154^{+}$ Tregs (2.55% mean ± 1,10% St.Dev.) showing that overlap between the polyclonal $CD25^{+}CD127^{-}$ Treg and Tcon compartment derived specifically from this heterogeneous $CD137^{+}CD154^{+}$ population (Figure 36A). It is important to note that $CD137^{+}CD154^{+}$ Tregs also shared a significant fraction (5.33% mean ± 2.05% St.Dev) of their repertoire with stable $CD137^{+}CD154^{-}$ Tregs (Figure 36C). These data further confirm heterogeneity of $CD137^{+}CD154^{+}$ Tregs which consisted similarly of epigenetically imprinted $CD137^{+}CD154^{-}$ Tregs and $CD137^{-}CD154^{+}$ Tcons (see 4.3.1). Therefore it can be assumed that overlap with $CD137^{+}CD154^{-}$ Tregs and $CD137^{-}CD154^{+}$ Tcons did not derive from transitional processes within this subset, but rather from cellular heterogeneity. In line with this notion, almost no sequences could be detected in all three populations which would be expected if $CD137^{+}CD154^{+}$ Tregs represented a transitional state of Treg-Tcon conversion (Figure 36C).

Taken together, TCR repertoire analysis provided further evidence for the thymic origin of $CD137^{+}CD154^{-}$ Tregs which exhibited a TCR repertoire that was distinct from Tcons. These data show their origin from different precursors and reveal separate TCR clones in the periphery. Furthermore, these data indicate no major contribution of potentially pathogenic Treg conversion to the Tcon compartment and also show no significant extrathymic Treg induction. In addition, absence of clones that appeared in all three populations, that is $CD137^{+}CD154^{-}$ Tregs, $CD137^{+}CD154^{+}$ Tregs and $CD137^{-}CD154^{+}$ Tcons, indicate that $CD137^{+}CD154^{+}$ Tregs did not identify Treg-Tcon conversion but confirm the co-existence of Tregs and Tcons within $CD137^{+}CD154^{+}$ Tregs suggesting that stable Tregs and Tcons converge but do not convert within this subset.

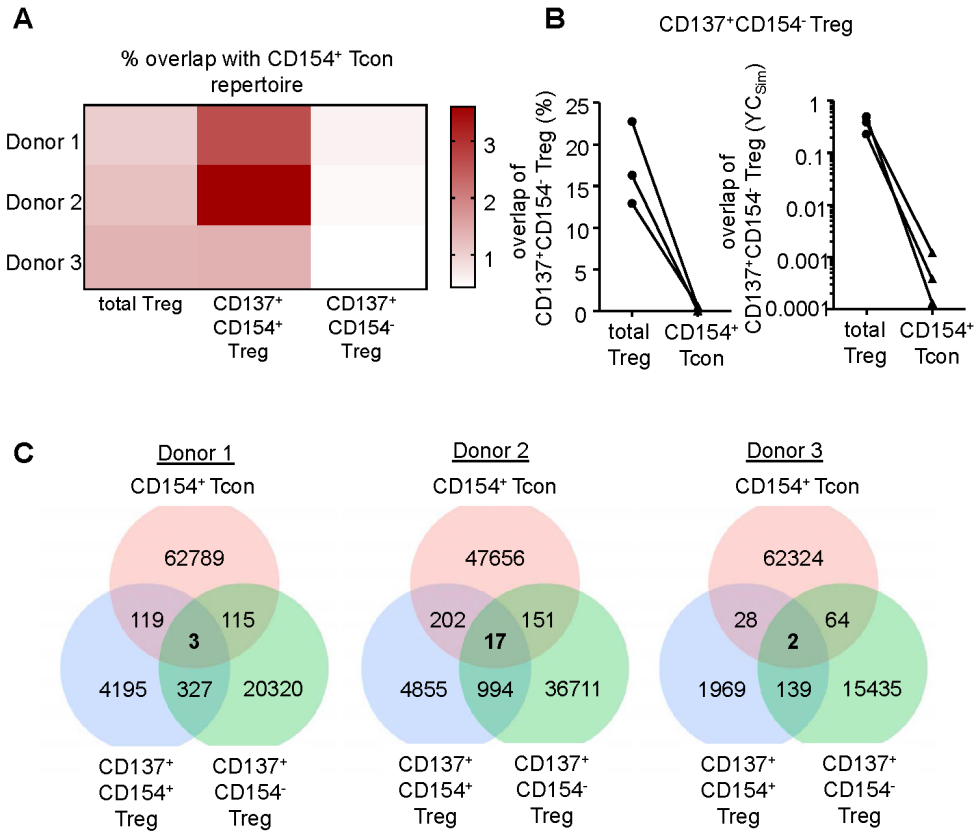

Figure 36: TCR repertoire of the peripheral Treg compartment. (A-C) Tregs ($CD45RO^+CD25^+CD127^-$) and Tcons ($CD45RO^+CD25^-CD127^+$) were sorted according to CD137 and CD154 expression for sequencing of the TCR-β repertoire (n=3, 2 independent experiments were performed). **(A)** Heatmap of the percentage of the Treg repertoire that overlaps with Tcons. **(B)** The percentage (left) and Yue-Clayton similarity index (right; $YC_{Sim,}$ all clonotypes were considered) of $CD137^+CD154^-$ Tregs that overlap with total Tregs ($CD137^-CD154^-$) and Tcons are shown; Yue-Clayton similarity index (YC_{Sim}) ranges from 0 indicating dissimilarity to 1 for identical populations. **(C)** The total number and distribution of clonotypes of the respective Treg and Tcon populations are shown. **(B)** Each symbol represents one donor.

4.3.4.2 The TCR repertoire of antigen-specific Tregs and Tcons

Analysis of the polyclonal TCR repertoires of $CD137^+CD154^-$ Tregs and $CD137^-CD154^+$ Tcons revealed only minor overlap indicating distinct TCR clones and providing no evidence for a contribution of Treg-Tcon conversion to the peripheral Treg compartment (Figure 36A-C). It has been proposed that extrathymic Treg induction contributes to regulatory immune responses in particular against foreign antigens such as allergens, microbiota or food (see 1.2.1.2). Similarly, it can be speculated that pathogenic conversion of Tregs preferentially occurs in particular situations e.g. to augment immune responses against pathogens. Consequently, it can be assumed that Treg-Tcon conversion occurs on an antigen-specific level and therefore minor clonal

overlap between polyclonal Tregs and Tcons does not inevitably exclude conversion during particular immune responses. Therefore, the contribution of Treg-Tcon conversion to physiological immune responses in humans needs to be analysed on an antigen-specific level.

Identification and isolation of rare antigen-specific T cells has been shown and also specificity of Tregs against foreign antigens (e.g. *A. fumigatus, C. albicans*, birch) has recently been demonstrated [92, 96, 97]. Furthermore, it has been shown that the repertoires of $CD137^{+}CD154^{-}$ Tregs and $CD137^{-}CD154^{+}$ Tcons specific for *A. fumigatus* and birch were distinct providing no evidence for Treg-Tcon conversion against these antigens [96]. To elucidate the clonality of Tregs and Tcons reactive against additional antigens that could potentially induce Treg-Tcon conversion, $CD137^{+}CD154^{-}$ Tregs and $CD137^{-}CD154^{+}$ Tcons specific for CMV, *E. coli* or *C. albicans* were magnetically enriched from PBMCs after 6h stimulation. It is important to note, that antigen-specific responses did not contain notable frequencies of $CD137^{+}CD154^{+}$ cells which were therefore not included in this analysis. Antigen-specific Tregs and Tcons were purified by FACS sorting before sequencing of the TCRVβ repertoires. As low frequencies of unspecific $CD137^{+}CD154^{-}$ Tregs could be detected independent of the stimulation, $CD137^{+}CD154^{-}$ Tregs were also sorted from unstimulated samples as internal control to determine maximum overlap between samples and to remove unspecific clonotypes for analysis.

Since antigen-specific cells are rare, only a limited number of cells could be sorted (<5000 cells/sample). To control for the sensitivity of the method for each individual sample, overlap of $CD137^{+}CD154^{-}$ Tregs from stimulated and unstimulated samples was analysed. Identical clonotypes could readily be detected between two samples indicating that overlapping sequences could be identified within two independently sorted samples from the same donor in spite of limited cell numbers (Figure 37A,D). For analysis of the antigen-specific responses, unspecific clonotypes that were detected in the unstimulated sample were excluded. In line with the distinct repertoires of Tregs and Tcons specific for *A. fumigatus* and birch [96], Tregs and Tcons specific for CMV, *E. coli* and *C. albicans* did not share the same clonotypes indicating their origin from different precursors (Figure 37B,C). These data provide no evidence for Treg-Tcon conversion in response to these antigens and furthermore show that specificities against non-self are found within the stable Treg compartment. In addition, there was no contribution of Treg clones that have converted to the Tcon compartment showing once more remarkable stability of Tregs on an antigen-specific level.

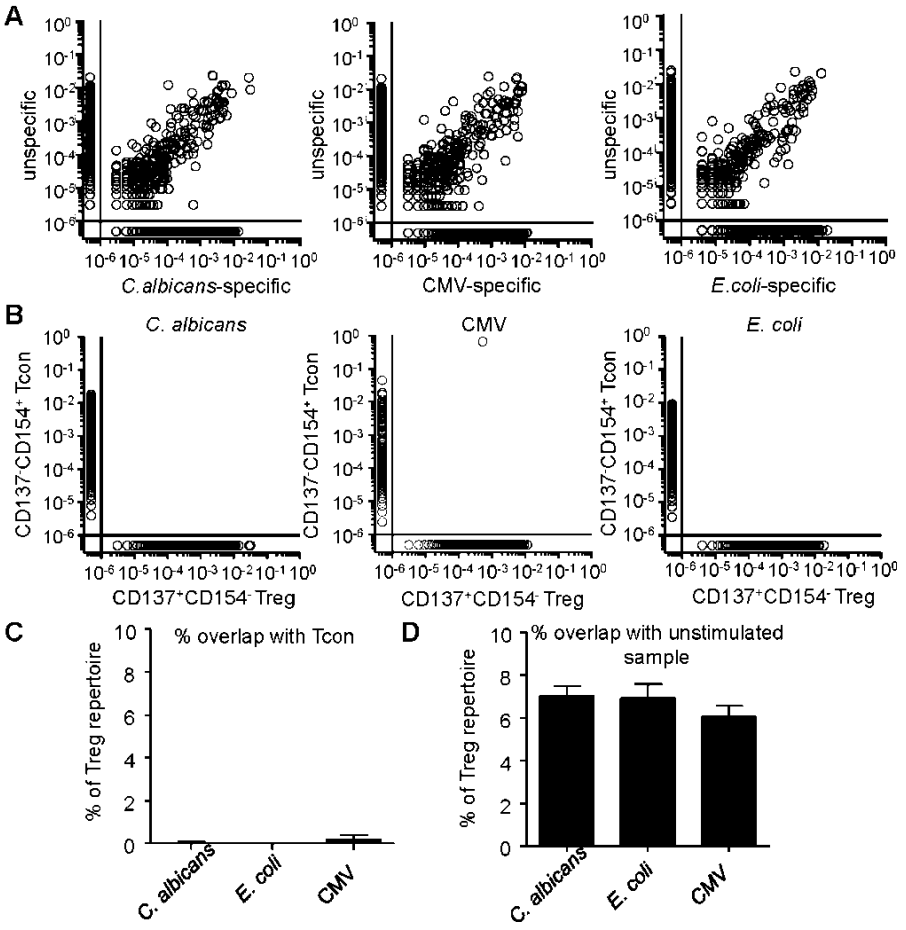

Figure 37: TCR repertoire of antigen-specific Tregs and Tcons. (A-D) $CD137^+CD154^-$ Tregs and $CD137^-CD154^+$ Tcons were sorted for TCRVβ sequencing. **(A,D)** Overlap of $CD137^+CD154^-$ Tregs after stimulation with *C. albicans* (left), CMV (middle) and *E. coli* (right) with $CD137^+CD154^-$ Tregs from unstimulated samples were analysed. **(B,C)** Overlap of $CD137^+CD154^-$ Tregs and $CD137^-CD154^+$ Tcons specific for *C. albicans* (left), CMV (middle) and *E. coli* (right) is shown. **(A,B)** Representative graph of one donor and **(C,D)** statistical summary of the percentage of clones within $CD137^+CD154^-$ Tregs that were also detected in **(C)** $CD137^-CD154^+$ Tcons or **(D)** unstimulated samples (n=3, 2 independent experiments were performed). **(A,B)** Each dot represents one clone, the proportion of each sequence in the respective sample is shown; clones below the line were only detected in one population; **(C,D)** mean + SEM is shown.

In conclusion, activation-induced CD154 expression on $CD137^+$ Tregs was shown to distinguish between stable, in all likelihood thymic-derived $CD137^+CD154^-$ Tregs and instable effector-like $CD137^+CD154^+$ Tregs. In-depth analysis, including TCR sequencing, single cell gene expression, epigenetics and cloning revealed that $CD137^+CD154^+$ Tregs were not derived from transitional Treg-Tcon intermediates but from a mixture of epigenetically imprinted Tregs and Tcons. In line with these findings, antigen-specific Treg responses against foreign antigens were generated by stable $CD137^+CD154^-$ Tregs with a distinct TCR repertoire indicating their separate

development, and not induction from Tcons. Collectively, these data highlight remarkable Treg stability *in vitro* and during antigen-specific immune responses against foreign antigens *in vivo* and therefore show that Treg instability and Treg-Tcon conversion only negligibly contribute to the human Treg compartment.

5 Discussion

5.1 $CD137^{+}CD154^{-}$ expression as Treg-specific activation signature for the identification and sorting of stable Tregs

The *in vitro* generation of therapeutic Tregs requires heightened safety measures as effector cell contaminations can enhance inflammatory immune pathologies. Studies from mice [42-51] and humans [45, 55-73] have shown notable Treg plasticity including the upregulation of effector cytokines and loss of FoxP3 expression. To date, stability of expanded Tregs depends on the purity of the starting population as there are no unambiguous markers to separate stable Tregs from non-Tregs after expansion. In this study, $CD137^{+}CD154^{-}$ expression was shown to selectively identify epigenetically stable antigen-activated Tregs *ex vivo* and within *in vitro* expanded cultures. There was a striking correlation of $CD137^{+}CD154^{-}$ expression with TSDR demethylation revealing its potential to purify epigenetically imprinted Tregs from unseparated *in vitro* expanded cultures. Therefore $CD137^{+}CD154^{-}$ expression emerges as Treg-specific activation signature for the identification, isolation and characterization of inherently stable Treg populations.

Upon *in vitro* expansion, most $CD137^{+}CD154^{-}$ Tregs maintained their phenotype and lacked expression of effector cytokines. However, low frequencies of e.g. IL-2, INF-γ and TNF-α were observed upon expansion, but it was shown that they were expressed selectively by cells that had acquired CD154 expression. Such transient phenotypic plasticity, including upregulation of CD154 and expression of effector cytokines, was shown to be restricted to few clones within the naive, memory and $CD137^{+}CD154^{-}$ Treg compartment while the majority of expanded clones maintained a stable $CD137^{+}CD154^{-}$ Treg phenotype. Furthermore, CD154 acquisition did not correlate with epigenetic instability as most clones were completely demethylated at the TSDR independent of CD154 expression by some cells. Therefore, it was shown that inherently stable Tregs that were defined by $CD137^{+}CD154^{-}$ expression were of remarkable stability *in vitro* with only few clones that exhibited minor phenotypic plasticity.

Previous data have shown that Treg instability occurred primarily within the memory compartment [60-65] and was associated with TCR activation [50, 61]. It was shown here that in spite of prolonged expansion and repetitive activation, most clonal populations were remarkably stable. Furthermore, clones that exhibited minor phenotypic plasticity were not selectively found within the memory Treg compartment

but similarly occurred within expanded naive cells. It can be speculated that instabilities that have been observed within the human $CD25^{+}CD127^{-}$ Treg compartment in previous studies most likely derived from contaminating effector cells due to an inability to unambiguously identify stable Tregs *ex vivo* [45, 55-73]. Therefore, the findings presented in this study underline the remarkable stability of Tregs and provide no evidence for inherent instability. These findings also have important clinical implications as higher numbers of memory Tregs can be isolated from patients and also potential disease-relevant antigen-specificities are most likely increased within this compartment. Collectively, $CD137^{+}CD154^{-}$ expression can enable the isolation of stable, highly potent antigen-specific memory Tregs to increase efficacy of adoptive Treg transfer.

Although only minor phenotypic plasticity was observed within stable Tregs, understanding mechanisms that can promote or inhibit such plasticity *in vitro* and *in vivo* can contribute to the optimization of Treg stability for therapeutic applications. It has been proposed that different cytokines such as IL-1ß, IL-6, IL-12, IL-21, IL-23, IL-15, IL1RA or TNF-α can negatively influence Treg stability *in vitro* [55-59, 68, 69]. However, it has not clearly been distinguished between inherent Treg instability and selective outgrowth of effector cell contaminations. Here, it was shown that phenotypic plasticity of lineage stable Tregs was restricted to cells that co-expressed CD137 and CD154. Therefore, tracking of CD154 acquisition by $CD137^{+}CD154^{-}$ Tregs can provide a novel tool for the rapid analysis of different factors (e.g. cytokines, antigens) that induce or prevent CD154 upregulation on stable Tregs. These findings can contribute to the phenotypic stabilization of the $CD137^{+}CD154^{-}$ Treg compartment *in vitro* and potentially also *in vivo*.

While CD137 was rapidly upregulated on Tregs, it has been shown that Tregs are unable to express CD154 [92, 96, 97, 107, 272]. In line with this notion, differential methylation of CD154 in Tregs and Tcons has been reported and was also described in this study [241]. Nevertheless, upregulation of CD154 was observed on stable Tregs, although expression was rare and only transient. It remains unclear whether differential methylation of *cd40lg* within individual cells accounted for an intrinsic ability to upregulate CD154. Further analysis regarding single cell methylation of *cd40lg* and its correlation with the ability to acquire effector functions are needed in the future. On a transcriptional level it has been shown that CD154 expression is suppressed by NFAT-FoxP3 complexes, but induced by NFAT-AP-1 complexes [273]. Higher levels of nuclear NFAT were observed in CD154-expressing Tregs which simultaneously

expressed lower levels of FoxP3. It can be speculated that increased levels of nuclear NFAT together with reduced levels of FoxP3 can favor interaction of NFAT with AP-1 resulting in expression of CD154 along with other effector molecules [244]. Differential levels of nuclear NFAT can be mediated by calcium signaling downstream of TCR activation which were shown to be increased in $CD137^{+}CD154^{+}$ Tregs. It has been shown that Tcons exhibited increased TCR activity compared to Tregs [274] and also in mice acquisition of a Th2 phenotype by Tregs has been associated with elevated expression levels of proteins associated with TCR activity [49]. Therefore, differences in the integration of TCR signals can account for phenotypic plasticity within Tregs. Taken together, understanding mechanisms that regulate CD154 expression and phenotypic plasticity on Tregs can reveal important targets for the stabilization of Tregs *in vitro* and *in vivo*. Based on the findings in this work, it can be hypothesized that differential signal transduction in $CD137^{+}CD154^{+}$ Tregs can account for different levels of nuclear NFAT which then induces, instead of represses, effector molecules and CD154 expression.

Taken together, $CD137^{+}CD154^{-}$ expression emerges as Treg-specific activation signature for the identification and isolation of lineage stable Tregs. It was shown that $CD137^{+}CD154^{-}$ Tregs were remarkably stable *in vitro* while transient phenotypic plasticity was limited to a minor subset that acquired CD154 expression.

5.1.1 Potential roles of CD137 expression on Tregs

CD137 is expressed selectively on Tregs after 5-7h stimulation although it can also be upregulated on $CD4^{+}$ Tcons after longer stimulation [107, 275]. To account for the different kinetics of CD137 expression in Tregs and Tcons, it can be speculated that accessibility of the region is regulated by epigenetic modifications as CD137 has been shown to be hypomethylated in Tregs compared to Tcons [241]. Similarly, *tnfrsf9* was almost completely demethylated in $CD137^{+}CD154^{-}$ Tregs providing a molecular basis for rapid CD137 upregulation on Tregs. There was a remarkable correlation of $CD137^{+}CD154^{-}$ expression with a stable Treg phenotype suggesting a link between FoxP3 and CD137 expression as well as TSDR demethylation. Regulation of Treg-associated genes (e.g. CTLA4) by FoxP3 has been shown [276]. Furthermore, Marson et al. (2007) showed that *tnfrsf9* (CD137) was a direct target of FoxP3 providing a possible link between CD137 upregulation with FoxP3 expression that was shown here [277]. It can be speculated that stable FoxP3 expression that induces CD137

expression is mediated by TSDR demethylation which therefore indirectly correlates with CD137 expression [31-34].

CD137 is an important co-stimulator for T cell activation upon binding of CD137L which is expressed on a variety of APCs and activated T cells [278]. CD137 ligation induces T cell activation and expansion which is currently investigated to heighten T cell responses against tumors. In contrast, the function of CD137 co-stimulation for Tregs remains unclear as studies have reported increased [279-283] or impaired [284] Treg function upon CD137L ligation. In contrast, CD28, CTLA-4 [285] and TIGIT [286] have been shown to augment Treg functionality while CD134 co-stimulation has been shown to abrogate Treg-mediated immunosuppression [287, 288]. Using a chimeric antigen receptor, it was shown here that intracellular CD137 co-stimulation was highly potent in activating and expanding CAR-Tregs suggesting augmented Treg functionality upon CD137L ligation. However, the impact of endogenous CD137-CD137L interaction on Treg functionality *in vitro* and *in vivo* needs to be determined in future studies.

In spite of their potent regulatory functions, mechanisms involved in Treg-mediated suppression are not clearly defined and are currently believed to contain contact-dependent as well as secreted factors [289]. CD137 expression was shown to be rapidly upregulated on antigen-activated Tregs, yet its role in the regulation of immune responses remains elusive [290]. It can be speculated that rapid upregulation of CD137 can enable early interactions of $CD137^+$ Tregs with CD137L-expressing APCs. This mechanism can block co-stimulation of $CD137^+$ Tcons resulting in diminished T cell activation and therefore can represent a potent regulatory mechanism of $CD137^+$ Tregs. CD137 expression was upregulated by the majority of $CD25^+CD127^-$ cells and therefore was not limited to a particular Treg subset. Consequently, its rapid upregulation can provide a versatile and wide-ranging mechanism enabling their interaction with various immune cells following antigen-specific activation. Understanding the interaction of CD137-CD137L as regulatory mechanism can reveal important targets for the fine-tuning of Treg-mediated immunosuppression.

In mice, IL-10 has been well-established as regulatory cytokine contributing to Treg-mediated immunosuppression [291]. In contrast, the abundance and function of Treg-derived IL-10 in humans remains unknown. Most importantly, as lack of markers has prevented tTreg identification, the identity of IL-10-producing cells in humans cannot be unequivocally determined. Interestingly, it was shown here that IL-10 expression, along with inflammatory effector cytokines, was increased in $CD137^+CD154^+$ Tregs, but

absent in stable $CD137^+CD154^-$ Tregs. However, single cell analysis revealed that IL-10 expression derived from only few cells within $CD137^+CD154^+$ Tregs while IL-10-expressing cells were highly abundant in $CD137^-CD154^+$ Tcons. Furthermore, it is important to note that $FoxP3^-$ cells within $CD137^+CD154^+$ Tregs were not characterized by increased IL-10 expression indicating that they do not represent Tr1 cells which are most likely part of the $FoxP3^-CD137^-$ T cell compartment. These data suggest that other than in mice, IL-10 expression does not significantly contribute to Treg-mediated immune regulation in humans. Treg-derived IL-10 has been shown to be most relevant for the maintenance of tolerance at mucosal surfaces, such as the intestine in mice [292]. However, significant IL-10 protein expression was not detected within any of the tissues that were analysed, including lung and colon (data not shown). In summary, it remains elusive to what degree Treg-derived IL-10 contributes to immune regulation in humans. Nevertheless, in this study it was shown that epigenetically imprinted Tregs lacked expression of effector cytokines as well as IL-10 suggesting alternative regulatory mechanisms, such as contact-dependent suppression or consumption of IL-2, that need to be determined in future studies.

5.1.2 Using chimeric antigen receptors to generate antigen-specific Tregs

Autoimmune diseases are the result of ongoing inflammatory immune reactions and local tissue damage, but the mechanisms of their development are complex and largely unknown. It is currently believed that loss of tolerance against autoantigens contributes to chronic inflammation and the destruction of healthy tissue, yet target antigens remain elusive. Therefore, current immunosuppressive approaches are based on a systemic inhibition of effector functions leaving patients severely immunocompromised. Particularly in regard to chronic inflammatory diseases such as rheumatoid arthritis (RA), multiple sclerosis (MS), systemic lupus erythematodes (SLE) or inflammatory bowel disease (IBD), novel therapies are required to directly target disease-relevant populations to restore tolerance while maintaining protective immune reactions.

Tregs exhibit a potent immunosuppressive potential and are important mediators of tolerance. It has been shown that antigen-independent expansion of Tregs *in vivo* by application of IL-2 can restore tolerance in patients with T1D [152], GvHD [148, 151], SLE [150] and HCV-induced vasculitis [149]. Alternatively, increasing Treg frequencies by adoptive transfer of polyclonal Tregs has been shown to be safe and effective in patients suffering from GvHD [174, 177-179, 182] and T1D [173, 175, 176, 180, 181]. For adoptive transfer, large numbers of Tregs are required to suppress inflammation *in*

vivo. As endogenous frequencies of Tregs are low, massive expansion is needed to generate these therapeutically relevant numbers. To increase potency, antigen-specific Tregs are currently evaluated for adoptive transfer whose superior suppressive potential has been shown in mice for the treatment of e.g. T1D [161, 203-205], GvHD [154-158, 166, 167, 201, 202], EAE [79, 200] and arthritis [206, 207]. Thus, transfer of Tregs targeting disease-relevant antigens increases efficacy and therefore lowers the numbers of required cells which reduces the risk of harmful side effects. However, identification and isolation of endogenous antigen-specific Tregs for clinical applications remains challenging and is currently limited by lack of technologies and also relevant Treg targets are mostly unknown [74, 75]. Alternatively, genetic engineering has been investigated to introduce defined specificities into Tregs by TCR or CAR expression. To this end, human Tregs have been redirected toward a melanoma antigen tyrosinase [208], NY-ESO-1 [209] or an islet antigen [210] by TCR gene transfer. Alternatively, CARs with an antibody-type specificity can be redirected toward a large variety of surface antigens which they can bind independent of MHC. In mice, CAR-Tregs have been shown to prevent colitis [227-229], EAE [226], GvHD [230-232], allergic airway inflammation [233] and neutralizing immune responses against Factor VIII [234]. However, treatment of many other inflammatory immune pathologies such as RA, SLE or IBD by antigen-specific CAR-Tregs is currently limited by lack of knowledge about disease-relevant Treg targets.

5.1.2.1 Redirection of Treg specificity toward an exogenous antigen

As disease-relevant Treg targets are mostly unknown, the redirection of Tregs toward an exogenous antigen emerges as promising approach for the controllable activation of Tregs *in vitro* and *in vivo*. For example, it has been shown that Treg activation by male-specific HY antigen can ameliorate GvHD in females when the antigen is applied showing systemic immunosuppression by an exogenous antigen in mice [293]. Furthermore, oral application of ovalbumin (OVA) locally activated OVA-specific IL-10 producing Tr1 cells in the intestine resulting in reduced severity of IBD in mice [21] and humans [294]. In addition, OVA-specific Tregs were able to locally suppress arthritis in a murine adjuvant-induced-arthritis model when ovalbumin was injected into the knee [206]. Collectively, these findings highlight the potential of redirecting regulatory cells toward an exogenous antigen to enable targeted induction of tolerance. However, in humans, endogenous frequencies of Tregs specific for foreign antigens (e.g. ovalbumin) are low and may originate from diverse precursors whose stability *in vivo*

remains elusive. Furthermore, it has been shown that Tcons that are specific for exogenous antigens (e.g. KLH) most likely express cross-reactive TCRs as they accumulated with immunological age which could result in harmful off-target T cell activation *in vivo* [106]. Therefore, in this work, human Tregs were genetically engineered to express a CAR to redirect Treg specificity toward an exogenous antigen to provide a system for targeted Treg activation.

The selection of suitable exogenous antigens represents a major challenge as antigens for targeted Treg activation need to fulfill particular requirements for their therapeutically safe application. Most importantly, they need to be (1) absent from endogenous or frequently encountered structures (2) therapeutically safe and stable upon application by different routes and (3) have a limited persistence *in vivo*. The branched polysaccharide dextran consists of several glucose molecules that are linked by α-1,6 and α-1,3 glycosidic linkages resulting in lengths of 3-2000 kDa. It is not endogenously expressed or regularly encountered but well-tolerated as it is commonly used e.g. as a plasma volume expander or as contrast agent for imaging in medicine. It has been shown that dextran can be applied systemically but also targeted e.g. to the gastrointestinal tract by oral application providing flexible routes of antigen application [295]. Finally, dextran is rather stable *in vivo* with its persistence depending on the molecular weight enabling controllable titration of the antigen [296]. Therefore, dextran emerges as therapeutically safe antigen for controllable and targeted activation of Tregs *in vivo*.

5.1.2.2 Enhancing CAR-Treg efficacy

Efficacy of *in vitro* generated CAR-Tregs depends on their antigen-specific activation and expansion. CARs are artificial constructs and it has been shown that the extracellular, the transmembrane and the intracellular domains can significantly impact T cell activation, expansion and persistence [270, 297]. To evaluate the functionality of different constructs, specific *in vitro* assays are needed which can provide insight into the potential efficacy of CARs *in vivo*. Functionality of CAR-Tcons can readily be analysed by upregulation of effector molecules (e.g. IFN-γ, IL-2) after *in vitro* stimulation. However, functional assays for the analysis of CAR-Treg efficacy are limited due to a lack of markers that are specifically involved in Treg function. Therefore, requirements for the activation and expansion of CAR-Tregs which can significantly differ from Tcons remain poorly understood.

To analyse Treg activation, CD121a/b, LAP, GARP [272, 298, 299] or Ox40/CD39 [300] have been described to identify activated Tregs *ex vivo*, yet they require long stimulation and expression is not limited to the Treg lineage. Recently, CD137 has been shown to be upregulated on Tregs after only 5-7 hours of antigenic stimulation and has been proven to be highly specific for Tregs allowing their *ex vivo* discrimination from $CD137^{-}CD154^{+}$ effector T cells [92, 96, 97, 107]. CD137 expression enabled specific enrichment of antigen-activated Tregs *ex vivo*, displaying all features of thymic Tregs, such as a demethylated TSDR and a Treg specific expression profile, including high levels of FoxP3, Helios, CTLA4 and lack of CD127 and effector cytokines [96]. In this study, CD137 was identified as Treg-specific activation marker for the identification and isolation of antigen-reactive Tregs after prior *in vitro* expansion which enabled the rapid screening of CAR-Treg activation. Furthermore, lack of CD154 expression on $CD137^{+}$ Tregs was shown to identify stable antigen-specific CAR-Tregs enabling the purification of *in vitro* generated Tregs for optimized safety.

Although there is accumulating data about the generation of CAR-Tregs, little is known about the impact of CAR design on Treg function as analysis has been limited by functional *in vitro* assays. In this study, CD137 expression was applied to rapidly optimize the extracellular spacer and the intracellular signaling domain for improved CAR-Treg activation and expansion *in vitro*. It has been shown that the extracellular spacer domain impacts CAR function depending on the size and expression pattern of the target antigen [251-257]. Furthermore, *in vivo* interactions with Fc domains within the spacer have been shown to result in off target activation [253, 301]. Therefore, Fc domains within the CAR constructs were altered to prevent off-target interactions and the impact of spacer length on CAR-Treg function was evaluated. Antigen-binding was significantly influenced by the size of the spacer and was most efficient with short spacer domains. Interestingly, antigen-binding alone was not sufficient for CAR-Treg activation as among dextran-binding cells, CD137 was only upregulated on CAR-Tregs with very short spacer domains (12aa). It can be speculated that full CAR-Treg activation requires not only antigen-binding *per se*, but depends on the affinity and persistence of the receptor-ligand interaction. In line with this hypothesis, Taylor et al. (2017) reported that T cell signaling required formation of submicron receptor clusters which were dependent on the time and affinity of the receptor-ligand interaction [302]. In particular, large antigens such as dextran can benefit from very short and therefore highly flexible spacer domains providing the basis for stable antigen-binding and Treg activation which can rapidly be analysed by CD137 upregulation. Taken together,

CD137 expression emerges as potent Treg-specific activation marker that enabled the rapid testing of CAR-Treg functionality *in vitro* which can provide insight into the specific requirements of Treg activation for augmented CAR-Treg efficacy.

5.1.2.3 CD137 co-stimulation augments CAR-Treg functionality *in vitro*

The *in vivo* function of effector CAR-T cells markedly depends on efficient T cell activation which has been shown to require proper co-stimulation [258-263]. However, lack of functional assays has limited analysis of the impact of different co-stimulatory domains on Treg functionality. In accordance with other reports [266-268], the intracellular signaling domain did not only have an impact on Treg activation, but also on antigen-binding which was almost completely abrogated in constructs with ICOS co-stimulation or CD3ε signaling. This effect was not limited to CAR-Tregs, but was similarly observed on conventional CAR-T cells and most likely derives from steric effects that influence stability of CAR complexes on the cellular surface. Remaining constructs with CD3ζ signaling and CD28, CD137, CD134, PD-1 or no co-stimulation were expressed on the surface and also shown to induce intracellular signaling by phosphorylation of ZAP70. However, Treg activation as measured by CD137 induction was only observed in CAR-Tregs with CD137-CD3ζ or to a lesser extent CD134-CD3ζ signaling. These data reveal significant differences in the functionality of different CAR constructs and underline the importance to carefully test *in vitro* Treg activation which can rapidly be analysed by CD137 expression.

Interestingly, ZAP70 was phosphorylated in only few CAR-Tregs with CD137 co-stimulation while pZAP70 was detected in a significant proportion of $LNGFR^+$ cells with CD28 or no co-stimulation. Nevertheless, signal transduction was highly efficient in CAR-Tregs with CD137 co-stimulation compared to other signaling domains resulting in activation of the majority of dextran-binding cells. It can be speculated that different kinetics can account for the variable levels of pZAP70 that were observed and can suggest a very rapid signal transduction in CAR-Tregs with CD137 co-stimulation compared to CAR-Tregs with CD28 or no co-stimulation. However, levels of ZAP70 phosphorylation upon CAR stimulation with different signaling domains were similar in $CD4^+$ Tcons although signaling output as measured in CD154 upregulation was strikingly different. Therefore, these data reveal surprisingly different requirements of Treg and Tcon activation upon CAR stimulation in spite of similar proximal signal transduction which can rapidly be tested by converse expression of CD137 and CD154. Although the detailed intracellular mechanisms that activate downstream

pathways upon CAR stimulation in Tregs and Tcons remain unclear, superiority of CD137 co-stimulation for Treg activation and expansion becomes evident.

In addition to stronger activation, CAR-Tregs with CD137-CD3ζ signaling expanded more efficiently *in vitro*, indicating augmented proliferation compared to other co-stimulatory domains. In contrast, CAR-Tregs with CD134 co-stimulation did not exhibit antigen-specific expansion suggesting inefficient activation or survival. It has been shown that CD134 co-stimulation negatively affects Treg function providing a possible explanation for their impaired functionality upon *in vitro* expansion [287, 288]. Although CD134 co-stimulation induced CD137 expression in most donors, protein levels were low and often only marginally above the background already indicating impaired functionality. Conversely, CD28 co-stimulation did not induce Treg activation, yet there was minor antigen-specific expansion in some donors. These data reveal some discrepancies between activation-induced CD137 upregulation and *in vitro* expansion indicating that lack of CD137 expression not necessarily showed complete dysfunction of a construct although it consistently correlated with impaired functionality. Collectively, CD137 expression enabled rapid analysis of Treg activation for improved CAR-Treg efficacy whose correlation with long-term persistence and proliferation *in vivo* needs to be analysed in future studies.

The requirement of CD137 co-stimulation for CAR-Treg activation that was shown here is in contrast to studies that have generated functional CAR-Tregs with CD28 co-stimulation [230-234]. In mice it has been shown that CD28, but not CD137 co-stimulation initiated tonic signaling in conventional T cells resulting in an exhaustion phenotype and limited efficacy [303]. However, in that particular study the degree of exhaustion varied between CARs in spite of identical signaling domains. Therefore, superiority of CD137 that was shown here is not in contrast to studies that have generated functional CAR-Tregs with CD28-CD3ζ signaling but suggests that CD137 provides superior co-stimulation resulting in augmented CAR-Treg functionality. These findings highlight the importance to carefully assess and optimize CARs for heightened potency.

In this work, generation and activation of dextran-specific Tregs was shown and CAR efficacy was optimized *in vitro* as prerequisite for their functionality *in vivo*. Future studies are needed to confirm their functionality in different mouse models. Most importantly, feasibility of local or systemic application of dextran to redirect Tregs to inflamed tissue e.g. during GvHD or colitis needs to be evaluated. Furthermore, the

composition of the antigen can significantly influence CAR-Treg efficacy as soluble or cross-linked dextran could differ in their ability to bind and activate CAR-Tregs. In addition, the coupling of rapamycin to biodegradable nanoparticles has been shown to increase their tolerogenic potential showing that additional modifications can contribute to heightened functionality of antigen-specific Tregs *in vivo* [304]. Similarly, the combination of CAR-Treg therapy with IL-2 treatment could enhance their *in vivo* expansion resulting in potent immunosuppression. In conclusion, dextran-specific CAR-Tregs have the potential to become a versatile therapeutic approach for targeted immunosuppression in multiple inflammatory immune pathologies.

Taken together, $CD137^{+}CD154^{-}$ expression emerges as Treg-specific activation signature to improve purity of *in vitro* generated Tregs. For clinical applications, Tregs can be isolated from peripheral blood by GMP-compliant CD25 expression. This results in heterogeneous cultures containing stable Tregs, instable Tregs and contaminating non-Tregs (Figure 38). Treg cultures can be expanded *in vitro* and their functionality can be modified, e.g. by genetic engineering of their antigen receptors to redirect their specificity. Sufficiently expanded Treg cultures can be restimulated by either polyclonal or antigen-specific activation to identify and isolate stable $CD137^{+}CD154^{-}$ Tregs while eliminating contaminating inflammatory CD154-expressing cells. Upon transfer, epigenetically stable Tregs with disease-relevant specificities can be activated locally and can suppress chronic immune pathologies within inflamed tissues (e.g. brain, gut, joints). If disease-relevant targets are unknown, Tregs can be redirected toward an exogenous antigen by CAR expression and application of the antigen can induce local or systemic Treg activation for targeted immunosuppression.

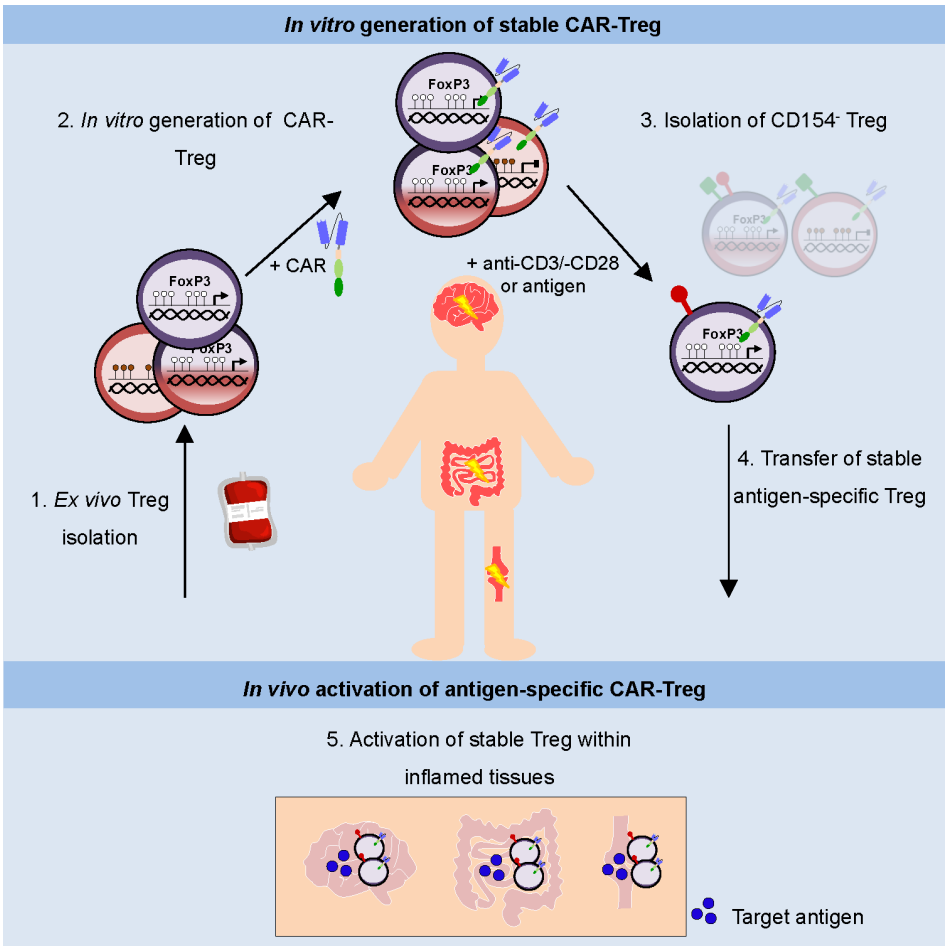

Figure 38: Schematic diagram of optimized Treg therapy. (1) Tregs can be isolated from peripheral blood of patients that suffer from chronic inflammation e.g. at the brain, gut or joints resulting in epigenetically imprinted stable and instable Tregs as well as contaminating effector cells. **(2)** Tregs can be expanded and engineered *in vitro* to express a CAR with defined specificity and **(3)** upon polyclonal or antigen-specific stimulation, CD154-expressing cells that are able to exert effector functions can be eliminated. **(4)** For adoptive transfer, stable $CD137^{+}CD154^{-}$ Tregs can be purified from *in vitro* cultures and **(5)** are redirected toward local tissues *in vivo* either by endogenous antigen expression or application of the target antigen.

5.2 The contribution of Treg-Tcon conversion to the peripheral Treg compartment

Although Tregs emerge as a promising target for the treatment of inflammatory immune pathologies, little has been known about the heterogeneity and stability of the physiological Treg compartment in humans. Conversion between the Treg and Tcon compartment have been shown, including Treg reprogramming and extrathymic pTreg induction, yet their contribution to human immune responses remains poorly understood.

Pathogenic conversion of Tregs has been observed *in vivo* in mice and has been shown to contribute to autoimmunity [44-46], allergy [47] and chronic inflammation [48]. Furthermore, pTregs have been shown to be induced in the periphery from Tcons and it is currently believed that pTregs contribute to peripheral tolerance, in particular against non-self antigens. For example, pTregs have been shown to be important for the maintenance of tolerance against commensal microbiota [88-91], dietary antigens [120, 121] and during maternal-fetal conflict in mice [305]. Furthermore, preventing extrathymic Treg induction resulted in spontaneous Th2-type pathologies at mucosal sites such as allergic inflammation and asthma [122]. These findings suggest a very distinct functional separation of thymic-derived Tregs that control autoimmunity and pTregs that prevent immune reactions against non-self. Collectively, the contribution of Treg-Tcon conversion to the peripheral Treg compartment and to human immune responses remains poorly understood.

Here it was shown that $CD137^{+}CD154^{-}$ expression identified epigenetically stable and clonally distinct Tregs which can be speculated to be of a thymic origin and can therefore provide insight into the specificity and stability of *bona fide* Tregs in humans. In contrast, the ability to exert effector functions was restricted to a $CD137^{+}CD154^{+}$ Treg subset within the $CD25^{+}CD127^{-}$ Treg compartment which was characterized by expression of pro-inflammatory cytokines, compromised suppressive capacity and a partially methylated TSDR, yet their origin and function remain elusive. Tracking of clonal progenitors by TCR sequencing showed that Tcon- and Treg-derived sequences were found within $CD137^{+}CD154^{+}$ Tregs. Furthermore, $CD137^{+}CD154^{+}$ Tregs exhibited an intermediate epigenetic and transcriptional Treg-Tcon signature and also single cell transcriptional analysis showed heterogeneity within $CD137^{+}CD154^{+}$ Tregs. Therefore it can be hypothesized that transitional processes of Treg-Tcon conversion occurred particularly within this effector-like $CD137^{+}CD154^{+}$ subset. In contrast, single cell methylation analysis and cloning revealed that there were no ongoing methylation processes within $CD137^{+}CD154^{+}$ Tregs indicating no epigenetic reprogramming. This distinct epigenetic pattern was observed at the TSDR, but also within the FoxP3 promoter. Transitional processes involving loss or acquisition of FoxP3 expression would most likely involve reprogramming within the promoter region to regulate gene expression. Therefore, $CD137^{+}CD154^{+}$ Tregs did not identify Treg-Tcon conversion, but represented a mixture of epigenetically imprinted Tregs and Tcons. These data show transient plasticity, but not transition, of Tregs and Tcons within the $CD137^{+}CD154^{+}$ subset.

Transitional processes were not detected within the polyclonal Treg compartment and also the polyclonal TCR repertoires of $CD137^{+}CD154^{-}$ Tregs and $CD137^{-}CD154^{+}$ Tcons were distinct. These data provide no evidence for Treg-Tcon conversion within the peripheral Treg compartment. However, it can be speculated that Treg-Tcon conversion occurs particularly against defined antigens during specific immune responses. For example, Treg conversion has been associated with TCR activation [50, 61] and has been shown during inflammatory immune responses against pathogens, e.g. during helminth infection [49] and Herpes simplex virus infection [48]. Induction of pTregs has particularly been associated with mucosal surfaces to maintain tolerance against microbiota and commensals as well as against other harmless environmental antigens [306]. Therefore it can be speculated that Treg-Tcon conversion was restricted to individual clones that can specifically contribute to immune responses against defined antigens. Antigen-specific Treg-Tcon conversion would result in low frequencies of cells that were undergoing transitional processes which most likely could not be detected within the polyclonal Treg compartment. To analyse Treg-Tcon conversion during antigen-specific immune responses, activation-induced CD137 and CD154 expression were used to isolate rare antigen-specific T cells [92, 96, 97, 107]. To track the clonal progenitors of Tregs and Tcons in response to a pathogen (CMV) and commensals (*E. coli* and *C. albicans*), the TCR repertoires of antigen-specific Tregs and Tcons were sequenced. *E. coli* and *C. albicans* are found at mucosal surfaces while CMV is a latent virus. Therefore, these antigens are frequently encountered by the immune system and it can be speculated that they require peripheral tolerance mechanisms (*E. coli* and *C. albicans*) or can contribute to Treg conversion (CMV). Within the antigen-specific repertoires, there were no overlapping clonotypes between Tregs and Tcons in response to CMV, *E. coli* and *C. albicans.* Similarly, distinct repertoires of Tregs against *A. fumigatus* and birch have recently been shown providing no evidence for Treg-Tcon conversion against these antigens [96]. As whole cell lysates were used for stimulation, it cannot be excluded that Tregs and Tcons that were specific for the same antigen were actually reactive against different proteins which has recently been shown for birch [96]. Nevertheless, independent of their peptide specificity, these data show that Tregs and Tcons specific for CMV, *E. coli* and *C. albicans* derived from distinct precursors providing no evidence for Treg-Tcon conversion on an antigen-specific level.

An alternative explanation for the absence of Treg-Tcon conversion in human blood could be lack of inflammation or the local conversion in tissues as seen in mice [88,

115, 119, 307-310]. However, this is unlikely, as albeit frequencies of converted Tregs in mice were increased in inflamed tissues, they could readily be detected during homeostasis and throughout peripheral organs [45, 46, 52, 100, 122, 125]. In humans, Tregs and Tcons specific for various antigens, including mucosa-associated antigens such as *E. coli*, *C. albicans* or *C. leptum*, were detected in peripheral blood showing the circulation of Tregs that were specific for local antigens [96]. It was now shown that the TCR repertoires of Tregs and Tcons specific for different antigens (*C. albicans, A. fumigatus*, birch, *E. coli,* CMV) were distinct indicating no Treg-Tcon conversion within the circulation. However, it cannot be excluded that pTregs or converted Tregs that are reprogrammed at local sites are retained within the tissue or undergo apoptosis once they enter the circulation and therefore cannot be detected in the periphery. Consequently, sequencing of the TCR repertoires of antigen-specific Tregs and Tcons from different tissues are required in the future.

Another explanation for the absence of overlapping clonotypes can be the conversion of all progeny of a single clonotype within an antigen-specific immune response. This would result in the complete conversion and therefore lack of overlap between Tregs and Tcons. However in mice, Treg-Tcon conversion never affected an entire clonal naive T cell population [47, 102, 115, 123]. Furthermore, Treg induction has been associated with strong proliferation which would result in pronounced TCR sequence overlap between related populations [310]. In addition, it can be hypothesized that such a massive conversion would result in notable reprogramming even within the polyclonal Treg compartment, which was shown here to be completely absent. It cannot be fully excluded that individual clones that have converted were no longer detected within the original population, yet this would require very rapid and complete conversion which is highly unlikely.

Comprehensive analysis of $CD137^{+}CD154^{-}$ Tregs and $CD137^{+}CD154^{+}$ Tregs revealed heterogeneity and transient phenotypic plasticity within the peripheral Treg compartment, but provided no evidence for conversion between Tregs and Tcons. It was shown that Tregs and Tcons in the periphery derived from separate lineages and exhibited distinct epigenetic signatures and individual TCR repertoires that similarly included specificities for foreign antigens such as CMV, *C. albicans* or *E. coli* (Figure 39). Collectively, it was shown that human $CD137^{+}CD154^{-}$ Tregs were remarkably stable *in vitro* and *in vivo* with only a small epigenetically imprinted subset that exhibited minor phenotypic plasticity and was prone to the acquisition of effector functions, including upregulation of CD154, whose immunological function needs to be

determined in the future. In addition, it was shown that some cells from the Tcon lineage that expressed CD154 after stimulation could upregulate CD137. Nevertheless, there was no conversion between the Treg and Tcon compartment, not even within the $CD137^{+}CD154^{+}$ Treg subset which contained a mixture, but not transition, of epigenetically imprinted Tregs and Tcons. It remains to be determined in future studies whether particular environmental conditions or antigens promote phenotypic plasticity, but collectively these findings provide no evidence for Treg reprogramming or peripheral Treg-Tcon conversion *in vitro* or during antigen-specific immune responses *in vivo* (Figure 39). It cannot be excluded that conversion might be increased during or even favor the development of certain immune pathologies in humans, but obviously it does not represent a major mechanism contributing to peripheral tolerance under steady-state conditions.

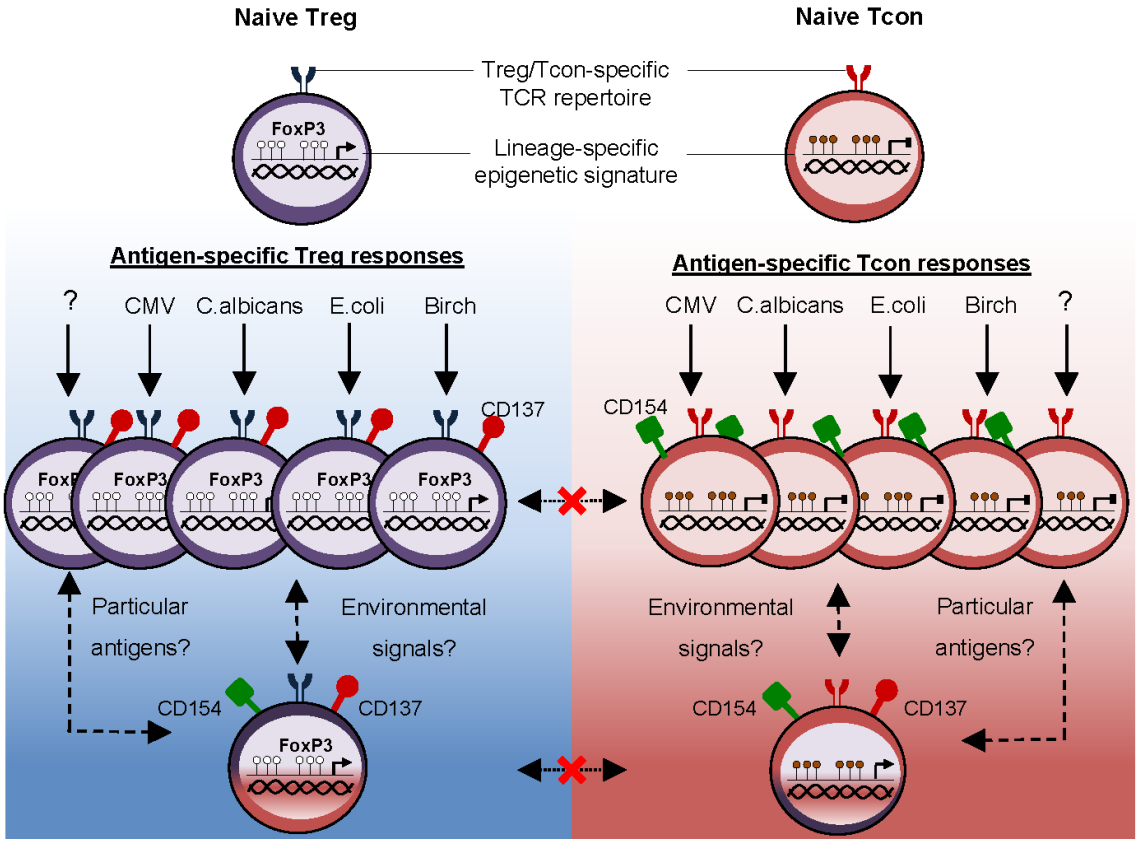

Figure 39: Stability of the Treg lineage during antigen-specific immune responses *in vivo*. Treg (left) and Tcon (right) develop as distinct lineages in the thymus with a specific epigenetic signature and TCR repertoire. Upon antigen encounter in the periphery, Treg upregulate CD137 while Tcon express CD154. Although under certain conditions (e.g. environmental signals or particular antigens) Treg and Tcon can co-express CD137 and CD154, there is no conversion between the Treg and Tcon compartment.

5.2.1 Plasticity within the peripheral Treg compartment

In this study, $CD137^{+}CD154^{-}$ expression was shown to identify a prototypic Treg subset with an epigenetic Treg signature and a distinct TCR repertoire which is in all likelihood thymic-derived whereas transient plasticity, but not conversion, was observed within $CD137^{+}CD154^{+}$ Tregs. $CD137^{+}CD154^{+}$ expression was not stably maintained but only transiently upregulated on epigenetically imprinted Tregs and Tcons that readily lost CD154 or CD137 expression, respectively, upon expansion. Therefore, $CD137^{+}CD154^{+}$ expression can provide insight into the contribution of transient Treg and Tcon plasticity to the peripheral Treg compartment.

Frequencies of $CD137^{+}CD154^{+}$ Tregs were low within the polyclonal Treg compartment indicating only minor plasticity in healthy individuals. However, it can be speculated that certain environmental conditions, e.g. inflammation or chronic activation can contribute to transient phenotypic plasticity of Tregs and Tcons. Treg stability has been shown to be influenced by culture conditions *in vitro* [55-59, 68, 69] and also, cytokine-producing Tregs have been shown to be increased in patients suffering from MS [66], T1D [67], arthritis [45, 68, 69], psoriasis [70] and IBD [71-73]. Thus, it can be hypothesized that inflammatory immune pathologies favor plasticity. To provide insight into the phenotypic plasticity of the peripheral Treg compartment that was exposed to different environmental conditions *in vivo*, CD137 and CD154 expression were analysed on Tregs isolated from thymus, tonsil, lung and colon. Compared to Tregs derived from the thymus, higher levels of $CD137^{+}CD154^{+}$ expression were detected in other analysed organs as well as in peripheral blood. These findings suggest that Treg plasticity was increased within the periphery. However, even Tregs that were isolated from tonsil, lung and colon that were most likely exposed to an inflammatory environment *in vivo* expressed only low levels of CD154. Since samples were obtained from various donors that were of different ages it cannot be clearly determined whether observed phenotypic differences derived from their differential localization or donor variability. For example, thymus samples were obtained from young individuals that were only a couple of days up to a few months old. Therefore, it cannot be determined whether lack of CD154 expression on thymic Tregs derived from their thymic origin or would similarly be observed within other organs of the same individual. Nevertheless, overall low levels of CD154 expression within tissue-derived Tregs provide further evidence for the remarkable stability of Tregs within the circulation and local tissues.

In addition to environmental conditions, it can be speculated that Treg and Tcon plasticity was restricted to particular clones. Within the polyclonal Treg compartment only low frequencies of $CD137^+CD154^+$ Tregs were detected, yet it cannot be excluded that these cells specifically contribute to particular immune responses. Therefore, CD137 and CD154 expression were analysed on antigen-specific T cells during different immune responses against numerous tolerogenic (e.g. *E. coli*, food), pathogenic (e.g. CMV, influenza A virus, *S. aureus*) and non-pathogenic (e.g. *C. albicans*, house dust mite, pollen antigens) antigens using antigen-reactive T cell enrichment (ARTE). However, none of the tested responses revealed significant frequencies of $CD137^+CD154^+$ Tregs (data not shown). ARTE is a highly sensitive assay which is able to detect ~1 cell within 10^5-10^6 [106]. However, the peripheral Treg compartment only contained low frequencies of $CD137^+CD154^+$ Tregs and therefore absence of $CD137^+CD154^+$ Tregs during antigen-specific immune responses can also derive from an inability to detect such low numbers. Nevertheless, the high frequencies of $CD137^+CD154^-$ Tregs that were reactive against the tested antigens suggest that a vast majority of antigen-specific immune responses were mediated by stable $CD137^+CD154^-$ Tregs [96]. However, a highly specific, yet undefined function of plasticity and $CD137^+CD154^+$ Tregs cannot be excluded.

Although it was shown that the majority of the peripheral Treg compartment comprised $CD137^+CD154^-$ Tregs, CD154 expression could transiently be acquired by lineage stable Tregs. However, it remains elusive whether transient acquisition of CD154 affects Treg function and in what way it may contribute to immune reactions or even pathology. CD154 is an important co-stimulator that is mainly expressed on activated T cells which enables interaction with CD40-expressing cells (e.g. B cells, DCs, macrophages). The CD154-CD40 interaction has been shown to impact many different immune pathways and initiate cellular and humoral immune responses such as germinal center formation, immunoglobulin isotype switching and formation of plasma cells and memory B cells [311, 312]. Therefore, it can be speculated that rapid upregulation of CD154 on Tregs can enable their interaction with various immune cells that express CD40. For example, CD154-expressing Tregs could augment immune reactions by initiation of humoral immune responses, yet whether they complement or dominate particular effector cell reactions remains unknown. Consequently, the function of CD154 upregulation by some Tregs during homeostasis but also during different immune pathologies needs to be focus of further research.

Here, it was shown that $CD137^+CD154^+$ Tregs contained epigenetically imprinted Tcon clones that had down-regulated effector functions which most likely represented pTregs. Single cell analysis revealed that $CD137^+CD154^+$ Tregs lacked expression of inflammatory cytokines (e.g. IFN-γ, IL-2) which were highly expressed in $CD137^-$ $CD154^+$ Tcons. Therefore, induction of rapid CD137 upregulation on Tcons can enable analysis of factors that have the potential to induce iTregs or pTregs *in vitro* and *in vivo*. Most commonly, TGF-β has been shown to induce a regulatory phenotype in Tcons, but also vitamin C [48, 313, 314], sodium butyrate [315, 316] or retinoic acid [48, 119, 308, 317-320] have been evaluated for their ability to induce Tregs. Although CD137 and CD154 co-expression can enable the rapid analysis of iTreg or pTreg induction, their relevance for the maintenance of tolerance in humans are questioned by the low frequencies of $CD137^+CD154^+$ Tregs and their absence during antigen-specific immune responses that were shown here. These findings suggest only a minor contribution of pTregs to the peripheral Treg compartment and indicate only negligible contribution to tolerance which is dominated by stable Tregs. Therefore, it can be proposed that tolerance induction *in vivo* needs to target stable Tregs, but not aim to induce or expand pTregs.

5.2.2 Non-self specificities within the peripheral Treg compartment do not derive from extrathymic Treg induction

It is currently believed that Tregs are selected based on their intermediate affinity to autoantigens in the thymus which directs their repertoire toward recognition of self [76-83]. In contrast, Tcons are directed toward foreign antigens by the positive selection of low affinity interactions with self-MHC-peptide complexes. However, this model of Treg-intrinsic self-reactivity is challenged by the fact that the Treg repertoire is similarly diverse as that of Tcons [321, 322] and that in mice thymic-derived Tregs can recognize foreign antigens such as intestinal commensals [84], pathogens [85-87] or ectopic antigens (e.g. Cre or OVA) [80, 323]. Furthermore, $FoxP3^+$ Tregs from human blood have been shown to recognize antigens derived from HIV, melanoma, influenza [94], Varicella zoster [95], hepatitis C [93], *A. fumigatus*, *C. albicans*, *S. aureus*, CMV, influenza A, mite, birch and grass [92, 96, 97]. Moreover, it has been demonstrated that human Tregs can suppress effector cell responses in an antigen-specific manner showing that Tregs and Tcons can target the same antigen [96]. Collectively, the occurrence of non-self specificities within the peripheral Treg compartment suggests

that thymic Treg selection is not exclusively limited to self-reactive TCRs and highlight the importance of Tregs for the maintenance of tolerance against foreign antigens.

Treg development is currently believed to be driven by intermediate affinity interactions with self-MHC-peptide complexes resulting in commitment to the Treg lineage upon TCR selection. However, if TCR selection was the main driver for Treg development, diversity of the Treg repertoire would strongly depend on the selecting ligands in the thymus. On the contrary, it was observed that presentation of a single peptide on MHCII in mice resulted in highly diverse Treg repertoires [127, 130]. Furthermore, increased overlap between the Treg and Tcon repertoires was observed in these mice indicating that expression of the same TCR did not selectively induce Treg or Tcon development. Similarly, it was shown that the same self-peptide can select Tregs and Tcons providing further evidence for TCR-independent commitment to the Treg lineage [324].

As alternative model to TCR-dependent, affinity-based Treg development, it has been proposed that the Treg repertoire is shaped by an increased resistance to negative selection which selectively affects Tcons [325, 326]. For example, van Santen et al. (2004) showed that increasing numbers of agonist ligand in the thymus had no impact on the numbers of developing Tregs but resulted in increased deletion of Tcons leading to a higher proportion of Tregs in the periphery [327]. Therefore, peptide expression in the thymus appeared to be a more potent driver of Tcon deletion rather that Treg induction [328]. The transcription factor *Aire* promotes presentation of tissue specific antigens in the thymus and therefore represents an important mechanism of central tolerance. However, *Aire* deficiency is mostly associated with lack of negative selection of Tcons while an impact on Tregs is less clear and remains controversial [17]. The selective model of Treg development suggests that Treg commitment is driven by TCR-independent processes and pre-committed Tregs undergo TCR selection with an intrinsic resistance to clonal deletion which leads to the generation of highly diverse repertoires with specificities against self and non-self. If such an unbiased TCR rearrangement is assumed to occur in Tregs, this could account for the observations of Tregs that have similar specificities compared to Tcons although they differ in their TCR clones [96, 128]. Based on this model, it can be speculated Tregs can recognize a highly diverse repertoire of non-self which can partly be mediated by cross-reactive TCRs [6, 329].

Collectively, TCR-independent commitment to the Treg lineage can provide an explanation for the enrichment of self-reactive TCRs within the Treg repertoire, but similarly account for highly diverse repertoires that match Tcon specificities. However, what drives this TCR-independent commitment to the Treg lineage remains unclear. FoxP3 expression has been observed independent of TCR signals, yet whether it identifies pre-committed Tregs remains elusive [330]. In addition, the importance of epigenetic imprinting of Tregs in the thymus becomes evident and has been shown to occur early during Treg development independent of FoxP3 expression [331, 332]. Consequently, the requirements for thymic Treg development and selection remain poorly understood and most likely contain a combination of various factors, including TCR-dependent and -independent mechanisms, such as secreted signals, co-stimulation, different APCs or individual niches. In summary, it becomes clear that Tregs and Tcons can similarly respond to foreign antigens in the periphery which enables their simultaneous contribution to antigen-specific immune responses. Future studies will need to address the mechanisms that promote Treg development and shaping of their repertoire in the thymus, but also elucidate the role of Treg specificity for the maintenance of tolerance, the regulation of antigen-specific Treg responses and consequently its contribution to the development of various immune pathologies.

6 Summary

Regulatory T cells (Tregs) are essential mediators of tolerance and crucial for the containment of inflammatory immune reactions. Their immunosuppressive potential is currently investigated for the treatment of inflammatory diseases. However, conversion between the Treg and conventional T cell (Tcon) compartment has been described, comprising the induction or loss of the regulatory phenotype *in vivo* which generates significant safety concerns for the therapeutic use of Tregs e.g. for adoptive transfer. To what extent such Treg plasticity affects the formation and stability of the human Treg compartment and how it influences specific immune responses *in vivo* is currently unknown. In addition, therapeutic Treg application often requires prolonged *in vitro* culture to generate sufficient Treg numbers or to optimize their functionality, e.g. via genetic engineering of their antigen receptors. However, purity of clinical Treg expansion cultures is highly variable and it is currently challenging to identify and separate stable Tregs from contaminating Tcons, either *ex vivo* or after prior expansion. Inaccuracy of the identification of stable Tregs also limits the development of protocols for specific manipulation of Treg functions. Therefore, this study aimed to identify markers for the unambiguous identification of stable Tregs to improve efficacy and safety of *in vitro* generated Tregs as well as to provide insight into the heterogeneity and stability of the physiological Treg compartment in humans.

Here, $CD137^{+}CD154^{-}$ expression was described as Treg-specific activation signature after short-term reactivation. It was shown to identify prototypic stable Tregs that were characterized by a phenotypic and epigenetic Treg signature, high suppressive potential and lack of inflammatory cytokine expression. This Treg-specific activation signature enabled the purification of stable *in vitro* generated Tregs and also allowed for the rapid *in vitro* optimization of chimeric antigen receptor (CAR) constructs for human Tregs which revealed major differences in the signaling requirements compared to Tcons. In addition, antigen-specific responses against various antigens were dominated by prototypic $CD137^{+}CD154^{-}$ Tregs and $CD137^{-}CD154^{+}$ Tcons with no overlapping TCR sequences indicating no major contribution of Treg-Tcon conversion to the Treg repertoire. In contrast, TCR overlap with Tcons was restricted to a minor $CD137^{+}CD154^{+}$ Treg subset with an epigenetically and transcriptionally intermediate Treg-Tcon phenotype whose function remains unknown. Nevertheless, CD137 and CD154 co-expression did not identify conversion, but a mixture of epigenetically imprinted Tregs and Tcons.

Taken together, $CD137^{+}CD154^{-}$ expression emerges as a universal Treg activation signature *ex vivo* and upon *in vitro* expansion allowing the identification and isolation of

stable antigen-activated Tregs and providing a means for their rapid functional testing *in vitro*. Furthermore, it was shown that most human Tregs represent a highly stable cell lineage which contributes to *in vivo* immune reactions suggesting minor Treg instability and negligible peripheral Treg-Tcon conversion during the majority of human Treg responses *in vivo*. Consequently, stable $CD137^{+}CD154^{-}$ Tregs emerge as important target for clinical applications and can contribute to the optimization of the efficacy and safety of therapeutic Tregs.

7 Zusammenfassung

Regulatorische T Zellen (Tregs) sind wichtig für die Aufrechterhaltung von Toleranz und die Eindämmung von entzündlichen Immunreaktionen. Die suppressiven Eigenschaften von Tregs können zur Entwicklung von neuen Therapien zur Behandlung von entzündlichen Immunerkrankungen beitragen. Es wurde jedoch gezeigt, dass Tregs und konventionelle T Zellen (Tcons) ineinander übergehen können, was den Verlust oder auch die Induktion von regulatorischen Eigenschaften *in vivo* beinhaltet und die therapeutische Anwendung von Tregs, z.B. durch adoptiven Transfer aufgrund von Sicherheitsbedenken limitiert. Inwiefern diese Treg Plastizität zur Bildung und Stabilität des menschlichen Treg Kompartiments, als auch zu spezifischen Immunreaktionen *in vivo* beiträgt, bleibt unklar. Die therapeutische Anwendung von Tregs bedarf langer *in vitro* Expansion um ausreichende Zellzahlen zu erlangen oder um deren Funktionalität, z.B. durch genetische Veränderung der Antigenrezeptoren, zu optimieren. Die Reinheit der expandierten Kulturen ist jedoch höchst variabel, da es momentan kaum möglich ist stabile Tregs von kontaminierenden Tcons *ex vivo* oder nach *in vitro* Expansion zu unterscheiden. Ferner begrenzen solche Ungenauigkeiten die Entwicklung von Protokollen zur spezifischen Manipulation von Tregs. Deshalb war es Ziel dieser Arbeit neue Marker für die eindeutige Identifizierung stabiler Tregs zu beschreiben welche zum einen zur verbesserten Wirksamkeit und Sicherheit von *in vitro* generierten Tregs beitragen können, als auch wichtige Einblicke in die Stabilität und Heterogenität des humanen Treg Kompartiments ermöglichen.

Es wurde gezeigt, dass $CD137^{+}CD154^{-}$ Expression nach kurzer Stimulation eine Treg-spezifische Aktivierungssignatur darstellt. Diese wurde auf stabilen Tregs exprimiert, welche eine phänotypische und epigenetische Treg Signatur sowie ein hohes suppressives Potential aufwiesen, jedoch keine pro-inflammatorischen Zytokine produzierten. Mithilfe dieser Treg-spezifischen Aktivierungssignatur konnten stabile Tregs aufgereinigt und chimäre Antigenrezeptoren (CARs) für Tregs *in vitro* optimiert werden, welche unterschiedliche Anforderungen bezüglich der Signaldomänen im Vergleich zu Tcons aufwiesen. Des Weiteren wurden antigen-spezifische Immunantworten gegen verschiedene Antigene von stabilen $CD137^{+}CD154^{-}$ Tregs und $CD137^{-}CD154^{+}$ Tcons mit unterschiedlichen T Zell Rezeptor (TCR) Sequenzen vermittelt, welches die Abwesenheit von Treg-Tcon Übergängen im Treg Repertoire aufzeigte. Es wurde ebenfalls eine kleine $CD137^{+}CD154^{+}$ Treg Population detektiert, welche TCR Überlappung mit Tcon und eine intermediäre epigenetische und transkriptionelle Treg-Tcon Signatur aufwies, deren Funktion bisher nicht geklärt

werden konnte. Diese Population identifizierte jedoch keine Übergänge, sondern eine Mischung aus stabilen Tregs und Tcons.

Zusammengefasst konnte gezeigt werden, dass $CD137^{+}CD154^{-}$ Expression als universelle Treg Aktivierungssignatur die Identifizierung und Isolierung von stabilen antigen-aktivierten Tregs *ex vivo* und nach *in vitro* Expansion, sowie deren schnelle funktionelle Testung *in vitro*, ermöglichte. Des Weiteren wurde gezeigt, dass die meisten menschlichen Tregs von einer stabilen Linie abstammen, welche zu Immunreaktionen *in vivo* beiträgt was ein nur geringes Aufkommen von Treg Instabilität und Treg-Tcon Übergängen aufzeigt. Dementsprechend kann eine gezielte Anwendung von $CD137^{+}CD154^{-}$ Tregs die Wirksamkeit und Sicherheit von therapeutischen Tregs maßgeblich verbessern.

8 References

[1] Janeway, C.A., Jr.,Medzhitov, R. Innate immune recognition. *Annu Rev Immunol* 20, 197-216 (2002).

[2] Boehm, T.,Swann, J.B. Origin and evolution of adaptive immunity. *Annu Rev Anim Biosci* 2, 259-83 (2014).

[3] Nemazee, D. Receptor selection in B and T lymphocytes. *Annu Rev Immunol* 18, 19-51 (2000).

[4] Schatz, D.G. V(D)J recombination. *Immunol Rev* 200, 5-11 (2004).

[5] Wucherpfennig, K.W., Gagnon, E., Call, M.J., Huseby, E.S.,Call, M.E. Structural biology of the T-cell receptor: insights into receptor assembly, ligand recognition, and initiation of signaling. *Cold Spring Harb Perspect Biol* 2, a005140 (2010).

[6] Zarnitsyna, V.I., Evavold, B.D., Schoettle, L.N., Blattman, J.N.,Antia, R. Estimating the diversity, completeness, and cross-reactivity of the T cell repertoire. *Front Immunol* 4, 485 (2013).

[7] Yates, A.J. Theories and quantification of thymic selection. *Front Immunol* 5, 13 (2014).

[8] Starr, T.K., Jameson, S.C.,Hogquist, K.A. Positive and negative selection of T cells. *Annu Rev Immunol* 21, 139-76 (2003).

[9] Zhang, N.,Bevan, M.J. CD8(+) T cells: foot soldiers of the immune system. *Immunity* 35, 161-8 (2011).

[10] Geginat, J., Paroni, M., Maglie, S., Alfen, J.S., Kastirr, I., Gruarin, P. et al. Plasticity of human CD4 T cell subsets. *Front Immunol* 5, 630 (2014).

[11] Xing, Y.,Hogquist, K.A. T-cell tolerance: central and peripheral. *Cold Spring Harb Perspect Biol* 4 (2012).

[12] Sakaguchi, S., Yamaguchi, T., Nomura, T.,Ono, M. Regulatory T cells and immune tolerance. *Cell* 133, 775-87 (2008).

[13] Anderson, M.S., Venanzi, E.S., Chen, Z., Berzins, S.P., Benoist, C.,Mathis, D. The cellular mechanism of Aire control of T cell tolerance. *Immunity* 23, 227-39 (2005).

[14] DeVoss, J., Hou, Y., Johannes, K., Lu, W., Liou, G.I., Rinn, J. et al. Spontaneous autoimmunity prevented by thymic expression of a single self-antigen. *J Exp Med* 203, 2727-35 (2006).

[15] Liston, A., Lesage, S., Wilson, J., Peltonen, L.,Goodnow, C.C. Aire regulates negative selection of organ-specific T cells. *Nat Immunol* 4, 350-4 (2003).

[16] Taniguchi, R.T., DeVoss, J.J., Moon, J.J., Sidney, J., Sette, A., Jenkins, M.K. et al. Detection of an autoreactive T-cell population within the polyclonal repertoire that undergoes distinct autoimmune regulator (Aire)-mediated selection. *Proc Natl Acad Sci U S A* 109, 7847-52 (2012).

[17] Anderson, M.S.,Su, M.A. AIRE expands: new roles in immune tolerance and beyond. *Nat Rev Immunol* 16, 247-58 (2016).

[18] Mathis, D.,Benoist, C. A decade of AIRE. *Nat Rev Immunol* 7, 645-50 (2007).

[19] Klein, L., Kyewski, B., Allen, P.M.,Hogquist, K.A. Positive and negative selection of the T cell repertoire: what thymocytes see (and don't see). *Nat Rev Immunol* 14, 377-91 (2014).

[20] Bluestone, J.A. Mechanisms of tolerance. *Immunol Rev* 241, 5-19 (2011).

[21] Groux, H., O'Garra, A., Bigler, M., Rouleau, M., Antonenko, S., de Vries, J.E. et al. A CD4+ T-cell subset inhibits antigen-specific T-cell responses and prevents colitis. *Nature* 389, 737-42 (1997).

[22] Bacchetta, R., Lucarelli, B., Sartirana, C., Gregori, S., Lupo Stanghellini, M.T., Miqueu, P. et al. Immunological Outcome in Haploidentical-HSC Transplanted Patients Treated with IL-10-Anergized Donor T Cells. *Front Immunol* 5, 16 (2014).

[23] Gagliani, N., Jofra, T., Stabilini, A., Valle, A., Atkinson, M., Roncarolo, M.G. et al. Antigen-specific dependence of Tr1-cell therapy in preclinical models of islet transplant. *Diabetes* 59, 433-9 (2010).

[24] Baecher-Allan, C., Wolf, E.,Hafler, D.A. Functional analysis of highly defined, FACS-isolated populations of human regulatory CD4+ CD25+ T cells. *Clin Immunol* 115, 10-8 (2005).

[25] Buckner, J.H. Mechanisms of impaired regulation by CD4(+)CD25(+)FOXP3(+) regulatory T cells in human autoimmune diseases. *Nat Rev Immunol* 10, 849-59 (2010).

[26] Bacchetta, R., Barzaghi, F.,Roncarolo, M.G. From IPEX syndrome to FOXP3 mutation: a lesson on immune dysregulation. *Ann N Y Acad Sci* (2016).

[27] Bennett, C.L., Christie, J., Ramsdell, F., Brunkow, M.E., Ferguson, P.J., Whitesell, L. et al. The immune dysregulation, polyendocrinopathy, enteropathy, X-linked syndrome (IPEX) is caused by mutations of FOXP3. *Nat Genet* 27, 20-1 (2001).

[28] Pillai, V., Ortega, S.B., Wang, C.K.,Karandikar, N.J. Transient regulatory T-cells: a state attained by all activated human T-cells. *Clin Immunol* 123, 18-29 (2007).

[29] Tran, D.Q., Ramsey, H.,Shevach, E.M. Induction of FOXP3 expression in naive human CD4+FOXP3 T cells by T-cell receptor stimulation is transforming growth factor-beta dependent but does not confer a regulatory phenotype. *Blood* 110, 2983-90 (2007).

[30] Wang, J., Ioan-Facsinay, A., van der Voort, E.I., Huizinga, T.W.,Toes, R.E. Transient expression of FOXP3 in human activated nonregulatory CD4+ T cells. *Eur J Immunol* 37, 129-38 (2007).

[31] Baron, U., Floess, S., Wieczorek, G., Baumann, K., Grutzkau, A., Dong, J. et al. DNA demethylation in the human FOXP3 locus discriminates regulatory T cells from activated FOXP3(+) conventional T cells. *Eur J Immunol* 37, 2378-89 (2007).

[32] Floess, S., Freyer, J., Siewert, C., Baron, U., Olek, S., Polansky, J. et al. Epigenetic control of the foxp3 locus in regulatory T cells. *PLoS Biol* 5, e38 (2007).

[33] Huehn, J., Polansky, J.K.,Hamann, A. Epigenetic control of FOXP3 expression: the key to a stable regulatory T-cell lineage? *Nat Rev Immunol* 9, 83-9 (2009).

[34] Polansky, J.K., Kretschmer, K., Freyer, J., Floess, S., Garbe, A., Baron, U. et al. DNA methylation controls Foxp3 gene expression. *Eur J Immunol* 38, 1654-63 (2008).

[35] Ohkura, N., Kitagawa, Y.,Sakaguchi, S. Development and maintenance of regulatory T cells. *Immunity* 38, 414-23 (2013).

[36] Hori, S. Lineage stability and phenotypic plasticity of Foxp3(+) regulatory T cells. *Immunol Rev* 259, 159-72 (2014).

[37] Overacre, A.E.,Vignali, D.A. T(reg) stability: to be or not to be. *Curr Opin Immunol* 39, 39-43 (2016).

[38] Abbas, A.K., Benoist, C., Bluestone, J.A., Campbell, D.J., Ghosh, S., Hori, S. et al. Regulatory T cells: recommendations to simplify the nomenclature. *Nat Immunol* 14, 307-8 (2013).

[39] Sakaguchi, S.,Powrie, F. Emerging challenges in regulatory T cell function and biology. *Science* 317, 627-9 (2007).

[40] Sawant, D.V.,Vignali, D.A. Once a Treg, always a Treg? *Immunol Rev* 259, 173-91 (2014).

[41] Sakaguchi, S., Vignali, D.A., Rudensky, A.Y., Niec, R.E.,Waldmann, H. The plasticity and stability of regulatory T cells. *Nat Rev Immunol* 13, 461-7 (2013).

[42] Zhou, X., Bailey-Bucktrout, S., Jeker, L.T.,Bluestone, J.A. Plasticity of CD4(+) FoxP3(+) T cells. *Curr Opin Immunol* 21, 281-5 (2009).

[43] Guo, J.,Zhou, X. Regulatory T cells turn pathogenic. *Cell Mol Immunol* 12, 525-32 (2015).

[44] Bailey-Bucktrout, S.L., Martinez-Llordella, M., Zhou, X., Anthony, B., Rosenthal, W., Luche, H. et al. Self-antigen-driven activation induces instability of regulatory T cells during an inflammatory autoimmune response. *Immunity* 39, 949-62 (2013).

[45] Komatsu, N., Okamoto, K., Sawa, S., Nakashima, T., Oh-hora, M., Kodama, T. et al. Pathogenic conversion of Foxp3+ T cells into TH17 cells in autoimmune arthritis. *Nat Med* 20, 62-8 (2014).

[46] Zhou, X., Bailey-Bucktrout, S.L., Jeker, L.T., Penaranda, C., Martinez-Llordella, M., Ashby, M. et al. Instability of the transcription factor Foxp3 leads to the generation of pathogenic memory T cells in vivo. *Nat Immunol* 10, 1000-7 (2009).

[47] Noval Rivas, M., Burton, O.T., Wise, P., Charbonnier, L.M., Georgiev, P., Oettgen, H.C. et al. Regulatory T cell reprogramming toward a Th2-cell-like lineage impairs oral tolerance and promotes food allergy. *Immunity* 42, 512-23 (2015).

[48] Bhela, S., Varanasi, S.K., Jaggi, U., Sloan, S.S., Rajasagi, N.K.,Rouse, B.T. The Plasticity and Stability of Regulatory T Cells during Viral-Induced Inflammatory Lesions. *J Immunol* 199, 1342-1352 (2017).

[49] Pelly, V.S., Coomes, S.M., Kannan, Y., Gialitakis, M., Entwistle, L.J., Perez-Lloret, J. et al. Interleukin 4 promotes the development of ex-Foxp3 Th2 cells during immunity to intestinal helminths. *J Exp Med* (2017).

[50] Zhang, Z., Zhang, W., Guo, J., Gu, Q., Zhu, X.,Zhou, X. Activation and Functional Specialization of Regulatory T Cells Lead to the Generation of Foxp3 Instability. *J Immunol* 198, 2612-2625 (2017).

[51] Duarte, J.H., Zelenay, S., Bergman, M.L., Martins, A.C.,Demengeot, J. Natural Treg cells spontaneously differentiate into pathogenic helper cells in lymphopenic conditions. *Eur J Immunol* 39, 948-55 (2009).

[52] Komatsu, N., Mariotti-Ferrandiz, M.E., Wang, Y., Malissen, B., Waldmann, H.,Hori, S. Heterogeneity of natural Foxp3+ T cells: a committed regulatory T-cell lineage and an uncommitted minor population retaining plasticity. *Proc Natl Acad Sci U S A* 106, 1903-8 (2009).

[53] Miyao, T., Floess, S., Setoguchi, R., Luche, H., Fehling, H.J., Waldmann, H. et al. Plasticity of Foxp3(+) T cells reflects promiscuous Foxp3 expression in conventional T cells but not reprogramming of regulatory T cells. *Immunity* 36, 262-75 (2012).

[54] Rubtsov, Y.P., Niec, R.E., Josefowicz, S., Li, L., Darce, J., Mathis, D. et al. Stability of the regulatory T cell lineage in vivo. *Science* 329, 1667-71 (2010).

[55] Beriou, G., Costantino, C.M., Ashley, C.W., Yang, L., Kuchroo, V.K., Baecher-Allan, C. et al. IL-17-producing human peripheral regulatory T cells retain suppressive function. *Blood* 113, 4240-9 (2009).

[56] Voo, K.S., Wang, Y.H., Santori, F.R., Boggiano, C., Wang, Y.H., Arima, K. et al. Identification of IL-17-producing FOXP3+ regulatory T cells in humans. *Proc Natl Acad Sci U S A* 106, 4793-8 (2009).

[57] Koenen, H.J., Smeets, R.L., Vink, P.M., van Rijssen, E., Boots, A.M.,Joosten, I. Human CD25highFoxp3pos regulatory T cells differentiate into IL-17-producing cells. *Blood* 112, 2340-52 (2008).

[58] Deknuydt, F., Bioley, G., Valmori, D.,Ayyoub, M. IL-1beta and IL-2 convert human Treg into T(H)17 cells. *Clin Immunol* 131, 298-307 (2009).

[59] Valencia, X., Stephens, G., Goldbach-Mansky, R., Wilson, M., Shevach, E.M.,Lipsky, P.E. TNF downmodulates the function of human CD4+CD25hi T-regulatory cells. *Blood* 108, 253-61 (2006).

[60] d'Hennezel, E., Yurchenko, E., Sgouroudis, E., Hay, V.,Piccirillo, C.A. Single-cell analysis of the human T regulatory population uncovers functional heterogeneity and instability within FOXP3+ cells. *J Immunol* 186, 6788-97 (2011).

[61] Hoffmann, P., Boeld, T.J., Eder, R., Huehn, J., Floess, S., Wieczorek, G. et al. Loss of FOXP3 expression in natural human CD4+CD25+ regulatory T cells upon repetitive in vitro stimulation. *Eur J Immunol* 39, 1088-97 (2009).

[62] Hoffmann, P., Eder, R., Boeld, T.J., Doser, K., Piseshka, B., Andreesen, R. et al. Only the CD45RA+ subpopulation of CD4+CD25high T cells gives rise to homogeneous regulatory T-cell lines upon in vitro expansion. *Blood* 108, 4260-7 (2006).

[63] Arroyo Hornero, R., Betts, G.J., Sawitzki, B., Vogt, K., Harden, P.N.,Wood, K.J. CD45RA Distinguishes CD4+CD25+CD127-/low TSDR Demethylated Regulatory T Cell Subpopulations With Differential Stability and Susceptibility to Tacrolimus-Mediated Inhibition of Suppression. *Transplantation* 101, 302-309 (2017).

[64] Miyara, M., Yoshioka, Y., Kitoh, A., Shima, T., Wing, K., Niwa, A. et al. Functional delineation and differentiation dynamics of human CD4+ T cells expressing the FoxP3 transcription factor. *Immunity* 30, 899-911 (2009).

[65] Ayyoub, M., Deknuydt, F., Raimbaud, I., Dousset, C., Leveque, L., Bioley, G. et al. Human memory FOXP3+ Tregs secrete IL-17 ex vivo and constitutively express the T(H)17 lineage-specific transcription factor RORgamma t. *Proc Natl Acad Sci U S A* 106, 8635-40 (2009).

[66] Dominguez-Villar, M., Baecher-Allan, C.M.,Hafler, D.A. Identification of T helper type 1-like, Foxp3+ regulatory T cells in human autoimmune disease. *Nat Med* 17, 673-5 (2011).

[67] McClymont, S.A., Putnam, A.L., Lee, M.R., Esensten, J.H., Liu, W., Hulme, M.A. et al. Plasticity of human regulatory T cells in healthy subjects and patients with type 1 diabetes. *J Immunol* 186, 3918-26 (2011).

[68] Pesenacker, A.M., Bending, D., Ursu, S., Wu, Q., Nistala, K.,Wedderburn, L.R. CD161 defines the subset of FoxP3+ T cells capable of producing proinflammatory cytokines. *Blood* 121, 2647-58 (2013).

[69] Afzali, B., Mitchell, P.J., Edozie, F.C., Povoleri, G.A., Dowson, S.E., Demandt, L. et al. CD161 expression characterizes a subpopulation of human regulatory T cells that produces IL-17 in a STAT3-dependent manner. *Eur J Immunol* 43, 2043-54 (2013).

[70] Bovenschen, H.J., van de Kerkhof, P.C., van Erp, P.E., Woestenenk, R., Joosten, I.,Koenen, H.J. Foxp3+ regulatory T cells of psoriasis patients easily differentiate into IL-17A-producing cells and are found in lesional skin. *J Invest Dermatol* 131, 1853-60 (2011).

[71] Kryczek, I., Wu, K., Zhao, E., Wei, S., Vatan, L., Szeliga, W. et al. IL-17+ regulatory T cells in the microenvironments of chronic inflammation and cancer. *J Immunol* 186, 4388-95 (2011).

[72] Hovhannisyan, Z., Treatman, J., Littman, D.R.,Mayer, L. Characterization of interleukin-17-producing regulatory T cells in inflamed intestinal mucosa from patients with inflammatory bowel diseases. *Gastroenterology* 140, 957-65 (2011).

[73] Ueno, A., Jijon, H., Chan, R., Ford, K., Hirota, C., Kaplan, G.G. et al. Increased prevalence of circulating novel IL-17 secreting Foxp3 expressing CD4+ T cells and defective suppressive function of circulating Foxp3+ regulatory cells support plasticity between Th17 and regulatory T cells in inflammatory bowel disease patients. *Inflamm Bowel Dis* 19, 2522-34 (2013).

[74] Bacher, P.,Scheffold, A. Flow-cytometric analysis of rare antigen-specific T cells. *Cytometry A* 83, 692-701 (2013).

[75] Bacher, P.,Scheffold, A. New technologies for monitoring human antigen-specific T cells and regulatory T cells by flow-cytometry. *Curr Opin Pharmacol* 23, 17-24 (2015).

[76] Hsieh, C.S., Liang, Y., Tyznik, A.J., Self, S.G., Liggitt, D.,Rudensky, A.Y. Recognition of the peripheral self by naturally arising CD25+ CD4+ T cell receptors. *Immunity* 21, 267-77 (2004).

[77] Hsieh, C.S., Zheng, Y., Liang, Y., Fontenot, J.D.,Rudensky, A.Y. An intersection between the self-reactive regulatory and nonregulatory T cell receptor repertoires. *Nat Immunol* 7, 401-10 (2006).

[78] Jordan, M.S., Boesteanu, A., Reed, A.J., Petrone, A.L., Holenbeck, A.E., Lerman, M.A. et al. Thymic selection of CD4+CD25+ regulatory T cells induced by an agonist self-peptide. *Nat Immunol* 2, 301-6 (2001).

[79] Kieback, E., Hilgenberg, E., Stervbo, U., Lampropoulou, V., Shen, P., Bunse, M. et al. Thymus-Derived Regulatory T Cells Are Positively Selected on Natural Self-Antigen through Cognate Interactions of High Functional Avidity. *Immunity* 44, 1114-26 (2016).

[80] Legoux, F.P., Lim, J.B., Cauley, A.W., Dikiy, S., Ertelt, J., Mariani, T.J. et al. CD4+ T Cell Tolerance to Tissue-Restricted Self Antigens Is Mediated by Antigen-Specific Regulatory T Cells Rather Than Deletion. *Immunity* 43, 896-908 (2015).

[81] Malchow, S., Leventhal, D.S., Lee, V., Nishi, S., Socci, N.D.,Savage, P.A. Aire Enforces Immune Tolerance by Directing Autoreactive T Cells into the Regulatory T Cell Lineage. *Immunity* 44, 1102-13 (2016).

[82] Malchow, S., Leventhal, D.S., Nishi, S., Fischer, B.I., Shen, L., Paner, G.P. et al. Aire-dependent thymic development of tumor-associated regulatory T cells. *Science* 339, 1219-24 (2013).

[83] Malhotra, D., Linehan, J.L., Dileepan, T., Lee, Y.J., Purtha, W.E., Lu, J.V. et al. Tolerance is established in polyclonal CD4(+) T cells by distinct mechanisms, according to self-peptide expression patterns. *Nat Immunol* 17, 187-95 (2016).

[84] Cebula, A., Seweryn, M., Rempala, G.A., Pabla, S.S., McIndoe, R.A., Denning, T.L. et al. Thymus-derived regulatory T cells contribute to tolerance to commensal microbiota. *Nature* 497, 258-62 (2013).

[85] Shafiani, S., Dinh, C., Ertelt, J.M., Moguche, A.O., Siddiqui, I., Smigiel, K.S. et al. Pathogen-specific Treg cells expand early during mycobacterium tuberculosis infection but are later eliminated in response to Interleukin-12. *Immunity* 38, 1261-70 (2013).

[86] Suffia, I.J., Reckling, S.K., Piccirillo, C.A., Goldszmid, R.S.,Belkaid, Y. Infected site-restricted Foxp3+ natural regulatory T cells are specific for microbial antigens. *J Exp Med* 203, 777-88 (2006).

[87] Zhao, J., Zhao, J., Fett, C., Trandem, K., Fleming, E.,Perlman, S. IFN-gamma- and IL-10-expressing virus epitope-specific Foxp3(+) T reg cells in the central nervous system during encephalomyelitis. *J Exp Med* 208, 1571-7 (2011).

[88] Lathrop, S.K., Bloom, S.M., Rao, S.M., Nutsch, K., Lio, C.W., Santacruz, N. et al. Peripheral education of the immune system by colonic commensal microbiota. *Nature* 478, 250-4 (2011).

[89] Atarashi, K., Tanoue, T., Oshima, K., Suda, W., Nagano, Y., Nishikawa, H. et al. Treg induction by a rationally selected mixture of Clostridia strains from the human microbiota. *Nature* 500, 232-6 (2013).

[90] Atarashi, K., Tanoue, T., Shima, T., Imaoka, A., Kuwahara, T., Momose, Y. et al. Induction of colonic regulatory T cells by indigenous Clostridium species. *Science* 331, 337-41 (2011).

[91] Round, J.L.,Mazmanian, S.K. Inducible Foxp3+ regulatory T-cell development by a commensal bacterium of the intestinal microbiota. *Proc Natl Acad Sci U S A* 107, 12204-9 (2010).

[92] Bacher, P., Kniemeyer, O., Schonbrunn, A., Sawitzki, B., Assenmacher, M., Rietschel, E. et al. Antigen-specific expansion of human regulatory T cells as a major tolerance mechanism against mucosal fungi. *Mucosal Immunol* 7, 916-28 (2014).

[93] Ebinuma, H., Nakamoto, N., Li, Y., Price, D.A., Gostick, E., Levine, B.L. et al. Identification and in vitro expansion of functional antigen-specific CD25+ FoxP3+ regulatory T cells in hepatitis C virus infection. *J Virol* 82, 5043-53 (2008).

[94] Su, L.F., Del Alcazar, D., Stelekati, E., Wherry, E.J.,Davis, M.M. Antigen exposure shapes the ratio between antigen-specific Tregs and conventional T cells in human peripheral blood. *Proc Natl Acad Sci U S A* 113, E6192-E6198 (2016).

[95] Vukmanovic-Stejic, M., Agius, E., Booth, N., Dunne, P.J., Lacy, K.E., Reed, J.R. et al. The kinetics of CD4+Foxp3+ T cell accumulation during a human

cutaneous antigen-specific memory response in vivo. *J Clin Invest* 118, 3639-50 (2008).

[96] Bacher, P., Heinrich, F., Stervbo, U., Nienen, M., Vahldieck, M., Iwert, C. et al. Regulatory T Cell Specificity Directs Tolerance versus Allergy against Aeroantigens in Humans. *Cell* 167, 1067-1078 e16 (2016).

[97] Bacher, P., Kniemeyer, O., Teutschbein, J., Thon, M., Vodisch, M., Wartenberg, D. et al. Identification of immunogenic antigens from Aspergillus fumigatus by direct multiparameter characterization of specific conventional and regulatory CD4+ T cells. *J Immunol* 193, 3332-43 (2014).

[98] Thornton, A.M., Korty, P.E., Tran, D.Q., Wohlfert, E.A., Murray, P.E., Belkaid, Y. et al. Expression of Helios, an Ikaros transcription factor family member, differentiates thymic-derived from peripherally induced Foxp3+ T regulatory cells. *J Immunol* 184, 3433-41 (2010).

[99] Singh, K., Hjort, M., Thorvaldson, L.,Sandler, S. Concomitant analysis of Helios and Neuropilin-1 as a marker to detect thymic derived regulatory T cells in naive mice. *Sci Rep* 5, 7767 (2015).

[100] Weiss, J.M., Bilate, A.M., Gobert, M., Ding, Y., Curotto de Lafaille, M.A., Parkhurst, C.N. et al. Neuropilin 1 is expressed on thymus-derived natural regulatory T cells, but not mucosa-generated induced Foxp3+ T reg cells. *J Exp Med* 209, 1723-42, S1 (2012).

[101] Yadav, M., Louvet, C., Davini, D., Gardner, J.M., Martinez-Llordella, M., Bailey-Bucktrout, S. et al. Neuropilin-1 distinguishes natural and inducible regulatory T cells among regulatory T cell subsets in vivo. *J Exp Med* 209, 1713-22, S1-19 (2012).

[102] Gottschalk, R.A., Corse, E.,Allison, J.P. Expression of Helios in peripherally induced Foxp3+ regulatory T cells. *J Immunol* 188, 976-80 (2012).

[103] Himmel, M.E., MacDonald, K.G., Garcia, R.V., Steiner, T.S.,Levings, M.K. Helios+ and Helios- cells coexist within the natural FOXP3+ T regulatory cell subset in humans. *J Immunol* 190, 2001-8 (2013).

[104] Szurek, E., Cebula, A., Wojciech, L., Pietrzak, M., Rempala, G., Kisielow, P. et al. Differences in Expression Level of Helios and Neuropilin-1 Do Not Distinguish Thymus-Derived from Extrathymically-Induced CD4+Foxp3+ Regulatory T Cells. *PLoS One* 10, e0141161 (2015).

[105] Milpied, P., Renand, A., Bruneau, J., Mendes-da-Cruz, D.A., Jacquelin, S., Asnafi, V. et al. Neuropilin-1 is not a marker of human Foxp3+ Treg. *Eur J Immunol* 39, 1466-71 (2009).

[106] Bacher, P., Schink, C., Teutschbein, J., Kniemeyer, O., Assenmacher, M., Brakhage, A.A. et al. Antigen-reactive T cell enrichment for direct, high-resolution analysis of the human naive and memory Th cell repertoire. *J Immunol* 190, 3967-76 (2013).

[107] Schoenbrunn, A., Frentsch, M., Kohler, S., Keye, J., Dooms, H., Moewes, B. et al. A converse 4-1BB and CD40 ligand expression pattern delineates

activated regulatory T cells (Treg) and conventional T cells enabling direct isolation of alloantigen-reactive natural Foxp3+ Treg. *J Immunol* 189, 5985-94 (2012).

[108] Chen, W., Jin, W., Hardegen, N., Lei, K.J., Li, L., Marinos, N. et al. Conversion of peripheral CD4+CD25- naive T cells to CD4+CD25+ regulatory T cells by TGF-beta induction of transcription factor Foxp3. *J Exp Med* 198, 1875-86 (2003).

[109] Davidson, T.S., DiPaolo, R.J., Andersson, J.,Shevach, E.M. Cutting Edge: IL-2 is essential for TGF-beta-mediated induction of Foxp3+ T regulatory cells. *J Immunol* 178, 4022-6 (2007).

[110] Walker, M.R., Kasprowicz, D.J., Gersuk, V.H., Benard, A., Van Landeghen, M., Buckner, J.H. et al. Induction of FoxP3 and acquisition of T regulatory activity by stimulated human CD4+CD25- T cells. *J Clin Invest* 112, 1437-43 (2003).

[111] Cobbold, S.P., Castejon, R., Adams, E., Zelenika, D., Graca, L., Humm, S. et al. Induction of foxP3+ regulatory T cells in the periphery of T cell receptor transgenic mice tolerized to transplants. *J Immunol* 172, 6003-10 (2004).

[112] Curotto de Lafaille, M.A., Kutchukhidze, N., Shen, S., Ding, Y., Yee, H.,Lafaille, J.J. Adaptive Foxp3+ regulatory T cell-dependent and -independent control of allergic inflammation. *Immunity* 29, 114-26 (2008).

[113] Haribhai, D., Lin, W., Edwards, B., Ziegelbauer, J., Salzman, N.H., Carlson, M.R. et al. A central role for induced regulatory T cells in tolerance induction in experimental colitis. *J Immunol* 182, 3461-8 (2009).

[114] Haribhai, D., Williams, J.B., Jia, S., Nickerson, D., Schmitt, E.G., Edwards, B. et al. A requisite role for induced regulatory T cells in tolerance based on expanding antigen receptor diversity. *Immunity* 35, 109-22 (2011).

[115] Thompson, L.J., Valladao, A.C.,Ziegler, S.F. Cutting edge: De novo induction of functional Foxp3+ regulatory CD4 T cells in response to tissue-restricted self antigen. *J Immunol* 186, 4551-5 (2011).

[116] Grainger, J.R., Smith, K.A., Hewitson, J.P., McSorley, H.J., Harcus, Y., Filbey, K.J. et al. Helminth secretions induce de novo T cell Foxp3 expression and regulatory function through the TGF-beta pathway. *J Exp Med* 207, 2331-41 (2010).

[117] Curotto de Lafaille, M.A., Lino, A.C., Kutchukhidze, N.,Lafaille, J.J. CD25- T cells generate CD25+Foxp3+ regulatory T cells by peripheral expansion. *J Immunol* 173, 7259-68 (2004).

[118] Thorstenson, K.M.,Khoruts, A. Generation of anergic and potentially immunoregulatory CD25+CD4 T cells in vivo after induction of peripheral tolerance with intravenous or oral antigen. *J Immunol* 167, 188-95 (2001).

[119] Sun, C.M., Hall, J.A., Blank, R.B., Bouladoux, N., Oukka, M., Mora, J.R. et al. Small intestine lamina propria dendritic cells promote de novo generation of Foxp3 T reg cells via retinoic acid. *J Exp Med* 204, 1775-85 (2007).

[120] Kim, K.S., Hong, S.W., Han, D., Yi, J., Jung, J., Yang, B.G. et al. Dietary antigens limit mucosal immunity by inducing regulatory T cells in the small intestine. *Science* 351, 858-63 (2016).

[121] Mucida, D., Kutchukhidze, N., Erazo, A., Russo, M., Lafaille, J.J.,Curotto de Lafaille, M.A. Oral tolerance in the absence of naturally occurring Tregs. *J Clin Invest* 115, 1923-33 (2005).

[122] Josefowicz, S.Z., Niec, R.E., Kim, H.Y., Treuting, P., Chinen, T., Zheng, Y. et al. Extrathymically generated regulatory T cells control mucosal TH2 inflammation. *Nature* 482, 395-9 (2012).

[123] Kretschmer, K., Apostolou, I., Hawiger, D., Khazaie, K., Nussenzweig, M.C.,von Boehmer, H. Inducing and expanding regulatory T cell populations by foreign antigen. *Nat Immunol* 6, 1219-27 (2005).

[124] Hindley, J.P., Ferreira, C., Jones, E., Lauder, S.N., Ladell, K., Wynn, K.K. et al. Analysis of the T-cell receptor repertoires of tumor-infiltrating conventional and regulatory T cells reveals no evidence for conversion in carcinogen-induced tumors. *Cancer Res* 71, 736-46 (2011).

[125] Lathrop, S.K., Santacruz, N.A., Pham, D., Luo, J.,Hsieh, C.S. Antigen-specific peripheral shaping of the natural regulatory T cell population. *J Exp Med* 205, 3105-17 (2008).

[126] Wong, J., Mathis, D.,Benoist, C. TCR-based lineage tracing: no evidence for conversion of conventional into regulatory T cells in response to a natural self-antigen in pancreatic islets. *J Exp Med* 204, 2039-45 (2007).

[127] Pacholczyk, R., Ignatowicz, H., Kraj, P.,Ignatowicz, L. Origin and T cell receptor diversity of Foxp3+CD4+CD25+ T cells. *Immunity* 25, 249-59 (2006).

[128] Relland, L.M., Williams, J.B., Relland, G.N., Haribhai, D., Ziegelbauer, J., Yassai, M. et al. The TCR repertoires of regulatory and conventional T cells specific for the same foreign antigen are distinct. *J Immunol* 189, 3566-74 (2012).

[129] Liu, X., Nguyen, P., Liu, W., Cheng, C., Steeves, M., Obenauer, J.C. et al. T cell receptor CDR3 sequence but not recognition characteristics distinguish autoreactive effector and Foxp3(+) regulatory T cells. *Immunity* 31, 909-20 (2009).

[130] Wong, J., Obst, R., Correia-Neves, M., Losyev, G., Mathis, D.,Benoist, C. Adaptation of TCR repertoires to self-peptides in regulatory and nonregulatory CD4+ T cells. *J Immunol* 178, 7032-41 (2007).

[131] Fazilleau, N., Bachelez, H., Gougeon, M.L.,Viguier, M. Cutting edge: size and diversity of CD4+CD25high Foxp3+ regulatory T cell repertoire in humans: evidence for similarities and partial overlapping with CD4+CD25- T cells. *J Immunol* 179, 3412-6 (2007).

[132] Fourcade, J., Sun, Z., Kudela, P., Janjic, B., Kirkwood, J.M., El-Hafnawy, T. et al. Human tumor antigen-specific helper and regulatory T cells share common

epitope specificity but exhibit distinct T cell repertoire. *J Immunol* 184, 6709-18 (2010).

[133] Schwele, S., Fischer, A.M., Brestrich, G., Wlodarski, M.W., Wagner, L., Schmueck, M. et al. Cytomegalovirus-specific regulatory and effector T cells share TCR clonality--possible relation to repetitive CMV infections. *Am J Transplant* 12, 669-81 (2012).

[134] Golding, A., Darko, S., Wylie, W.H., Douek, D.C.,Shevach, E.M. Deep sequencing of the TCR-beta repertoire of human forkhead box protein 3 (FoxP3)+ and FoxP3- T cells suggests that they are completely distinct and non-overlapping. *Clin Exp Immunol* 188, 12-21 (2017).

[135] Lei, H., Kuchenbecker, L., Streitz, M., Sawitzki, B., Vogt, K., Landwehr-Kenzel, S. et al. Human CD45RA(-) FoxP3(hi) Memory-Type Regulatory T Cells Show Distinct TCR Repertoires With Conventional T Cells and Play an Important Role in Controlling Early Immune Activation. *Am J Transplant* 15, 2625-35 (2015).

[136] Viglietta, V., Baecher-Allan, C., Weiner, H.L.,Hafler, D.A. Loss of functional suppression by CD4+CD25+ regulatory T cells in patients with multiple sclerosis. *J Exp Med* 199, 971-9 (2004).

[137] Kumar, M., Putzki, N., Limmroth, V., Remus, R., Lindemann, M., Knop, D. et al. CD4+CD25+FoxP3+ T lymphocytes fail to suppress myelin basic protein-induced proliferation in patients with multiple sclerosis. *J Neuroimmunol* 180, 178-84 (2006).

[138] Venken, K., Hellings, N., Thewissen, M., Somers, V., Hensen, K., Rummens, J.L. et al. Compromised CD4+ CD25(high) regulatory T-cell function in patients with relapsing-remitting multiple sclerosis is correlated with a reduced frequency of FOXP3-positive cells and reduced FOXP3 expression at the single-cell level. *Immunology* 123, 79-89 (2008).

[139] Jamshidian, A., Shaygannejad, V., Pourazar, A., Zarkesh-Esfahani, S.H.,Gharagozloo, M. Biased Treg/Th17 balance away from regulatory toward inflammatory phenotype in relapsed multiple sclerosis and its correlation with severity of symptoms. *J Neuroimmunol* 262, 106-12 (2013).

[140] Haas, J., Hug, A., Viehover, A., Fritzsching, B., Falk, C.S., Filser, A. et al. Reduced suppressive effect of CD4+CD25high regulatory T cells on the T cell immune response against myelin oligodendrocyte glycoprotein in patients with multiple sclerosis. *Eur J Immunol* 35, 3343-52 (2005).

[141] Ehrenstein, M.R., Evans, J.G., Singh, A., Moore, S., Warnes, G., Isenberg, D.A. et al. Compromised function of regulatory T cells in rheumatoid arthritis and reversal by anti-TNFalpha therapy. *J Exp Med* 200, 277-85 (2004).

[142] Lawson, C.A., Brown, A.K., Bejarano, V., Douglas, S.H., Burgoyne, C.H., Greenstein, A.S. et al. Early rheumatoid arthritis is associated with a deficit in the CD4+CD25high regulatory T cell population in peripheral blood. *Rheumatology (Oxford)* 45, 1210-7 (2006).

[143] Crispin, J.C., Martinez, A.,Alcocer-Varela, J. Quantification of regulatory T cells in patients with systemic lupus erythematosus. *J Autoimmun* 21, 273-6 (2003).

[144] Lee, J.H., Wang, L.C., Lin, Y.T., Yang, Y.H., Lin, D.T.,Chiang, B.L. Inverse correlation between CD4+ regulatory T-cell population and autoantibody levels in paediatric patients with systemic lupus erythematosus. *Immunology* 117, 280-6 (2006).

[145] Mellor-Pita, S., Citores, M.J., Castejon, R., Tutor-Ureta, P., Yebra-Bango, M., Andreu, J.L. et al. Decrease of regulatory T cells in patients with systemic lupus erythematosus. *Ann Rheum Dis* 65, 553-4 (2006).

[146] Miyara, M., Amoura, Z., Parizot, C., Badoual, C., Dorgham, K., Trad, S. et al. Global natural regulatory T cell depletion in active systemic lupus erythematosus. *J Immunol* 175, 8392-400 (2005).

[147] Suen, J.L., Li, H.T., Jong, Y.J., Chiang, B.L.,Yen, J.H. Altered homeostasis of CD4(+) FoxP3(+) regulatory T-cell subpopulations in systemic lupus erythematosus. *Immunology* 127, 196-205 (2009).

[148] Koreth, J., Matsuoka, K., Kim, H.T., McDonough, S.M., Bindra, B., Alyea, E.P., 3rd et al. Interleukin-2 and regulatory T cells in graft-versus-host disease. *N Engl J Med* 365, 2055-66 (2011).

[149] Saadoun, D., Rosenzwajg, M., Joly, F., Six, A., Carrat, F., Thibault, V. et al. Regulatory T-cell responses to low-dose interleukin-2 in HCV-induced vasculitis. *N Engl J Med* 365, 2067-77 (2011).

[150] von Spee-Mayer, C., Siegert, E., Abdirama, D., Rose, A., Klaus, A., Alexander, T. et al. Low-dose interleukin-2 selectively corrects regulatory T cell defects in patients with systemic lupus erythematosus. *Ann Rheum Dis* 75, 1407-15 (2016).

[151] Matsuoka, K., Koreth, J., Kim, H.T., Bascug, G., McDonough, S., Kawano, Y. et al. Low-dose interleukin-2 therapy restores regulatory T cell homeostasis in patients with chronic graft-versus-host disease. *Sci Transl Med* 5, 179ra43 (2013).

[152] Rosenzwajg, M., Churlaud, G., Mallone, R., Six, A., Derian, N., Chaara, W. et al. Low-dose interleukin-2 fosters a dose-dependent regulatory T cell tuned milieu in T1D patients. *J Autoimmun* 58, 48-58 (2015).

[153] Singer, B.D., King, L.S.,D'Alessio, F.R. Regulatory T cells as immunotherapy. *Front Immunol* 5, 46 (2014).

[154] Golshayan, D., Jiang, S., Tsang, J., Garin, M.I., Mottet, C.,Lechler, R.I. In vitro-expanded donor alloantigen-specific CD4+CD25+ regulatory T cells promote experimental transplantation tolerance. *Blood* 109, 827-35 (2007).

[155] Joffre, O., Santolaria, T., Calise, D., Al Saati, T., Hudrisier, D., Romagnoli, P. et al. Prevention of acute and chronic allograft rejection with CD4+CD25+Foxp3+ regulatory T lymphocytes. *Nat Med* 14, 88-92 (2008).

[156] Nishimura, E., Sakihama, T., Setoguchi, R., Tanaka, K.,Sakaguchi, S. Induction of antigen-specific immunologic tolerance by in vivo and in vitro antigen-specific expansion of naturally arising Foxp3+CD25+CD4+ regulatory T cells. *Int Immunol* 16, 1189-201 (2004).

[157] Trenado, A., Charlotte, F., Fisson, S., Yagello, M., Klatzmann, D., Salomon, B.L. et al. Recipient-type specific CD4+CD25+ regulatory T cells favor immune reconstitution and control graft-versus-host disease while maintaining graft-versus-leukemia. *J Clin Invest* 112, 1688-96 (2003).

[158] Taylor, P.A., Lees, C.J.,Blazar, B.R. The infusion of ex vivo activated and expanded CD4(+)CD25(+) immune regulatory cells inhibits graft-versus-host disease lethality. *Blood* 99, 3493-9 (2002).

[159] Kohm, A.P., Carpentier, P.A., Anger, H.A.,Miller, S.D. Cutting edge: CD4+CD25+ regulatory T cells suppress antigen-specific autoreactive immune responses and central nervous system inflammation during active experimental autoimmune encephalomyelitis. *J Immunol* 169, 4712-6 (2002).

[160] Mottet, C., Uhlig, H.H.,Powrie, F. Cutting edge: cure of colitis by CD4+CD25+ regulatory T cells. *J Immunol* 170, 3939-43 (2003).

[161] Masteller, E.L., Warner, M.R., Tang, Q., Tarbell, K.V., McDevitt, H.,Bluestone, J.A. Expansion of functional endogenous antigen-specific CD4+CD25+ regulatory T cells from nonobese diabetic mice. *J Immunol* 175, 3053-9 (2005).

[162] Morgan, M.E., Flierman, R., van Duivenvoorde, L.M., Witteveen, H.J., van Ewijk, W., van Laar, J.M. et al. Effective treatment of collagen-induced arthritis by adoptive transfer of CD25+ regulatory T cells. *Arthritis Rheum* 52, 2212-21 (2005).

[163] van Herwijnen, M.J., Wieten, L., van der Zee, R., van Kooten, P.J., Wagenaar-Hilbers, J.P., Hoek, A. et al. Regulatory T cells that recognize a ubiquitous stress-inducible self-antigen are long-lived suppressors of autoimmune arthritis. *Proc Natl Acad Sci U S A* 109, 14134-9 (2012).

[164] Nadig, S.N., Wieckiewicz, J., Wu, D.C., Warnecke, G., Zhang, W., Luo, S. et al. In vivo prevention of transplant arteriosclerosis by ex vivo-expanded human regulatory T cells. *Nat Med* 16, 809-13 (2010).

[165] Issa, F., Hester, J., Goto, R., Nadig, S.N., Goodacre, T.E.,Wood, K. Ex vivo-expanded human regulatory T cells prevent the rejection of skin allografts in a humanized mouse model. *Transplantation* 90, 1321-7 (2010).

[166] Sagoo, P., Ali, N., Garg, G., Nestle, F.O., Lechler, R.I.,Lombardi, G. Human regulatory T cells with alloantigen specificity are more potent inhibitors of alloimmune skin graft damage than polyclonal regulatory T cells. *Sci Transl Med* 3, 83ra42 (2011).

[167] Putnam, A.L., Safinia, N., Medvec, A., Laszkowska, M., Wray, M., Mintz, M.A. et al. Clinical grade manufacturing of human alloantigen-reactive regulatory T cells for use in transplantation. *Am J Transplant* 13, 3010-20 (2013).

[168] Wu, D.C., Hester, J., Nadig, S.N., Zhang, W., Trzonkowski, P., Gray, D. et al. Ex vivo expanded human regulatory T cells can prolong survival of a human islet allograft in a humanized mouse model. *Transplantation* 96, 707-16 (2013).

[169] Safinia, N., Scotta, C., Vaikunthanathan, T., Lechler, R.I.,Lombardi, G. Regulatory T Cells: Serious Contenders in the Promise for Immunological Tolerance in Transplantation. *Front Immunol* 6, 438 (2015).

[170] Trzonkowski, P., Bacchetta, R., Battaglia, M., Berglund, D., Bohnenkamp, H.R., ten Brinke, A. et al. Hurdles in therapy with regulatory T cells. *Sci Transl Med* 7, 304ps18 (2015).

[171] Di Ianni, M., Falzetti, F., Carotti, A., Terenzi, A., Castellino, F., Bonifacio, E. et al. Tregs prevent GVHD and promote immune reconstitution in HLA-haploidentical transplantation. *Blood* 117, 3921-8 (2011).

[172] Martelli, M.F., Di Ianni, M., Ruggeri, L., Falzetti, F., Carotti, A., Terenzi, A. et al. HLA-haploidentical transplantation with regulatory and conventional T-cell adoptive immunotherapy prevents acute leukemia relapse. *Blood* 124, 638-44 (2014).

[173] Bluestone, J.A., Buckner, J.H., Fitch, M., Gitelman, S.E., Gupta, S., Hellerstein, M.K. et al. Type 1 diabetes immunotherapy using polyclonal regulatory T cells. *Sci Transl Med* 7, 315ra189 (2015).

[174] Brunstein, C.G., Miller, J.S., Cao, Q., McKenna, D.H., Hippen, K.L., Curtsinger, J. et al. Infusion of ex vivo expanded T regulatory cells in adults transplanted with umbilical cord blood: safety profile and detection kinetics. *Blood* 117, 1061-70 (2011).

[175] Marek-Trzonkowska, N., Mysliwec, M., Siebert, J.,Trzonkowski, P. Clinical application of regulatory T cells in type 1 diabetes. *Pediatr Diabetes* 14, 322-32 (2013).

[176] Marek-Trzonkowska, N., Mysliwiec, M., Dobyszuk, A., Grabowska, M., Techmanska, I., Juscinska, J. et al. Administration of CD4+CD25highCD127-regulatory T cells preserves beta-cell function in type 1 diabetes in children. *Diabetes Care* 35, 1817-20 (2012).

[177] Trzonkowski, P., Bieniaszewska, M., Juscinska, J., Dobyszuk, A., Krzystyniak, A., Marek, N. et al. First-in-man clinical results of the treatment of patients with graft versus host disease with human ex vivo expanded CD4+CD25+CD127- T regulatory cells. *Clin Immunol* 133, 22-6 (2009).

[178] Brunstein, C.G., Blazar, B.R., Miller, J.S., Cao, Q., Hippen, K.L., McKenna, D.H. et al. Adoptive transfer of umbilical cord blood-derived regulatory T cells and early viral reactivation. *Biol Blood Marrow Transplant* 19, 1271-3 (2013).

[179] Brunstein, C.G., Miller, J.S., McKenna, D.H., Hippen, K.L., DeFor, T.E., Sumstad, D. et al. Umbilical cord blood-derived T regulatory cells to prevent GVHD: kinetics, toxicity profile, and clinical effect. *Blood* 127, 1044-51 (2016).

[180] Marek-Trzonkowska, N., Mysliwiec, M., Iwaszkiewicz-Grzes, D., Gliwinski, M., Derkowska, I., Zalinska, M. et al. Factors affecting long-term efficacy of T regulatory cell-based therapy in type 1 diabetes. *J Transl Med* 14, 332 (2016).

[181] Marek-Trzonkowska, N., Mysliwiec, M., Dobyszuk, A., Grabowska, M., Derkowska, I., Juscinska, J. et al. Therapy of type 1 diabetes with CD4(+)CD25(high)CD127-regulatory T cells prolongs survival of pancreatic islets - results of one year follow-up. *Clin Immunol* 153, 23-30 (2014).

[182] Theil, A., Tuve, S., Oelschlagel, U., Maiwald, A., Dohler, D., Ossmann, D. et al. Adoptive transfer of allogeneic regulatory T cells into patients with chronic graft-versus-host disease. *Cytotherapy* 17, 473-86 (2015).

[183] Putnam, A.L., Brusko, T.M., Lee, M.R., Liu, W., Szot, G.L., Ghosh, T. et al. Expansion of human regulatory T-cells from patients with type 1 diabetes. *Diabetes* 58, 652-62 (2009).

[184] Seay, H.R., Putnam, A.L., Cserny, J., Posgai, A.L., Rosenau, E.H., Wingard, J.R. et al. Expansion of Human Tregs from Cryopreserved Umbilical Cord Blood for GMP-Compliant Autologous Adoptive Cell Transfer Therapy. *Mol Ther Methods Clin Dev* 4, 178-191 (2017).

[185] Hippen, K.L., Merkel, S.C., Schirm, D.K., Sieben, C.M., Sumstad, D., Kadidlo, D.M. et al. Massive ex vivo expansion of human natural regulatory T cells (T(regs)) with minimal loss of in vivo functional activity. *Sci Transl Med* 3, 83ra41 (2011).

[186] Hoffmann, P., Boeld, T.J., Eder, R., Albrecht, J., Doser, K., Piseshka, B. et al. Isolation of CD4+CD25+ regulatory T cells for clinical trials. *Biol Blood Marrow Transplant* 12, 267-74 (2006).

[187] Hoffmann, P., Eder, R., Kunz-Schughart, L.A., Andreesen, R.,Edinger, M. Large-scale in vitro expansion of polyclonal human CD4(+)CD25high regulatory T cells. *Blood* 104, 895-903 (2004).

[188] Ukena, S.N., Hopting, M., Velaga, S., Ivanyi, P., Grosse, J., Baron, U. et al. Isolation strategies of regulatory T cells for clinical trials: phenotype, function, stability, and expansion capacity. *Exp Hematol* 39, 1152-60 (2011).

[189] Boardman, D., Maher, J., Lechler, R., Smyth, L.,Lombardi, G. Antigen-specificity using chimeric antigen receptors: the future of regulatory T-cell therapy? *Biochem Soc Trans* 44, 342-8 (2016).

[190] Cherai, M., Hamel, Y., Baillou, C., Touil, S., Guillot-Delost, M., Charlotte, F. et al. Generation of Human Alloantigen-Specific Regulatory T Cells Under Good Manufacturing Practice-Compliant Conditions for Cell Therapy. *Cell Transplant* 24, 2527-40 (2015).

[191] Veerapathran, A., Pidala, J., Beato, F., Betts, B., Kim, J., Turner, J.G. et al. Human regulatory T cells against minor histocompatibility antigens: ex vivo expansion for prevention of graft-versus-host disease. *Blood* 122, 2251-61 (2013).

[192] Peters, J.H., Preijers, F.W., Woestenenk, R., Hilbrands, L.B., Koenen, H.J.,Joosten, I. Clinical grade Treg: GMP isolation, improvement of purity by CD127 Depletion, Treg expansion, and Treg cryopreservation. *PLoS One* 3, e3161 (2008).

[193] Sharpe, M.,Mount, N. Genetically modified T cells in cancer therapy: opportunities and challenges. *Dis Model Mech* 8, 337-50 (2015).

[194] Johnson, L.A., Morgan, R.A., Dudley, M.E., Cassard, L., Yang, J.C., Hughes, M.S. et al. Gene therapy with human and mouse T-cell receptors mediates cancer regression and targets normal tissues expressing cognate antigen. *Blood* 114, 535-46 (2009).

[195] Morgan, R.A., Dudley, M.E., Wunderlich, J.R., Hughes, M.S., Yang, J.C., Sherry, R.M. et al. Cancer regression in patients after transfer of genetically engineered lymphocytes. *Science* 314, 126-9 (2006).

[196] Parkhurst, M.R., Yang, J.C., Langan, R.C., Dudley, M.E., Nathan, D.A., Feldman, S.A. et al. T cells targeting carcinoembryonic antigen can mediate regression of metastatic colorectal cancer but induce severe transient colitis. *Mol Ther* 19, 620-6 (2011).

[197] Robbins, P.F., Kassim, S.H., Tran, T.L., Crystal, J.S., Morgan, R.A., Feldman, S.A. et al. A pilot trial using lymphocytes genetically engineered with an NY-ESO-1-reactive T-cell receptor: long-term follow-up and correlates with response. *Clin Cancer Res* 21, 1019-27 (2015).

[198] Robbins, P.F., Morgan, R.A., Feldman, S.A., Yang, J.C., Sherry, R.M., Dudley, M.E. et al. Tumor regression in patients with metastatic synovial cell sarcoma and melanoma using genetically engineered lymphocytes reactive with NY-ESO-1. *J Clin Oncol* 29, 917-24 (2011).

[199] Rapoport, A.P., Stadtmauer, E.A., Binder-Scholl, G.K., Goloubeva, O., Vogl, D.T., Lacey, S.F. et al. NY-ESO-1-specific TCR-engineered T cells mediate sustained antigen-specific antitumor effects in myeloma. *Nat Med* 21, 914-21 (2015).

[200] Stephens, L.A., Malpass, K.H.,Anderton, S.M. Curing CNS autoimmune disease with myelin-reactive Foxp3+ Treg. *Eur J Immunol* 39, 1108-17 (2009).

[201] Tsang, J.Y., Ratnasothy, K., Li, D., Chen, Y., Bucy, R.P., Lau, K.F. et al. The potency of allospecific Tregs cells appears to correlate with T cell receptor functional avidity. *Am J Transplant* 11, 1610-20 (2011).

[202] Tsang, J.Y., Tanriver, Y., Jiang, S., Xue, S.A., Ratnasothy, K., Chen, D. et al. Conferring indirect allospecificity on CD4+CD25+ Tregs by TCR gene transfer favors transplantation tolerance in mice. *J Clin Invest* 118, 3619-28 (2008).

[203] Tang, Q., Henriksen, K.J., Bi, M., Finger, E.B., Szot, G., Ye, J. et al. In vitro-expanded antigen-specific regulatory T cells suppress autoimmune diabetes. *J Exp Med* 199, 1455-65 (2004).

[204] Tarbell, K.V., Petit, L., Zuo, X., Toy, P., Luo, X., Mqadmi, A. et al. Dendritic cell-expanded, islet-specific CD4+ CD25+ CD62L+ regulatory T cells restore normoglycemia in diabetic NOD mice. *J Exp Med* 204, 191-201 (2007).

[205] Tarbell, K.V., Yamazaki, S., Olson, K., Toy, P.,Steinman, R.M. CD25+ CD4+ T cells, expanded with dendritic cells presenting a single autoantigenic peptide, suppress autoimmune diabetes. *J Exp Med* 199, 1467-77 (2004).

[206] Wright, G.P., Notley, C.A., Xue, S.A., Bendle, G.M., Holler, A., Schumacher, T.N. et al. Adoptive therapy with redirected primary regulatory T cells results in antigen-specific suppression of arthritis. *Proc Natl Acad Sci U S A* 106, 19078-83 (2009).

[207] Fujio, K., Okamoto, A., Araki, Y., Shoda, H., Tahara, H., Tsuno, N.H. et al. Gene therapy of arthritis with TCR isolated from the inflamed paw. *J Immunol* 177, 8140-7 (2006).

[208] Brusko, T.M., Koya, R.C., Zhu, S., Lee, M.R., Putnam, A.L., McClymont, S.A. et al. Human antigen-specific regulatory T cells generated by T cell receptor gene transfer. *PLoS One* 5, e11726 (2010).

[209] Plesa, G., Zheng, L., Medvec, A., Wilson, C.B., Robles-Oteiza, C., Liddy, N. et al. TCR affinity and specificity requirements for human regulatory T-cell function. *Blood* 119, 3420-30 (2012).

[210] Hull, C.M., Nickolay, L.E., Estorninho, M., Richardson, M.W., Riley, J.L., Peakman, M. et al. Generation of human islet-specific regulatory T cells by TCR gene transfer. *J Autoimmun* 79, 63-73 (2017).

[211] Gross, G., Waks, T.,Eshhar, Z. Expression of immunoglobulin-T-cell receptor chimeric molecules as functional receptors with antibody-type specificity. *Proc Natl Acad Sci U S A* 86, 10024-8 (1989).

[212] Kuwana, Y., Asakura, Y., Utsunomiya, N., Nakanishi, M., Arata, Y., Itoh, S. et al. Expression of chimeric receptor composed of immunoglobulin-derived V regions and T-cell receptor-derived C regions. *Biochem Biophys Res Commun* 149, 960-8 (1987).

[213] Gross, G., Gorochov, G., Waks, T.,Eshhar, Z. Generation of effector T cells expressing chimeric T cell receptor with antibody type-specificity. *Transplant Proc* 21, 127-30 (1989).

[214] Eshhar, Z., Waks, T., Gross, G.,Schindler, D.G. Specific activation and targeting of cytotoxic lymphocytes through chimeric single chains consisting of antibody-binding domains and the gamma or zeta subunits of the immunoglobulin and T-cell receptors. *Proc Natl Acad Sci U S A* 90, 720-4 (1993).

[215] Eshhar, Z.,Gross, G. Chimeric T cell receptor which incorporates the anti-tumour specificity of a monoclonal antibody with the cytolytic activity of T cells: a model system for immunotherapeutical approach. *Br J Cancer Suppl* 10, 27-9 (1990).

[216] Hwu, P., Shafer, G.E., Treisman, J., Schindler, D.G., Gross, G., Cowherd, R. et al. Lysis of ovarian cancer cells by human lymphocytes redirected with a chimeric gene composed of an antibody variable region and the Fc receptor gamma chain. *J Exp Med* 178, 361-6 (1993).

[217] Hwu, P., Yang, J.C., Cowherd, R., Treisman, J., Shafer, G.E., Eshhar, Z. et al. In vivo antitumor activity of T cells redirected with chimeric antibody/T-cell receptor genes. *Cancer Res* 55, 3369-73 (1995).

[218] Gill, S.,June, C.H. Going viral: chimeric antigen receptor T-cell therapy for hematological malignancies. *Immunol Rev* 263, 68-89 (2015).

[219] Sadelain, M. CAR therapy: the CD19 paradigm. *J Clin Invest* 125, 3392-400 (2015).

[220] Geyer, M.B.,Brentjens, R.J. Review: Current clinical applications of chimeric antigen receptor (CAR) modified T cells. *Cytotherapy* 18, 1393-1409 (2016).

[221] Fesnak, A.D., June, C.H.,Levine, B.L. Engineered T cells: the promise and challenges of cancer immunotherapy. *Nat Rev Cancer* 16, 566-81 (2016).

[222] Ali, A., Kitchen, S.G., Chen, I.S., Ng, H.L., Zack, J.A.,Yang, O.O. HIV-1-Specific Chimeric Antigen Receptors Based on Broadly Neutralizing Antibodies. *J Virol* 90, 6999-7006 (2016).

[223] Deeks, S.G., Wagner, B., Anton, P.A., Mitsuyasu, R.T., Scadden, D.T., Huang, C. et al. A phase II randomized study of HIV-specific T-cell gene therapy in subjects with undetectable plasma viremia on combination antiretroviral therapy. *Mol Ther* 5, 788-97 (2002).

[224] Mitsuyasu, R.T., Anton, P.A., Deeks, S.G., Scadden, D.T., Connick, E., Downs, M.T. et al. Prolonged survival and tissue trafficking following adoptive transfer of CD4zeta gene-modified autologous CD4(+) and CD8(+) T cells in human immunodeficiency virus-infected subjects. *Blood* 96, 785-93 (2000).

[225] Kumaresan, P.R., Manuri, P.R., Albert, N.D., Maiti, S., Singh, H., Mi, T. et al. Bioengineering T cells to target carbohydrate to treat opportunistic fungal infection. *Proc Natl Acad Sci U S A* 111, 10660-5 (2014).

[226] Mekala, D.J.,Geiger, T.L. Immunotherapy of autoimmune encephalomyelitis with redirected CD4+CD25+ T lymphocytes. *Blood* 105, 2090-2 (2005).

[227] Blat, D., Zigmond, E., Alteber, Z., Waks, T.,Eshhar, Z. Suppression of murine colitis and its associated cancer by carcinoembryonic antigen-specific regulatory T cells. *Mol Ther* 22, 1018-28 (2014).

[228] Elinav, E., Adam, N., Waks, T.,Eshhar, Z. Amelioration of colitis by genetically engineered murine regulatory T cells redirected by antigen-specific chimeric receptor. *Gastroenterology* 136, 1721-31 (2009).

[229] Elinav, E., Waks, T.,Eshhar, Z. Redirection of regulatory T cells with predetermined specificity for the treatment of experimental colitis in mice. *Gastroenterology* 134, 2014-24 (2008).

[230] MacDonald, K.G., Hoeppli, R.E., Huang, Q., Gillies, J., Luciani, D.S., Orban, P.C. et al. Alloantigen-specific regulatory T cells generated with a chimeric antigen receptor. *J Clin Invest* 126, 1413-24 (2016).

[231] Noyan, F., Zimmermann, K., Hardtke-Wolenski, M., Knoefel, A., Schulde, E., Geffers, R. et al. Prevention of Allograft Rejection by Use of Regulatory T Cells With an MHC-Specific Chimeric Antigen Receptor. *Am J Transplant* 17, 917-930 (2017).

[232] Boardman, D.A., Philippeos, C., Fruhwirth, G.O., Ibrahim, M.A., Hannen, R.F., Cooper, D. et al. Expression of a Chimeric Antigen Receptor Specific for Donor HLA Class I Enhances the Potency of Human Regulatory T Cells in Preventing Human Skin Transplant Rejection. *Am J Transplant* 17, 931-943 (2017).

[233] Skuljec, J., Chmielewski, M., Happle, C., Habener, A., Busse, M., Abken, H. et al. Chimeric Antigen Receptor-Redirected Regulatory T Cells Suppress Experimental Allergic Airway Inflammation, a Model of Asthma. *Front Immunol* 8, 1125 (2017).

[234] Yoon, J., Schmidt, A., Zhang, A.H., Konigs, C., Kim, Y.C.,Scott, D.W. FVIII-specific human chimeric antigen receptor T-regulatory cells suppress T- and B-cell responses to FVIII. *Blood* 129, 238-245 (2017).

[235] Frischbutter, S., Schultheis, K., Patzel, M., Radbruch, A.,Baumgrass, R. Evaluation of calcineurin/NFAT inhibitor selectivity in primary human Th cells using bar-coding and phospho-flow cytometry. *Cytometry A* 81, 1005-11 (2012).

[236] Lutsik, P., Feuerbach, L., Arand, J., Lengauer, T., Walter, J.,Bock, C. BiQ Analyzer HT: locus-specific analysis of DNA methylation by high-throughput bisulfite sequencing. *Nucleic Acids Res* 39, W551-6 (2011).

[237] Dziubianau, M., Hecht, J., Kuchenbecker, L., Sattler, A., Stervbo, U., Rodelsperger, C. et al. TCR repertoire analysis by next generation sequencing allows complex differential diagnosis of T cell-related pathology. *Am J Transplant* 13, 2842-54 (2013).

[238] Kuchenbecker, L., Nienen, M., Hecht, J., Neumann, A.U., Babel, N., Reinert, K. et al. IMSEQ--a fast and error aware approach to immunogenetic sequence analysis. *Bioinformatics* 31, 2963-71 (2015).

[239] Yue, J.C., Clayton, M.K.,Lin, F.C. A nonparametric estimator of species overlap. *Biometrics* 57, 743-9 (2001).

[240] Arvey, A., van der Veeken, J., Plitas, G., Rich, S.S., Concannon, P.,Rudensky, A.Y. Genetic and epigenetic variation in the lineage specification of regulatory T cells. *Elife* 4, e07571 (2015).

[241] Schmidl, C., Klug, M., Boeld, T.J., Andreesen, R., Hoffmann, P., Edinger, M. et al. Lineage-specific DNA methylation in T cells correlates with histone methylation and enhancer activity. *Genome Res* 19, 1165-74 (2009).

[242] Durek, P., Nordstrom, K., Gasparoni, G., Salhab, A., Kressler, C., de Almeida, M. et al. Epigenomic Profiling of Human CD4+ T Cells Supports a Linear Differentiation Model and Highlights Molecular Regulators of Memory Development. *Immunity* 45, 1148-1161 (2016).

[243] Kim, J.O., Kim, H.W., Baek, K.M.,Kang, C.Y. NF-kappaB and AP-1 regulate activation-dependent CD137 (4-1BB) expression in T cells. *FEBS Lett* 541, 163-70 (2003).

[244] Macian, F. NFAT proteins: key regulators of T-cell development and function. *Nat Rev Immunol* 5, 472-84 (2005).

[245] Hogan, P.G., Chen, L., Nardone, J.,Rao, A. Transcriptional regulation by calcium, calcineurin, and NFAT. *Genes Dev* 17, 2205-32 (2003).

[246] Tresoldi, E., Dell'Albani, I., Stabilini, A., Jofra, T., Valle, A., Gagliani, N. et al. Stability of human rapamycin-expanded CD4+CD25+ T regulatory cells. *Haematologica* 96, 1357-65 (2011).

[247] Battaglia, M., Stabilini, A.,Tresoldi, E. Expanding human T regulatory cells with the mTOR-inhibitor rapamycin. *Methods Mol Biol* 821, 279-93 (2012).

[248] Battaglia, M.,Roncarolo, M.G. The Tregs' world according to GARP. *Eur J Immunol* 39, 3296-300 (2009).

[249] Mocci, S., Lafferty, K.,Howard, M. The role of autoantigens in autoimmune disease. *Curr Opin Immunol* 12, 725-30 (2000).

[250] Liu, H., Rhodes, M., Wiest, D.L.,Vignali, D.A. On the dynamics of TCR:CD3 complex cell surface expression and downmodulation. *Immunity* 13, 665-75 (2000).

[251] Guest, R.D., Hawkins, R.E., Kirillova, N., Cheadle, E.J., Arnold, J., O'Neill, A. et al. The role of extracellular spacer regions in the optimal design of chimeric immune receptors: evaluation of four different scFvs and antigens. *J Immunother* 28, 203-11 (2005).

[252] Hudecek, M., Lupo-Stanghellini, M.T., Kosasih, P.L., Sommermeyer, D., Jensen, M.C., Rader, C. et al. Receptor affinity and extracellular domain modifications affect tumor recognition by ROR1-specific chimeric antigen receptor T cells. *Clin Cancer Res* 19, 3153-64 (2013).

[253] Hudecek, M., Sommermeyer, D., Kosasih, P.L., Silva-Benedict, A., Liu, L., Rader, C. et al. The nonsignaling extracellular spacer domain of chimeric antigen receptors is decisive for in vivo antitumor activity. *Cancer Immunol Res* 3, 125-35 (2015).

[254] James, S.E., Greenberg, P.D., Jensen, M.C., Lin, Y., Wang, J., Till, B.G. et al. Antigen sensitivity of CD22-specific chimeric TCR is modulated by target epitope distance from the cell membrane. *J Immunol* 180, 7028-38 (2008).

[255] Wilkie, S., Picco, G., Foster, J., Davies, D.M., Julien, S., Cooper, L. et al. Retargeting of human T cells to tumor-associated MUC1: the evolution of a chimeric antigen receptor. *J Immunol* 180, 4901-9 (2008).

[256] Hombach, A., Heuser, C., Gerken, M., Fischer, B., Lewalter, K., Diehl, V. et al. T cell activation by recombinant FcepsilonRI gamma-chain immune receptors: an extracellular spacer domain impairs antigen-dependent T cell activation but not antigen recognition. *Gene Ther* 7, 1067-75 (2000).

[257] Alabanza, L., Pegues, M., Geldres, C., Shi, V., Wiltzius, J.J.W., Sievers, S.A. et al. Function of Novel Anti-CD19 Chimeric Antigen Receptors with Human Variable Regions Is Affected by Hinge and Transmembrane Domains. *Mol Ther* 25, 2452-2465 (2017).

[258] Finney, H.M., Akbar, A.N.,Lawson, A.D. Activation of resting human primary T cells with chimeric receptors: costimulation from CD28, inducible costimulator, CD134, and CD137 in series with signals from the TCR zeta chain. *J Immunol* 172, 104-13 (2004).

[259] Kowolik, C.M., Topp, M.S., Gonzalez, S., Pfeiffer, T., Olivares, S., Gonzalez, N. et al. CD28 costimulation provided through a CD19-specific chimeric antigen receptor enhances in vivo persistence and antitumor efficacy of adoptively transferred T cells. *Cancer Res* 66, 10995-1004 (2006).

[260] Loskog, A., Giandomenico, V., Rossig, C., Pule, M., Dotti, G.,Brenner, M.K. Addition of the CD28 signaling domain to chimeric T-cell receptors enhances chimeric T-cell resistance to T regulatory cells. *Leukemia* 20, 1819-28 (2006).

[261] Milone, M.C., Fish, J.D., Carpenito, C., Carroll, R.G., Binder, G.K., Teachey, D. et al. Chimeric receptors containing CD137 signal transduction domains mediate enhanced survival of T cells and increased antileukemic efficacy in vivo. *Mol Ther* 17, 1453-64 (2009).

[262] Savoldo, B., Ramos, C.A., Liu, E., Mims, M.P., Keating, M.J., Carrum, G. et al. CD28 costimulation improves expansion and persistence of chimeric antigen receptor-modified T cells in lymphoma patients. *J Clin Invest* 121, 1822-6 (2011).

[263] Wang, J., Jensen, M., Lin, Y., Sui, X., Chen, E., Lindgren, C.G. et al. Optimizing adoptive polyclonal T cell immunotherapy of lymphomas, using a chimeric T cell receptor possessing CD28 and CD137 costimulatory domains. *Hum Gene Ther* 18, 712-25 (2007).

[264] Zhang, H., Snyder, K.M., Suhoski, M.M., Maus, M.V., Kapoor, V., June, C.H. et al. 4-1BB is superior to CD28 costimulation for generating CD8+ cytotoxic lymphocytes for adoptive immunotherapy. *J Immunol* 179, 4910-8 (2007).

[265] Kalos, M., Levine, B.L., Porter, D.L., Katz, S., Grupp, S.A., Bagg, A. et al. T cells with chimeric antigen receptors have potent antitumor effects and can establish memory in patients with advanced leukemia. *Sci Transl Med* 3, 95ra73 (2011).

[266] Heuser, C., Hombach, A., Losch, C., Manista, K.,Abken, H. T-cell activation by recombinant immunoreceptors: impact of the intracellular signalling domain on the stability of receptor expression and antigen-specific activation of grafted T cells. *Gene Ther* 10, 1408-19 (2003).

[267] Nolan, K.F., Yun, C.O., Akamatsu, Y., Murphy, J.C., Leung, S.O., Beecham, E.J. et al. Bypassing immunization: optimized design of "designer T cells" against carcinoembryonic antigen (CEA)-expressing tumors, and lack of suppression by soluble CEA. *Clin Cancer Res* 5, 3928-41 (1999).

[268] Zhao, Y., Wang, Q.J., Yang, S., Kochenderfer, J.N., Zheng, Z., Zhong, X. et al. A herceptin-based chimeric antigen receptor with modified signaling domains leads to enhanced survival of transduced T lymphocytes and antitumor activity. *J Immunol* 183, 5563-74 (2009).

[269] Wang, H., Kadlecek, T.A., Au-Yeung, B.B., Goodfellow, H.E., Hsu, L.Y., Freedman, T.S. et al. ZAP-70: an essential kinase in T-cell signaling. *Cold Spring Harb Perspect Biol* 2, a002279 (2010).

[270] Maus, M.V.,June, C.H. Making Better Chimeric Antigen Receptors for Adoptive T-cell Therapy. *Clin Cancer Res* 22, 1875-84 (2016).

[271] Stockis, J., Fink, W., Francois, V., Connerotte, T., de Smet, C., Knoops, L. et al. Comparison of stable human Treg and Th clones by transcriptional profiling. *Eur J Immunol* 39, 869-82 (2009).

[272] Noyan, F., Lee, Y.S., Zimmermann, K., Hardtke-Wolenski, M., Taubert, R., Warnecke, G. et al. Isolation of human antigen-specific regulatory T cells with high suppressive function. *Eur J Immunol* 44, 2592-602 (2014).

[273] Lozano, T., Villanueva, L., Durantez, M., Gorraiz, M., Ruiz, M., Belsue, V. et al. Inhibition of FOXP3/NFAT Interaction Enhances T Cell Function after TCR Stimulation. *J Immunol* 195, 3180-9 (2015).

[274] Campbell, D.J.,Ziegler, S.F. FOXP3 modifies the phenotypic and functional properties of regulatory T cells. *Nat Rev Immunol* 7, 305-10 (2007).

[275] Wehler, T.C., Karg, M., Distler, E., Konur, A., Nonn, M., Meyer, R.G. et al. Rapid identification and sorting of viable virus-reactive CD4(+) and CD8(+) T cells based on antigen-triggered CD137 expression. *J Immunol Methods* 339, 23-37 (2008).

[276] Wu, Y., Borde, M., Heissmeyer, V., Feuerer, M., Lapan, A.D., Stroud, J.C. et al. FOXP3 controls regulatory T cell function through cooperation with NFAT. *Cell* 126, 375-87 (2006).

[277] Marson, A., Kretschmer, K., Frampton, G.M., Jacobsen, E.S., Polansky, J.K., MacIsaac, K.D. et al. Foxp3 occupancy and regulation of key target genes during T-cell stimulation. *Nature* 445, 931-5 (2007).

[278] DeBenedette, M.A., Chu, N.R., Pollok, K.E., Hurtado, J., Wade, W.F., Kwon, B.S. et al. Role of 4-1BB ligand in costimulation of T lymphocyte growth and its upregulation on M12 B lymphomas by cAMP. *J Exp Med* 181, 985-92 (1995).

[279] Zheng, G., Wang, B.,Chen, A. The 4-1BB costimulation augments the proliferation of CD4+CD25+ regulatory T cells. *J Immunol* 173, 2428-34 (2004).

[280] Zhang, P., Gao, F., Wang, Q., Wang, X., Zhu, F., Ma, C. et al. Agonistic anti-4-1BB antibody promotes the expansion of natural regulatory T cells while maintaining Foxp3 expression. *Scand J Immunol* 66, 435-40 (2007).

[281] Elpek, K.G., Yolcu, E.S., Franke, D.D., Lacelle, C., Schabowsky, R.H.,Shirwan, H. Ex vivo expansion of CD4+CD25+FoxP3+ T regulatory cells based on synergy between IL-2 and 4-1BB signaling. *J Immunol* 179, 7295-304 (2007).

[282] Kim, J., Kim, W., Kim, H.J., Park, S., Kim, H.A., Jung, D. et al. Host CD25+CD4+Foxp3+ regulatory T cells primed by anti-CD137 mAbs inhibit graft-versus-host disease. *Biol Blood Marrow Transplant* 18, 44-54 (2012).

[283] Lee, J., Lee, E.N., Kim, E.Y., Park, H.J., Chang, C.Y., Jung, D.Y. et al. Administration of agonistic anti-4-1BB monoclonal antibody leads to the amelioration of inflammatory bowel disease. *Immunol Lett* 101, 210-6 (2005).

[284] Choi, B.K., Bae, J.S., Choi, E.M., Kang, W.J., Sakaguchi, S., Vinay, D.S. et al. 4-1BB-dependent inhibition of immunosuppression by activated CD4+CD25+ T cells. *J Leukoc Biol* 75, 785-91 (2004).

[285] Bour-Jordan, H.,Bluestone, J.A. Regulating the regulators: costimulatory signals control the homeostasis and function of regulatory T cells. *Immunol Rev* 229, 41-66 (2009).

[286] Joller, N., Lozano, E., Burkett, P.R., Patel, B., Xiao, S., Zhu, C. et al. Treg cells expressing the coinhibitory molecule TIGIT selectively inhibit proinflammatory Th1 and Th17 cell responses. *Immunity* 40, 569-81 (2014).

[287] Kitamura, N., Murata, S., Ueki, T., Mekata, E., Reilly, R.T., Jaffee, E.M. et al. OX40 costimulation can abrogate Foxp3+ regulatory T cell-mediated suppression of antitumor immunity. *Int J Cancer* 125, 630-8 (2009).

[288] Vu, M.D., Xiao, X., Gao, W., Degauque, N., Chen, M., Kroemer, A. et al. OX40 costimulation turns off Foxp3+ Tregs. *Blood* 110, 2501-10 (2007).

[289] Schmidt, A., Oberle, N.,Krammer, P.H. Molecular mechanisms of treg-mediated T cell suppression. *Front Immunol* 3, 51 (2012).

[290] Kwon, B. Is CD137 Ligand (CD137L) Signaling a Fine Tuner of Immune Responses? *Immune Netw* 15, 121-4 (2015).

[291] Rubtsov, Y.P., Rasmussen, J.P., Chi, E.Y., Fontenot, J., Castelli, L., Ye, X. et al. Regulatory T cell-derived interleukin-10 limits inflammation at environmental interfaces. *Immunity* 28, 546-58 (2008).

[292] Harrison, O.J.,Powrie, F.M. Regulatory T cells and immune tolerance in the intestine. *Cold Spring Harb Perspect Biol* 5 (2013).

[293] Martin, G.H., Gregoire, S., Landau, D.A., Pilon, C., Grinberg-Bleyer, Y., Charlotte, F. et al. In vivo activation of transferred regulatory T cells specific for third-party exogenous antigen controls GVH disease in mice. *Eur J Immunol* 43, 2263-72 (2013).

[294] Desreumaux, P., Foussat, A., Allez, M., Beaugerie, L., Hebuterne, X., Bouhnik, Y. et al. Safety and efficacy of antigen-specific regulatory T-cell therapy for patients with refractory Crohn's disease. *Gastroenterology* 143, 1207-17 e1-2 (2012).

[295] Mehvar, R. Dextrans for targeted and sustained delivery of therapeutic and imaging agents. *J Control Release* 69, 1-25 (2000).

[296] Klotz, U.,Kroemer, H. Clinical pharmacokinetic considerations in the use of plasma expanders. *Clin Pharmacokinet* 12, 123-35 (1987).

[297] Sadelain, M., Brentjens, R.,Riviere, I. The basic principles of chimeric antigen receptor design. *Cancer Discov* 3, 388-98 (2013).

[298] Tran, D.Q., Andersson, J., Wang, R., Ramsey, H., Unutmaz, D.,Shevach, E.M. GARP (LRRC32) is essential for the surface expression of latent TGF-beta on platelets and activated FOXP3+ regulatory T cells. *Proc Natl Acad Sci U S A* 106, 13445-50 (2009).

[299] Tran, D.Q., Andersson, J., Hardwick, D., Bebris, L., Illei, G.G.,Shevach, E.M. Selective expression of latency-associated peptide (LAP) and IL-1 receptor type I/II (CD121a/CD121b) on activated human FOXP3+ regulatory T cells allows for their purification from expansion cultures. *Blood* 113, 5125-33 (2009).

[300] Seddiki, N., Cook, L., Hsu, D.C., Phetsouphanh, C., Brown, K., Xu, Y. et al. Human antigen-specific CD4(+) CD25(+) CD134(+) CD39(+) T cells are enriched for regulatory T cells and comprise a substantial proportion of recall responses. *Eur J Immunol* 44, 1644-61 (2014).

[301] Jonnalagadda, M., Mardiros, A., Urak, R., Wang, X., Hoffman, L.J., Bernanke, A. et al. Chimeric antigen receptors with mutated IgG4 Fc spacer avoid fc receptor binding and improve T cell persistence and antitumor efficacy. *Mol Ther* 23, 757-68 (2015).

[302] Taylor, M.J., Husain, K., Gartner, Z.J., Mayor, S.,Vale, R.D. A DNA-Based T Cell Receptor Reveals a Role for Receptor Clustering in Ligand Discrimination. *Cell* 169, 108-119 e20 (2017).

[303] Long, A.H., Haso, W.M., Shern, J.F., Wanhainen, K.M., Murgai, M., Ingaramo, M. et al. 4-1BB costimulation ameliorates T cell exhaustion induced by tonic signaling of chimeric antigen receptors. *Nat Med* 21, 581-90 (2015).

[304] Maldonado, R.A., LaMothe, R.A., Ferrari, J.D., Zhang, A.H., Rossi, R.J., Kolte, P.N. et al. Polymeric synthetic nanoparticles for the induction of antigen-specific immunological tolerance. *Proc Natl Acad Sci U S A* 112, E156-65 (2015).

[305] Samstein, R.M., Josefowicz, S.Z., Arvey, A., Treuting, P.M.,Rudensky, A.Y. Extrathymic generation of regulatory T cells in placental mammals mitigates maternal-fetal conflict. *Cell* 150, 29-38 (2012).

[306] Yadav, M., Stephan, S.,Bluestone, J.A. Peripherally induced tregs - role in immune homeostasis and autoimmunity. *Front Immunol* 4, 232 (2013).

[307] Tsuji, M., Komatsu, N., Kawamoto, S., Suzuki, K., Kanagawa, O., Honjo, T. et al. Preferential generation of follicular B helper T cells from Foxp3+ T cells in gut Peyer's patches. *Science* 323, 1488-92 (2009).

[308] Coombes, J.L., Siddiqui, K.R., Arancibia-Carcamo, C.V., Hall, J., Sun, C.M., Belkaid, Y. et al. A functionally specialized population of mucosal CD103+ DCs induces Foxp3+ regulatory T cells via a TGF-beta and retinoic acid-dependent mechanism. *J Exp Med* 204, 1757-64 (2007).

[309] Soroosh, P., Doherty, T.A., Duan, W., Mehta, A.K., Choi, H., Adams, Y.F. et al. Lung-resident tissue macrophages generate Foxp3+ regulatory T cells and promote airway tolerance. *J Exp Med* 210, 775-88 (2013).

[310] Nutsch, K., Chai, J.N., Ai, T.L., Russler-Germain, E., Feehley, T., Nagler, C.R. et al. Rapid and Efficient Generation of Regulatory T Cells to Commensal Antigens in the Periphery. *Cell Rep* 17, 206-20 (2016).

[311] Grewal, I.S.,Flavell, R.A. CD40 and CD154 in cell-mediated immunity. *Annu Rev Immunol* 16, 111-35 (1998).

[312] Elgueta, R., Benson, M.J., de Vries, V.C., Wasiuk, A., Guo, Y.,Noelle, R.J. Molecular mechanism and function of CD40/CD40L engagement in the immune system. *Immunol Rev* 229, 152-72 (2009).

[313] Sasidharan Nair, V., Song, M.H.,Oh, K.I. Vitamin C Facilitates Demethylation of the Foxp3 Enhancer in a Tet-Dependent Manner. *J Immunol* 196, 2119-31 (2016).

[314] Yue, X., Trifari, S., Aijo, T., Tsagaratou, A., Pastor, W.A., Zepeda-Martinez, J.A. et al. Control of Foxp3 stability through modulation of TET activity. *J Exp Med* 213, 377-97 (2016).

[315] Arpaia, N., Campbell, C., Fan, X., Dikiy, S., van der Veeken, J., deRoos, P. et al. Metabolites produced by commensal bacteria promote peripheral regulatory T-cell generation. *Nature* 504, 451-5 (2013).

[316] Furusawa, Y., Obata, Y., Fukuda, S., Endo, T.A., Nakato, G., Takahashi, D. et al. Commensal microbe-derived butyrate induces the differentiation of colonic regulatory T cells. *Nature* 504, 446-50 (2013).

[317] Mucida, D., Park, Y., Kim, G., Turovskaya, O., Scott, I., Kronenberg, M. et al. Reciprocal TH17 and regulatory T cell differentiation mediated by retinoic acid. *Science* 317, 256-60 (2007).

[318] Schmidt, A., Eriksson, M., Shang, M.M., Weyd, H.,Tegner, J. Comparative Analysis of Protocols to Induce Human CD4+Foxp3+ Regulatory T Cells by Combinations of IL-2, TGF-beta, Retinoic Acid, Rapamycin and Butyrate. *PLoS One* 11, e0148474 (2016).

[319] Lu, L., Zhou, X., Wang, J., Zheng, S.G.,Horwitz, D.A. Characterization of protective human CD4CD25 FOXP3 regulatory T cells generated with IL-2, TGF-beta and retinoic acid. *PLoS One* 5, e15150 (2010).

[320] Wang, J., Huizinga, T.W.,Toes, R.E. De novo generation and enhanced suppression of human CD4+CD25+ regulatory T cells by retinoic acid. *J Immunol* 183, 4119-26 (2009).

[321] Fujishima, M., Hirokawa, M., Fujishima, N.,Sawada, K. TCRalphabeta repertoire diversity of human naturally occurring CD4+CD25+ regulatory T cells. *Immunol Lett* 99, 193-7 (2005).

[322] Kasow, K.A., Chen, X., Knowles, J., Wichlan, D., Handgretinger, R.,Riberdy, J.M. Human CD4+CD25+ regulatory T cells share equally complex and comparable repertoires with CD4+CD25- counterparts. *J Immunol* 172, 6123-8 (2004).

[323] Lee, H.M., Bautista, J.L., Scott-Browne, J., Mohan, J.F.,Hsieh, C.S. A broad range of self-reactivity drives thymic regulatory T cell selection to limit responses to self. *Immunity* 37, 475-86 (2012).

[324] Wojciech, L., Ignatowicz, A., Seweryn, M., Rempala, G., Pabla, S.S., McIndoe, R.A. et al. The same self-peptide selects conventional and regulatory CD4(+) T cells with identical antigen receptors. *Nat Commun* 5, 5061 (2014).

[325] Hsieh, C.S., Lee, H.M.,Lio, C.W. Selection of regulatory T cells in the thymus. *Nat Rev Immunol* 12, 157-67 (2012).

[326] Pacholczyk, R.,Kern, J. The T-cell receptor repertoire of regulatory T cells. *Immunology* 125, 450-8 (2008).

[327] van Santen, H.M., Benoist, C.,Mathis, D. Number of T reg cells that differentiate does not increase upon encounter of agonist ligand on thymic epithelial cells. *J Exp Med* 200, 1221-30 (2004).

[328] Bonasio, R., Scimone, M.L., Schaerli, P., Grabie, N., Lichtman, A.H.,von Andrian, U.H. Clonal deletion of thymocytes by circulating dendritic cells homing to the thymus. *Nat Immunol* 7, 1092-100 (2006).

[329] Mason, D. A very high level of crossreactivity is an essential feature of the T-cell receptor. *Immunol Today* 19, 395-404 (1998).

[330] Tuovinen, H., Kekalainen, E., Rossi, L.H., Puntila, J.,Arstila, T.P. Cutting edge: human CD4-CD8- thymocytes express FOXP3 in the absence of a TCR. *J Immunol* 180, 3651-4 (2008).

[331] Beyer, M.,Huehn, J. Epigenetic orchestration of thymic Treg cell development. *Nat Immunol* 18, 144-146 (2017).

[332] Kitagawa, Y., Ohkura, N.,Sakaguchi, S. Epigenetic control of thymic Treg-cell development. *Eur J Immunol* 45, 11-6 (2015).

9 Appendix

9.1 Table of figures

9.2 Table of tables

9.3 Abbreviations

Aire	Autoimmune regulator
AP-1	Activator protein 1
APC	Antigen presenting cell / Allophycocyanin
APS-1	Autoimmune polyendocrine syndrome type 1
ATP	Adenosine triphosphate
B2M	β2-microglobulin
BSA	Bovine serum albumin
BTP1	3,5-bistrifluoromethyl pyrazole
CAR	Chimeric antigen receptor
CD	Cluster of differentiation
CD40L	CD40 ligand
CEA	Carcinoembryonic antigen
CMV	Cytomegalovirus
CpG	5'—Cytosine—phosphate—Guanine—3'
CSF2	Colony Stimulating Factor 2
CTL	Cytotoxic T lymphocyte
CTLA4	Cytotoxic T-lymphocyte-associated Protein 4
DAPI	4’,6-diamidino-2-phenylindole
Dex	Dextran
DNA	Deoxyribonucleic acid
dNTP	Deoxynucleotide
EAE	Experimental autoimmune encephalomyelitis
EDTA	Ethylenediaminetetraacetic acid
FACS	Fluorescence-activated cell sorting
FITC	Fluorescein isothiocyanate
FoxP3	Forkhead Box Protein P3
GAPDH	Glyceraldehyde-3-phosphate dehydrogenase
GARP	Glycoprotein A repetitions predominant
GvHD	Graft-versus-host-disease
HIV	Human immunodeficiency virus
HLA	Human leucocyte antigen
ICOS	Inducible T-cell costimulator
IFC	Integrated fluidic circuit

IFN	Interferon
IgG	Immunoglobulin
IKZF	Ikaros family of zinc finger proteins
IL	Interleukin
IPEX	Immune dysregulation, polyendocrinopathy, enteropathy, X-linked
ITAM	Immunoreceptor tyrosine-based activation motif
iTreg	In vitro induced Treg
kDa	Kilodalton
LAP	Latency-associated peptide
LNGFR	Low-affinity nerve growth factor receptor
LRRC32	Leucine rich repeat containing 32
MHC	Major histocompatibility complex
MS	Multiple sclerosis
mTEC	Medullary thymic epithelial cells
mTOR	Mechanistic target of rapamycin
NFAT	Nuclear factor of activated T cells
NFκB	Nuclear factor ‘kappa-light-chain-enhancer’ of activated B-cells
NGS	Next generation sequencing
PBS	Phosphate buffered saline
PCR	Polymerase chain reaction
PD-1	Programmed cell death protein 1
PE	Phycoerythrin
Percp	Peridinin-chlorophyll-protein
PMA	Phorbol-12-myristat-13-acetat
pTreg	Peripherally-induced Treg
RA	Rheumatoid arthritis
RNA	Ribonucleic acid
RT	Room temperature
scFv	Single chain variable fragment
SLE	Systemic lupus erythematosus
T1D	Type 1 diabetes
T_{CM}	Central memory T cell
Tcon	Conventional T cell
TCR	T cell receptor
TGFβ	Transforming growth factor beta

Th	T helper
TIGIT	T-cell immunoreceptor with Ig and ITIM domains
TLR	Toll-like receptor
TNF	Tumor necrosis factor
TNFRSF9	Tumor necrosis factor receptor superfamily
TNP	Trinitrophenol
Tr1	Type 1 regulatory cells
Treg	Regulatory T cell
Tresp	Responder T cells
TSDR	Treg-specific demethylated region
tTreg	Thymic-derived Treg
ZAP70	Zeta chain of T-cell receptor associated protein kinase 70

9.4 Acknowledgements

An dieser Stelle möchte ich allen Personen danken, die mich in den letzten Jahren bei dieser Arbeit begleitet und unterstützt haben.

Mein großer Dank gilt Roland Lauster für die Begutachtung dieser Arbeit, die freundliche Betreuung und den unkomplizierten Ablauf des Promotionsverfahrens. Ebenfalls möchte ich Jens Kurreck für die Begutachtung dieser Arbeit danken.

Mein ganz besonderer Dank gilt Alexander Scheffold, der mir die Bearbeitung dieses interessanten Projekts in seiner Arbeitsgruppe ermöglicht hat und durch die freundliche Betreuung und anregenden Diskussionen diese Arbeit während der letzten Jahre begleitet und unterstützt hat.

Den derzeitigen und ehemaligen Mitgliedern der AG Scheffold möchte ich ganz herzlich für die außerordentlich angenehme Zusammenarbeit und konstruktive Unterstützung während der letzten Jahre danken. Insbesondere Petra Bacher möchte ich für die fachliche Unterstützung und das Korrekturlesen dieser Arbeit danken, sowie Frederik Heinrich und Thordis Hohnstein für die freundschaftliche Atmosphäre.

Dem gesamten DRFZ, sowie unseren internen und externen Kooperationspartnern Jörn Walter, Birgit Sawitzki, Katrin Vogt, Julia Polansky-Biskup, Nina Babel, Ulrik Stervbo, Mikalai Nienen, Laura Lozza, Manuela Stäber, Pascal Giehr, Judith Gottfreund, Andrew Kaiser und Dominik Lock möchte ich für die konstruktive Zusammenarbeit danken, die wesentlich zur Anfertigung dieser Arbeit beigetragen hat.

Mein tiefempfundener Dank gilt meinen Eltern und meiner Familie, die mir in jeder Lebenslage zur Seite stehen und auf die ich mit zu jeder Zeit ausnahmslos verlassen kann. Mein größter Dank gilt Paul, für seine uneingeschränkte und liebevolle Unterstützung, Motivation und Geduld. Danke.

9.5 Publikationsliste

Nowak A., Lock D., Bacher P., Hohnstein T., Vogt K., Gottfreund J., Giehr P., Polansky J.K., Sawitzki B., Kaiser A., Walter J. and Scheffold A. (2018). CD137+CD154− Expression As a Regulatory T Cell (Treg)-Specific Activation Signature for Identification and Sorting of Stable Human Tregs from In Vitro Expansion Cultures. Front. Immunol. 9:199. https://doi.org/10.3389/fimmu.2018.00199

(Dieser Artikel enthält Teile der Dissertation).

9.6 Eidesstattliche Versicherung

Hiermit erkläre ich, Anna Nowak, geboren am 15.06.1989 in Berlin, die vorliegende Dissertation mit dem Titel: "Optimizing human Treg stability and target specificity for therapeutic applications" selbstständig und ohne unerlaubte Hilfe angefertigt zu haben und alle verwendeten Hilfsmittel und Inhalte aus anderen Quellen als solche kenntlich gemacht zu haben. Des Weiteren erkläre ich, dass ich nicht schon anderweitig einmal die Promotionsabsicht angemeldet oder ein Promotionseröffnungsverfahren beantragt habe. Die geltende Promotionsordnung der TU Berlin vom 23. Oktober 2006, zuletzt geändert mit der Änderungssatzung vom 15. Januar 2014, ist mir bekannt.

Berlin, im Dezember 2017

Anna Nowak